APPROVED FOR RELEASE: 2007/02/08: CIA-RDP82-00850R000300080046-0

JPRS L/9563

23 February 1981

USSR Report

METEOROLOGY AND HYDROLOGY

No. 10, October 1980

FBIS FOREIGN BROADCAST INFORMATION SERVICE

APPROVED FOR RELEASE: 2007/02/08: CIA-RDP82-00850R000300080046-0

APPROVED FOR RELEASE: 2007/02/08: CIA-RDP82-00850R000300080046-0

NOTE

JPRS publications contain information primarily from foreign newspapers, periodicals and books, but also from news agency transmissions and broadcasts. Materials from foreign-language sources are translated; those from English-language sources are transcribed or reprinted, with the original phrasing and other characteristics retained.

Headlines, editorial reports, and material enclosed in brackets [] are supplied by JPRS. Prccessing indicators such as [Text] or [Excerpt] in the first line of each item, or following the last line of a brief, indicate how the original information was processed. Where no processing indicator is given, the information was summarized or extracted.

Unfamiliar names rendered phonetically or transliterated are enclosed in parentheses. Words or names preceded by a question mark and enclosed in parentheses were not clear in the original but have been supplied as appropriate in context. Other unattributed parenthetical notes within the body of an item originate with the source. Times within items are as given by source.

The contents of this publication in no way represent the policies, views or attitudes of the U.S. Government.

COPYRIGHT LAWS AND REGULATIONS GOVERNING OWNERSHIP OF MATERIALS REPRODUCED HEREIN REQUIRE THAT DISSEMINATION OF THIS PUBLICATION BE RESTRICTED FOR OFFICIAL USE ONLY.

APPROVED FOR RELEASE: 2007/02/08: CIA-RDP82-00850R000300080046-0

APPROVED FOR RELEASE: 2007/02/08: CIA-RDP82-00850R000300080046-0

JPRS L/9563

23 February 1981

USSR REPORT

METEOROLOGY AND HYDROLOGY

No. 10, October 1980

Translation of the Russian-language monthly journal METEOROLOGIYA I GIDROLOGIYA published in Moscow by Gidrometeoizdat.

CONTENTS

APPROVED FOR RELEASE: 2007/02/08: CIA-RDP82-00850R000300080046-0

APPROVED FOR RELEASE: 2007/02/08: CIA-RDP82-00850R000300080046-0

APPROVED FOR RELEASE: 2007/02/08: CIA-RDP82-00850R000300080046-0

APPROVED FOR RELEASE: 2007/02/08: CIA-RDP82-00850R000300080046-0

UDC 551.509.313

FORMULATION OF BOUNDARY CONDITIONS FOR THE FORECASTING PROBLEM USING NESTED GRIDS

Moscow METEOROLOGIYA I GIDROLOGIYA in Russian No 10, Oct 80 pp 5-12

[Article by Candidate of Physical and Mathematical Sciences Ye. Ye. Kalenkovich and I. V. Cholakh, West Siberian Regional Scientific Research Institute, manuscript submitted 24 Dec 79]

[Text]

Abstract: The problem of formulation of boundary conditions for a regional forecast, which is computed jointly with a forecast for an expanded territory, is considered. The derivation of the boundary conditions adequate for coincidence of solutions of discrete approximations of problems within the internal region of telescoping is given, taking into account use of the splitting method. The results of computations using real data are presented.

Telescoping techniques have developed intensively during recent years. The essence of this technique is that within a large prognostic region, where a grid with large space variables intervals is used, a smaller region with a fine grid (mesh) is defined. In solving the problem in the fine grid use is made of information obtained in the course of forecasting for a large territory [7, 12, 13]. In forecasts for a hemisphere and region use is made of telescoping with a unidirectional effect (the results of computations in the fine grid are not used for correcting the forecast in the coarse grid). Such a telescoping version makes it possible to improve the approximation without a substantial increase in the requirements on the size of computer memory or greater computer speed and at the boundaries of the region with a fine grid use time-dependent boundary conditions.

Figure 1 shows the trajectories of particles which at the initial moment are at the boundary of the region of telescoping, tracked over a 24-hour period when computing a forecast for a hemisphere. In order to obtain the trajectories in each time interval the coordinates of the particles were scaled using the velocity values at these points interpolated from the adjacent points of grid intersection. The figure gives some idea of how substantially the fields can be distorted by stipulating time-constant values of the functions at the boundary of the region. In this connection it was of interest to clarify what the model gives if real values are stipulated at the boundaries. Table 1 gives the values of the

APPROVED FOR RELEASE: 2007/02/08: CIA-RDP82-00850R000300080046-0

APPROVED FOR RELEASE: 2007/02/08: CIA-RDP82-00850R000300080046-0

evaluations of a forecast using a regional model with boundary conditions close to the actual boundary conditions, obtained using the formula

[Φ= act(ual)] $$H_{boun}(t) = \alpha(t) H_{\Phi}^{24} + (1 - \alpha(t)) H_{\Phi}^{0},$$

where H_{act}^{0}, H_{act}^{24} are the actual values of the meteorological elements at the initial moment and after 24 hours and $\alpha(t)$ changes linearly in the course of the forecast from 0 to 1. Although such boundary conditions can only conditionally be called "actual," in real computations at the present time it is scarcely possible to obtain such a success in a forecast.

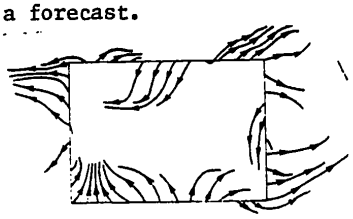

Fig. 1. Predicted trajectories of particles after 24 hours.

Table 1

Evaluation of Forecast With Actual Boundary Conditions (ε -- Relative Error, r -- Correlation Coefficient)

	Level, mb		
	1000	500	200
ε	0.53	0.34	0.43
r	0.85	0.95	0.91

Several telescoped models [8, 11] have now been created and are being used in routine practice. Their use has made it possible to improve the quality of forecasts. The development and testing of such schemes has shown that the success in use of telescoping to a very great degree is dependent on the methods for stipulating the boundary conditions. The difficulties in formulating the boundary conditions ensuring correctness of the problem for a system of primitive equations are related to the mathematical properties of the system itself [1] and the presence of angles at the boundary of the region. Sometimes overdetermined boundary conditions are used in combination with different methods for suppressing reflected waves [7, 9, 13]. Attempts at formulating boundary conditions not allowing wave reflections meet with considerable mathematical difficulties. Conditions of the total absorption type and their local approximations [6, 10] defined for simpler problems for the time being have not been applied to the case of a system of primitive equations in a region with angles.

The realization of a prognostic algorithm on the basis of the splitting method [5] used in the model in [2] makes it possible to avoid these difficulties and in each splitting stage define boundary conditions making it possible to avoid overdetermination and ensuring correctness of the problem. This was done in [4] for the

APPROVED FOR RELEASE: 2007/02/08: CIA-RDP82-00850R000300080046-0

APPROVED FOR RELEASE: 2007/02/08: CIA-RDP82-00850R000300080046-0

initial differential problem. It was found that at the lateral boundaries in the transfer stage it is necessary to stipulate the velocity, temperature and geopotential values for the lower level only at the inflow points, and in the adaptation stage -- geopotential or the normal velocity component at each point of the lateral boundary.

In [2] the system of primitive equations was written in a stereographic projection. The vertical coordinate is pressure. The problem is solved by the splitting method [5]. The evolutionary equations are first reduced to a skew-symmetric form. This facilitates the formulation of stable difference schemes which in an adiabatic approximation in the transfer stage retain the mean squares of the computed values, and in the adaptation stage -- a finite-difference analogue of total energy.

The problem is solved for two territories. The outer region is a square taking in the greater part of the northern hemisphere, at whose boundaries the conditions of absence of flows are stipulated. The inner region is a rectangle on a map in a stereographic projection with sides parallel to the sides of the square. The extent of the inner region is 4800 x 7200 km. The interval in horizontal coordinates is half as great as for the larger territory. Values obtained in the course of a "hemisphere" forecast are used at the boundaries.

In this article the proofs are presented with use of the energy method. In [2] this method (with some assumptions) was used in demonstrating the stability of the finite-difference scheme for the large territory in the sense of conservation (or nonincrease in the presence of turbulent terms) of a quadratic functional -- the difference analogue of energy. Assume that the problem for the inner region is solved using the same scheme and in this same grid. We will select the lateral boundary conditions in such a way that the solutions of both problems within the small region coincide. This ensures the stability and uniqueness of solution of the regional model. The advantage of the constructed boundary conditions is a method for taking into account the time-dependent values of the meteorological elements at the boundaries of the region which is rather simple from the point of view of computational procedures.

Now we will examine a system of equations in the stage of transfer in horizontal coordinates. Taking into account the parameterization of horizontal turbulence used at the present time [3], the system assumes the form

$$\varphi_t + \frac{1}{2} m^2 u \varphi_x + \frac{1}{2}(m^2 u \varphi)_x + \frac{1}{2} m^2 v \varphi_y + \frac{1}{2}(m^2 v \varphi)_y = F_\varphi,$$

$$F_\varphi = \frac{\partial}{\partial x} K \frac{\partial \varphi}{\partial x} + \frac{\partial}{\partial y} K \frac{\partial \varphi}{\partial y},$$

$$K = a h^2 D,$$

$$a = \text{const} > 0,$$

$$D = |u_x + v_y|.$$

APPROVED FOR RELEASE: 2007/02/08: CIA-RDP82-00850R000300080046-0

APPROVED FOR RELEASE: 2007/02/08: CIA-RDP82-00850R000300080046-0

Here $$\varphi = \left| u, v, \frac{T}{m} \right|,$$

T is temperature, u, v are the velocity components, m is a cartographic factor, h is the horizontal grid interval.

It is possible to limit ourselves to the first fractional interval -- transfer along x:

$$\varphi_t + \frac{1}{2} m^2 u \varphi_x + \frac{1}{2} (m^2 u \varphi)_x = \frac{\partial}{\partial x} K \frac{\partial \varphi}{\partial x}.$$

As the difference approximation we use the scheme

$$\frac{\varphi_i^{n+1} - \varphi_i^n}{\Delta t} + \frac{1}{2h}[(m^2u)^n_{i+1/2} \varphi^{n+1/2}_{i+1} - (m^2u)^n_{i-1/2} \varphi^{n+1/2}_{i-1}] = \tag{1}$$

$$= \frac{1}{h^2}[(K^n_{i-1/2} \varphi^{n+1/2}_{i-1} - (K^n_{i-1/2} + K^n_{i+1/2}) \varphi^{n+1/2}_i + K^n_{i+1/2} \varphi^{n+1/2}_{i+1}]; \; i = 1, \ldots, N,$$

where n is the time index, i is an index along x (as a simplification the remaining indices are omitted), Δ t is a time interval.

The sought-for boundary conditions are the least complete conditions ensuring the coincidence in the time interval of n+1 solutions of two discrete problems in the region of telescoping on the assumption that in the preceding n interval these solutions coincided. Assume that $\tilde{\varphi}$ is the solution of the problem for a large territory within the region of telescoping, φ is the solution of the problem for the inner region and $\varphi' = \tilde{\varphi} - \varphi$. Taking into account that $\tilde{\varphi}^n = \varphi^n$ the difference of equations (1) for these two problems assumes the form

$$\frac{\varphi'^{n+1}}{\Delta t} + \frac{1}{4h}(\alpha_{i+1/2} \varphi'^{n+1}_{i+1} - \alpha_{i-1/2} \varphi'^{n+1}_{i-1}) =$$

$$= \frac{1}{2h^2}[\beta_{i-1/2} \varphi'^{n+1}_{i-1} - (\beta_{i-1/2} + \beta_{i+1/2}) \varphi'^{n+1}_i + \beta_{i+1/2} \varphi'^{n+1}_{i+1}].$$

Here $\alpha_i = (m^2u)^n_i$, $\beta_i = K^n_i$. After multiplying the i-th equation of the system by φ_i^{n+1} we obtain

$$\varphi_i'^2 + \frac{\Delta t}{4h}(\alpha_{i+1/2} \varphi'_i \varphi'_{i+1} - \alpha_{i-1/2} \varphi'_{i-1} \varphi'_i) +$$

$$+ \frac{\Delta t}{2h^2}[(\beta_{i-1/2} + \beta_{i+1/2}) \varphi_i'^2 - \beta_{i-1/2} \varphi_{i-1} \varphi'_i - \beta_{i+1/2} \varphi'_i \varphi'_{i+1}] = 0. \tag{2}$$

Here and in the text which follows the time indices have been omitted. The summation of (2) for i gives

$$\sum_{i=1}^{N} \varphi_i'^2 + \frac{\Delta t}{4h}(\alpha_{N+1/2} \varphi'_N \varphi'_{N+1} - \alpha_{1/2} \varphi'_0 \varphi'_1) +$$

$$+ \frac{\Delta t}{2h^2}\left[\sum_{i=1}^{N} (\beta_{i-1/2} + \beta_{i+1/2}) \varphi_i'^2 - \sum_{i=1}^{N} \beta_{i-1/2} \varphi'_{i-1} \varphi'_i - \sum_{i=1}^{N} \beta_{i+1/2} \varphi'_i \varphi'_{i+1}\right] = 0.$$

We will transform the terms in the brackets:

APPROVED FOR RELEASE: 2007/02/08: CIA-RDP82-00850R000300080046-0

APPROVED FOR RELEASE: 2007/02/08: CIA-RDP82-00850R000300080046-0

$$\sum_{i=1}^{N}(\beta_{i-1/2}+\beta_{i+1/2})\varphi_i'^2-\sum_{i=1}^{N}\beta_{i-1/2}\varphi'_{i-1}\varphi'_i-\sum_{i=1}^{N}\beta_{i+1/2}\varphi'_i\varphi'_{i+1}=$$

$$=\sum_{i=1}^{N}\beta_{i-1/2}\varphi_i'^2-\beta_{1/2}\varphi'_0\varphi'_1+\beta_{N+1/2}\varphi'_N\varphi'_{N+1}+\sum_{i=1}^{N}\beta_{i+1/2}(\varphi_i'^2-2\varphi'_i\varphi'_{i+1})=$$

$$=\sum_{i=1}^{N}\beta_{i-1/2}\varphi_i'^2-\sum_{i=1}^{N}\beta_{i+1/2}\varphi_{i+1}'^2-\beta_{1/2}\varphi'_0\varphi'_1+\beta_{N+1/2}\varphi'_N\varphi'_{N+1}+$$

$$+\sum_{i=1}^{N}\beta_{i+1/2}(\varphi'_i-\varphi'_{i+1})^2=\sum_{i=1}^{N}\beta_{i+1/2}(\varphi'_i-\varphi'_{i+1})^2+\beta_{1/2}\varphi_1'^2-\beta_{N+1/2}\varphi_{N+1}'^2-$$

$$-\beta_{1/2}\varphi'_0\varphi'_1+\beta_{N+1/2}\varphi'_N\varphi'_{N+1}.$$

Finally we obtain

$$\sum_{i=1}^{N}\varphi_i'^2+\frac{\Delta t}{2h^2}\left[\beta_{1/2}\varphi_1'^2+\sum_{i=1}^{N}\beta_{i+1/2}(\varphi'_i-\varphi'_{i+1})^2\right]+$$

$$+\frac{\Delta t}{4h}(\alpha_{N+1/2}\varphi'_N\varphi'_{N+1}-\alpha_{1/2}\varphi'_0\varphi'_1)-$$

$$-\frac{\Delta t}{2h^2}(\beta_{1/2}\varphi'_0\varphi'_1-\beta_{N+1/2}\varphi'_N\varphi'_{N+1}+\beta_{N+1/2}\varphi_{N+1}'^2)=0.$$

With $\varphi'_0=\varphi'_{N+1}=0$ we have

$$\sum_{i=1}^{N}\varphi_i'^2+\frac{\Delta t}{2h^2}\left[\beta_{1/2}\varphi_1'^2+\sum_{i=1}^{N}\beta_{i+1/2}(\varphi'_i-\varphi'_{i+1})^2\right]=0.$$

Hence, because β is positive, it follows that $\varphi'=0$. Thus, the stipulation of boundary conditions in the form $\varphi_0=\tilde{\varphi}_0$ and $\varphi_{N+1}=\tilde{\varphi}_{N+1}$ ensures coincidence of the solution of the discrete problem for the inner region and the solution of the discrete problem for the large territory within the limits of this region in the stage of transfer along x. Transfer along y is examined in exactly the same way.

The following system of equations [2] is solved in the adaptation stage:

$$\begin{aligned}&\frac{u^{n+1}-u^n}{\Delta t}+fv^{n+1/2}=-\Phi_x^{n+1/2},\\&\frac{v^{n+1}-v^n}{\Delta t}-fu^{n+1/2}=-\Phi_y^{n+1/2},\\&\frac{T^{n+1}-T^n}{\Delta t}-\frac{R}{p^{\circ}}T^{n+1/2}=0,\end{aligned}\qquad(3)$$

APPROVED FOR RELEASE: 2007/02/08: CIA-RDP82-00850R000300080046-0

APPROVED FOR RELEASE: 2007/02/08: CIA-RDP82-00850R000300080046-0

$$T^{n+1} = -\frac{p}{R}\Phi_p^{n+1},$$

$$\tau_p^{n+1} + m^2(u_\tau^{n+1} + v_y^{n+1}) = 0, \tag{3}$$

where Φ is geopotential, f is the Coriolis parameter, p is pressure, $\tau^2 = \frac{g}{(\gamma_a - \bar{\gamma})\bar{T}}$.

Again we will examine two problems: the problem for the large territory and the problem for the inner region. The system is linear and therefore it can be assumed that it was written in deviations and its solution is identically equal to zero. Assuming the solutions of the two problems in the n-th interval to coicide, and applying the method of biorthogonalization for the vertical coordinate [5], system (3) can be reduced to the form

$$\left(\lambda + \left(\frac{\Delta t}{2}\right)^2 \Lambda_1 + \frac{\Delta t}{2}\Lambda_2\right)\varphi = 0. \tag{4}$$

Here $\lambda = \frac{2h^2}{m^2}\mu$, $\mu > 0$ are the eigenvalues of the vertical operator, φ are the Fourier coefficients in the expansion of Φ in the eigenfunctions of the vertical operator,

$$(\Lambda_1\varphi)_{j,i} = (f\gamma)_{j+1/2,\,i+1/2}(\varphi_{j+1,\,i} - \varphi_{j,\,i+1}) + (f\gamma)_{j-1/2,\,i+1/2}(\varphi_{j,\,i+1} - \varphi_{j-1,\,i}) -$$
$$- (f\gamma)_{j+1/2,\,i-1/2}(\varphi_{j+1,\,i} - \varphi_{j,\,i-1}) - (f\gamma)_{j-1/2,\,i-1/2}(\varphi_{j,\,i-1} - \varphi_{j-1,\,i}),$$
$$(\Lambda_2)\varphi_{j,i} = (\gamma_{j+1/2,\,i+1/2} + \gamma_{j-1/2,\,i+1/2} + \gamma_{j+1/2,\,i-1/2} + \gamma_{j-1/2,\,i-1/2})\varphi_{j,i} -$$
$$- \gamma_{j+1/2,\,i+1/2}\varphi_{j+1,\,i+1} - \gamma_{j-1/2,\,i+1/2}\varphi_{j-1,\,i+1} -$$
$$- \gamma_{j+1/2,\,i-1/2}\gamma_{j+1,\,i-1} - \gamma_{j-1/2,\,i-1/2}\varphi_{j-1,\,i-1},$$
$$\gamma = |1 + (f\Delta t/2)^2|^{-1},\ i = 1, \ldots, N;\ j = 1, \ldots, M.$$

This approximation was obtained taking into account [2] that the u, v values were determined at the centers of the squares in the main grid for φ. Scalarly we multiply (4) by φ.

$$(\Lambda_1\varphi, \varphi) = \sum_{i=1}^{\Lambda}[(f\gamma)_{M+1/2,\,i+1/2} - (f\gamma)_{M+1/2,\,i-1/2}]\varphi_{M,i}\varphi_{M+1,i} -$$

$$- \sum_{i=1}^{N}[(f\gamma)_{1/2,\,i+1/2} - (f\gamma)_{1/2,\,i-1/2}]\varphi_{0,i}\varphi_{1,i} + \sum_{j=1}^{M}[(f\gamma)_{j+1/2,\,1/2} -$$

$$-(f\gamma)_{j-1/2,\,1/2}]\varphi_{j,0}\varphi_{j,1} - \sum_{j=1}^{M}[(f\gamma)_{j+1/2,\,N+1/2} - (f\gamma)_{j-1/2,\,N+1/2}]\varphi_{j,N}\varphi_{j,N+1},$$

$$(\Lambda_2\varphi, \varphi) = \sum_{j=1}^{M-1}\sum_{i=1}^{N-1}\gamma_{j+1/2,\,i+1/2}(\varphi_{j+1,\,i+1} - \varphi_{j,\,i})^2 +$$

APPROVED FOR RELEASE: 2007/02/08: CIA-RDP82-00850R000300080046-0

APPROVED FOR RELEASE: 2007/02/08: CIA-RDP82-00850R000300080046-0

$$+\sum_{j=2}^{M}\sum_{i=1}^{N-1}\gamma_{j-1/2,\,i+1/2}(\varphi_{j,i}-\varphi_{j-1,\,i+1})^2+\sum_{i=1}^{N}(\gamma_{1/2,\,i-1/2}+\gamma_{1/2,\,i+1/2})\varphi_{1,i}^2+$$

$$+\sum_{i=1}^{N}(\gamma_{M+1/2,\,i-1/2}+\gamma_{M+1/2,\,i+1/2})\varphi_{M,\,i}^2+\sum_{j=2}^{M-1}(\gamma_{j-1/2,\,1/2}+\gamma_{j+1/2,\,1/2})\varphi_{j,\,1}^2+$$

$$+\sum_{j=2}^{M-1}(\gamma_{j-1/2,\,N+1/2}+\gamma_{j-1/2,\,N+1/2})\varphi_{j,\,N}^2-\sum_{i=1}^{N}\gamma_{M+1/2,\,i+1/2}\,\varphi_{M+1,\,i+1}\,\varphi_{M,\,i}-$$

$$-\sum_{j=2}^{M-1}\gamma_{j+1/2,\,N+1/2}\,\varphi_{j+1,\,N+1}\,\varphi_{j,\,N}-\sum_{i=1}^{N}\gamma_{1/2,\,i-1/2}\,\varphi_{0,\,i-1}\,\varphi_{1,\,i}-$$

$$-\sum_{j=2}^{M-1}\gamma_{j-1/2,\,1/2}\,\varphi_{j-1,\,0}\,\varphi_{j,\,1}-\sum_{i=1}^{N}\gamma_{1/2,\,i+1/2}\,\varphi_{0,\,i+1}\,\varphi_{1,\,i}-$$

$$-\sum_{j=2}^{M-1}\gamma_{j-1/2,\,N+1/2}\,\varphi_{j-1,\,N+1}\,\varphi_{j,\,N}-\sum_{i=1}^{N}\gamma_{M+1/2,\,i-1/2}\,\varphi_{M+1,\,i-1}\,\varphi_{M,\,i}-$$

$$-\sum_{j=2}^{M-1}\gamma_{j+1/2,\,1/2}\,\varphi_{j+1,\,0}\,\varphi_{j,\,1}.$$

Stipulation of $\varphi_{j,0}=\varphi_{j,\,A+1}=\varphi_{0,i}=\varphi_{M+1,\,i}=0$ at the boundaries, which corresponds to the boundary conditions $\tilde{\Phi}=\bar{\Phi}$, leads to the equality

$$\left(\left(\lambda+\left(\frac{\Delta t}{2}\right)^2\Lambda_1+\left(\frac{\Delta t}{2}\right)\Lambda_2\right)\varphi_1,\,\varphi\right)=\lambda\sum_{j=1}^{M}\sum_{i=1}^{N}\varphi_{j,\,i}^2+$$

$$+\frac{\Delta t}{2}\left[\sum_{j=1}^{M-1}\sum_{i=1}^{N-1}\gamma_{j+1/2,\,i+1/2}(\varphi_{j+1,\,i+1}-\varphi_{j,\,i})^2+\right.$$

$$+\sum_{j=2}^{M}\sum_{i=1}^{N-1}\gamma_{j-1/2,\,i+1/2}(\varphi_{j,\,i}-\varphi_{j-1,\,i+1})^2+\sum_{i=1}^{N}(\gamma_{1/2,\,i-1/2}+\gamma_{1/2,\,i+1/2})\varphi_{1,\,i}^2+$$

$$+\sum_{i=1}^{N}(\gamma_{M+1/2,\,i-1/2}+\gamma_{M+1/2,\,i+1/2})\varphi_{M,\,i}^2+\sum_{j=2}^{M-1}(\gamma_{j-1/2,\,1/2}+\gamma_{j+1/2,\,1/2})\varphi_{j,\,1}^2+$$

APPROVED FOR RELEASE: 2007/02/08: CIA-RDP82-00850R000300080046-0

APPROVED FOR RELEASE: 2007/02/08: CIA-RDP82-00850R000300080046-0

$$+\sum_{j=2}^{M-1}(\gamma_{j-1/2,\,N+1/2}+\gamma_{j+1/2,\,N+1/2})\,\varphi^2_{j,\,N}\Big]=0.$$

It follows from this equation, since the squared coefficients are positive, that $\varphi \equiv 0$.

Table 2

Evaluation of Forecast With Constant Boundary Conditions (1) and Telescoping Problem (2)

Level, mb	1		2	
	ε	r	ε	r
1000	0.70	0.67	0.61	0.79
500	0.67	0.71	0.68	0.71
200	0.87	0.52	0.83	0.64

Thus, in the adaptation stage the stipulation of the geopotential values at the boundaries from the problem for the large territory ensures a coincidence of the solutions of this problem and the problem for the inner region in a discrete case.

We note that in the proofs cited above it is assumed that the computations for both territories are made in coinciding grids. In actuality, the forecast for the inner region is computed with lesser intervals. Accordingly, the boundary values are obtained from the hemisphere forecast by means of interpolation in time and horizontal coordinates with some error. But if the scheme is convergent (unfortunately, convergence cannot be demonstrated for nonlinear problems), applying interpolation formulas with an order of magnitude not less than the order of magnitude of approximation of the difference scheme we obtain a coincidence of the solutions with a corresponding accuracy.

In conclusion, in Table 2 we give the results of one of the preliminary computations. In the first forecast we used boundary conditions constant in time; in the second forecast the telescoping problem was solved. Both variants were computed with intervals Δt = 30 min and h = 300 km and with very simple parameterization of horizontal turbulence

$$\varphi_t + \ldots = K\Delta\varphi,\ K = 5_{10}5\ \ m^2/sec.$$

The estimates show that the use of telescoping made possible a considerable improvement in the forecast at the lower and upper levels.

BIBLIOGRAPHY

1. Kadyshnikov, V. M., "Boundary Conditions in the Short-Range Weather Forecasting Problem Using a Baroclinic Atmospheric Model," IZV. AN SSSR, FIZIKA ATMOSFERY I OKEANA (News of the USSR Academy of Sciences, Physics of the Atmosphere and Ocean), Vol 9, No 1, 1973.

APPROVED FOR RELEASE: 2007/02/08: CIA-RDP82-00850R000300080046-0

APPROVED FOR RELEASE: 2007/02/08: CIA-RDP82-00850R000300080046-0

2. Kalenkovich, Ye. Ye., Novikova, N. V., Cholakh, I. V., "The Forecasting Problem for the Northern Hemisphere and a Region," TRUDY ZapSibRNIGMI (Transactions of the West Siberian Regional Scientific Research Hydrometeorological Institute), No 41, 1978.

3. Kalenkovich, Ye. Ye., Novikova, N. V., Cholakh, I. V., "Some Methods for the Parameterization of Subgrid Processes," METEOROLOGIYA I GIDROLOGIYA (Meteorology and Hydrology), in press.

4. Kalenkovich, Ye. Ye., Cholakh, I. V., "Formulation of Boundary Conditions in Computing a Forecast for Nested Territories With Use of the Splitting Method," TRUDY ZapSibRNIGMI, No 41, 1978.

5. Marchuk, G. I., CHISLENNYYE METODY V PROGNOZE POGODY (Numerical Methods in Weather Forecasting), Leningrad, Gidrometeoizdat, 1967.

6. Bennett, A. F., "Open Boundary Conditions for Dispersive Waves," J. ATMOS. SCI., Vol 33, No 2, 1976.

7. Chen, J. H., Miyakoda, K. A., "Nested Grid Computation for the Barotropic Free Atmosphere," MON. WEATHER REV., Vol 102, No 2, 1974.

8. Cooley, D. S., THE LIMITED-AREA FINE MESH MODEL, U. S. Dep. Commer. Nat. Ocean. and Atmos. Admin. Nat Weather Serv. Techn. Proced. Bull., No 232, 1978.

9. Davies, H. C., "A Lateral Boundary Formulation for Multilevel Prediction Models," QUART. J. ROY. METEOROL. SOC., Vol 102, No 432, 1976.

10. Enquist, B., Majda, A., "Absorbing Boundary Conditions for the Numerical Simulation of Waves," MATH. COMP., Vol 31, No 139, 1977.

11. Gaunlett, D. J., Leslie, L. M., McGregor, J. L., Hincksman, D. R., "Recent Results from the ANMRC Limited Area Nested Model," ANN. METEOROL. NEUE FOLGE, No 11, 1976.

12. Hill, G. E., "Grid Telescoping in Numerical Weather Prediction," J. APPL. METEOROL., Vol 7, No 1, 1968.

13. Perkey, D. J., Kreitzberg, C. W., "A Time-Dependent Boundary Scheme for Limited-Area Primitive Equation Models," MON. WEATHER REV., Vol 104, No 6, 1976.

APPROVED FOR RELEASE: 2007/02/08: CIA-RDP82-00850R000300080046-0

APPROVED FOR RELEASE: 2007/02/08: CIA-RDP82-00850R000300080046-0

UDC 551.509.313

VARIATIONAL PRINCIPLE AND SPLITTING METHOD

Moscow METEOROLOGIYA I GIDROLOGIYA in Russian No 10, Oct 80 pp 13-24

[Article by Doctor of Physical and Mathematical Sciences V. V. Penenko, Computation Center Siberian Department USSR Academy of Sciences, manuscript submitted 20 Mar 80]

[Text]

Abstract: The article describes a method for constructing splitting schemes for solving multidimensional problems on the basis of the variational principle. The splitting schemes are obtained from the conditions of stationarity of a summator functional formed in a special way by the method of weak approximation with fractional time intervals. The best qualities of both are manifested in the combination of the splitting method with the variational principle. The splitting method leads to computation algorithms which are economical and simple in application and the variational principle guarantees their stability and ensures matching of all stages in solution of the problem.

The splitting method is now used rather frequently in practical work for solving multidimensional problems in mathematical physics [2,4,8,9]. It has a great many good qualities and in particular it affords a possibility for development of stable numerical schemes which are economical and simple in application. Such a possibility follows from the very essence of the splitting method, whose basic idea is that solution of a complex problem is reduced to solution of a set of simpler problems. In formulating discrete models this method can be conveniently examined from two points of view: as a method for the splitting of "physical processes," by means of which the initial model, describing a complex physical system, is represented in a quite small time interval in the form of a set of simpler models, each of which describes one or more aspects of the studied process; and as a method for the splitting of "space variables," making it possible to reduce the solution of the multidimensional problem to subsequent solution of problems of a lesser dimensionality.

APPROVED FOR RELEASE: 2007/02/08: CIA-RDP82-00850R000300080046-0

APPROVED FOR RELEASE: 2007/02/08: CIA-RDP82-00850R000300080046-0

The structure of computation algorithms based on these principles is very convenient for solving problems in the mathematical modeling of physical processes in such complex systems as the atmosphere and ocean. In the splitting method the problems of atmospheric dynamics can be regarded as one of the stages in a more complex model of a climatic system consisting of the atmosphere, ocean, continents and biosphere. The splitting method naturally is also consistent with the modular principle for the formulation of computation algorithms and complexes of programs for the application of the models on computers.

The article describes a method for the formulation of discrete models on the basis of the variational principle in combination with the splitting method. With respect to its content it must be regarded as a continuation of [6], which describes a method for constructing energetically balanced approximations by means of an integral identity, and as a component part of studies [5, 7], which set forth the use of the methods of the theory of perturbations and optimization in problems of dynamics of the atmosphere and ocean. In this case the splitting schemes are obtained from the conditions of stationarity of a summator functional, formed in a special way by the weak approximation method with fractional time intervals. This functional and the splitting schemes generated by it constitute the constructive basis for numerical methods for investigating sensitivity and identification of models of hydrothermodynamics of the atmosphere and ocean [5, 7]. A variational interpretation of the splitting method makes it a very convenient means in solving optimization problems in models described by multidimensional differential equations in partial derivatives.

The proposed method is quite universal and therefore in order to make the following exposition more specific all the constructions will be presented using the same example of a model of atmospheric dynamics in isobaric coordinates on a sphere as in [6]. In order to save space we will omit a description of the model in a differential formulation and represent it at once in the form of an integral identity (3.3) from [6]. Since the subject of our examination is the construction of time approximations, as a convenience we will rewrite this identity, first collecting together all the integrals in space variables and specially discriminating only time integration. Assume that $D = \{[S \times (p_T \leqslant p \leqslant p_a)]$; $S = [0 \leqslant \psi \leqslant 2\pi, 0 \leqslant \theta \leqslant \pi]\}$ is the region of change of the horizontal coordinates ψ, θ on a sphere and pressure p (ψ is longitude, θ is the complement to latitude, p_T, p_a are the pressures at the upper and lower boundaries of the air mass),

is the vector of state of the model, u, v, τ are the components of the velocity vector $\vec{u}$ in the directions ψ, θ, p respectively, T, H are the deviations of temperature and geopotential from the standard values,

is an arbitrary vector-function of the same structure as $\vec{\varphi}$, with adequately smooth components. We will determine the scalar product of the functions $\vec{\varphi}$ and $\vec{\varphi}^*$ in the following way:

$$(\vec{\varphi}, \vec{\varphi}^*) = \int_D (uu^* + vv^* + \varkappa TT^*)\, dD + \int_S \bar{p} HH^*|_{p=p_a}\, ds, \qquad (1)$$

APPROVED FOR RELEASE: 2007/02/08: CIA-RDP82-00850R000300080046-0

APPROVED FOR RELEASE: 2007/02/08: CIA-RDP82-00850R000300080046-0

where $\vec{\varphi} \in Q(D_t)$, $\vec{\varphi}^* \in Q^*(D_t)$, $D_t = D \times [0, \bar{t}]$, $dD = ds\,dt$,

$$ds = a^2 \sin\Theta\, d\Theta\, d\psi,$$

$\bar{\rho}$ is the standard density value, $\varkappa$ is a scale factor, $Q(D_t)$, $Q^*(D_t)$ are function spaces determined in D_t and the functional

$$A(\vec{\varphi}, \vec{\varphi}^*) = \int_D \Big\{ (\tilde{\Lambda} u, u^*) + (\tilde{\Lambda} v, v^*) + \varkappa(\tilde{\Lambda} T, T^*) + (\vec{u}^* \operatorname{grad} H - \vec{u} \operatorname{grad} H^*) + \tag{2}$$

$$+ \left(l + \frac{\operatorname{ctg}\Theta}{a} u\right)(uv^* - u^*v) + \frac{R}{p}\left(T\tau^* - \varkappa\frac{\gamma_a - \gamma}{g}\tau T^*\right) + \frac{\tilde{\varkappa}\varepsilon}{c_p} T^* +$$

$$+ \mu_1 [D_T(\vec{u}_s)\, D_T(\vec{u}_s^*) + D_s(\vec{u}_s)\, D_s(\vec{u}_s^*)] + \chi_1\left[\frac{\partial u}{\partial p}\frac{\partial u^*}{\partial p} + \frac{\partial v}{\partial p}\frac{\partial v^*}{\partial p}\right] +$$

$$+ \varkappa\left[\frac{\mu_2}{a^2}\left(\frac{1}{\sin^2\Theta}\frac{\partial T}{\partial\psi}\frac{\partial T^*}{\partial\psi} + \frac{\partial T}{\partial\Theta}\frac{\partial T^*}{\partial\Theta}\right) + \chi_2\frac{\partial T}{\partial p}\frac{\partial T^*}{\partial p}\right]\Big\} dD +$$

$$+ \int_S (u^*\tau_\psi + v^*\tau_\theta + \varkappa q_s T^*)|_{p=p_0}\, dS,$$

where

$$(\tilde{\Lambda}\varphi, \varphi) = \frac{1}{2}(\varphi^*\vec{u} \operatorname{grad}\varphi - \varphi\vec{u} \operatorname{grad}\vec{\varphi}^*),\ \vec{u}_s = (u, v),\ \vec{u}_s^* = (u^*, v^*),$$

$$\vec{u} = (u, v, \tau),\quad \vec{u}^* = (u^*, v^*, \tau^*),\quad \chi_i = \left(\frac{gp}{RT}\right)^2 \nu_i,\ \nu_i,\ \mu_i \quad (i=1, 2)$$

are coefficients of vertical and horizontal turbulent exchange, l is the Coriolis parameter, a is the earth's radius, R is the universal gas constant, c_p is the heat capacity of air at a constant pressure, $\tilde{\varepsilon}$ is the heat influx to a unit volume, g is the acceleration of free falling, γ_a is the adiabatic temperature gradient, γ is the vertical gradient of standard temperature, τ_ψ, τ_θ are functions characterizing the dynamic and q_s the thermal interaction of the atmosphere with the underlying surface.

With these notations taken into account, the identity (3.3) from [6] is written in the following way:

$$I(\vec{\varphi}, \vec{\varphi}^*) \equiv \int_0^{\bar{t}} \left\{ \frac{1}{2}\left[\left(\frac{\partial\vec{\varphi}}{\partial t}, \vec{\varphi}^*\right) - \left(\frac{\partial\vec{\varphi}^*}{\partial t}, \vec{\varphi}\right)\right] + \right. \tag{3}$$

$$\left. + A(\vec{\varphi}, \vec{\varphi}^*)\right\} dt + \frac{1}{2}(\vec{\varphi}, \vec{\varphi}^*)\Big|_0^{\bar{t}} = 0.$$

APPROVED FOR RELEASE: 2007/02/08: CIA-RDP82-00850R000300080046-0

APPROVED FOR RELEASE: 2007/02/08: CIA-RDP82-00850R000300080046-0

The sense of the notations (1) and (2) becomes clear if we compare (3) with (3.3) from [6]. The scalar product (1) gives an abbreviated writing of the integrals in space variables of expressions containing time derivatives and expressions obtained as a result of integration by parts and time integration and the functional $A(\vec{\varphi}, \vec{\varphi}^*)$ includes all the integrals for the regions D and S of the expressions not containing time derivatives. External sources and boundary conditions are also taken into account in this functional.

The methods for the discretization of the identity (3) in space variables have been described in considerable detail in [6]. Now we will consider the formulation of time approximations. Taking into account the property of additivity of the integrals, we will represent the functional $A(\vec{\varphi}, \vec{\varphi}^*)$ in the form of the sum

$$A(\vec{\varphi}, \vec{\varphi}^*) = \sum_{k=1}^{r} A_k(\vec{\varphi}, \vec{\varphi}^*), \quad (r \geqslant 1), \tag{4}$$

where r is the number of terms which can be discriminated from the functional $A(\vec{\varphi}, \vec{\varphi}^*)$ under the condition that the antisymmetric pairs of terms are not disrupted. Satisfaction of this condition guarantees energy balancing of the discrete approximations of the differential operators. It is evident that with such a restriction there is a great degree of freedom in selecting the representation (4). We will cite an example of determination of the functionals $A_k(\vec{\varphi}, \vec{\varphi}^*)$ in (4):

$$A_1(\vec{\varphi}, \vec{\varphi}^*) = \int_D \Big[(\Lambda_\varphi u, u^*) + (\Lambda_\varphi v, v^*) + \varkappa(\Lambda_\varphi T, T^*) + \frac{\operatorname{ctg}\Theta}{a} u\,(uv^* - u^*v)\Big]\,dD,$$

$$A_2(\vec{\varphi}, \vec{\varphi}^*) = \int_D |(\Lambda_\Theta u, u^*) + (\Lambda_\Theta v, v^*) + \varkappa(\Lambda_\Theta T, T^*)|\,dD,$$

$$A_3(\vec{\varphi}, \vec{\varphi}^*) = \int_D |(\Lambda_p u, u^*) + (\Lambda_p v, v^*) + \varkappa(\Lambda_p T, T^*)|\,dD,$$

$$A_4(\vec{\varphi}, \vec{\varphi}^*) = \int_D \Big\{ \mu_1 [D_T(\vec{u}_s) D_T(\vec{u}_s^*) + D_s(\vec{u}_s) D_s(\vec{u}_s^*)] + \frac{\varkappa\mu_2}{a^2 \sin^2\Theta}\left[\frac{\partial T}{\partial \psi}\frac{\partial T^*}{\partial \psi} + \frac{1}{a^2}\frac{\partial T}{\partial \Theta}\frac{\partial T^*}{\partial \Theta}\right]\Big\}\,dD,$$

$$A_5(\vec{\varphi}, \vec{\varphi}^*) = \int_D \left[\lambda_1\left(\frac{\partial u}{\partial p}\frac{\partial u^*}{\partial p} + \frac{\partial v}{\partial p}\frac{\partial v^*}{\partial p}\right) + \varkappa\chi_2\frac{\partial T}{\partial p}\frac{\partial T^*}{\partial p}\right] dD + \int_S (u^*\tau_\psi + v^*\tau_\Theta + \varkappa q_s T^*)\,|_{p=p_0}\,dS,$$

$$A_6(\vec{\varphi}, \vec{\varphi}^*) = \int_D \Big\{ (\vec{u}^* \operatorname{grad} H - \vec{u} \operatorname{grad} H^*) + l(u^*v - uv^*) + \frac{R}{p}\Big(T\tau^* - \varkappa\frac{(\gamma_a - \gamma)\overline{T}}{g}\tau T^*\Big) - \frac{\widetilde{\varkappa\varepsilon}}{cp} T^*\Big\}\,dD, \tag{5}$$

where

$$(\widetilde{\Lambda}\varphi, \varphi^*) \equiv (\Lambda_\psi\varphi, \varphi^*) + (\Lambda_\Theta\varphi, \varphi^*) + (\Lambda_p\varphi, \varphi^*),$$

$$(\Lambda_\psi\varphi, \varphi^*) = \frac{1}{2a\sin\Theta}\left(\varphi^* u\frac{\partial\varphi}{\partial\psi} - \varphi u\frac{\partial\varphi^*}{\partial\psi}\right),$$

APPROVED FOR RELEASE: 2007/02/08: CIA-RDP82-00850R000300080046-0

APPROVED FOR RELEASE: 2007/02/08: CIA-RDP82-00850R000300080046-0

$$(\Lambda_\theta \varphi, \varphi^*) = \frac{1}{2a}\left(\varphi^* v \frac{\partial \varphi}{\partial \theta} - \varphi v \frac{\partial \varphi^*}{\partial \theta}\right),$$

$$(\Lambda_p \varphi, \varphi^*) = \frac{1}{2}\left(\varphi^* \omega \frac{\partial \varphi}{\partial p} - \varphi \omega \frac{\partial \varphi^*}{\partial p}\right).$$

The example of the breakdown of the functional was selected in such a way that it was possible to make an analogy with the splitting scheme [2] usually used in numerical weather forecasting models. This scheme is formulated in accordance with the ideas of the splitting method for physical processes and in each time interval $t_j \leqslant t \leqslant t_{j+1}$ consists of the following three stages:

1) Transfer of meteorological substances along trajectories

$$\begin{aligned} &\frac{\partial u_1}{\partial t} + \Lambda u_1 + \frac{\operatorname{ctg}\theta}{a} u^j v_1 = 0, \\ &\frac{\partial v_1}{\partial t} + \Lambda v_1 - \frac{\operatorname{ctg}\theta}{a} u^j u_1 = 0, \\ &\frac{\partial T_1}{\partial t} + \Lambda T_2 = 0, \end{aligned} \tag{6a}$$

where the operator $\Delta\varphi$ ($\varphi = u_1, v_1, T_1$) is determined by one of the expressions

$$\Lambda\varphi = \begin{cases} \vec{u}\operatorname{grad}\varphi - & \text{gradient form,} \\ \operatorname{div}\varphi\vec{u} - & \text{divergent form,} \\ \frac{1}{2}(\vec{u}\operatorname{grad}\varphi + \operatorname{div}\varphi\vec{u}) - & \text{antisymmetric form.} \end{cases} \tag{6b}$$

The problem (6) is solved with the following initial conditions:

$$\vec{\Phi}_1(t_j) = \vec{\Phi}^j, \ \vec{\Phi}_1 = (u_1, v_1, T_1), \ \vec{\Phi}^j = (u^j, v^j, T^j). \tag{6c}$$

The components of the $\vec{\Phi}^j$ vector coincide with the components u^j, v^j, T^j of the vector of state of the $\vec{\varphi}$ system at the time $t = t_j$.

2) Turbulent exchange

$$\begin{aligned} &\frac{\partial u_2}{\partial t} - F_u = 0, \\ &\frac{\partial v_2}{\partial t} - F_v = 0, \\ &\frac{\partial T_2}{\partial t} - F_T = 0, \end{aligned} \tag{7a}$$

where F_α ($\alpha = u, v, T$) are turbulent exchange operators with the initial conditions

APPROVED FOR RELEASE: 2007/02/08: CIA-RDP82-00850R000300080046-0

APPROVED FOR RELEASE: 2007/02/08: CIA-RDP82-00850R000300080046-0

$$\vec{\Phi}_2(t_j) = \vec{\Phi}_1(t_{j+1}),\ \vec{\Phi}_2 = (u_2,\ v_2,\ T_2). \tag{7b}$$

3) Dynamic assimilation of fields

$$\begin{gathered}\frac{\partial u_3}{\partial t} + lv_3 + \frac{1}{a\sin\theta}\frac{\partial H_3}{\partial\theta} = 0,\\ \frac{\partial v_3}{\partial t} - lu_3 + \frac{1}{a}\frac{\partial H_3}{\partial\theta} = 0,\\ \frac{\partial T_3}{\partial t} - \frac{R(\tau_a-\gamma)\overline{T}}{gp}\tau_3 - \frac{\tilde{\varepsilon}}{c_p} = 0,\\ \operatorname{div}\vec{U}_3 = 0,\quad \vec{U}_3 = (u_3,\ v_3,\ \tau_3),\\ \frac{\partial H_3}{\partial t} + \frac{RT_3}{p} = 0\end{gathered} \tag{8a}$$

with the initial conditions

$$\vec{\Phi}_3(t_j) = \vec{\Phi}_2(t_{j+1}),\ \vec{\Phi}_3 = (u_3,\ v_3,\ T_3). \tag{8b}$$

The boundary-value conditions with $p = p_a$ and $p = p_T$, as a result of the method which we selected for discretization of the model in space variables using an integral identity, are taken into account by coefficients and the right-hand sides of the corresponding difference analogues of the problem (6)-(8). Judging from the names of the stages, they can be given a definite physical sense, but the functions $\vec{\Phi}_1$ and $\vec{\Phi}_2$ in (6)-(8) do not have physical sense and are intermediate results of the computations. Physical sense can be given only to the function $\varphi_3 = (u_3, v_3, T_3, \tau_3, H_3)$, assuming that at the time $t = t_{j+1}$ its value is equal to the value of the vector of state, that is, $\vec{\varphi}_3(t_{j+1}) = \vec{\varphi}^{j+1}$. Splitting of the problem into three stages is not mandatory. For example, the problems of transfer of substances and turbulent exchange can be combined into one. For solution of each of the problems (6)-(8) in turn it is possible to use splitting of space variables. Then the number of elementary splitting intervals will be considerably greater.

In the splitting of the functional (2), given by formulas (5), the first three functionals correspond to the problem (6), the fourth and fifth -- to the problem (7), and the sixth -- to the problem (8). The balance properties of each of the functionals $A_k(\vec{\varphi}, \vec{\varphi}^*)$ $(k = \overline{1,6})$ with the substitution $\vec{\varphi}^* = \vec{\varphi}$ are checked directly.

In order to be specific, we will examine construction of discrete splitting schemes equivalent in accuracy to the Crank-Nicholson schemes. The simplest case of representation of (4) is obtained with $r = 1$, which corresponds to a family of two-layer time schemes having the property of energy balancing. These are implicit schemes and energy balancing guarantees their stability independently of dimensionality of the problem. However, in order to find solutions in each time interval in two-layer schemes one cannot avoid iteration processes. The problems

APPROVED FOR RELEASE: 2007/02/08: CIA-RDP82-00850R000300080046-0

APPROVED FOR RELEASE: 2007/02/08: CIA-RDP82-00850R000300080046-0

arising in this case, related to investigation of convergence and algorithmic realization of the iterations, are not attributable to the physical formulation of the problem, but the approach to its solution.

We will examine the case $r \geqslant 2$. We introduce into D_t the grid region $D_t^h = D^h \times \omega_t^h$, where D^h is the grid in the region D and $\omega_t^h = \{t_j, (j = \overline{0, J+1}, t_0 = 0; t_{j+1} = t_j + \Delta t_j; t_{J+1}$ is the time grid, which as a convenience will also be made uniform. In the grid ω_t^h we determine the components of the vector of state, representing solution of the problem. Together with ω_t^h we introduce a grid with fractional intervals. For this purpose each interval $[t_j, t_{j+1}]$ of the length Δt is broken down into 2r equal subintervals of the length $\Delta t/2r$ which we will call fractional intervals. The grid constructed in this way will be denoted ω_t^{2r}, that is

$$\omega_t^{2r} = \left\{ t_{j+\frac{k}{2r}} \quad (j = \overline{0, J},\ k = \overline{0, 2r}),\ t_0 = 0,\ t_{J+1} = T \right\}. \tag{9}$$

It is evident that ω_t^h is embedded in ω_t^{2r} and the points of intersection of the grid ω_t^{2r} with the whole-number indices coincide with the ω_t^h points of intersection. Thus, each interval $[t_j, t_{j+1}]$ has its own local system for the reading of fractional intervals and the number of the fractional interval determines the numerator of the fraction $k/2r$, $k = \overline{1, 2r-1}$. Such a structure of the time grids is in common use in splitting schemes [4, 9]. We will predetermine the spaces of the grid functions $Q^h(D_t^h)$ and $Q^{*h}(D_t^h)$ by the vectors $\vec{\varphi}^{j+k/2r}$ and $\vec{\varphi}^{*j+k/2r}$ ($j = \overline{0, J}$, $k = \overline{1, 2r-1}$) at the times

$$t = t_j + \frac{k\Delta t}{2r} \quad (j = \overline{0, J},\ k = \overline{1, 2r-1})$$

We also need the values of the grid functions at the points

$$t = t_j + \frac{(2k-1)\Delta t}{4r} \quad (j = \overline{0, J},\ k = \overline{1, 2r}),$$

and in order not to expand the spaces $Q^h(D_t)$ and $Q^{*h}(D_t^h)$ still more, we will determine these functions in the following way:

$$\vec{\gamma}_l^{\,j+\frac{2k-1}{4r}} = \frac{1}{2}\left(\vec{\gamma}_l^{\,j+\frac{k-1}{2r}} + \vec{\gamma}_l^{\,j+\frac{k}{2r}}\right), \tag{10}$$

$$\vec{\gamma}_l = \vec{\varphi}, \vec{\varphi}^* \quad (j = \overline{0, J},\ k = \overline{1, 2r}).$$

Taking into account the representation of (4) and the determination of the grid region (9), we will represent the integral in the identity (3) in the form of the sum

$$\sum_{j=0}^{J}\left\{\frac{1}{2}\sum_{k=1}^{2r}\left[\int_{t_j+\frac{(k-1)\Delta t}{2r}}^{t_j+\frac{k\Delta t}{2r}}\left[\left(\frac{\partial\vec{\varphi}}{\partial t}, \vec{\varphi}^*\right) - \left(\frac{\partial\vec{\varphi}^*}{\partial t}, \vec{\varphi}\right)\right]dt - \right.\right.$$
$$\left.\left. - \int_{t_j}^{t_{j+1}}\left[\sum_{k=1}^{r} A_k(\vec{\varphi}, \vec{\varphi}^*)\right]dt\right\} + \frac{1}{2}(\vec{\varphi}, \vec{\varphi}^*)\Big|_{t_0}^{t_{J+1}} = 0. \tag{11}$$

Now we will undertake approximation of the integrals in (11). We will use quadratic time formulas with a symmetric arrangement of the points of intersection relative to the middle of each of the integration intervals. In this case our choice is governed by the fact that the symmetric quadrature formulas with one and the same number of points of intersection in a general case have a higher order of accuracy than the asymmetric formulas (see [1]).

APPROVED FOR RELEASE: 2007/02/08: CIA-RDP82-00850R000300080046-0

APPROVED FOR RELEASE: 2007/02/08: CIA-RDP82-00850R000300080046-0

The integrals containing time derivatives are approximated in each fractional interval using the formulas of central rectangles employing antisymmetric constructions of the following type:

$$\int_{t_1}^{t_2}\left[\left(\frac{\partial\varphi}{\partial t},\ \varphi^*\right)-\left(\frac{\partial\varphi^*}{\partial t},\ \varphi\right)\right]dt\approx\left(\frac{\varphi^2-\varphi^1}{t_2-t_1}\frac{\varphi^{*2}+\varphi^{*1}}{2}-\frac{\varphi^{*2}-\varphi^{*1}}{t_2-t_1}\frac{\varphi^2+\varphi^1}{2}\right)(t_2-t_1). \tag{12}$$

Assuming that the functionals $A_k(\vec{\varphi}, \vec{\varphi}^*)$, $(k = \overline{1,r})$ are continuously dependent on time, we will write the quadrature formula

$$\int_{t_j}^{t_{j+1}}A(\vec{\varphi},\vec{\varphi}^*)\,dt=\int_{t_j}^{t_{j+1}}\left[\sum_{k=1}^{r}A_k(\vec{\varphi},\vec{\varphi}^*)\right]dt\approx\frac{\Delta t}{2}\sum_{k=1}^{r}\left[A_k(\vec{\varphi},\vec{\varphi}^*)\Big|_{t_j-\frac{(2k-1)\Delta t}{4r}}+\right.$$
$$\left.-A_k(\vec{\varphi},\vec{\varphi}^*)\Big|_{t_{j-1}-\frac{(2k-1)\Delta t}{4r}}\right], \tag{13}$$

whose residual term is of the order $0(\Delta t^3)$. In (13) each of the functionals Ak $(\vec{\varphi}, \vec{\varphi}^*)$ is computed at the two points

$$t=t_j+\frac{(2k-1)\Delta t}{4r}\qquad\text{and}\qquad t=t_{j+1}-\frac{(2k-1)\Delta t}{4r},$$

arranged symmetrically relative to the middle of the interval $t = t_j + \Delta t/2$, that is, with approximation of the integrals

$$\int_{t_j}^{t_{j+1}}A(\vec{\varphi},\vec{\varphi})\,dt$$

the different terms in the representation of the functional (4) are spaced in different fractional intervals. Such quadrature formulas are obtained on the basis of the weak approximation method.

Finally, using formulas (12)-(13) and performing discretization in space variables, we obtain the summator identity

$$I^h(\vec{\varphi},\vec{\varphi}^*)\equiv\frac{1}{2}\sum_{j=0}^{J}\left\{\sum_{k=1}^{2r}\left[\left(\left(\frac{\vec{\varphi}^{j+\frac{k}{2r}}-\vec{\varphi}^{j+\frac{k-1}{2r}}}{(\Delta t/2r)},\ \frac{\vec{\varphi}^{*j+\frac{k}{2r}}+\vec{\varphi}^{*j+\frac{k-1}{2r}}}{2}\right)^h-\right.\right.$$
$$\left.\left.-\left(\frac{\vec{\varphi}^{*j+\frac{k}{2r}}-\vec{\varphi}^{*j+\frac{k-1}{2r}}}{(\Delta t/2r)},\ \frac{\vec{\varphi}^{j+\frac{k}{2r}}+\vec{\varphi}^{j+\frac{k-1}{2r}}}{2}\right)^h\right)\right]\frac{\Delta t}{2r}+ \tag{14}$$
$$+\sum_{k=1}^{r}\left[(A_k^h(\vec{\varphi},\vec{\varphi}^*))^{j+\frac{2k-1}{4r}}+(A_k^h(\vec{\varphi},\vec{\varphi}^*))^{j+1-\frac{2k-1}{4r}}\right]\Delta t\Big\}+$$
$$+\frac{1}{2}(\vec{\varphi},\vec{\varphi}^*)\Big|_0^{t_{J+1}}=0.$$

APPROVED FOR RELEASE: 2007/02/08: CIA-RDP82-00850R000300080046-0

APPROVED FOR RELEASE: 2007/02/08: CIA-RDP82-00850R000300080046-0

approximating the identity (11) in time with the accuracy $0(\Delta t^2)$. The superscript h denotes discretization in space variables.

By analogy with [6], from the conditions of stationarity of the summator functional (14) with arbitrary and independent variations of the functions $\vec{\varphi}^*$ and $\vec{\varphi}$ at the points of intersection of the grid region $D_t^h = D^h \times \omega^{2r}$ we obtain systems of fundamental and conjugate equations in discrete form. These conditions are expressed in the following way:

$$\frac{\partial}{\partial \vec{\varphi}^*} I^h(\vec{\varphi}, \vec{\varphi}^*) = 0, \tag{15a}$$

$$\frac{\partial}{\partial \varepsilon}\left[\lim_{\xi \to 0} \frac{\partial}{\partial \xi} I^h(\vec{\varphi} + \xi\vec{\varphi}', \vec{\varphi}^*)\right] = 0, \tag{15b}$$

$$\vec{\varphi} \in Q^h(D_t^h), \ \vec{\varphi}^* \in Q^{*h}(D_t^h), \ \vec{\varphi} + \xi\vec{\varphi}' \in Q^h(D_t^h),$$

where ξ is a real parameter, $\vec{\varphi}'$ is the variation of the vector of state in the neighborhood of the stipulated unperturbed $\vec{\varphi}$ value. The difference equations (15) represent a family of splitting schemes satisfying the energy balance equation

$$I^h(\vec{\varphi}, \vec{\varphi}) = 0, \ \vec{\varphi} \in Q^h(D_t^h), \tag{16}$$

which is obtained from (14) by the substitution $\vec{\varphi}^* = \vec{\varphi}$. An evaluation of the approximation (14) shows that the discrete energy balance equation (16) in time approximates the equation

$$I(\vec{\varphi}, \vec{\varphi}) = 0. \tag{17}$$

The approximation is understood in a weak sense as the degree of closeness of the two functionals

$$\varepsilon = |(I(\vec{\varphi}, \vec{\varphi}) - I^h(\vec{\varphi}, \vec{\varphi}))|.$$

The quadrature time formulas which we used have residual terms with an order not less than the second and the integrands are also approximated with the second order.

The specific splitting scheme is determined by the choice of the representation (4), the quadrature formulas for approximating the integrals containing the time derivatives in (11), by the choice of the integration points in formulas of the type (13).

Now we will cite an example of a splitting scheme constructed using the variational principle. Assume that $\Im_k^h (k = \overline{1,r})$ are operators generated by the functionals $A_k^h(\vec{\varphi}, \vec{\varphi}^*)$, that is

$$A_k^h(\vec{\varphi}, \vec{\varphi}^*) = |\Im_k^h \vec{\varphi}, \vec{\varphi}^*| \quad (k = \overline{1, r}), \quad \vec{\varphi} \in Q^h(D_t^h), \quad \vec{\varphi}^* \in Q^{*h}(D_t^h), \tag{18}$$

APPROVED FOR RELEASE: 2007/02/08: CIA-RDP82-00850R000300080046-0

APPROVED FOR RELEASE: 2007/02/08: CIA-RDP82-00850R000300080046-0

where the symbol [,] denotes the scalar product. The form of the operators $\mathcal{Э}_k$ is established by direct transformations of the functionals $A_k^h(\vec{\varphi}, \vec{\varphi}^*)$, to wit

$$\mathcal{Э}_k^h \vec{\varphi} = \frac{\partial}{\partial \vec{\varphi}^*} A_k^h(\vec{\varphi}, \vec{\varphi}^*). \tag{19}$$

The summator analogues (13), entering into (14), are written in the form

$$(A_k^h(\vec{\varphi}, \vec{\varphi}^*))_{\vec{\varphi}}^{j+\frac{2k-1}{4r}} = |\mathcal{Э}_k^h \vec{\varphi}, \vec{\varphi}^*|^{hj-\frac{2k-1}{4r}} \equiv \tag{20}$$

$$\equiv \left[\mathcal{Э}_k^h \frac{\vec{\varphi}^{j+\frac{k}{2r}} + \vec{\varphi}^{j+\frac{k-1}{2r}}}{2}, \frac{\vec{\varphi}^{*j+\frac{k}{2r}} + \vec{\varphi}^{*j-\frac{k-1}{2r}}}{2}\right]^h,$$

and we transform the summator identity (14) with allowance for the introduced notations:

$$\sum_{j=0}^{J}\left\{\sum_{k=1}^{r}\left(\frac{\Delta t}{2r}\right)\left(\frac{\vec{\varphi}^{j+\frac{k}{2r}} - \vec{\varphi}^{j-\frac{k-1}{2r}}}{(\Delta t/2r)}, \frac{\vec{\varphi}^{*j+\frac{k}{2r}} + \vec{\varphi}^{*j+\frac{k-1}{2r}}}{2}\right)^h + \right. \tag{21}$$

$$\left. + \frac{1}{2}\sum_{k=1}^{r}(|\mathcal{Э}_k^h \vec{\varphi}, \vec{\varphi}^*|^{j+\frac{2k-1}{4r}} + |\mathcal{Э}_k^h \vec{\varphi}, \vec{\varphi}^*|^{j+1-\frac{2k-1}{4r}})\Delta t\right\} = 0.$$

The conditions of stationarity of the functional standing on the left-hand side of (21), with arbitrary and independent variations of the components of the $\vec{\varphi}^*$ vector at the grid points of intersection $D_t^h = D^h \times \omega_t^{2r}$, lead to the system of equations

$$B^h \frac{\vec{\varphi}^{j+\frac{k}{2r}} - \vec{\varphi}^{j+\frac{k-1}{2r}}}{(\Delta t/2)} + \mathcal{Э}_k^h \frac{\vec{\varphi}^{j+\frac{k}{2r}} + \vec{\varphi}^{j+\frac{k-1}{2r}}}{2} = 0 \quad (k = \overline{1, r}),$$

$$B^h \frac{\vec{\varphi}^{j+\frac{k}{2r}} - \vec{\varphi}^{j+\frac{k-1}{2r}}}{(\Delta t/2)} + \mathcal{Э}_{(2r+1-k)}^h \frac{\vec{\varphi}^{j+\frac{k}{2r}} + \vec{\varphi}^{j+\frac{k-1}{2r}}}{2} = 0 \quad (k = \overline{r+1, 2r}), \tag{22}$$

where k is the number of the splitting stage. The B^h matrix in (22) is diagonal, with nonnegative elements. It is generated by a discrete analogue of the scalar product (1) in the grid $D^h \times \omega_t^{2r}$. In approximations of equations not containing time derivatives the elements of the B^h matrix are equal to 0. A system of conjugate equations (15) is also similarly obtained. For this it is better that the identity (14) first be transformed to the form

$$\sum_{j=0}^{J}\left\{\sum_{k=1}^{r}\left(\frac{\Delta t}{2r}\right)\left(-\frac{\vec{\varphi}^{*j-\frac{k}{2r}} - \vec{\varphi}^{*j+\frac{k-1}{2r}}}{(\Delta t/2r)}, \frac{\vec{\varphi}^{j+\frac{k}{2r}} + \vec{\varphi}^{j+\frac{k-1}{2r}}}{2}\right)^h + \right. \tag{23}$$

$$\left. + \frac{\Delta t}{2}\sum_{k=1}^{r}(|\mathcal{Э}_k^h \vec{\varphi}, \vec{\varphi}^*|^{j+\frac{2k-1}{4r}} + |\mathcal{Э}_k^h \vec{\varphi}, \vec{\varphi}^*|^{j+1-\frac{2k-1}{4r}})\right\} +$$

$$+ (\vec{\varphi}, \vec{\varphi}^*)^{hJ+1} - (\vec{\varphi}, \vec{\varphi}^*)^{h0} = 0.$$

APPROVED FOR RELEASE: 2007/02/08: CIA-RDP82-00850R000300080046-0

APPROVED FOR RELEASE: 2007/02/08: CIA-RDP82-00850R000300080046-0

If it is assumed that the operators $\Im_k^h$ ($k = \overline{1,r}$) are not dependent on the vector of state, the conditions (15b) lead to a system of conjugate equations

$$-B^{j}\frac{\overset{\rightarrow}{\varphi}^{*j+\frac{k}{2r}}-\overset{\rightarrow}{\varphi}^{j+\frac{k-1}{2r}}}{(\Delta t/2)}+\Im_k^{hT}\frac{\overset{\rightarrow}{\varphi}^{*j+\frac{k}{2r}}+\overset{\rightarrow}{\varphi}^{*j+\frac{k-1}{2r}}}{2}=0\quad(k=\overline{1,\ r}),\tag{24}$$

$$-B^{h}\frac{\overset{\rightarrow}{\varphi}^{*j+\frac{k}{2r}}-\overset{\rightarrow}{\varphi}^{*j+\frac{k-1}{2r}}}{(\Delta t/2)}+$$

$$+\Im_{2r+1-k}^{hT}\frac{\overset{\rightarrow}{\varphi}^{*j+\frac{k}{2r}}+\overset{\rightarrow}{\varphi}^{*j+\frac{k-1}{2r}}}{2}=0\quad(k=\overline{r+1,\ 2r}),$$

where the superscript T denotes the transposing operation. Whereas the operators $\Im_k^h(k = \overline{1,r})$ are dependent on the components of the vector of state, the operation of differentiation for ξ with $\xi = 0$ in (15b) determines the Hato derivatives of the nonlinear operators in the neighborhood of a stipulated undisturbed state. In nonlinear problems in computing the coefficients of the $\Im_k^h$ operators it is customary to use information on the vector of state from the preceding time intervals and therefore linearization leads to the appearance of additional terms which are explicitly taken into account in (24).

According to the definition given by G. I. Marchuk in [3,4], schemes of the type (22) are called two-cycle multicomponent splitting schemes. Each of the equations (22) represents a two-layer Crank-Nicholson time approximation. The first r equations constitute one cycle and are solved successively in the order of increase of the numbers of the splitting stages and the $\Im_k^h$ operators from 1 to r, and the next r constitute a second cycle and with an increase in the number of the splitting stage from r+1 to 2r the numbers of the $\Im_k$ operators decrease from r to 1. The solution of each preceding equation serves as an initial condition for the next. It follows from (14) that the splitting schemes obtained by this method will be energetically balanced not only as a whole in the entire $[0, \overline{t}]$ interval, but in each fractional interval.

A comparison of systems (22) and (24) reveals that whereas the basic problem (22) is correct in the direction of an increase in time from 0 to $\overline{t}$ the conjugate problem (24), on the contrary, is correct in the direction of a decrease from $\overline{t}$ to 0. Accordingly, the initial conditions for it are stipulated with $t = \overline{t}$ and the equations (24) are solved in each time interval $[t_{j+1}, t_j]$ in the reverse order in comparison with (22), that is, the subscript k, determining the number of the splitting stage, varies from 2r to 1.

Thus, the combination of the variational principle with the splitting method makes it possible to construct a broad class of economical and stable numerical schemes for solving problems in the mathematical modeling of atmospheric and oceanic processes. The fundamental requirement which is imposed on splitting schemes is that the terms of the same type entering into the integral identity be taken into account in the same splitting stage and be uniformly approximated. The stability of the splitting schemes (15) follows from the energy balance equation (16). It is a

APPROVED FOR RELEASE: 2007/02/08: CIA-RDP82-00850R000300080046-0

APPROVED FOR RELEASE: 2007/02/08: CIA-RDP82-00850R000300080046-0

noteworthy fact that the conditions (15) lead to splitting schemes for the fundamental and conjugate equations and these schemes are made mutually consistent through the summator functional (14). The latter circumstance is important to use in the formulation and application of methods in the theory of perturbations and optimization [5, 7].

The combination of the splitting method with the variational principle manifests their best qualities. The splitting method leads to computation algorithms which are economical and simple to apply and the variational principle guarantees their stability and ensures consistency in all stages of solution of the problem. This means that by introducing a sufficiently large number of fractional intervals and elementary splitting stages it is possible to achieve a considerable simplification of the practical realization of the model. At the same time, the summator identity (14), generating the splitting schemes, makes possible the automatic checking of the behavior of the model as a whole independently of the number of splitting stages.

BIBLIOGRAPHY

1. Bakhvalov, N. S., CHISLENNYYE METODY (Numerical Methods), Vol 1, Moscow, Nauka, 1973.

2. Marchuk, G. I., CHISLENNYYE METODY V PROGNOZE POGODY (Numerical Methods in Weather Forecasting), Leningrad, Gidrometeoizdat, 1967.

3. Marchuk, G. I., CHISLENNOYE RESHENIYE ZADACH DINAMIKI ATMOSFERY I OKEANA (Numerical Solution of Problems in the Dynamics of the Atmosphere and Ocean), Leningrad, Gidrometeoizdat, 1974.

4. Marchuk, G. I., METODY VYCHISLITEL'NOY MATEMATIKI (Methods in Computational Mathematics), Moscow, Nauka, 1977.

5. Marchuk, G. I., Penenko, V. V., "Investigation of the Sensitivity of Discrete Models of Dynamics of the Atmosphere and Ocean," IZV. AN SSSR, FIZIKA ATMOSFERY I OKEANA (News of the USSR Academy of Sciences, Physics of Atmosphere and Ocean), Vol 15, No 11, 1979.

6. Penenko, V. V., "Energetically Balanced Discrete Models of Dynamics of Atmospheric Processes," METEOROLOGIYA I GIDROLOGIYA (Meteorology and Hydrology), No 10, 1977.

7. Penenko, V. V., "Evaluation of the Parameters of Discrete Models of Dynamics of the Atmosphere and Ocean," METEOROLOGIYA I GIDROLOGIYA, No 10, 1979.

8. Samarskiy, A. A., VVEDENIYE V TEORIYU RAZNOSTNYKH SKHEM (Introduction to the Theory of Difference Schemes), Moscow, Nauka, 1971.

9. Yanenko, N. N., METOD DROBNYKH SHAGOV RESHENIYA MNOGOMERNYKH ZADACH MATEMATICHESKOY FIZIKI (Fractional Intervals Method for Solving Multidimensional Problems in Mathematical Physics), Novosibirsk, Nauka, 1967.

APPROVED FOR RELEASE: 2007/02/08: CIA-RDP82-00850R000300080046-0

APPROVED FOR RELEASE: 2007/02/08: CIA-RDP82-00850R000300080046-0

UDC 551.558.1

EFFECT OF AIR ENTRAINMENT ON STABILITY OF A THERMAL

Moscow METEOROLOGIYA I GIDROLOGIYA in Russian No 10, Oct 80 pp 25-28

[Article by Candidate of Physical and Mathematical Sciences Ye. Sirakov, Sofia University, Bulgaria, manuscript submitted 17 Apr 80]

[Text]

Abstract: The influence of air entrainment on the atmospheric equilibrium criterion is investigated on the basis of solution of the equations of thermohydrodynamics for a nonadiabatic particle.

In the adiabatic model of convection it is assumed that an air particle during its vertical movement does not interact with the surrounding medium, that is, it moves adiabatically. On the basis of this model an appropriate adiabatic equilibrium criterion is introduced characterizing the parameter $(\gamma - \gamma_a)$, where $\gamma = -dT_e/dz$, T_e is atmospheric temperature, γ_a is the dry adiabatic temperature gradient.

Now we will attempt to take into account the influence of nonadiabaticity on the equilibrium criterion. For this we will turn to equations describing the dynamics of a nonadiabatic particle [the literature also contains such terms as "thermal" and "bubble"], taking into account the buoyancy force $\beta_1 \delta q$ generated by a nonuniformity of humidity (in application to the ocean this can be salinity) [2, 4, 6],

$$\frac{dw^2}{dz} = 2\beta\delta T + 2\beta_1\delta q - \left(\frac{2}{m}\frac{dm}{dz} + \frac{3c_d}{4R}\right)w^2, \quad (1)$$

$$\frac{dT_i}{dz} = -\gamma_a - \frac{1}{m}\frac{dm}{dz}\delta T, \quad (2)$$

$$\frac{dq_i}{dz} = -\frac{1}{m}\frac{dm}{dz}\delta q, \quad (3)$$

Here T_i, q_i, w, m, R are temperature, specific humidity, vertical velocity, mass and equivalent radius of the particle, β and β_1 are the parameters of temperature and humidity buoyancy, c_d is the drag coefficient, $\delta T = T_i - T_e$ and $\delta q = q_i - q_e$ are the temperature and humidity deficits. q_e is atmospheric humidity, z is the vertical coordinate.

APPROVED FOR RELEASE: 2007/02/08: CIA-RDP82-00850R000300080046-0

APPROVED FOR RELEASE: 2007/02/08: CIA-RDP82-00850R000300080046-0

The system (1)-(3) is not closed since the rate of entrainment $\alpha(z) = (1/m)dm/dz$ is an unknown function of altitude z. This function, determined in [5] and described in [2], has the form

$$\alpha(z) = \frac{1}{m}\frac{dm}{dz} = \frac{3}{R}\frac{dR}{dz} - \frac{1}{T_{vi}}\frac{dT_{vi}}{dz} - \frac{\Gamma_A}{T_{ve}}. \tag{4}$$

where T_{vi} and T_{ve} are the virtual temperatures of the particle and atmosphere, Γ_A is the autoconvective gradient.

For normal atmospheric conditions with an adequate accuracy there is satisfaction of the condition [2]

$$\alpha(z) = \frac{3}{R}\frac{dR}{dz}. \tag{5}$$

The solution of the system of equations (1)-(3), (5) with the initial conditions

$$w = w_0,\ \delta T = \delta_0 T,\ \delta q = \delta_0 q,\ R = R_0 \qquad \text{with } z = 0 \tag{6}$$

has the form

$$\delta T = \left(\frac{R_0}{R}\right)^3\left[\delta_0 T + \int_0^z (\gamma - \gamma_a)\left(\frac{R}{R_0}\right)^3 dz\right],$$

$$\delta q = \left(\frac{R_0}{R}\right)^3\left[\delta_0 q + \int_0^z \gamma_q\left(\frac{R}{R_0}\right)^3 dz\right], \tag{7}$$

$$w^2 = \left(\frac{R_0}{R}\right)^6 \exp\left[-\frac{3c_d}{4}\int_0^z \frac{dz}{R}\right]\left\{w_0^2 + 2\int_0^z\left(\frac{R}{R_0}\right)^3\left[\delta_0\Pi + \int_0^z \Gamma_*\left(\frac{R}{R_0}\right)^3 dz\right]\times\right.$$

$$\left.\times \exp\left[\frac{3c_d}{4}\int_0^z \frac{dz}{R}\right]dz\right\},$$

where

$$\delta_0\Pi = \beta\delta_0 T + \beta_1\delta_0 q,\ \Gamma_* = \beta(\gamma - \gamma_a) + \beta_1\gamma_q,\ \gamma_q = -\frac{dq_r}{dz}.$$

The change R(z) with altitude is described by the law

$$R(z) = R_0 + bz^n, \tag{8}$$

in this case most frequently n = 1 (see [6]). The entrainment constant b characterizes the intensity of mixing. We note in passing that in the case of a spontaneously arising thermal [3], developing in an unstable atmosphere, the degree of whose instability changes in conformity to the power law

$$(\gamma - \gamma_a) = cz^{-p},\ \gamma_q = c_1 z^{-p_1}, \tag{9}$$

where c and c_1 are positive constants, the initial conditions (6) must be replaced by the following:

$$w_0 = \delta_0 T = \delta_0 q = R_0 \to 0 \qquad \text{with } z = 0. \tag{10}$$

APPROVED FOR RELEASE: 2007/02/08: CIA-RDP82-00850R000300080046-0

APPROVED FOR RELEASE: 2007/02/08: CIA-RDP82-00850R000300080046-0

Then the solution for a spontaneous thermal is written in the form

$$\delta T = \frac{c}{3n+1-p} z^{1-p}, \quad \delta q = \frac{c_1}{3n+1-p_1} z^{1-p_1}, \tag{11}$$

$$w = \left[\frac{2\beta c}{(3n+1-p)(8+s-p)} z^{2-p} + \frac{2\beta_1 c_1}{(3n+1-p_1)(8+s-p_1)} z^{2-p_1}\right]^{1/2} \tag{12}$$

In the special case n = 1, p = p_1, $c_1 = \beta_1 = 0$, s = $3c_d/4 = 0$, from (11)-(12) we have the expressions

$$\delta T = \frac{c}{4-p} z^{1-p}, \quad w = \frac{2\beta c}{(4-p)(8-p)} z^{2-p}, \tag{13}$$

obtained in [1]. In this study the conclusion is drawn that convective movements in an unstable layer of the atmosphere must be realized in a form closer to jets since with such a geometry of convection currents heat exchange and the evening-out of temperature nonuniformity occurs more effectively than in the case of realization of convective movements in the form of bubbles. The general solution (12), where drag was also taken into account, still further confirms such a conclusion. In actuality, the value s > 0, figuring in the denominator (12), additionally decreases w (in comparison with the case s = 0), that is, the intensity of exchange, accomplished by means of thermals in the form of bubbles, is slowed.

Now we will proceed to a discussion of the influence of nonadiabaticity (mass exchange) on the atmospheric equilibrium criterion. We will examine a particle of finite size R_0 whose characteristics at the initial level z = 0 do not differ from the corresponding characteristics in the surrounding air:

$$\delta_0 T = \delta_0 q = w_0 = 0, \quad R = R_0 \qquad \text{with } z = 0. \tag{14}$$

As a result of the initial displacement the particle moves upward (z > 0), u the question arises as to the nature of its further behavior. This can be investigated on the basis of the solution (7), with (14) taken into account. We will assume that γ and γ_q are constant with altitude. Then it is easy to obtain the following expressions for the characteristics of a nonadiabatic particle:

(15)

$$\beta\delta T + \beta_1 \delta q = \Gamma_* \frac{R}{3b} \Phi, \tag{16}$$

$$\frac{1}{2}\frac{dw^2}{dz} \equiv \frac{dw}{dt} = \Gamma_*^{\text{н}} \frac{R}{3b} \Phi, \tag{17}$$

$$\Gamma_*^{\text{н}} = \beta(\gamma - \gamma_l) + \beta_1(\gamma_q - \gamma_{ql}) = \Gamma_*(1 - \Phi),$$

$$\frac{dw/dt}{\beta\delta T + \beta_1 \delta q} = (1 - \Phi) = \frac{\Gamma_*^{\text{н}}}{\Gamma_*} > 0, \tag{18}$$

$$\Phi = \frac{3(R^4 - R_0^4)}{4R^4} \equiv \frac{3}{4}[1 - (1+\eta)^{-4}], \quad \eta = b\frac{z}{R_0}, \tag{19}$$

APPROVED FOR RELEASE: 2007/02/08: CIA-RDP82-00850R000300080046-0

APPROVED FOR RELEASE: 2007/02/08: CIA-RDP82-00850R000300080046-0

where $\gamma_i = -dT_i/dz$ and $\gamma_{qi} = -dq_i/dz$ are the nonadiabatic temperature and humidity gradients of the particle respectively.

With $\beta_1 = 0$ expressions (15)-(19) describe purely thermal convection, with $\beta_1 \neq 0$, $\beta = 0$ is convection in the humidity field, but with $\beta_1 \neq 0$, $\beta \neq 0$ is the mixed convection regime.

For an adiabatic thermal ($\alpha \to 0$, $R \to R_0$) with $c_d = 0$ the expressions (15)-(19) are reduced to the known adiabatic equilibrium criteria

$$\beta\delta T + \beta_1 \delta q = \Gamma_* z, \tag{20}$$

$$\frac{dw}{dt} = \Gamma_* z, \tag{21}$$

[H = non(adiabatic)]

$$\frac{dw/dt}{\beta\delta T + \beta_1 \delta q} = \frac{\Gamma_*^H}{\Gamma_*} = 1, \Phi = 1. \tag{22}$$

From a comparison of (15)-(19) and (20)-(22) it is easy to ascertain the influence of nonadiabaticity on the equilibrium criterion. According to the adiabatic equilibrium criterion (20)-(21) $dw/dt \gtreqless 0$ and accordingly $\beta\delta T + \beta_1 \delta q \gtreqless 0$ with $\Gamma_* \gtreqless 0$ (the symbols $>$, $=$, $<$ relate to unstable, neutral and stable stratifications respectively). In a nonadiabatic case in formulas (17) and (18) the nonadiabatic correction factor $(1 - \bar{\Phi})$ appears, replacing unity. In the general case of mixed convection the adiabatic equilibrium criterion Γ_* is replaced by the nonadiabatic equilibrium criterion $\Gamma_*^{non} = \Gamma_*(1 - \bar{\Phi})$. In special cases $\beta_1 = 0(\gamma - \gamma_a)$ is replaced by $(\gamma - \gamma_i) = (\gamma - \gamma_a)(1 - \bar{\Phi})$, but with $\beta = 0$ γ_q is replaced by $(\gamma_q - \gamma_{qi}) = \gamma_q(1 - \bar{\Phi})$. It is important that the adiabatic criteria Γ_*, $(\gamma - \gamma_a)$, γ_q and the corresponding nonadiabatic criteria Γ_*^{non}, $(\gamma - \gamma_i)$, $(\gamma_q - \gamma_{qi})$ always have identical signs since $\bar{\Phi}$ is a nonnegative monotonically increasing function limited with height ($\bar{\Phi}(0) = 0 \leqslant \bar{\Phi} \leqslant \bar{\Phi}(\infty) = 3/4$) and always $(1 - \bar{\Phi}) > 0$. This means that mass exchange does not change the type of equilibrium (stable, neutral, unstable), but changes its degree.

In contrast to the constant Γ_*, $(\gamma - \gamma_a)$ and γ_q values, the Γ_*^{non}, $(\gamma - \gamma_i)$ and $(\gamma_q - \gamma_{qi})$ values are dependent on z and the characteristics of the thermal b and R_0, in this case not on them separately, but on the dimensionless combination $\eta = b\, z/R_0$. With $\eta \to 0$ we have $(1 - \bar{\Phi}) \to 1$ and $\Gamma_*^{non} \to \Gamma_*$, that is, the difference between the adiabatic and nonadiabatic equilibrium criteria disappears. With a fixed z th[redacted]dition $\eta \to 0$ is realized with $b \to 0$ (little mixing) or $R_0 \to \infty$ (large thermals). [redacted]e other hand, the maximum difference between the adiabatic and nonadiabatic criteria is observed with $\eta \to \infty$, as is realized (z is fixed) with $b \to \infty$ (great mixing) with $R_0 \to 0$ (very small thermals). Since the numerical value of expansion coefficient for atmospheric thermals does not vary very significantly ($b \simeq 0.2$ [3, 5]), the above-mentioned conclusions are equivalent to the assertion that with fixed z the difference in the criteria Γ_*^{non} and Γ_* is considerable for very small thermals and decreases with an increase in R_0. For any specific case the precise value of the difference between Γ_*^{non} and Γ_* can be computed using formula (18).

APPROVED FOR RELEASE: 2007/02/08: CIA-RDP82-00850R000300080046-0

APPROVED FOR RELEASE: 2007/02/08: CIA-RDP82-00850R000300080046-0

We will also briefly examine the influence of drag ($c_d \neq 0$) on the equilibrium criterion. It is easy to show that instead of (18) it is possible to obtain

$$0 < \frac{dw\,dt}{\beta_0 T + \beta_1 \partial q} < (1 - \Phi).$$

Evidently, the type of stability again does not change, but under identical conditions the acceleration dw/dt with $c_d \neq 0$ at any level z is always less than the corresponding acceleration with $c_d = 0$.

The next problem is allowance for the mutual influence of nonadiabaticity and phase transitions of water on the stability criterion. This can be done on the basis of analytical solutions for a nonadiabatic moist thermal above the condensation level obtained in [7].

These problems will be dealt with in a separate study.

BIBLIOGRAPHY

1. Andreyev, V., Panchev, S., DINAMIKA ATMOSFERNYKH TERMIKOV (Dynamics of Atmospheric Thermals), Leningrad, Gidrometeoizdat, 1975.

2. Andreyev, V., Sirakov, E., "Interaction Between an Isolated Thermal and the Surrounding Medium," KHIDROLOGIYA I METEOROLOGIYA (Hydrology and Meteorology), Vol XIX, No 6, Sofia, 1970.

3. Vul'fson, N., Levin, I. O., "Form of Realization of Spontaneous Convective Movements in the Atmosphere," IZV. AN SSSR, FIZIKA ATMOSFERY I OKEANA (News of the USSR Academy of Sciences, Physics of the Atmosphere and Ocean), Vol 10, No 4, 1974.

4. Matveyev, L. T., OSNOVY OBSHCHEY METEOROLOGII (Principles of General Meteorology), Leningrad, Gidrometeoizdat, 1965.

5. Sirakov, E., "A Model of Nonadiabatic Thermal Convection in Dry Air," Diploma Work, SU "Kl. Okhridski," 1969.

6. Sirakov, E., "Periodic Solutions for a Nonadiabatic Thermal in a Stratified Atmosphere," COMP. REND. BULG. AK. SCI., Tome 29, No 1, 1976.

7. Sirakov, E., "Dynamics of Nonadiabatic Thermal in a Stratified Atmosphere Taking Into Account the Co-effect of Mass Exchange and Water's Phase Transition," COMP. REND. BULG. AK. SCI., Tome 31, No 9, 1978.

APPROVED FOR RELEASE: 2007/02/08: CIA-RDP82-00850R000300080046-0

APPROVED FOR RELEASE: 2007/02/08: CIA-RDP82-00850R000300080046-0

UDC 551.576.1:621.396.969

OPERATIONAL RADAR DISPLAY OF THE STRUCTURE OF THUNDERSTORM-HAIL CLOUDS

Moscow METEOROLOGIYA I GIDROLOGIYA in Russian No 10, Oct 80 pp 29-38

[Article by Candidate of Physical and Mathematical Sciences M. T. Abshayev, High-Mountain Geophysical Institute, manuscript submitted 14 Jan 80]

[Text]

Abstract: The article describes the methods and apparatus used in the routine collection and graphic display of data on the cellular structure of thunderstorm-hail clouds which ensure a considerable increase in the information yield of meteorological radars. The principle of the method is obtaining the cellular structure of the radioechoes of clouds in isolines of radar reflectivity, against whose background it is possible to discriminate hail centers, bearings of lightning discharges and zones of turbulence, discriminated by the simultaneous processing of data in several channels. Some results of investigation of the structure and dynamics of development of hail clouds obtained by the proposed method are presented.

Introduction. The widespread use of radar apparatus in routine hail protection work, in the storm warning service, in ensuring the safety of aircraft flights, etc., requires the routine automation of the processing and graphic display of information in a form easily comprehensible to users, not requiring high skills of personnel in the interpretation of the observational results. For example, the services for hail protection, storm warning and ensuring the safety of air traffic require routine materials on the structure of hail clouds with the simultaneous discrimination, at a real time scale, of each convective cell, the hail and thunderstorm centers in them, zones of increased turbulence and zones of ordered jets of ascending currents.

In hail protection work the need for this method is dictated by the fact that the scheme for the modification of hail processes is determined by the cellular structure of the cloud (unicellular, multicellular, supercellular), stages of development (hail or potentially hail stage), relative spatial position and configuration of the zone of localization of the hail and the zone of the ascending

APPROVED FOR RELEASE: 2007/02/08: CIA-RDP82-00850R000300080046-0

APPROVED FOR RELEASE: 2007/02/08: CIA-RDP82-00850R000300080046-0

flow [3]. The expenditure of means on modification is determined by the transverse dimensions and rate of movement of the center of hail formation.

Known methods and apparatus for the processing of radar information on meteorological objects do not ensure collection of information on the total structure of radioechoes of clouds and because of this have an information yield inadequate for practical purposes.

The method for discriminating hail centers used in hail protection work does not ensure the detection of jets of ascending currents and determination of the structure of clouds, on the basis of which the technology and intensity of modification are selected for the purpose of interrupting and preventing hailfalls.

The methods for discriminating zones of increased turbulence [7, 8] make it possible for aircraft to avoid zones of dangerous bumping, but do not provide warnings concerning large hail capable of inflicting serious mechanical damage to them. In addition, with the existing method for the display of turbulence zones there is a loss of information concerning the spatial position of this zone relative to the boundaries of the radioecho, zone of enhanced reflectivity and hail center.

In turn, known methods for obtaining a multicontour isoecho [4, 5, 10 and others] ensure only the collection of information on the structure of radioechoes of clouds and give no idea concerning the presence and location of hail centers, ordered jets of ascending currents, zones of dangerous bumping, etc.

In this article we propose a method and apparatus for operational collection of the total structure of radioechoes of hail clouds with the discrimination of hail centers, zones of increased turbulence and zones of ordered ascending currents against a background of the pattern of a radioecho in the form of a multicontour isoecho.

Principle of Method

The principle of the method is as follows. Hail centers, bearings of lightning discharges and zones of increased turbulence, simultaneously discriminated in different data processing channels, show up in the form of bright pips against the background of the cellular structure of thunderstorm-hail clouds displayed on radar screens in the form of a multicontour isoecho by means of thin reflectivity isolines.

In this method the structure of radioechoes of clouds in the form of a multicontour isoecho is obtained, in accordance with [4], by the introduction of a correction for the square of distance, spatial-temporal averaging of the radioecho in many range channels (192) for 16 successive signals, quantization with the selected interval and the formation of narrow (0.5-1.0 msec) pulses which during radial-circular scanning define reflectivity isocontours. The adopted quantization interval was 10 db, this ensuring the necessary detail and adequate clarity of radioecho structure. The first contour, representing the outer boundary of the cloud radioecho, is discriminated in the form of a dashed line, which makes it possible to

APPROVED FOR RELEASE: 2007/02/08: CIA-RDP82-00850R000300080046-0

APPROVED FOR RELEASE: 2007/02/08: CIA-RDP82-00850R000300080046-0

identify natural clearings in clouds and simplifies the interpretation of the isoecho pattern.

The discrimination of the hail centers is accomplished, in accordance with [1], by the two-wave method by the subtraction of the logarithm of strength of a radioecho obtained in the 3.2 cm channel of a MRL-5 radar from the logarithm of the strength of a radioecho obtained in its 10 cm channel. Neglecting the attenuation of the 10-cm radiation, we have

$$\lg \frac{\overline{P}_{10}(R)}{\overline{P}_{3.2}(R)} = \lg \frac{C_{10}}{C_{3.2}} + \lg \frac{\eta_{10}(R)}{\eta_{3.2}(R)} + 0{,}2 \int_0^R K_{3.2}(R)dR, \qquad (1)$$

where $\overline{P}_{3.2}$ and $\overline{P}_{10}$ is the mean strength of the radioecho in the channels 3.2 and 10 cm respectively; $C_{3.2}$ and C_{10} are the meteorological potentials of the channels 3.2 and 10 cm of the MRL-5 radar; $\eta_{3.2}$ and η_{10} are the radar reflectivities of a cloud in the channels 3.2 and 10 cm; $K_{3.2}$ is the coefficient of attenuation of radiation at 3.2 cm.

In a rain zone the ratio of the radar reflectivities at wavelengths 3.2 and 10 cm $\eta_{10}/\eta_{3.2}$ regardless of the intensity of the precipitation is a constant value and equal to $\lambda_1^4/\lambda_2^4 \approx 0.01$, but in the presence of hail with a maximum diameter $d_{max} > 0.8$–1.0 cm this ratio increases with an increase in the diameter of the hail and for large hail attains values $\eta_{10}/\eta_{3.2} \geqslant 1$ or more. Accordingly, selection of a cloud cover field where the value $\eta_{10}/\eta_{3.2} > 0.01$ is observed ensures the discrimination of zones of localization of hail with a maximum diameter of more than 0.8–1.0 cm. The errors associated with the attenuation of 3.2 cm radiation are eliminated by the introduction of a correction by means of a special device for the correction of attenuation.

Apparatus

The method for obtaining the structure of thunderstorm-hail clouds described above can be applied using specialized devices for the processing of information or using an electronic computer. In both cases high requirements are imposed on the processing apparatus: speed not less than 10^6 operations, memory unit volume $\approx$ 30 kbyte, high accuracy and clarity of data display.

In this article we examine specialized apparatus for obtaining the structure of thunderstorm-hail clouds. Figure 1 is a structural diagram of such apparatus, built into a two-wave MRL-5 meteorological radar.

The apparatus for obtaining the structure of thunderstorm-hail clouds includes the MRL-5 radar, a multicontour isoecho device, device for the selection of hail centers, turbulence indicator, thunderstorm direction finder, commutator and signal mixer. With respect to actual construction, the multicontour isoecho unit, turbulence indicator and thunderstorm direction finder are enclosed in individual cabinets with their own current sources.

The principle of operation of the apparatus for obtaining the structure of thunderstorm-hail clouds is as follows. The power of the radioecho is fed from the output of the receiver for the 3.2 cm channel of the MRL-5 radar, corrected by $1/R^2$ (for the SHF of a p-i-n diode attenuator), to the device for the selection of

APPROVED FOR RELEASE: 2007/02/08: CIA-RDP82-00850R000300080046-0

APPROVED FOR RELEASE: 2007/02/08: CIA-RDP82-00850R000300080046-0

hail centers and the commutator I.

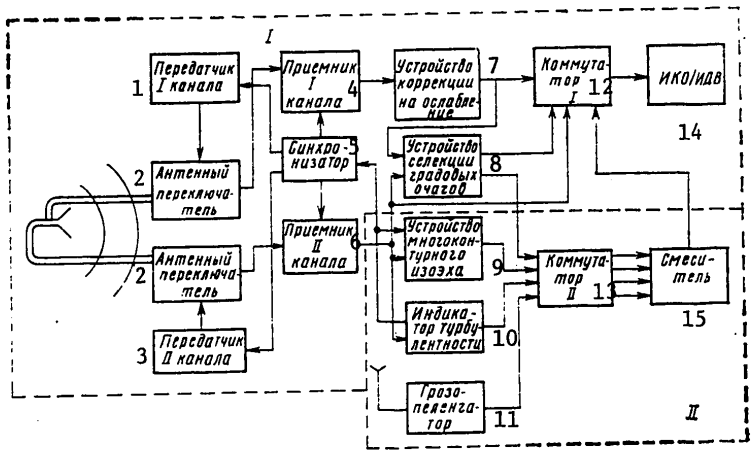

Fig. 1. Functional diagram of apparatus for obtaining structure of thunderstorm-hail clouds. I) standard MRL-5 meteorological radar; II) additional devices.

KEY:

1. Transmitter of channel I
2. Antenna switch
3. Transmitter of channel II
4. Receiver of channel I
5. Synchronizer
6. Receiver of channel II
7. Device for correction for attenuation
8. Device for selection of hail centers
9. Multicontour isoecho device
10. Turbulence indicator
11. Thunderstorm direction finder
12. Commutator I
13. Commutator II
14. IKO/IDV
15. Mixer

The power of the radioecho in the 10 cm channel of the MRL-5 radar, also with the $1/R^2$ correction, is fed simultaneously to the commutator I, the multicontour isoecho device and the turbulence indicator. The commutator I ensures the possibility for alternate indication on IKO/IDV displays of the MRL-5 radar of the videosignals $\lg P_{3.2}$ and $\lg P_{10}$, as well as the difference signals $\lg P_{3.2}/P_{10}$ and $\lg P_{10}/P_{3.2}$. In the device for the selection of hail centers and the multicontour isoecho device there is spatial-temporal averaging of the meteorological radioecho. The averaging of $\lg P_{3.2}$ and $\lg P_{10}$ is accomplished by selection of the meteorological radioecho in 192 range and integration channels in RC circuits with a time constant $\tau \approx 0.04$ sec [4]. The schemes for the averaging of $\lg P_{3.2}$ and $\lg P_{10}$ are identical and consist of a generator of cadence pulses (triggered by a triggering pulse from the MRL-5) with a frequency divider, shaper of strobing pulses, shaper of shifting pulses, eight-digit shifting register and a unit of 192 time selectors with integrators.

APPROVED FOR RELEASE: 2007/02/08: CIA-RDP82-00850R000300080046-0

APPROVED FOR RELEASE: 2007/02/08: CIA-RDP82-00850R000300080046-0

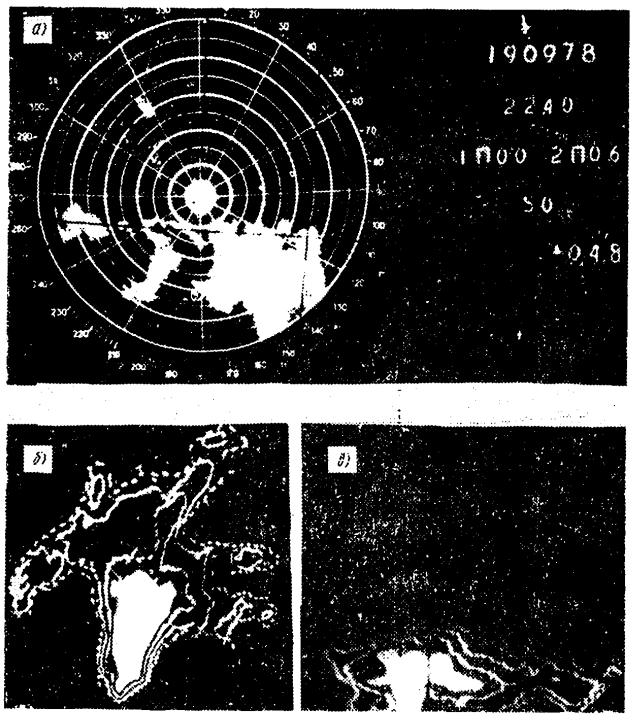

Fig. 2. Pattern of radioechoes of hail clouds on IKO and IDV displays. a) ordinary pattern of radioechoes on IKO display. (The display shows the date, time, sign of the norm for the energy potential for the meteorological radar (letter П), scanning scale, antenna angle of elevation); b) structure of hail cloud on IKO display in reflectivity isolines at $\lambda = 10$ cm, with 10 db interval. (The outer dashed contour corresponds to $\eta_{10} = 10^{-12}$ cm^{-1}. The hail center is discriminated from the solid white pip); c) structure of radioecho of hail cloud on IDV indicator.

The number of range channels in the averaging scheme is selected in such a way as to ensure the necessary range resolution of 0.25 km with a scanning scale M$\leq$ 50 km, 0.5 km with M = 100 km and 1.5 km with M = 300 km.

In the hail center selection device the averaged signals lg $\overline{P}_{3.2}$ and lg $\overline{P}_{10}(R)$ are subtracted in the operational amplifier and the difference signal is fed to the commutators I and II through an amplifier-limiter shaping the boundaries of the hail center. The averaged signal lg $\overline{P}_{10}$ in the multicontour isoecho unit is fed to the input of the quantizer, ensuring parallel quantization at six levels with a stipulated interval (for example, 10 db). At the output of the threshold devices in each quantizer channel pulse shapers (duration 1μsec) are cut in, which during radial-circular scanning define the isolines of reflectivity (or radioecho strength). In order to define the outer boundary of the radioecho

APPROVED FOR RELEASE: 2007/02/08: CIA-RDP82-00850R000300080046-0

APPROVED FOR RELEASE: 2007/02/08: CIA-RDP82-00850R000300080046-0

by a dashed line the pulses from the first quantization level are fed to a coincidence circuit ensuring the selection of output pulses by the pulses of a "64 counter," which first divides the MRL triggering frequency.

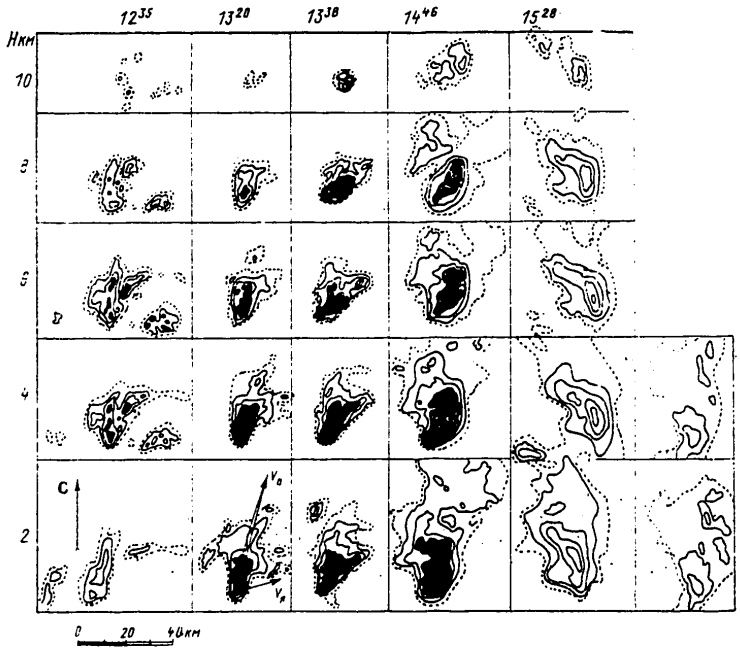

Fig. 3. Spatial structure of radioecho and dynamics of development of one of supercellular hail clouds observed on 13 August 1977 obtained by circular sections at indicated altitude levels. The cloud structure in η_{10} isolines without revelation of hail center is shown at 1528 hours. V_{sc} = 70 km/hour is the velocity of the steering current, V_{cell} = 40 km/hour is the velocity of movement of the supercell.

The turbulence indicator [7] consists of the limiter amplifier, a phase detector, an ultrasonic delay line, a device for period-by-period subtraction and ensures obtaining the fields of the difference of radial velocities of hydrometeors caused for the most part by turbulence (scale 0.5 km). A detailed description of the turbulence indicator and thunderstorm rangefinder, ensuring determination of the bearings of the lightning discharges, and the MRL-5 radar is given in [2, 6, 7] and therefore they will not be discussed here.

The commutator II is used in sending signals from the output of the multicontour isoecho unit, unit for the selection of hail centers and the lightning direction finder to the input of the videosignal mixer.

APPROVED FOR RELEASE: 2007/02/08: CIA-RDP82-00850R000300080046-0

APPROVED FOR RELEASE: 2007/02/08: CIA-RDP82-00850R000300080046-0

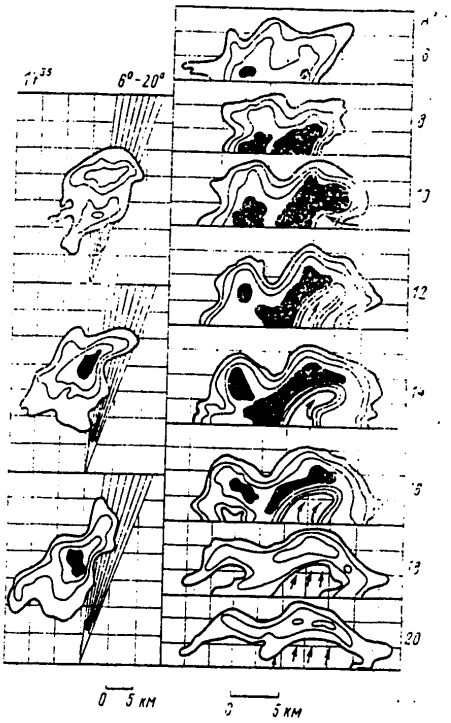

Fig. 4. Structure of supercellular hail cloud observed on 20 August 1976 on IDV display in indicated azimuths (at right). In the IKO display patterns (at left) the lines represent the directions in which vertical sections were made. (The arrows indicate the region of the jet of powerful ascending currents.)

The videosignal mixer is used for mixing the pulses outlining the cloud cover field by reflectivity isolines at all quantization levels with additional information arriving through the other processing channels. In particular, the mixer can be fed (simultaneously or alternately) the thunderstorm direction-finding pulse and echo signals from the thunderstorm center selection device and the turbulence indicator.

The total signal, containing total information on the structure of thunderstorm-hail clouds, is fed to the IKO and IDV standard displays of the meteorological radar through the commutator I.

The clarity of data display can be enhanced by using a system for the color display of signals (for example, reflectivity isolines in white, hail centers and thunderstorm bearings -- in red, turbulence -- in green, etc.

The operation of all the apparatus is synchronized by MRL-5 triggering pulses. When the turbulence indicator is cut in the MRL-5 synchronizer is triggered from it.

APPROVED FOR RELEASE: 2007/02/08: CIA-RDP82-00850R000300080046-0

APPROVED FOR RELEASE: 2007/02/08: CIA-RDP82-00850R000300080046-0

Some Results of Experimental Investigations of the Structure of Thunderstorm-Hail Clouds

The use of several models of apparatus for the routine determination of the structure of thunderstorm-hail clouds under different regional conditions (Northern Caucasus, Transcaucasia, Leningradskaya and Volgogradskaya Oblasts) revealed that:
— apparatus for determining the structure of thunderstorm-hail clouds is easily coupled with the meteorological radars MRL-1, MRL-2, MRL-4, MRL-5 and MRL-6 without changes in their circuitry and design (however, the MRL-1, MRL-2, MRL-4 and MRL-6 radars do not ensure the discrimination of hail centers using formula (1) and instead of them zones of enhanced radioechoes of clouds stand out in the structure of the radioechoes);
-- obtaining a graphic picture of the structure of thunderstorm-hail clouds is ensured in the tempo of automatic circular and vertical scanning of space with rates of rotation of the MRL antenna up to 6 rpm;
— use of apparatus for obtaining the structure of thunderstorm-hail clouds considerably increases the information yield from meteorological radars, by several times reducing the time required for obtaining information on the cellular structure of clouds, about the location of hail centers, thunderstorm discharges, jets of ordered ascending currents, on the relative position of all these zones in clouds, etc.

The pattern of structure of radioechoes of a hail cloud on the IKO and IDV indicators in isolines of radar reflectivity at $\lambda = 10$ cm with the clear revelation of hail centers is shown in Fig. 2. Comparison of the usual pattern of radioechoes of a hail cloud on the IKO indicator (Fig. 2a) and the pattern obtained using the considered apparatus (Fig. 2b,c) indicates a considerable increase in the information yield from the meteorological radar.

The use of the apparatus ensures obtaining the spatial structure of cloud cover in 1.5-2 minutes by photoregistry of the IKO and IDV indicators with different angles of elevation and azimuths of the antenna respectively and also makes it possible to trace the dynamics of development of thunderstorm-hail clouds (Figures 3 and 4), establish the site of generation of new convective cells, detect the zone of maximum hail-forming activity of clouds, determine the altitude of the layer of generation and growth of hail, study the characteristics of hail formation and the nature of propagation of the hail formation process in space, localize the region of ordered ascending currents, etc. For example, the region of ascending currents (even in the absence of a turbulence indicator) is easily detected by superposing the structure of the radioechoes on the IKO indicator at an altitude of 6-7 km above sea level on the structure of the radioechoes at an altitude of 1-2 km above sea level (Fig. 3) as a region of a weak radioecho situated under the cover of a powerful radioecho. It is quite easy to discriminate zones of ascending currents in the structure of radioechoes of hail clouds on the IDV indicator (Fig. 4).

The error in drawing the isolines of reflectivity, consisting of the errors in calibrating the multicontour isoecho unit, time instability of the quantization levels (caused by instability of the power sources for the threshold devices) and

APPROVED FOR RELEASE: 2007/02/08: CIA-RDP82-00850R000300080046-0

APPROVED FOR RELEASE: 2007/02/08: CIA-RDP82-00850R000300080046-0

the errors in averaging the meteorological radar echo, does not exceed ± 3 db.

This causes some noncorrespondence of the position of reflectivity isolines ΔL. In the region of maximum reflectivity gradients ($d\bar{P}_r/dR \approx 30$-60 db/km), observed in hail clouds, ΔL does not exceed the duration of the range discretization interval ($\Delta L_{min} \leq 0.25$ km), whereas in the region of small reflectivity gradients ($d\bar{P}_r/dR \approx 1$-2 db/km) ΔL_{max} is about 1.5-3 km. The accuracy in determining the boundaries of the hail centers with a hail size greater than 1 cm is estimated at 0.2-0.3 km. The error in correction for attenuation does not exceed 2.0 db.

During the period 1976-1978 this apparatus was used in obtaining extensive material on the structure and development of 104 thunderstorm-hail processes in the Northern Caucasus and classifying them on the basis of cellular structure and dynamics of development. It was established that under the conditions prevailing in the Northern Caucasus, depending on the structure of the wind in the troposphere, as under the conditions prevailing in North America [9 and others], there are three types of hail processes: unicellular, multicellular and supercellular. In turn the multicellular processes in the Northern Caucasus are subdivided into three subtypes: ordered, nonordered and weakly organized.

The most intensive and destructive hailfalls, covering areas of about 500-1500 km^2, are observed in the case of supercellular processes consisting of one enormous (measuring 30 x 50 km) asymmetric cell (see Fig. 3) having a lifetime of 0.5-3 hours. Supercellular processes are observed in 12% of the cases of observations.

Multicellular processes are observed most frequently (in 64% of the cases). They consist of several asymmetric convective cells in different stages of development. New convective cells in ordered multicellular processes are generated on the right windward flank of the cloud system, old cells are destroyed on its leeward flank and in nonordered multicellular processes this is noted in any part of the cloud system. The greatest hail-forming activity in supercellular and multicellular processes is also observed on the windward flank of the cloud system. In unicellular processes, observed in 24% of the cases and consisting of axisymmetric cells which have low mobility with a minimum lifetime, hail formation is observed in their central part.

The hail formation process in unicellular processes has a discrete spatial propagation, in multicellular processes hail formation has a discrete-continuous propagation (as a result of the continuous propagation of individual cells and the periodic development of new cells on the right flank), and in supercellular processes -- continuous propagation in the direction of movement.

Powerful hail cells usually move 30-60° to the right of the direction of the steering current, although in the development and dissipation stages they move along the steering current. Jets of powerful ascending currents in powerful hail-forming cells of supercellular and multicellular processes are also displaced toward the windward flank, somewhat to the right of the hail center. The region of powerful radioechoes, hanging over the ascending flows, extends forward and to the right (by 0-90°) relative to the direction of movement of the hail center.

APPROVED FOR RELEASE: 2007/02/08: CIA-RDP82-00850R000300080046-0

APPROVED FOR RELEASE: 2007/02/08: CIA-RDP82-00850R000300080046-0

The velocity of movement of powerful hail clouds is 1.5-2 times less than the velocity of the steering current and only weak convective cells can virtually completely entrain them.

Since the structure, dynamics of development and character of propagation of the hail formation process in unicellular, multicellular and supercellular hail processes are substantially different, a scheme for modification for the purpose of interrupting and preventing hail formation should be differentiated with respect to the types of hail processes [3]. The apparatus for determining the structure of the thunderstorm-hail clouds will make it possible to carry out routine identification of their types and choose optimum seeding schemes. In addition, the graphic display of the cellular structure of thunderstorm-hail clouds with an indication of the position of the hail centers and jets of ascending currents will ensure exclusion of many standard errors of operators in the modification of hail processes (for example, the seeding of the zone of localization of hail, regions of the most powerful ascending currents, etc.) and will make it possible to carry out a more purposeful modification, which evidently will make possible a substantial increase in the effectiveness of hail protection and a reduction of the means spent on modification.

The positions of the zones of localization of hail, increased turbulence, lightning discharges and heavy precipitation, dangerous for aircraft flights, discriminated against the background of the field of reflectivity of clouds, can be of great importance for ensuring the safety of aircraft flights under complex meteorological conditions.

Summary

The operational radar method and apparatus for graphic display of the structure of thunderstorm-hail clouds, including a multicontour isoecho unit, a unit for the discrimination of hail centers, a unit for making corrections for attenuation, a turbulence indicator and a thunderstorm direction finder, ensuring the discrimination of hail centers, lightning discharges, zones of increased turbulence and zones of ascending currents against the background of cloud structure in the form of a multicontour isoecho, will considerably increase the meteorological information yield of meteorological radars and can be used:
-- in the hail protection service for identifying types of hail processes, localization of the object and zone to be modified, selection of the optimum seeding scheme and monitoring the modification results;
-- in the storm warning service for the localization of thunderstorm and hail centers, zones of dangerous bumping, increased liquid-water content and heavy precipitation;
-- in the monitoring of air movement for ensuring flight safety in a zone with a cumulonimbus cloud cover;
-- in investigating thunderstorm and hail clouds for study of their cellular structure and dynamics of development under different regional conditions, for investigating the hail formation process and the nature of its spatial propagation, position and characteristics of hail centers, zones of ascending currents, zones of increased turbulence and thunderstorm activity, relative position of these zones in clouds of different structure and their mutual influence, remote measurement of areas of falling of hail, development of experimental models of

APPROVED FOR RELEASE: 2007/02/08: CIA-RDP82-00850R000300080046-0

APPROVED FOR RELEASE: 2007/02/08: CIA-RDP82-00850R000300080046-0

thunderstorm-hail clouds, etc. In this connection it is evidently desirable that the standard-produced MRL-5 meteorological radar and its single-wave modifications MRL-4 and MRL-6 be supplied with attachments for the routine determination of the structure of thunderstorm-hail clouds.

BIBLIOGRAPHY

1. Anshayev, M. T., Dadali, Yu. A., "Localization of Hail Centers and Cumulonimbus Clouds," METEOROLOGIYA I GIDROLOGIYA (Meteorology and Hydrology), No 9, 1970.

2. Abshayev, M. T., et al., "Specialized Radar for Hail Protection and Storm Warning (MRL-5) and its Meteorological Effectiveness," TRUDY VGI (Transactions of the High-Mountain Geophysical Institute), No 33, 1976.

3. Abshayev, M. T., Zhuboyev, M. M., "Principles for the Modification of Unicellular, Multicellular and Supercellular Hail Processes," TRUDY VGI, No 39, 1978.

4. Abshayev, M. T., Pashkevich, M. Yu., "Methods and Units for Display of the Structure of Radioechoes of Meteorological Objects on Black-and-White Radar Screens," TRUDY VGI, No 33, 1976.

5. Author's Certificate 253178 (USSR), "Indicator Device of a Radar Station for Determining the Parameters of Atmospheric Inhomogeneities," I. M. Baranov, Mezhd. Kl. $G10l_S$, 1967.

6. Baru, N. V., Kononov, I. I., Solomonik, M. Ye., RADIOPELENGATORY-DAL'NOMERY BLIZHNIKH GROZ (Radio Direction Finders for Remote Range Determination of Near Thunderstorms), Leningrad, Gidrometeoizdat, 1976.

7. Mel'nichuk, Yu. V., Chernikov, A. A., "Operational Method for Detecting Turbulence in Clouds and Precipitation," TRUDY TsAO (Transactions of the Central Aerological Observatory), No 110, 1973.

8. Atlas, D., "Method and Apparatus for Radar Turbulence Detection," United States Patent No 3646555, Int. Cl. G01s9/02, G 01, No 1/00.

9. Chisholm, A. J., Renick, J. H., "Supercell and Multicell Alberta Hailstorms," INT. CLOUD PHYSICS CONF., London, 1972.

10. Lhermitte, R. M., Shreeve, K. H., Erdahl, R. J., "Waveform Averaging and Continuing Device for Weather Radar and the Like," United States Patent Office, No 3366951, Int. Cl., 343-5, 1968.

11. Marwitz, J. D., Auer, A. H., "Locating the Organized Updraft on Severe Thunderstorms," J. APPL. METEOROL., No 11, 1972.

APPROVED FOR RELEASE: 2007/02/08: CIA-RDP82-00850R000300080046-0

APPROVED FOR RELEASE: 2007/02/08: CIA-RDP82-00850R000300080046-0

UDC 551.577.21

PRINCIPLES FOR DETERMINING THE MAXIMUM LAYER OF PRECIPITATION DURING A COMPUTATION TIME INTERVAL

Moscow METEOROLOGIYA I GIDROLOGIYA in Russian No 10, Oct 80 pp 39-43

[Article by Candidate of Geographical Sciences M. N. Sosedko, Ukrainian Regional Scientific Research Institute, manuscript submitted 4 Apr 80]

[Text]

Abstract: It is shown that the approaches used in the generalization of precipitation gage data do not make it possible to obtain reliable information on the maximum quantities of precipitation during definite summation intervals. In this connection proposals are expressed concerning improvement of the processing of data from standard measurements of precipitation in the hydrometeorological network.

The maximum quantity of precipitation during a definite time interval whose probability of recurrence or nonexcess is known, is an important climatic parameter which can be used in many practical problems, especially in water management planning. The most widely used characteristic of rain of this type is the diurnal precipitation maximum. With respect to the problem of description, analysis and computation of the maximum diurnal layers of precipitation of different probability there are numerous publications, maps of their spatial distribution have been published, and also reference aids. We will mention only some of the studies, including those relating to the territory of the Ukraine [3-6, 8-10, 14].

The values of the diurnal precipitation maxima P_{day}^{max} are usually selected from their quantities computed as the sum for all scheduled observation times of meteorological (sometimes calendar) days. However, it must be noted that such an approach to the generalization of precipitation can be legitimate only for determining its total quantity for long time intervals (10-day period, month, etc.). But with respect to the diurnal precipitation maxima such a processing procedure is in principle unsubstantiated. Indeed, by such an operation parts of one and the same rain can fall on different (successive) days, although in practice the greatest layer of precipitation for a meteorological day is usually identified with the precipitation maximum for 24 hours ($P_{\Delta t = 24}^{max}$). Thus, as a result of time shifts in the falling of rain (especially advance of its "core") with one and the same quantity

APPROVED FOR RELEASE: 2007/02/08: CIA-RDP82-00850R000300080046-0

APPROVED FOR RELEASE: 2007/02/08: CIA-RDP82-00850R000300080046-0

of precipitation registered in 24 hours when using the adopted processing scheme it is possible to obtain different values of the diurnal sums. Naturally, the diurnal precipitation sums will usually be less than the 24-hour values. This circumstance has already been pointed out, especially in [11].

Now we will cite a number of characteristic examples.

Source [13] described a very heavy rain during which on 3-4 August 1959 in the neighborhood of Lutsk in Volynskaya Oblast the precipitation total was 179-192 mm. At Lutsk meteorological station the quantity of precipitation in 6 hours (from 1810 hours on 3 August to 0010 hours on 4 August) was 179 mm, of which during the meteorological day 3 August 65 mm fell, whereas the remaining 114 mm, as a result of such a time breakdown, was assigned to 4 August. Then these same 114 mm were included in the processing as the maximum observed layer of precipitation for the HANDBOOK OF USSR CLIMATE [14] with an indication of this value in giving a precipitation maximum with a 1% probability equal to 116 mm.

During the period 8-10 June considerable rains fell in the Ukrainian Carpathians and over Ciscarpathia. The rain-induced high waters caused by them had a catastrophic character. However, the diurnal precipitation maxima registered during this period do not give an adequately complete idea concerning the spatial distribution of the principal centers of intensive runoff formation. As indicated by a comparison of the P^{max}_{day} and $P^{max}_{\Delta t=24}$ values (see Table 1), the difference between them attains 35-40%. Among the 29 observation points, only at 10 do these characteristics coincide.

The value of the difference between P^{max}_{day} and $P^{max}_{\Delta t=24}$ is dependent in each individual case on the position of the core of the precipitation on the time axis. Accordingly, it is entirely obvious that it is impossible to assume the presence of any pattern in the variation of these deviations or their dependence on physiographic factors. It is only possible to judge the existence of a definite, significant range of variation of this difference, attaining 50% of the $P^{max}_{\Delta t=24}$ value. In a general case the values of the characteristics of the maximum layers of precipitation are interrelated by the inequality

$$P^{max}_{\Delta t=24} \geqslant P^{max}_{day} \geqslant 0.5P^{max}_{\Delta t=24}. \quad (1)$$

In addition, the P^{max}_{day} values not only inadequately precisely reflect the conditions for the formation and the precipitation regime in some physiographic region with respect to the quantity of maximum precipitation with a rare frequency of occurrence, but also distort its distribution with respect to the frequency ranges. This can be seen, for example, from a comparison of the curves for the probability of these characteristics on the basis of data for the meteorological station Turka during 1946-1975. In this case the diurnal maximum of precipitation with a 1% probability is 44 mm (34%) less than the corresponding maximum for the 24-hour interval (see Fig. 1).

Thus, it can be stated that the values of the maximum diurnal layers of precipitation have an uncertainty caused by the method employed in obtaining them. As a result, sets of P^{max}_{day} values are statistically inhomogeneous.

APPROVED FOR RELEASE: 2007/02/08: CIA-RDP82-00850R000300080046-0

APPROVED FOR RELEASE: 2007/02/08: CIA-RDP82-00850R000300080046-0

A similar situation exists in the statistical generalization of the maximum layers of precipitation for shorter time intervals. As indicated by experimental computations on the basis of data from the precipitation gage network in the basin of the upper Dnestr, the limitation of the computation interval to the times at which precipitation is measured (0300, 0900, 1500, 2100 hours at meteorological stations and 0800 and 2000 hours at posts) creates different variants of breakdown of the rainfall hyetograph. The latter circumstance in turn leads to an understatement of the computed precipitation values in the same limits as in a 24-hour summation interval (1). This is noted especially frequently when processing heavy prolonged rains, when we operate with the parameters most important for practical purposes: precipitation with a rare frequency of occurrence.

A generalization of sets of maximum precipitation values during time intervals not tied in to definite times of onset, but established by means of discriminating the parts of the hyetographs with the greatest rainfall intensity, is genetically and statistically justified. With adherence to this principle we ascertain the actual maximum layers of precipitation during a computation interval. And only with such an approach will the numerical values of the precipitation maxima reflect the conditions of shower activity and characterize the processes of formation of precipitation in some physiographic region and can also constitute sets of random values whose patterns can be determined by the methods of mathematical statistics.

The principle for generalization of the maximum layers of precipitation, excluding the tie-in of the computation intervals of their summation to the limits of the meteorological day, was used by G. A. Alekseyev in computations of the maximum discharges of rain-induced high waters on the basis of the limiting intensity formula which he proposed [1, 2], which subsequently was included in the norms-instructions for determining the computed hydrological characteristics [12]. The author of the recommendations [1, 2] developed a method for determining and territorial generalization of precipitation layers for computation time intervals Δt equal to the travel time of the water to the lowest-lying station in the fluvial drainage basin.

However, due to the limited amount of information on precipitation during different time intervals, in this method the diurnal precipitation layers were also used as the initial parameter. The computations essentially involve construction of regional precipitation reduction curves whose ordinates $\psi^p_{\Delta t}$ are determined from the ratio

$$\psi^p_{\Delta t} = \frac{P^p_{\Delta t}}{P^p_{\text{сут}}}, \qquad (2)$$

[СУТ = day]

that is, are expressed in fractions of the diurnal sums of precipitation of the same probability p% as the value of the maximum precipitation layer during the interval Δt - $P^p_{\Delta t}$.

In case of necessity the sought-for value of the precipitation layer with a stipulated probability of excess for any time interval is obtained by multiplying the diurnal precipitation layer, read, for example, from the map of the spatial distribution of precipitation maxima of this same probability, by the

APPROVED FOR RELEASE: 2007/02/08: CIA-RDP82-00850R000300080046-0

APPROVED FOR RELEASE: 2007/02/08: CIA-RDP82-00850R000300080046-0

Table 1

Maximum Quantity of Precipitation in Meteorological Day P^{max}_{day} and 24-Hour Interval $P^{max}_{\Delta t=24}$ in June 1969 in Upper (Right-Bank) Dnestr Basin

Precipitation gage stations	P^{max}_{day}, mm	$P^{max}_{\Delta t=24}$, mm	$P^{max}_{\Delta t=24} - P^{max}_{day}$	
			mm	%
Strelki	73	112	39	35
Sambor	46	54	8	15
Rozdol	28	47	19	40
Galich	26	33	7	21
Ozimina	27	34	7	21
Drogobych	39	45	6	13
Matkov	55	65	10	15
Novyy Kropivnik	136	205	69	34
Verkhneye Sinevidnoye	97	120	23	19
Stryy	51	51	0	0
Turka	66	101	35	35
Rybnik	117	175	58	33
Skole	131	138	7	5
Slavskoye	81	85	4	5
Ruzhanka	113	134	21	16
Tukhlya	109	146	37	25
Svyatoslav	172	205	33	16
Oleksichi	54	54	0	0
Myslovka	164	175	11	6
Zarechnoye	53	58	5	9
Goshev	51	51	0	0
Tisov	113	113	0	0
Osmoloda	166	194	28	14
Pervozets	48	48	0	0
Spas	88	88	0	0
Guta	239	239	0	0
Pasechna	214	214	0	0
Dolina	88	88	0	0
Ivano-Frankovsk	75	75	0	0

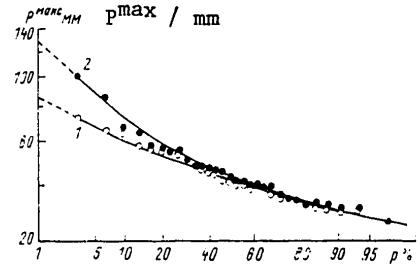

Fig. 1. Curve of probability of maximum diurnal and 24-hour sums of precipitation p^{max} (1 and 2 respectively) according to data for Turka meteorological station.

APPROVED FOR RELEASE: 2007/02/08: CIA-RDP82-00850R000300080046-0

APPROVED FOR RELEASE: 2007/02/08: CIA-RDP82-00850R000300080046-0

corresponding ordinate $\psi^{P}_{\Delta t}$. Thus, in this method as well the main computation characteristic is the maximum precipitation sum during the meteorological day.

It is impossible to deny the fact that the approach proposed by G. A. Alekseyev for generalization of the maximum precipitation layers, which has come into wide use (in particular, for the Ukrainian Carpathians region [6, 9]), is a substantial contribution to solution of one of the most important problems in hydrological computations. Nevertheless, orientation in the determination of the computed layers of precipitation on their maximum values for a meteorological day, although this is attributable to the limited volume of detailed information, to a certain degree lessens the value of this method. For this purpose it would be more valid to use the generalized characteristics of precipitation maxima for a 24-hour summation interval not tied into a constant initial reading time.

Summary

1. The employed procedures for the generalization of precipitation do not ensure obtaining their maximum values during definite summation intervals. The tie-in of the limits of the time interval to the established times set for the measurement of precipitation often leads to an understatement of their computed layers by 30-50%. As a result of such a time breakdown of the hyetograph there is a loss of important information on the precipitation regime and the frequency of occurrence of its maximum levels.

2. The maximum diurnal layers of precipitation, which in actual practice are identified with the maxima of precipitation falling in 24 hours, in many cases are considerably understated in comparison with the latter. It is not precluded that such information is not of high informative value for the user and may even lead him astray.

In addition, the statistical description of sets of maximum diurnal precipitation sums in principle is not legitimate since they were formed from nonuniform elements.

3. Due to the limited extent of the network of automatic rain recorders, whose data are used in determining the precipitation maxima during the computation intervals, regardless of the position of their summation limits on the time axis, it is extremely desirable to use the entire precipitation gage network for this purpose. Special difficulties are not foreseen here; it is only necessary to introduce additional characteristics of rains which in the processing of standard meteorological observations would be included in the summaries of the TM-1 (TM-8) tables. From observational data collected at meteorological stations it is possible to select the maximum precipitation sums for 1200 and 2400 hours, and from data for hydrometeorological posts, for 2400 hours, close to the true values.

BIBLIOGRAPHY

1. Alekseyev, G. A., "Method for Computing the Maximum Rain Discharges of Water from Precipitation Reduction Curves," TRUDY GGI (Transactions of the State Hydrological Institute), No 107, 1963.

APPROVED FOR RELEASE: 2007/02/08: CIA-RDP82-00850R000300080046-0

APPROVED FOR RELEASE: 2007/02/08: CIA-RDP82-00850R000300080046-0

2. Alekseyev, G. A., "Objective Statistical Methods for Determining the Characteristics of Shower Precipitation," METEOROLOGIYA I GIDROLOGIYA (Meteorology and Hydrology), No 7, 1966.

3. ATLAS RASCHETNYKH KHARAKTERISTIK DOZHDEVYKH OSADKOV ZA TEPLYY (KHOLODNYY) PERIOD GODA PO TERRITORII UKRAINSKOY SSR (Atlas of Computed Characteristics of Rain Precipitation During the Warm (Cold) Period of the Year Over the Territory of the Ukrainian SSR), edited by M. M. Ayzenberg, Kiev, Izd. UGMS UkrSSR, 1967.

4. Vishnevskiy, P. F., "Variability of the Maximum Shower and Allowance for This Phenomenon in Hydrological Computations," TRUDY UkrNIGMI (Transactions of the Ukrainian Scientific Research Hydrometeorological Institute), No 123, 1973.

5. Golub, Ye. V., "Catastrophic Precipitation in the Ukrainian Carpathians," METEOROLOGIYA I GIDROLOGIYA, No 7, 1971.

6. Kiptenko, Ye. N., Lyutik, P. M., "Maximum Diurnal Precipitation in the Ukrainian Carpathians," TRUDY UkrNIGMI, No 147, 1976.

7. Lebedev, A. N., Fan, A. A., "Investigation of the Maximum Semidiurnal and Diurnal Precipitation Sums," METEOROLOGIYA I GIDROLOGIYA, No 11, 1975.

8. Loyeva, I. D., "On Investigation of Abundant Rains in the Ukrainian Carpathians," TRUDY GGO (Transactions of the Main Geophysical Observatory), No 266, 1970.

9. Lyutik, P. M., Kiptenko, Ye. N., Bedratenko, V. T., "Computed Characteristics of Rain Precipitation in the Carpathians," TRUDY UkrNIGMI, No 119, 1972.

10. MATERIALY PO RASCHETNYM KHARAKTERISTIKAM DOZHDEVYKH NAVODKOV (Materials on the Computed Characteristics of Rain-Induced Floods), Leningrad, Gidrometeoizdat, 1969.

11. "Computations of Maximum Rain-Induced Runoff in the Rivers of Primorskiy Kray Using Nonlinear Electronic Analog Computers," TRUDY GGI, No 211, 1973.

12. RUKOVODSTVO PO OPREDELENIYU RASCHETNYKH GIDROLOGICHESKIKH KHARAKTERISTIK (Manual on Determination of Computed Hydrological Characteristics), Leningrad, Gidrometeoizdat, 1973.

13. Sosedko, M. N., "Strong Shower in Volynskaya Oblast," METEOROLOGIYA I GIDROLOGIYA, No 6, 1960.

14. SPRAVOCHNIK PO KLIMATU SSSR (Handbook of USSR Climate), No 10, Part IV, Leningrad, Gidrometeoizdat, 1969.

APPROVED FOR RELEASE: 2007/02/08: CIA-RDP82-00850R000300080046-0

APPROVED FOR RELEASE: 2007/02/08: CIA-RDP82-00850R000300080046-0

UDC 551.555(267)

NATURE OF EQUATORIAL WESTERLIES IN THE INDIAN OCEAN

Moscow METEOROLOGIYA I GIDROLOGIYA in Russian No 10, Oct 80 pp 44-51

[Article by Candidate of Physical and Mathematical Sciences L. M. Krivelevich and Candidate of Geographical Sciences Yu. A. Romanov, Institute of Oceanology USSR Academy of Sciences, manuscript submitted 28 Dec 79]

[Text]

Abstract: Within the framework of a zonal model of the equatorial circulation of the atmosphere the authors have computed the wind velocity components in the lower troposphere near the equator on the basis of stipulated meridional profiles of surface atmospheric pressure. The analysis shows that whatever may be the meridional surface pressure profile observed in the Indian Ocean it is not possible to model any westerly flow at the equator of such an intensity as is observed in nature. It is therefore concluded that the zonal pressure gradient must play an important role in formation of equatorial westerly winds in the Indian Ocean.

In this article a study is made to ascertain to what degree meridional gradients of atmospheric pressure can cause the appearance of equatorial westerlies in the Indian Ocean. The latter, as is well known, can be traced year-round in the lower troposphere over virtually the entire eastern hemisphere [6], but this element of global circulation of the atmosphere attains its greatest spatial distribution, intensity and regularity in the Indian Ocean, in the zone 60 and 90°E.

Figure 1a, taken from a study by Ye. K. Semenov [7], shows that in the northern summer the zone of equatorial westerlies (ZEW) at the center of the Indian Ocean (at 75°E) is displaced northward and expands, in winter it shifts southward and becomes narrower, whereas in the transition seasons it occupies a position approximately symmetric relative to the equator, at the 850-mb level occupying a zone from 5-7°S to 5-7°N.

Hypotheses

APPROVED FOR RELEASE: 2007/02/08: CIA-RDP82-00850R000300080046-0

APPROVED FOR RELEASE: 2007/02/08: CIA-RDP82-00850R000300080046-0

Several different hypotheses have been expressed at different times concerning the reasons for formation of the ZEW [5]. The classical hypothesis of "deflected Trades" attributes the equatorial westerlies to monsoonal pressure troughs developing in summer in the northern hemisphere in the northern part of India and in winter in the southern hemisphere, at latitudes 10-15°S. According to this hypothesis, the Trades in the winter hemisphere, flowing across the equator into the southern hemisphere, gradually enter into geostrophic equilibrium with the meridional pressure gradient on the equatorial side of the monsoonal trough and thereby acquire a westerly wind velocity component.

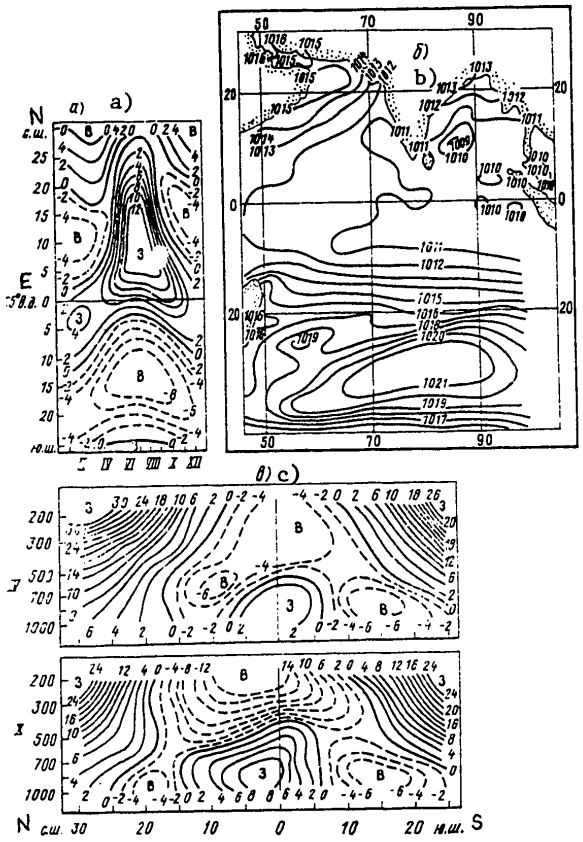

Fig. 1. Annual variation of the zonal wind velocity component in the Indian Ocean at meridian 75°E at the 850-mb surface [7] (a), mean long-term surface pressure field in the Indian Ocean in November [13] (b) and meridional sections of zonal wind component along 80°E in April and October [7] (c).

APPROVED FOR RELEASE: 2007/02/08: CIA-RDP82-00850R000300080046-0

APPROVED FOR RELEASE: 2007/02/08: CIA-RDP82-00850R000300080046-0

This hypothesis is correct for the westerlies developing in the neighborhood of a monsoonal trough far from the equator, but it cannot explain the presence of westerlies at the equator itself, much less than in the zone adjacent to the equator in the direction of the winter hemisphere (Fig. 1). This is confirmed by model computations of atmospheric circulation near the equator [1, 2] which show that with a more or less uniform decrease in atmospheric pressure from the winter to the summer hemisphere the easterly winds of the winter hemisphere must reach the equator, under the influence of inertia should cross into the summer hemisphere and be replaced there by westerly winds only at a distance of several degrees from the equator.

Figure 1a shows that westerly winds at the equator itself and near it are observed virtually throughout the year but the factor of greatest interest for analysis is the distribution of westerlies in the transitional seasons, quasisymmetric relative to the equator. It can be surmised that the mechanism of formation of westerlies at the equator itself is manifested during this period in the most explicit form, whereas in winter and summer together with it a powerful influence on the distribution of equatorial westerlies is exerted by the already mentioned monsoonal troughs.

There are several hypotheses explaining the presence of westerly winds at the equator and near it which can be divided roughly into two groups depending on what pressure gradients, meridional or zonal, are considered most important in the formation of these winds.

According to Fletcher [10], the equatorial westerlies develop under the influence of meridional pressure gradients caused by the presence of two pressure troughs (one of which can be monsoonal), situated approximately parallel to one another, one on each side of the equator. Fletcher [5] proposed an interesting, although not universal hypothesis concerning the mechanism of periodic formation of such troughs. Such troughs are actually observed on the synoptic charts of the Indian Ocean [5, 6] and are traced rather clearly on climatic charts of surface pressure for the spring and autumn months. As an example, Fig. 1b shows a chart of the mean long-term surface pressure for November on the basis of data in [13].

Palmer, who investigated atmospheric circulation in the western tropical part of the Pacific Ocean [12], assumes that the equatorial westerlies owe their origin to tropical depressions moving from east to west, often developing simultaneously on the two sides of the equator. In actuality, the principal role in the formation of the equatorial westerlies is here once again assigned to the meridional pressure gradients, but not constant, as indicated by Fletcher, but arising periodically with the frequency of passage of tropical depressions. This hypothesis is supported in [8].

In contrast to the above-mentioned authors, Khromov [9], and also Frost and Stephenson [11], assume that the main reason for the equatorial westerlies in the Indian Ocean is the pressure drop in the zonal direction caused by more intensive heating and accordingly the lower surface pressure over the region of Indonesia and New Guinea in comparison with the equatorial zone at the center of the Indian

APPROVED FOR RELEASE: 2007/02/08: CIA-RDP82-00850R000300080046-0

APPROVED FOR RELEASE: 2007/02/08: CIA-RDP82-00850R000300080046-0

Ocean. This hypothesis also has its supporters [5], who indicate, in particular, that the formation of the pressure lows on the boundary of the equatorial westerlies on both sides of the equator can be one of the consequences of and not the reason for the appearance of equatorial westerlies.

Checking of One of Hypotheses

In order to check the correctness of the hypothesis of formation of the zone of equatorial westerlies in the Indian Ocean under the influence of meridional pressure gradients we decided to use a zonal stationary "dry" model of equatorial circulation which we described in detail in [1]. We recall that in the equations of motion in this model, in addition to the pressure gradient and Coriolis forces, an allowance is made for advective acceleration, and also vertical and horizontal turbulent exchange with exchange coefficients equal to 10^5 and 1 m/sec^2 respectively. The computations are made for a meridional section from 13°S to 13°N with an altitude of 11 km, along which is stipulated a meridional profile of the surface pressure gradient decreasing with altitude in conformity to the law e^{-az}, and at the northern and southern boundaries of the section it is necessary to have a geostrophic balance with vertical friction taken into account. As a result of numerical computations we obtain the distribution of the wind velocity components u, v and w at all the internal points of the section.

Earlier, using this model, we succeeded in obtaining a pattern of equatorial circulation in the lower troposphere for a case characteristic for the Tropical Atlantic with one pressure trough asymmetric to the equator [2], which is close to that actually observed. On this basis we assumed that by stipulating in the model the profile of the meridional pressure gradient characteristic of regions of the prevalence of the equatorial westerlies and by comparing the computed distribution of the wind velocity components with the actual distribution for these regions we will be able to make a correct evaluation of how adequately the real atmospheric circulation near the equator is reflected in such computations and it will be possible to draw conclusions concerning the correctness of the hypothesis relating the equatorial westerlies in the Indian Ocean to meridional pressure gradients.

We note that the equatorial westerlies at the center of the Indian Ocean in the transition seasons have some distinguishing characteristics which can serve as points of reference in a comparison of the results of observations and the results of computations.

Figure 1c shows that the intensity of equatorial westerlies can vary in dependence on season, but in both April and in October the maximum velocity of the westerly wind is observed in the central part of the zone, approximately at the equator, at an altitude of about 1.5 km. Such a pattern in the distribution of the westerlies is traced both on the basis of mean long-term data and on the basis of data from regularly scheduled observations [5].

Judging from satellite observations [3], as well as observational data collected by ships [5], along the northern and southern boundaries of the ZEW in the Indian Ocean there are usually thick concentrations of clouds forming the so-called northern and southern branches of the ICZ.

APPROVED FOR RELEASE: 2007/02/08: CIA-RDP82-00850R000300080046-0

APPROVED FOR RELEASE: 2007/02/08: CIA-RDP82-00850R000300080046-0

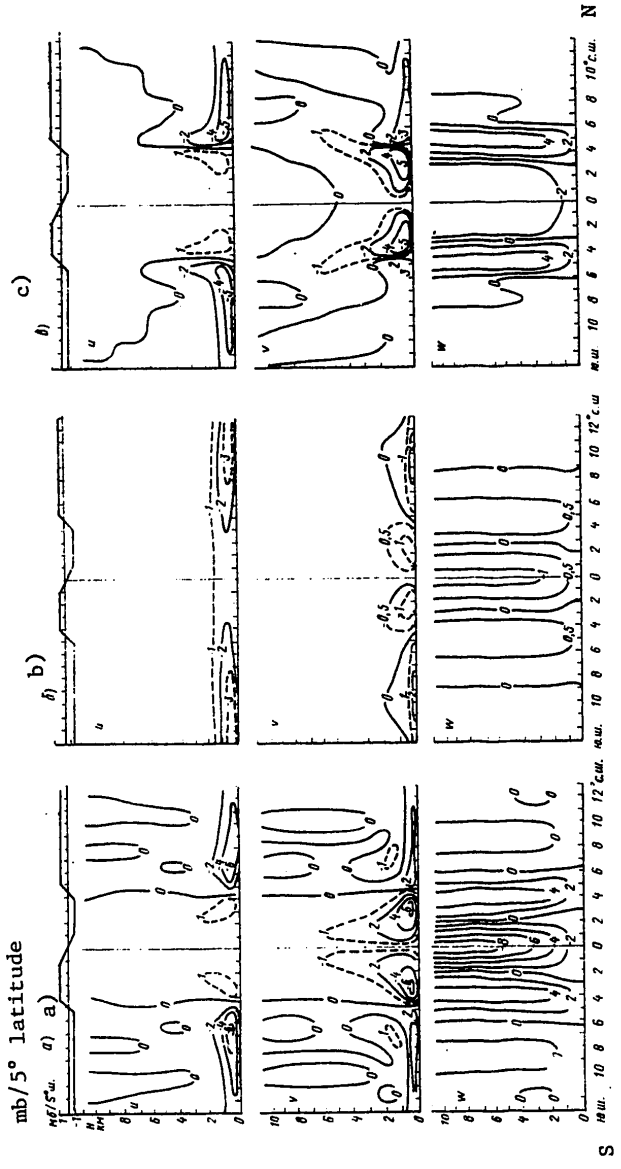

Fig. 2. Results of computations of zonal, meridional and vertical components of wind velocity for different values of coefficient of horizontal turbulent exchange. a) $A_1 = 10^5$ m^2/sec, b) $A_1 = 3 \cdot 10^6$ m^2/sec, c) $A_1 = 0$.

APPROVED FOR RELEASE: 2007/02/08: CIA-RDP82-00850R000300080046-0

APPROVED FOR RELEASE: 2007/02/08: CIA-RDP82-00850R000300080046-0

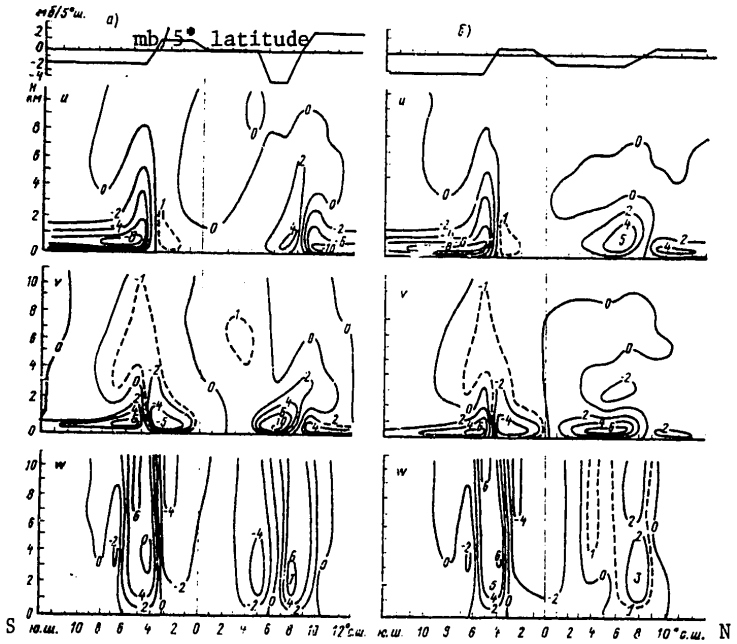

Fig. 3. Results of computations of zonal, meridional and vertical wind velocity components with $A_t = 10^5$ m^2/sec for different profiles of meridional surface pressure gradient.

The presence of the latter indicates the intensity of the ascending air flows in these regions of the ocean, that is, at the boundaries of the ZEW. On the other hand, at the equator itself, for example on Gan Island [11], the development of cloud cover in general is suppressed, which indicates the predominance of descending air flows here. Unfortunately, for the ZEW we did not find representative sections of the meridional wind component, and accordingly, could not note any distinguishing characteristics in its distribution.

It should be noted that in the Indian Ocean, in the ZEW, insofar as we know, on not a single one of the expeditions were there synchronous measurements of atmospheric pressure on the many ships which might have been at different latitudes along one and the same meridian, as was the case in the Atlantic Ocean during the TROPEKS-74 expedition [4]. Accordingly, in stipulating the initial profiles of meridional surface pressure gradients for the computations we relied on climatic charts (see Fig. 1b), as well as data from meteorological observations on the scientific research ship "Vityaz'" when carrying out a series of meridional runs intersecting the ZEW [5].

We note further that it scarcely makes sense to compare the results of numerical computations with the actual distribution of the wind above 3-5 km because in all the variants of the computations in our model we stipulated a decrease in the

APPROVED FOR RELEASE: 2007/02/08: CIA-RDP82-00850R000300080046-0

APPROVED FOR RELEASE: 2007/02/08: CIA-RDP82-00850R000300080046-0

gradient with altitude in conformity to the law e^{-az}, which at great altitudes can lead to substantial differences of the values in the model and real pressure gradients.

Now we will proceed to an analysis of the results of the numerical computations presented in Figures 2 and 3.

In the upper part of each of these figures we have shown the profiles of meridional surface pressure gradients for which computations of the wind velocity components were made.

Figure 2a shows the results of computations for a case characteristic of the transition seasons with two pressure troughs symmetric relative to the equator whose axes are situated at 6°S and 6°N and with values of the pressure gradients equal to 1 mb/5° latitude typical for the equatorial zone.

This figure shows that in the distribution of the vertical wind velocity component there is clear manifestation of those peculiarities which, as noted above, are characteristic of the ZEW in the Indian Ocean. At the equator there are in fact descending currents, whereas at the boundaries there are ascending currents with the possible vertical velocity values. However, there is so such agreement in the distribution of the zonal wind velocity component. Instead of one central core with the maximum value of the westerly wind velocity component there are two cores displaced toward the boundaries of the ZEW. At the equator, however, the maximum value of the westerly wind velocity component is at an altitude of 1-2 km and is only 0.3 m/sec.

With an increase in the meridional pressure gradients by double in comparison with those shown in Fig. 2a the values of the westerly wind velocity component are also approximately doubled (this is not shown in the figure), but the two-core pattern of distribution of these components remains unchanged. All this means that horizontal turbulent exchange and flow inertia in such a formulation of the problem (presence only of meridional pressure gradients) are not capable of redistributing the wind flows in such a way that the greatest values of the westerly wind velocity component would fall in the central part of this zone.

Despite the fact that in our earlier computations [1, 2] the best agreement with observational data was obtained when using a coefficient of horizontal turbulent exchange A_λ equal to 10^5 m^2/sec, we nevertheless decided to check whether our present result would improve if some other A_λ values were stipulated.

An extremely interesting pattern is obtained with an increase in A_λ to $3 \cdot 10^6$ m^2/sec. In this case (Fig. 2b), with the same pressure gradients as in the first variant of the computations, the westerlies completely disappear from the equatorial region. The isolines of equal wind velocities are smoother, but in the entire section there is a prevalence only of winds of easterly directions, which still more diverges from the actual distribution than the results of the first variant of the computations. However, it is interesting that in the distribution of the vertical wind velocity component this time as well in the equatorial region there are

APPROVED FOR RELEASE: 2007/02/08: CIA-RDP82-00850R000300080046-0

APPROVED FOR RELEASE: 2007/02/08: CIA-RDP82-00850R000300080046-0

descending currents, whereas near the axes of the pressure troughs there are ascending currents, although with lesser wind velocities than in Fig. 2a.

Figure 2c shows the results of computations obtained with $A_l = 0$. We see that all the wind velocity components, especially the vertical component, increase considerably in comparison with the computations in the first variant but the two-core pattern of distribution of the westerly wind velocity component is still more accentuated, so that at the equator the westerly component even becomes equal to zero.

The results of two other variants of the computations are presented in Fig. 3. They relate to cases when the pressure troughs are situated at different distances from the equator and in the neighborhood of the trough more distant from the equator the pressure gradient is stipulated greater than for the other trough, which can be interpreted as an accentuation of the corresponding trough and the development of a tropical depression in it. In this case in the distribution of the wind velocity component there is found to be a whole series of peculiarities, among which we should note the following. First, there is an entirely understandable increase in all the wind velocity components in the neighborhood of the deeper pressure trough. Second, there are secondary axes of ascending currents, somewhat raised above the ocean, in the neighborhood of both troughs, and also splitting of the region of descending movements, as a result of which the maximum velocities of "settling" are not observed at the equator, but in regions situated on the equatorial side of the trough axes. Without discussing a number of interesting details in the distribution of the wind velocity components, in Fig. 3 we present the principal result: at the equator the westerlies at the equator in this case as well do not attain any significant values and above 1.5 km they are completely replaced by easterly winds with a velocity up to 0.7 m/sec.

Summary

We see that in no variant of the computations could we obtain westerly winds at the equator with the velocities 4-8 m/sec really observed in nature (often more than 10 m/sec [5]). In our opinion this is evidence that some meridional pressure gradients cannot create a westerly flow of such intensity at the equator. Thus, the results which we obtained give basis for assuming that zonal pressure gradients must play a significant role in forming the ZEW in the Indian Ocean.

BIBLIOGRAPHY

1. Krivelevich, L. M., Romanov, Yu. A., "Some Characteristics of Atmospheric Circulation in the Equatorial Latitudes of the Oceans," METEOROLOGIYA I GIDROLOGIYA (Meteorology and Hydrology), No 5, 1977.

2. Krivelevich, L. M., Romanov, Yu. A., "Results of Computations of Equatorial Circulation of the Atmosphere for a Zonal Pressure Field," METEOROLOGIYA I GIDROLOGIYA, No 10, 1978.

3. Minina, L. S., PRAKTIKA NEFANALIZA (Practical Nephanalysis), Leningrad, Gidrometeoizdat, 1970.

APPROVED FOR RELEASE: 2007/02/08: CIA-RDP82-00850R000300080046-0

APPROVED FOR RELEASE: 2007/02/08: CIA-RDP82-00850R000300080046-0

4. Petrosyants, M. A., "First Results of the TROPEKS-74 Expedition," METEOROLOGIYA I GIDROLOGIYA, No 3, 1975.

5. Romanov, Yu. A., Luk'yanov, [illegible] V., "Some Peculiarities of Tropospheric Circulation in the Equatorial Part of the Indian Ocean," REZUL'TATY ISSLEDOVANIY PO MEZHDUNARODNYM GEOFIZICHESKIM PROYEKTAM. OKEANOLOGICHESKIYE ISSLEDOVANIYA (Results of Investigations Under the International Programs. Oceanological Research), No 19, 1968.

6. Semenov, Ye. K., "Aeroclimatology of Equatorial Westerlies in the Lower Troposphere," METEOROLOGIYA I GIDROLOGIYA, No 2, 1974.

7. Semenov, Ye. K., "Structure and Migration of the Equatorial Zone of Westerlies in the Eastern Hemisphere," METEOROLOGIYA I GIDROLOGIYA, No 9, 1974.

8. Solntseva, N. I., "Equatorial Westerlies in the Pacific Ocean According to Observations of Soviet Expeditions," TRUDY IOAN (Transactions of the Institute of Oceanology), Vol 78, 1965.

9. Khromov, S. P., "Types of Surface Distribution of Wind Near the Equator," IZV. VSESOYUZNOGO GEOGRAFICHESKOGO OBSHCHESTVA (News of the All-Union Geographical Society), Vol 93, No 2, 1961.

10. Fletcher, R. D., "The General Circulation of the Tropical and Equatorial Atmosphere," J. METEOROL., Vol 2, No 3, 1945.

11. Frost, R., Stephenson, P. M., "Mean Streamlines and Isotachs at Standard Pressure Level Over the Indian and West Pacific Oceans and Adjacent Areas," GEOPHYS. MEM., No 109, 1965.

12. Palmer, C. E., TROPICAL METEOROLOGY, Boston, Waverly Press, 1955.

13. Weickman, L., "Mittlere Luftdruckverteilung in Meersniveau Wahrend der Hauptjahreszeitung in Bereiche um Africa in dem Indischen Ozean under der angrenzenden teilen Asie," METEOROLOGISCHE RUNDSCHAU, Jahr. 16, No 4, 1963.

APPROVED FOR RELEASE: 2007/02/08: CIA-RDP82-00850R000300080046-0

APPROVED FOR RELEASE: 2007/02/08: CIA-RDP82-00850R000300080046-0

UDC 551.584.5(574)

AERATION-CLIMATIC MODEL OF A CITY

Moscow METEOROLOGIYA I GIDROLOGIYA in Russian No 10, Oct 80 pp 52-58

[Article by V. I. Degtyarev, Kazakh Regional Scientific Research Institute, manuscript submitted 8 Apr 80]

[Text]

Abstract: It was established on the basis of a great number (about 6,000) of field measurements that the dynamics of the wind velocity field around a building and different fragments of a built-up area exhibits considerable changes in dependence on the flow angle (the wind factor K varies in the range $2.00 > K > 0.00$), wind velocity (u_0) ($0.83 > K > 0.34$), height of the structure and density of tree stands. An aeration-climatic model of a city is formulated for the first time on the basis of the functional dependence of the wind factor on wind velocity $K = f(u_0)$ and the location of the building fragment in the city.

In the purification of the air basins of cities and the creation of favorable microclimatic conditions the principal role is played by the wind regime, making it possible to achieve aeration of residential areas and the entire city.

The long-term wind regime of a city is reliably evaluated using data from meteorological stations. A knowledge of the wind resources of a populated place still does not make it possible to clarify the nature of movement of air currents in the built-up area of a city. Existing recommendations on computation of the influence of wind on the microclimate of a built-up area still have an approximate character [5-7]. The inadequacy of field observations has not made possible an approach to formulation of an aeration-climatic model of a city. Accordingly, the need has arisen for carrying out studies of this type and making the first generalizations along these lines.

As the principal method for making investigations of aeration and creating an aeration-climatic model we employed a method which we adopted for anemometer surveys in the field, on a frequent time schedule, employing MS-13 anemometers and cloth pennants at a height of 2 m with 10-minute averaging [1, 2]. In implementing this

APPROVED FOR RELEASE: 2007/02/08: CIA-RDP82-00850R000300080046-0

APPROVED FOR RELEASE: 2007/02/08: CIA-RDP82-00850R000300080046-0

method in different parts of a city it is necessary to select several fragments of structures of the same type in the direction of the prevailing winds and perpendicular to them: at the center, at a distance of 3-5 km from it in the four cardinal directions and at the outskirts. In each fragment it is necessary to make observations at the 30-50 points most characteristic with respect to aerodynamics with their siting each 15-20 m in a chessboard fashion, which will ensure drawing the wind isotachs with a great accuracy.

The wind field and factors (K -- ratio of wind velocity in the built-up area to the velocity at a control point) in the fragments of the built-up area vary in dependence on the velocity and therefore it is necessary to carry out 3-5 anemometer surveys for all the selected fragments of the built-up areas in the velocity range from 1 to 20 m/sec with an interval 2-3 m/sec. It is virtually impossible to carry out observations simultaneously even in one fragment and therefore a "moving readings" method is proposed in which 6-10 observers ensure observations at 10-18 points simultaneously. One of the observers constantly works at the control point and the others in the built-up area, each ensuring simultaneous observations at two points. After each working 10-minute period, a time of 5-10 minutes is allocated, depending on the efficiency of the observers, for setting up the anemometers at the appropriate points. Prior to beginning the work it is necessary to prepare a diagram of the fragment of the built-up area and anemometric cards. The observations are rigorously regulated in time.

In order to determine the free wind velocity it is more reliable to use information from a control point situated at a distance of 200-300 m on the windward side, depending on the height H of the structures, but in any case it must be at a distance of not less than 6 H from the built-up area on a level or somewhat dominating sector. Prior to the onset of the investigations in all cases it is necessary to carry out reconnaissance work for determining the representativeness of the control point.

The "moving readings" method can be used with adherence to the following conditions: the mean wind velocity during the period when the anemometric surveys is carried out must not deviate from the initial velocity by more than ±20% (according to data at the control point) and the wind direction during this period must not exceed the limits ±22.5°. Accordingly, the surveys must be made in stable weather.

In this method in the analysis of aeration of a built-up area it is recommended that use be made of the wind factors as being the most stable characteristics, not the absolute velocities. The wind factors are computed as the ratio

$$K = \frac{u_i}{u_0}, \qquad (1)$$

where u_i is the wind velocity in the built-up area, u_0 is the wind velocity at the control point in m/sec.

A six-year experiment (1969-1974) with field investigations of aeration of urban built-up areas in Alma-Ata, Kapchagay, Balkhash and Novyy Uzen' has indicated that such surveys make possible a rather precise evaluation of the character of the wind field and its mapping in a complex built-up area with different wind

APPROVED FOR RELEASE: 2007/02/08: CIA-RDP82-00850R000300080046-0

APPROVED FOR RELEASE: 2007/02/08: CIA-RDP82-00850R000300080046-0

directions and velocities in dependence on the height and density of the built-up area, density of tree stand and location of the investigated types of built-up area in a city. A total of about 6,000 measurements was used in investigating the aeration of buildings, different types of built-up area and the city as a whole. All the investigations of aeration of a built-up area were made detailed for cities with weak wind velocities, which includes Alma-Ata, and cities with strong winds — Novyy Uzen' and Balkhash. It was established that the dynamics of the wind velocity field around a building and different fragments of built-up areas varies in a considerable range in dependence on the flow angle (the wind factor varies in the range $2.00 > K > 0.00$) and the air flow velocity ($0.83 > K > 0.34$). The aeration regime, which can be established with different directions and velocities of the basic wind, is represented in Fig. 1.

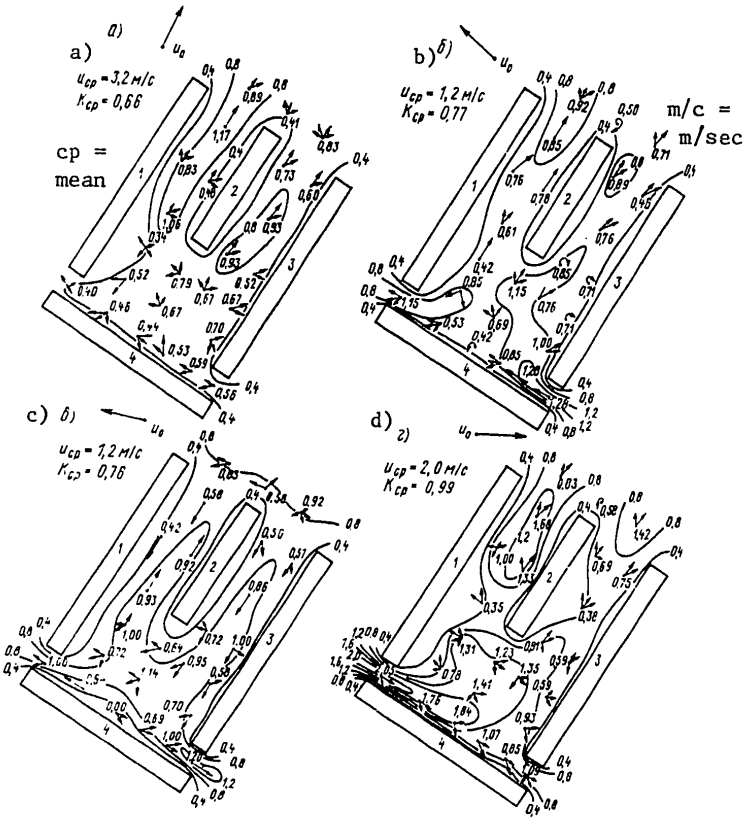

Fig. 1. Aeration regime of fragment of alined-perimetral built-up area of southwestern part of Alma-Ata with different wind directions, summer 1973.

APPROVED FOR RELEASE: 2007/02/08: CIA-RDP82-00850R000300080046-0

APPROVED FOR RELEASE: 2007/02/08: CIA-RDP82-00850R000300080046-0

Centers of intensification of wind velocities are observed at corner openings, in this case constituting 0.5H, and in the passages between the long sides of buildings in the built-up area. These intensifications occur as a result of the joining of the flows bending around the buildings from above and from the sides. If the onflow of the air current occurs at a right angle to the wind-shielding body of the building 4 (Fig. 1a) the mean wind coefficient with a velocity 3.2 m/sec is 0.66. Weak centers of wind intensification are observed only between the buildings 1 and 2. A state of wind exposure of the built-up fragment which is quite similar is observed with onflow of the air current at a right angle to the buildings 1, 2, 3. Insignificant deviations of the onflow of the air current from a right angle cause substantial changes in the wind field in the built-up area. For example, wind deviations from the initial direction by approximately ±15-20° cause countercurrents behind buildings 3 and 4 and an increase of the wind coefficients at a corner end to 1.28. However, at the center and corner end of buildings 4 and 1 -- to 1.15 (Fig. 1b). With directions of onflow to the built-up area somewhat less than +45° there is also an increase of the coefficients and accordingly, an improvement in the conditions for ventilation of the residential block (Fig. 1c). Flow around the built-up area by an air flow at an angle close to -45° (Fig. 1d) creates conditions for maximum increases in the wind coefficients (to 2.05) at the corner ends of buildings 4 and 1. [Here and in the remainder of the text the term "corner end" refers to the openings at the ends of the buildings arranged in a four-building complex as illustrated in Fig. 1.] The mean wind coefficient attains values 0.99 with a velocity 2.0 m/sec. Thus, with angles of onflow close to 45° the best conditions are observed for the built-up area, as can also be traced using data from investigations in a wind tunnel [3, 6].

Table 1

Distribution of Wind Coefficients in Built-Up Areas of Different Height and Different Tree Density

Stories	Tree plantings			
	none	slight	moderate	dense
4-5	222 / 0.70	132 / 0.61	78 / 0.42	172 / 0.31
2-3		12 / 0.38	12 / 0.31	12 / 0.18
Single-story barracks	54 / 0.64			
With sectors near farms		12 / 0.43	12 / 0.20	12 / 0.04

Note. Numerator -- number of measurements, denominator -- wind coefficient.

It should be noted that the effect of an improvement in the ventilation of a residential block with an air flow around it at angles close to 45° also persists for perimetral fragments situated both at the center and on the leeward margin of a city with the single difference that the values of the mean wind coefficients are considerably lower on the leeward margin. Corners and gaps

APPROVED FOR RELEASE: 2007/02/08: CIA-RDP82-00850R000300080046-0

APPROVED FOR RELEASE: 2007/02/08: CIA-RDP82-00850R000300080046-0

(passageways) favor an improvement in ventilation of the block, whereas closed corners create conditions for the total stagnation of air. A perimetral built-up area with gaps at the corners is ventilated to a lesser degree than an alined-perimetral built-up area. The absence of gaps at the corners in a built-up area of this type considerably complicates ventilation. The air in its territory flows in for the most part from above, bending around the windward buildings, flows onto the opposite parallely standing building, is reflected and creates low countercurrents, forming horizontal eddies. In this case the entry of contaminated air directly from the streets becomes quite difficult, but during a period of strong squally winds the horizontal eddies, intensifying sharply, raise dust and trash from the area and cast it at the windows of the leeward facade of the building. The dust, supported by the eddy currents, for a long time remains in a suspended state. As a result, instead of the anticipated improvement in microclimate in the territory of a perimetral-closed courtyard which is poorly maintained it is possible to trace its worsening.

With approach to the center in all types of built-up area there is a deterioration of ventilation conditions. On the margin, on the leeward side, there is again some improvement in ventilation in comparison with the center as a result of better developed countercurrents. Accordingly, not only the type of built-up area, but also its location in the city determine the degree of ventilation of the residential area.

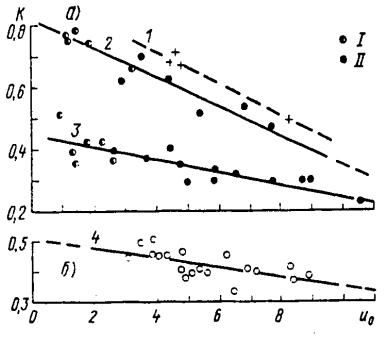

Fig. 2. Dependence of wind coefficient in built-up area with four or five stories on wind velocity. a) windward, b) leeward side of city: I) Alma-Ata, II) Balkhash; 1) alined-perimetral built-up area on outskirts of Novyy Uzen' city, 2) same 1-2 km from outskirts on windward side, 3) perimetral built-up area at center of city, 4) alined-perimetral built-up area on leeward margin of Kapchagay city.

The greatest zone of calm with the maximum extinction of wind velocity is created by buildings with a curvature of 120°, oriented with their convex side toward the wind, and closed fragments of built-up areas of this same type. The degree of wind extinction is further intensified in the case of double or triple blocking of built-up areas.

APPROVED FOR RELEASE: 2007/02/08: CIA-RDP82-00850R000300080046-0

APPROVED FOR RELEASE: 2007/02/08: CIA-RDP82-00850R000300080046-0

The height of the built-up area and forest plantings play a definite role in the ventilation of residential blocks in the city. It was possible to investigate the nature of the ventilation of built-up areas in dependence on their height and the density of tree plantings only in small cities. The influence of each type of built-up area individually is traced more clearly under these conditions. Table 1 gives materials from expeditionary observations characterizing the ventilation of Novyy Uzen' (1969) and Balkhash (1972) cities in dependence on the height of the built-up area and the density of tree plantings with velocities of the main wind 2-7 m/sec. With an increase in the number of stories in the built-up area from one to four there is an improvement in ventilation conditions in the city up to 20%. With an increase in the density of the tree plantings the ventilation of the built-up area is sharply reduced (in a built-up area with four stories -- up to 40%, in an area of one-story buildings -- up to 60%).

Now we will examine an aeration-climatic model of a section of a city in the direction of the prevailing winds for the widely used perimetral and alined-perimetral types of built-up areas with four stories, constructed on the dependence of the mean wind coefficients on free wind velocity.

With an increase in the velocity of onflow of the wind on different types of built-up areas and the city as a whole the wind coefficients decrease, as is confirmed by all the materials from field investigations (Fig. 2). The correlation is almost linear. On the graph, with approach to the center of the city (and from the leeward side -- also to its outskirts) the steepness of the correlation straight line decreases and approaches the horizontal straight line, which is evidence of weakening of the correlation and a decrease in the wind coefficient with an increase in velocity to a definite value. If the correlation straight lines are arbitrarily extended to their intersection, it is found that with a wind not less than 15 m/sec the wind coefficient is virtually not dependent on velocity.

The functional dependence of the wind coefficient on velocity can be written in the general form

$$K = -Au_0 + B, \tag{2}$$

where A, B are constant coefficients, computed by the least squares method, u_0 is wind velocity outside the built-up area.

As a result, for an alined-perimetral built-up area under the cover of a 1-2-km zone of mixed built-up area on the outskirts on the windward side of the city the formula has the form

$$K = -0{,}048\,u_0 + 0{,}825;$$
$$\sigma_K = 0{,}114;\ A_K = -0{,}423;\ E_K = -1{,}182. \tag{3}$$

For perimetral built-up areas with dense forest plantings at the center of the city

APPROVED FOR RELEASE: 2007/02/08: CIA-RDP82-00850R000300080046-0

APPROVED FOR RELEASE: 2007/02/08: CIA-RDP82-00850R000300080046-0

$$K = -0{,}020\, u_0 + 0{,}441;$$
$$\sigma_K = 0{,}069;\ A_K = 0{,}389;\ E_K = 0{,}764. \quad (4)$$

For an alined-perimetral built-up area with moderate tree plantings on the leeward side of the city

$$K = -0{,}015\, u_0 + 0{,}511;$$
$$\sigma_K = 0{,}042;\ A_K = 0{,}038;\ E_K = 0{,}029, \quad (5)$$

where σ_K is the standard deviation, A_K is the asymmetry coefficient, E_K is the excess coefficient.

The initial formula for computing the wind velocity in the built-up area is derived from formula (1):

$$\frac{u_l}{u_0} = -Au_0 + B. \quad (6)$$

Hence

$$u_l = -Au_0^2 + Bu_0. \quad (7)$$

Formulas (3)-(5), (7) serve reliably for low and high wind velocities.

The lessening of the ventilation of residential blocks with approach to the center is also confirmed by the data in Table 2.

Table 2

Distribution of Wind Coefficients in Residential Blocks

	K					Total number of measurements
	1.00	0.99-0.80	0.79-0.60	0.59-0.40	0.40	
			Alined-perimetral built-up area			
Windward side of city. Outskirts	97 18	87 16	151 30	123 23	55 13	513 100
1-2 km from outskirts	35 13	57 21	73 27	74 27	31 12	270 100
Center of city	25 10	18 7	43 16	88 34	83 33	257 100
Leeward side of city. Outskirts	19 3	29 5	105 18	164 28	263 46	580 100
			Perimetral built-up area			
Center of city	9 3	8 3	28 10	79 27	169 57	293 100

Note. Numerator -- number of cases, denominator -- percent.

APPROVED FOR RELEASE: 2007/02/08: CIA-RDP82-00850R000300080046-0

APPROVED FOR RELEASE: 2007/02/08: CIA-RDP82-00850R000300080046-0

On the outskirts on the leeward side of the city there is some improvement in ventilation in comparison with the center as a result of better developed countercurrents. If it is taken into account that measurements of wind velocity in a built-up area were made in conformity to a rigorously uniform scheme, the percentage of frequency of recurrence of the wind coefficient by gradations also gives a relative characteristic of the aeration regime over an area, which is a supplement to the considered graph and formulas. This increases the information yield of the considered aeration-climatic model.

The examined functional dependence $K = f(u_0)$ and all the mean wind coefficients of different types of built-up areas, cited in this article, can be used in corresponding computations of the wind coefficients and the velocity itself in a built-up area in the range from 1 to 10 m/sec.

The considered characteristics of the wind flow in the built-up area of a city represent only some of the changes which the wind component penetrating into the city experiences.

The wind flow during passage over a city, under the influence of the built-up area and the barrier effect of the "heat island," envelopes the city for the most part from above, and in the presence of inversions over the city a jet is formed. The appearance, intensification and disappearance of mesojets, according to the investigations of F. Ya. Klinov [4], occurs simultaneously with the appearance, deepening and disappearance of the inversion.

The considered materials indicate the great possibilities of in situ investigations. It must be expected that the collection of experimental data on the aeration of the built-up area and the microclimate of cities will in the future make it possible to formulate a more rigorous aeration-climatic model and computation model of urban microclimate.

BIBLIOGRAPHY

1. Degtyarev, V. I., "Method for In Situ Investigations of Aeration of the Built-up Area of a City," TRUDY ZSRNIGMI (Transactions of the West Siberian Regional Scientific Research Hydrometeorological Institute), No 33, 1977.

2. Degtyarev, V. I., "In Situ Investigations of Aeration of Traditional Methods for Residential Construction in the Cities of Kazakhstan," TRUDY KazNIGMI (Transactions of the Kazakh Scientific Research Hydrometeorological Institute), No 72, 1977.

3. Kalyuzhnyy, D. N., et al., "Influence of Nature of a Built-up Area on Change in Insolation and Aeration in the UkrSSR," VOPROSY PRIKLADNOY KLIMATOLOGII (Problems in Applied Climatology), Leningrad, Gidrometeoizdat, 1960.

4. Klinov, F. Ya., "Mesoscale Inhomogeneities in the Lower 500-m Layer of the Atmosphere," TRUDY TsVGMO (Transactions of the Central Volga Hydrometeorological Observatory), No 6, 1975.

APPROVED FOR RELEASE: 2007/02/08: CIA-RDP82-00850R000300080046-0

APPROVED FOR RELEASE: 2007/02/08: CIA-RDP82-00850R000300080046-0

5. Retter, E. I., "Aerodynamic Characteristics and Methods for Computing Aeration in a Residential Microregion," VLIYANIYE MESTNYKH PRIRODNO-KLIMATICHESKIKH USLOVIY NA PROYEKTIROVANIYE GORODOV (Influence of Local Natural-Climatic Conditions on the Planning of Cities), Moscow, Gidrometeoizdat, 1974.

6. Semashko, K. I., "Investigation of the Wind Regime of a Territory of Residential Construction," VLIYANIYE MESTNYKH PRIRODNO-KLIMATICHESKIKH USLOVIY NA PROYEKTIROVANIYE GORODOV, Moscow, Gidrometeoizdat, 1974.

7. Serebrovskiy, F. L., METODY RASCHETA AERATSII NASELENNYKH MEST (Methods for Computing Aeration of Populated Places), Leningrad, Gidrometeoizdat, 1973.

APPROVED FOR RELEASE: 2007/02/08: CIA-RDP82-00850R000300080046-0

APPROVED FOR RELEASE: 2007/02/08: CIA-RDP82-00850R000300080046-0

UDC 551.515.2

REACTION OF AN AXIALLY SYMMETRIC TROPICAL CYCLONE TO CHANGES IN OCEAN TEMPERATURE AND EVAPORATION

Moscow METEOROLOGIYA I GIDROLOGIYA in Russian No 10, Oct 80 pp 59-63

[Article by Candidate of Physical and Mathematical Sciences A. P. Khain, State Oceanographic Institute, manuscript submitted 22 Apr 80]

[Text]

Abstract: Using numerical experiments with a 12-level axially symmetric model of a tropical cyclone (TC) a study is made of its reaction to change in the temperature of the ocean surface by 1°C both under the entire region of the TC and under individual regions bounded by the radii 0-300, 300-480 and 480-540 km. The results of the computations are compared with the results of a control experiment in which the surface temperature does not change. In the second series of numerical experiments the surface temperature remained unchanged but the moisture fluxes from the surface were decreased by 30% both in the entire region and alternately over the above-mentioned regions. It is shown that the central region of the TC plays a decisive role in supplying the TC with moisture and heat, in bringing the humidity in the boundary layer to the level necessary for maintaining the intensity of the TC.

The reaction of model axially symmetric TC to change in the temperature of the water surface has been studied in a number of investigations [2, 3, 7-9]. In [2], where the model included a rather complex parameterization of the boundary layer, the reaction to the change in surface temperature was essentially less than in [7-9], and the change in the intensity of the TC did not occur immediately after the moment of decrease in water temperature, as in [7-9], but only after 6-10 hours, which is related to a gradual adaptation of the model boundary layer. In [3], using this same model of a TC [2], the authors compared the results of two numerical experiments. In the first experiment the temperature instantaneously

APPROVED FOR RELEASE: 2007/02/08: CIA-RDP82-00850R000300080046-0

APPROVED FOR RELEASE: 2007/02/08: CIA-RDP82-00850R000300080046-0

decreased by 2 degrees within the limits of a region with a radius of 300 km; in the second experiment the surface temperature decreased by 2 degrees outside this central region. The results indicated that in the first experiment the intensity of the TC decreases substantially, whereas in the second experiment it virtually does not change.

In this article we give an analysis of the results of numerical experiments with an axially symmetric model of a TC described in [1]. We studied the reaction of the TC to a decrease in the temperature of the water surface by 1° both under the entire region of the TC and under individual regions bounded by the radii 0-300, 300-480 and 480-540 km. These radii were selected in such a way that the regions of the surface bounded by them had approximately identical areas. This makes it possible to determine the relative contribution of these zones to maintenance of the intensity of the TC. The results of the computations are compared with the results of a control experiment (CE) in which the surface temperature did not change. In the second series of numerical experiments the surface temperature remained constant and the moisture fluxes from the surface decreased by 30% both in the entire region and alternately over the above-mentioned regions.

Description of model. The experiments were made with an axially symmetric 12-level model of a TC in a z coordinate system described in detail in [1]. The level heights of the finite-difference grid are as follows: 0, 574, 1042, 1530, 2042, 1530, 2042, 3154, 5105, 7380, 9655, 11 915, 14 175 and 16 590 m. The vertical velocity is computed at these levels. The other components of velocity, temperature and humidity are computed at intermediate levels. The horizontal grid interval is 60 km. The number of points in the finite-difference grid is 10 (horizontally). The time interval is 1 min. The model includes an explicit moisture cycle. There is a parameterization of the convective transfer of heat, moisture and the moment of momentum and also convective heating due to the condensation of vapor in cumulus clouds. In computing precipitation it was divided into convective and large-scale. It was assumed that macroscale condensation occurs when the mixing ratio, computed at the grid points of intersection, exceeds a saturating value. It was assumed that the entire excess of moisture under a saturating value is condensed and forms macroscale precipitation. During condensation the temperature increases (macroscale heating), so that the final saturating value, naturally, differs from the initial value.

Convective heating was computed by the following method. The discriminated column of the atmosphere was broken down by horizontal planes (coinciding with the model levels) into layers. It was assumed that the clouds can develop from the lower m layers in which there is moisture convergence. The heating of the atmosphere due to clouds arising from each of these m layers was computed by a method close to the Kuo method [5]. It was assumed that the clouds arising from different levels develop independently of one another and total convective heating was computed as the sum of heatings due to clouds arising from different levels.

Parameterization of the boundary layer by the Deardorff method is used in the model [4]. It is known that the Deardorff method makes it possible, on the basis of the mean values of wind velocity, potential temperature and the mixing ratio in

APPROVED FOR RELEASE: 2007/02/08: CIA-RDP82-00850R000300080046-0

APPROVED FOR RELEASE: 2007/02/08: CIA-RDP82-00850R000300080046-0

the boundary layer (in this case in the mixing layer), its height and water temperature at the surface to determine the fluxes of momentum, heat and moisture from the surface. The height of the mixing layer was assumed equal to the height of the condensation level. The Charnok formula was used in determining the roughness level.

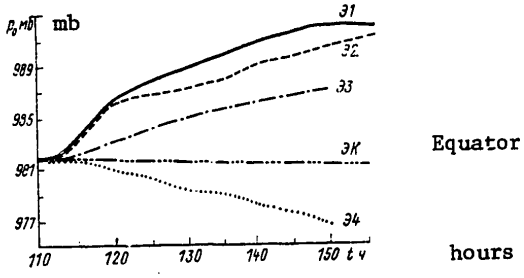

Fig. 1. Dependence of pressure at center of TC at surface on time for experiments with change in temperature of ocean surface.

As the initial state for numerical experiments we used a quasistationary typhoon (t = 110 hours) having the following characteristics: pressure at the center at the surface -- 982 mb, pressure drop at the surface between the center and periphery -- 30 mb, maximum wind velocity -- 36 m/sec, maximum wind velocity at surface -- 27.5 m/sec. The radius of the maximum winds was 90 km. The maximum rate of evaporation was 2.7 cm/day and the mean rate of evaporation over an area with a radius of 540 km was about 1.7 cm/day.

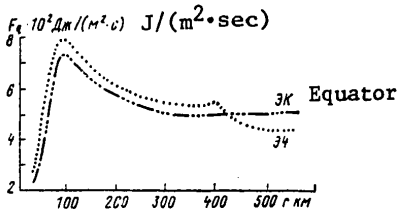

Fig. 2. Radial distribution of moisture fluxes in experiment E4 and control experiment CE at time t = 130 hours.

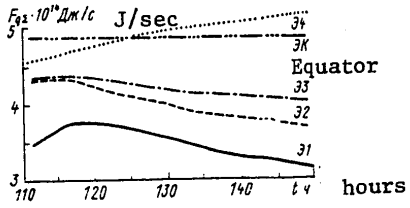

Fig. 3. Dependence of total moisture fluxes from entire region with radius 570 km on time in different experiments.

Results of numerical experiments. Figure 1 shows the dependence of pressure p_0 at the center of a TC at the earth's surface on time, determined in experiments with changes in temperature of the ocean surface T_w. The temperature change occurred at the time t = 110 hours (E1 -- experiment with a temperature decrease by 1°C in the entire region under the TC, E2 -- experiment with a temperature decrease by 1°C in a region with a radius 300 km, E3 -- experiment with a decrease

APPROVED FOR RELEASE: 2007/02/08: CIA-RDP82-00850R000300080046-0

APPROVED FOR RELEASE: 2007/02/08: CIA-RDP82-00850R000300080046-0

in temperature by 1°C in a region situated between the radii 300 and 480 km, E4 -- experiment in which the temperature decreased by 1°C outside the region with the radius 480 km, CE -- control experiment).

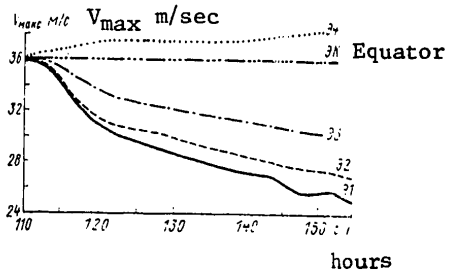

Fig. 4. Dependence of maximum wind velocity on time in described experiments.

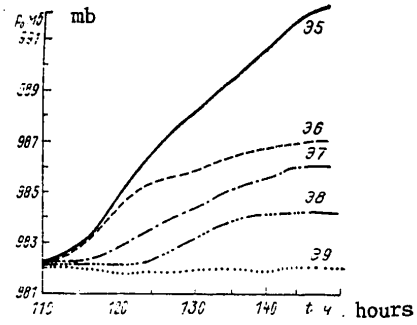

Fig. 5. Dependence of pressure at center of TC at surface on time in experiments with decrease in moisture flux by 30% at constant temperature.

Figure 1 shows that in all the experiments the intensity of the TC begins to change 3-4 hours after the decrease in surface temperature. It should be noted that in experiment E2 the TC attenuates almost as strongly as in the experiment E1. This indicates a decisive role of the central region in the supply of the TC with moisture and heat, in bringing the humidity of the boundary layer to the level necessary for maintaining the intensity of the TC. On the other hand, there can be still another mechanism explaining the role of surface temperature in the central region for model TC. A decrease in surface temperature in the central region leads to some decrease in the temperature in the boundary layer. Most of the methods for the parameterization of convection make use of the condition that the air, rising in clouds in a zone of well-developed convection, at the level of the cloud base has a temperature equal to the temperature of the boundary layer. If the temperature at the cloud base is reduced, the height of the upper boundary of the clouds is reduced, and in addition, there is a redistribution of vertical convective heating with a greater decrease in heating at the upper levels than at the lower levels (in a simple case the heating is proportional to the difference in the temperatures of the moist adiabat, reconstructed from the condensation level, and the mean temperature computed at the points of grid intersection). This can result in a decrease of the warm "core" and an attenuation of the TC.

APPROVED FOR RELEASE: 2007/02/08: CIA-RDP82-00850R000300080046-0

APPROVED FOR RELEASE: 2007/02/08: CIA-RDP82-00850R000300080046-0

There was an interesting peculiarity of the behavior of a TC in experiment E4. With a decrease in surface temperature the TC is not attenuated, but on the contrary is somewhat intensified. Such an evolution of a TC can be attributed to two factors. First, to the fact that the cooling of water on the periphery of the TC leads to a decrease in temperature in the boundary layer. Thus, in the TC boundary layer there is advection of cold air. The water-air temperature difference in the central region of the TC increases, which leads to an increase in the fluxes of heat and moisture from the surface. The increase in these fluxes is such that already at a distance of 200 km from the center the values of the mixing ratio and temperature virtually do not differ from the corresponding values in the control experiment.

Second, a temperature decrease in the boundary layer on the periphery leads to an increase of surface pressure in this region. Thus, the pressure drop between the center and the periphery in the boundary layer decreases, which leads to an increase in the radial, and accordingly, in the tangential velocity components, which in turn increases evaporation from the surface.

Figure 2 shows the radial distribution of moisture fluxes from the surface at the time t = 130 hours. It can be seen that a decrease in the moisture flux at the periphery in the experiment E4 is compensated by its increase in the central region.

Figure 3 shows the dependence of the total moisture fluxes from the entire region (r = 570 km) under a TC on time in different experiments.

Figure 4 shows the dependence of maximum wind velocities on time in the mentioned experiments. There is a velocity increase in experiment E4 and a decrease in experiments E1 and E2 and E3. In [5], in an experiment with a temperature decrease by 2°C outside a region with a radius 300 km, as was already mentioned, the intensity of the TC remained virtually constant. In our opinion, this occurred because a zone of intermediate radii (for example, as in the experiments in this study between the radii 300 and 480 km) and the periphery falls in a zone with a radius greater than 300 km; with a decrease in surface temperature the influence of these regions on the change in intensity of the TC is opposite. We note that an intensification of a tropical depression during the advection of cold air is observed in nature [6].

Figure 5 shows the dependence of pressure at the center at the surface on time for experiments with a decrease in the moisture fluxes by 30% at a constant temperature. (E5 -- experiment with a decrease in the moisture fluxes in the entire TC region, E6 -- experiment in which the moisture fluxes decreased in a region with a radius of 300 km, E7 -- experiment with a change in moisture fluxes in the region between radii of 300 and 480 km, E8 -- experiment in which the moisture fluxes decreased everywhere outside a region with the radius 420 km. Finally, E9 -- an experiment in which the moisture fluxes decreased outside a region with the radius 480 km).

Figure 5 also shows that a decrease in the fluxes in the central region (E6) leads to a strong attenuation of the TC. This once again confirms the role of the central region in supplying the TC with moisture. We note that in experiment E9 the

APPROVED FOR RELEASE: 2007/02/08: CIA-RDP82-00850R000300080046-0

APPROVED FOR RELEASE: 2007/02/08: CIA-RDP82-00850R000300080046-0

intensity of the TC virtually did not change (in contrast to experiment E4, in which the temperature decreased in this same region, which led to an intensification of the TC). Here a decrease in evaporation on the periphery leads to a decrease in the mixing ratio in the boundary layer. Also in the region with lesser radii there is advection of drier air. Since evaporation from the surface is proportional to the difference in the mixing ratios between the saturating value at the surface temperature and the mixing ratio at the anemometer level, the evaporation in the central region increases, compensating the decrease in evaporation at the periphery.

In conclusion we will formulate the conclusions. The central region of a TC with a radius of about 300 km plays the principal role in maintaining the intensity of the TC. A decrease in the fluxes of heat and moisture with a decrease in surface temperature or evaporation outside this region to a considerable degree is compensated by an increase in the fluxes within the limits of this region. A decrease in the surface temperature at the periphery of the TC outside a region with a radius of about 500 km can lead to an intensification of the TC. A decrease in the moisture fluxes on the TC periphery leads to an attenuation of the TC in a case when this decrease occurs quite close to the center of the TC (approximately 400 km). If the decrease in evaporation occurs at a distance r = 480-500 km from the center of the TC, changes in the intensity of the TC do not occur.

BIBLIOGRAPHY

1. Khain, A. P., "Twelve-Level Axially Symmetric Model of a Tropical Cyclone," METEOROLOGIYA I GIDROLOGIYA (Meteorology and Hydrology), No 10, 1979.

2. Anthes, R. A., Chang, S. W., "Response of the Hurricane Boundary Layer to Changes of Sea Surface Temperature in a Numerical Model," J. ATMOS. SCI., Vol 35, No 7, 1978.

3. Chang, S. W., "The Response of an Axisymmetric Model Tropical Cyclone to Local Variations of Sea Surface Temperature," MON. WEATHER REV., Vol 107, No 6, 1979.

4. Deardorff, J. W., "Parameterization of the Planetary Boundary Layer for Use in General Circulation Models," MON. WEATHER REV., Vol 10, No 2, 1972.

5. Kuo, H. L., "On Formation and Intensification of Tropical Cyclones Through Latent Heat Release by Cumulus Convection," J. ATMOS. SCI., Vol 22, No 1, 1965.

6. Namias, J., "Birth of Hurricane Agnes Triggered by the Transequatorial Movement of a Mesoscale System into a Favorable Large-Scale Environment," MON. WEATHER REV., Vol 101, No 1, 1973.

7. Ooyama, K., "Numerical Simulation of the Life Cycle of Tropical Cyclones," J. ATMOS. SCI., Vol 26, No 1, 1969.

8. Rosenthal, S. L., "The Response of a Tropical Model to Variations in Boundary Layer Parameters, Initial Conditions, Lateral Boundary Conditions and Domain Size," MON. WEATHER REV., Vol 99, 1971.

9. Sundqvist, H., "Mean Tropical Storm Behavior in Experiments Related to Modification Attempts," TELLUS, Vol 24, No 1, 1972.

APPROVED FOR RELEASE: 2007/02/08: CIA-RDP82-00850R000300080046-0

APPROVED FOR RELEASE: 2007/02/08: CIA-RDP82-00850R000300080046-0

UDC 551.465.4(263.5)

STRUCTURE OF ACTIVE LAYER IN SOUTHEASTERN CARIBBEAN SEA

Moscow METEOROLOGIYA I GIDROLOGIYA in Russian No 10, Oct 80 pp 64-69

[Article by A. Moreno, Candidate of Physical and Mathematical Sciences A. P. Nagurnyy and O. Padiya, Arctic and Antarctic Scientific Research Institute and Meteorology Institute, Havana, manuscript submitted 4 Feb 80]

[Text]

Abstract: In the upper layer with a thickness of 30-50 m there is water freshened by river runoff which causes a stable vertical density structure. This does not favor the penetration of heat into the deep layers of the active layer of the ocean, which in turn lessens the probability of the appearance and development of hurricanes in the southeastern part of the Caribbean Sea. Characteristic profiles of change of density and temperature in the upper water layers are shown.

During joint Soviet-Cuban investigations of the conditions for the formation of atmospheric cyclonic disturbances in the southeastern part of the Caribbean Sea in September-October 1979 aboard the scientific research ship "Professor Zubov" it was possible to determine the principal characteristics and peculiarities of the active layer of water in this region.

The active layer actively participates in energy exchange with the atmosphere and to a great extent determines the appearance and development of cyclonic formations from small eddies to hurricanes. The energy of solar radiation absorbed at the water surface is transferred into the depths of the active layer of the sea and is partially expended on the evaporation of water vapor and the heating of the near-water boundary layer of the atmosphere. The intensity of these processes is dependent for the most part on the vertical structure of the active layer of the sea and meteorological conditions near the water surface.

At the time of making of polygon observations of the state of the atmosphere and hydrosphere during the period 24 September-10 October 1979 in the southeastern part of the Caribbean Sea (coordinates of center of polygon 13°30'N, 65°00'W) specialists carried out frequent vertical soundings of the upper 1,000-m water layer. A probe-bathometer was used for these purposes. This apparatus makes it

APPROVED FOR RELEASE: 2007/02/08: CIA-RDP82-00850R000300080046-0

APPROVED FOR RELEASE: 2007/02/08: CIA-RDP82-00850R000300080046-0

possible to carry out remote measurements and to register temperature, as well as conductivity and hydrostatic pressure each 1-2 m of depth. The accuracy in measuring temperature was +0.01°C and for conductivity +0.004 cm/m. Soundings were made each three hours. At individual horizons there was registry of the temporal variation of temperature with exposure of the instrument at the stipulated horizon from two to three hours.

The hydrological regime of the particular region is characterized by strong currents directed from the straits of the Lesser Antilles to the Gulf of Mexico. These currents are a branch of the South Trades Current, which, meeting with the shores of South America, divides into a southerly branch (Brazilian Current) and a northerly branch (Guiana Current). The Guiana Current, moving northward along the shores of South America, draws along a great quantity of sea water freshened by large rivers, such as the Amazon, Orinoco, and reaching the straits of the Lesser Antilles, carries these waters into the southeastern part of the Caribbean Sea at a velocity of 1-1.5 knot per hour, forming a surface water in this region with 33.5°/oo, 28-29°C [2]. Below there are intermediate water masses with a greater salinity (35°/oo) arriving from the North Atlantic through the straits and entering the eastern part of the Caribbean Sea. At a depth of 1,000 m and extending to the bottom there are water masses with stable characteristics, changing little in time and space.

The data from the drifting bathometric stations and the probe-bathometer indicated that in the region of these investigations there were surface water masses of nonuniform density whose conditional density varied in the range 21-22.5 g/cm^3 and whose salinity varied from 33 to 34°/oo. The thickness of this layer varied from 10 to 60 m. The area of propagation of surface freshened waters attained a great extent. On the track from the region of the polygon to the northwest through all the eastern part of the Caribbean Sea it was possible to observe a region of reduced salinity at the water surface with an extent of more than 200 km (see Table 1).

Table 1

Change in Salinity and Temperature at Water Surface in Eastern Caribbean Sea on 11 October 1979

Sampling time	Coordinates N - W	Salinity °/oo	Temperature °C
08 h 15m	13°29′ — 65°23′	34,309	28,6
09 15	13 42 — 65 30	34,373	28,6
10 15	13 53 — 65 37	34,446	28,6
11 15	14 09 — 65 44	34,820	28,4
12 15	14 23 — 65 50	35,115	28,4
13 15	14 36 — 65 57	34,453	28,4
14 15	14 44 — 66 00	33,953	28,8
19 45	15 00 — 66 11	33,886	29,0
20 45	15 13 — 66 18	33,807	29,0
21 45	15 28 — 66 26	34,212	28,8
22 45	15 44 — 66 34	34,904	28,4
23 45	15 58 — 66 41	34,969	28,3
00 45	16 06 — 66 53	35,016	28,3

APPROVED FOR RELEASE: 2007/02/08: CIA-RDP82-00850R000300080046-0

APPROVED FOR RELEASE: 2007/02/08: CIA-RDP82-00850R000300080046-0

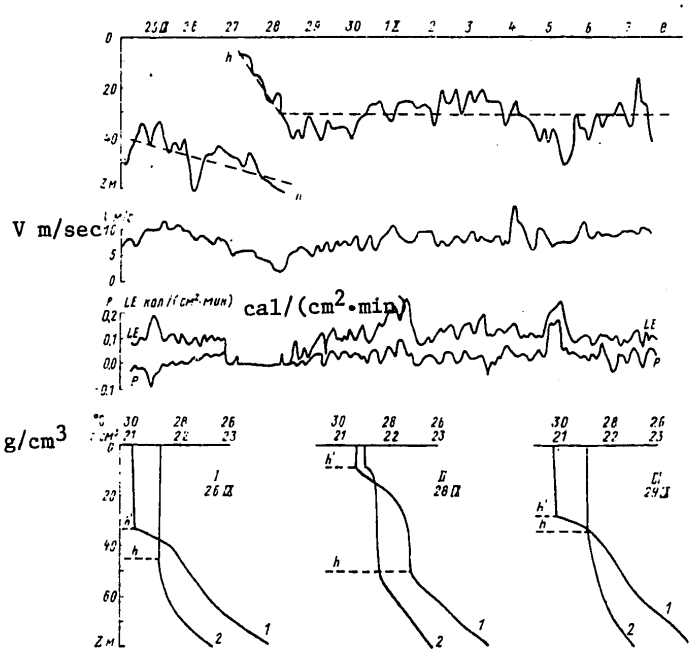

Fig. 1. Temporal change in thickness of upper homogeneous water layer (h), wind velocity (V), turbulent fluxes (P) and latent heat (LE) and three types (I-III) of vertical distribution of density (1) and temperature (2).

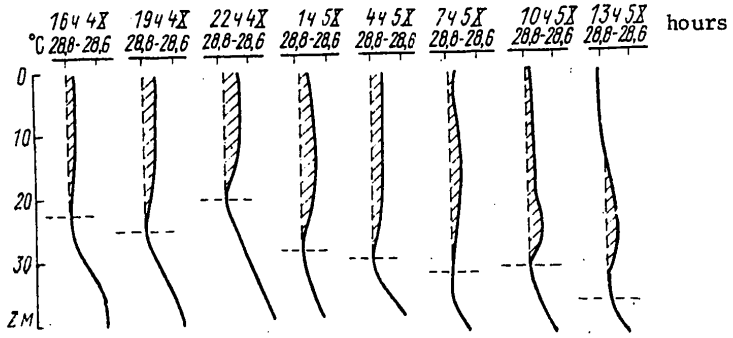

Fig. 2. Vertical distribution of temperature 4-5 October 1979. The shaded region represents the temperature curve deviation from the initial position on 4 October 1979.

Figure 1 illustrates the three most typical temperature distributions (curve 2) and most typical conditional density distributions (curve 1) in the upper water layer. In all three types of distributions there is a well-expressed density gradient

APPROVED FOR RELEASE: 2007/02/08: CIA-RDP82-00850R000300080046-0

APPROVED FOR RELEASE: 2007/02/08: CIA-RDP82-00850R000300080046-0

above which the density distribution is constant. The second type of distribution is characterized by two peculiarities of density distribution. This is evidently a result of active interaction between the atmosphere and the sea and also advective processes in the presence of a horizontal nonuniformity of density distribution. The latter is confirmed by the strong currents and the great salinity variations in the course of the entire observation period. The first and third types of distributions have an identical structure, differing with respect to the depth of the lower boundary of the homogeneous layer (h). In the first case the thickness of the homogeneous layer was 45-50 m. These values were characteristic for the time period from 24 to 28 September when the mean wind velocity was 10 m/sec and the turbulent fluxes of latent and apparent heat from the sea surface were in the range 0.05-0.10 cal/(cm^2·min). At the time of weakening of the wind to 2 m/sec and a decrease in the fluxes of latent and apparent heat to zero, that is, a decrease in the expended part of heat balance and accordingly an increase in the quantity of heat absorbed by the sea (28 September), the lower boundary of the homogeneous layer began to drop and at the same time a new, warmer homogeneous layer appeared in the upper decimeter horizon. With a subsequent intensification of the wind to 10-12 m/sec the initial boundary lost its outlines, the boundary of the new homogeneous layer in a day dropped from 10 to 30 m, on the average remaining at this depth during the period 29 September-8 October. For the transition period at the time of weakening of the wind (28 September) and an increase in the quantity of heat absorbed at the sea surface there was characteristically a temperature distribution of the second type (Fig. 1, II), whereas for the period of appearance of a new homogeneous layer and wind intensification a distribution of the third type was characteristic (Fig. 1, III). In this case the time of transition from one structure to another did not exceed one day. It can be concluded from Fig. 1 that there is a close relationship between the velocity of the surface wind and also the heat fluxes at the sea surface and the vertical structure of the upper homogeneous water layer.

The lower boundaries of the homogeneous layer, established on the basis of the density and temperature distribution, do not coincide, which indicates a difference in the intensity of the mechanism of turbulent diffusion of mass and heat in the stably stratified active layer.

Figure 2 shows a series of temperature profiles in the active layer of water obtained using a probe-bathometer on 4-5 October each three hours. It is characteristic of this series that it makes it possible to trace progressively the process of change in the heat content of a homogeneous water layer in the course of 24 hours. The area of the shaded region is proportional to the quantity of heat lost by the homogeneous layer beginning at the initial time 1300 LT on 4 October 1979. In the considered case a stable wind (10-15 m/sec), cloudy weather (7/10-10/10) and a decrease in total solar radiation as a result of its diurnal change favored heat transfer from the active layer of the sea into the atmosphere. The transfer of heat below the homogeneous layer into the thermocline region was difficult due to the stable density stratification at the depth h, which is also manifested in the formation of a temperature inversion at this depth. If the quantity of heat of a vertical column of a homogeneous water layer is expressed in the form

$$Q_n = c_p \rho \Delta T \Delta Sh,$$

APPROVED FOR RELEASE: 2007/02/08: CIA-RDP82-00850R000300080046-0

APPROVED FOR RELEASE: 2007/02/08: CIA-RDP82-00850R000300080046-0

where $c_p \cong 1$ cal/(g·°C); $\rho \cong 1.0$ g/cm^3; h is the thickness of the homogeneous water layer; $\Delta S = 1$ cm^2; $\Delta T = T_N - T_n$; T_N is the temperature of the homogeneous layer at the initial moment; T_n is the temperature of the homogeneous layer at the investigated moment in time, it can be computed that the upper homogeneous water layer in several hours imparts to the atmosphere 250 cal of heat through 1 cm^2 of sea surface area. The heat flux from the ocean to the atmosphere $(Q_{n+1} - Q_n)/\Delta t$ at the time 0200 hours on 5 October was 0.5 cal/(cm^2·min). This value can completely compensate the heat flux from the sea surface as a result of water vapor evaporation and turbulent exchange in the near-water layer of the atmosphere. With an increase in total solar radiation during the daytime (0800-1400 hours on 5 October 1979) the active layer absorbs heat replenishing the losses during the dark time of day (contraction of the shaded area in Fig. 2). It should be noted that the process of heat transfer from the sea into the atmosphere almost simultaneously affects the entire homogeneous water layer. There is a change not only of temperature, but also the thickness of the homogeneous layer. This is evidence of intensive processes of turbulent and convective diffusion of mass and heat in the upper layer caused by destruction of surface waves, vertical shift of the velocity of drift currents and subsidence of the water cooled at the surface. Turbulent diffusion and convection are generated only at the depth of the maximum density gradient. According to the estimates in [1], the characteristic time of action of turbulent diffusion is 0.5-1 hour, which evidently is also characteristic for the investigated region.

The thickness of the thermocline in this region was very great and occupied the water layer with an upper boundary 30-60 m, a lower boundary 750 m and a temperature drop from 28 to 6°C.

Investigations of the temporal variability of temperature in the thermocline layer were made using a probe-bathometer which was held at the stipulated horizon for two or three hours and registered temperature with a discreteness of 9.6 sec. Great vertical temperature gradients favor a stability of the fluctuations propagating in the stratified fluid layer. Fluctuations with a period more than an hour and several minutes were detected. Correlation analysis made it possible to discriminate fluctuations with a period of 8 minutes at the 100-m horizon, 9 minutes at the 200-m horizon and 10 minutes at the 250-m horizon. Fluctuations with such periods were characteristic for free internal waves. The amplitude of the wave attained 0.5°C. Manifestations of instability of these fluctuations were not discovered. Accordingly, the mechanism of intermittent turbulence associated with the destruction of internal waves is evidently not typical for the southeastern part of the Caribbean Sea.

The high-frequency fluctuations with an amplitude of 0.05°C characteristic for the time series were evidently associated with small-scale turbulence caused by the vertical velocity shear of currents.

Conclusions

The southeastern part of the Caribbean Sea is characterized by a stable vertical density stratification due to the transport of surface waters with relatively low salinity along the shores of South America through the straits of the Lesser Antilles.

APPROVED FOR RELEASE: 2007/02/08: CIA-RDP82-00850R000300080046-0

APPROVED FOR RELEASE: 2007/02/08: CIA-RDP82-00850R000300080046-0

The active layer of the sea consists of a homogeneous upper layer with a thickness of 30-50 m and the thermocline, whose lower boundary is situated at a depth of 750 m. The thicknesses of the homogeneous layers, determined from the temperature and density distribution, do not coincide with one another. As a rule, the density jump is situated above the temperature jump, which indicates a difference in the intensity of turbulent diffusion of heat and mass.

The variability of the lower boundary of the homogeneous layer is dependent to a considerable degree on wind velocity and the heat fluxes at the water surface. During the period 24 September-8 October the lower boundary varied in the range 20-50 m.

Intensive processes of heat exchange between the active layer of the sea and the atmosphere were detected. The heat content of a vertical column of the upper homogeneous layer can vary in several hours by 250 cal/cm^2. The heat flux from the homogeneous layer into the atmosphere is comparable to the heat fluxes at the water surface due to evaporation and turbulent exchange and can completely compensate them. In the thermocline at the horizons 100 and 200 m there were free internal waves with a period 8-9 minutes. The amplitude of the internal waves was small (0.5°). No manifestations of the instability of these waves were discovered.

The presence of water with relatively low salinity in the upper part of the active layer in the southeastern region of the Caribbean Sea leads to a stable density stratification below the boundary of the homogeneous layer. This weakens the processes of heat accumulation beyond the limits of the homogeneous layer. At the same time, the homogeneous layer is capable, very rapidly, of both accumulating heat and releasing it into the atmosphere. As a rule this does not favor the accumulation of heat in the active layer, which in turn reduces the probability of the appearance of cyclonic formations, whose development requires the heat reserves not only of the homogeneous layer, but also deeper layers [3]. It is possible that precisely the stable stratification of the active layer explains the small frequency of recurrence of cyclonic formations in the southeastern part of the Caribbean Sea. This frequency of recurrence is approximately half as great as in the northeastern, and approximately a third as great as in the northwestern part of the Caribbean basin, which receives virtually no freshened river runoff of surface waters. A similar situation was analyzed by Academician V. V. Shuleykin [3] in the example of the Gulf of Guinea, in which the surface waters are freshened by the runoff of the Niger River, as a result of which cyclonic eddies are not observed in the atmosphere.

It is necessary to make detailed oceanographic investigations of the southeastern part of the Caribbean Sea in order to ascertain the scales of horizontal nonuniformity of the distribution of surface waters with a low density and salinity and evaluate their temporal variability. This will assist in determining the statistical relationship between the frequency of recurrence of cyclonic disturbances and the temporal and spatial distribution of freshened surface waters in the southeastern part of the Caribbean Sea for formulating predictions of the appearance and development of hurricanes in this region.

APPROVED FOR RELEASE: 2007/02/08: CIA-RDP82-00850R000300080046-0

APPROVED FOR RELEASE: 2007/02/08: CIA-RDP82-00850R000300080046-0

BIBLIOGRAPHY

1. Kalatskiy, V. I., MODELIROVANIYE VERTIKAL'NOY TERMICHESKOY STRUKTURY DEYATEL'-NOGO SLOYA OKEANA (Modeling of the Vertical Thermal Structure of the Active Layer of the Ocean), Leningrad, Gidrometeoizdat, 1978.

2. Muromtsev, A. M., OSNOVNYYE CHERTY GIDROLOGII ATLANTICHESKOGO OKEANA (Principal Characteristics of Atlantic Ocean Hydrology), Moscow, Gidrometeoizdat, 1963.

3. Shuleykin, V. V., RASCHET RAZVITIYA, DVIZHENIYA I ZATUKHANIYA TROPICHESKIKH URAGANOV I GLAVNYKH VOLN, SOZDAVAYEMYKH URAGANOM (Computation of Development, Movement and Attenuation of Tropical Hurricanes and Main Waves Created by a Hurricane), Leningrad, Gidrometeoizdat, 1978.

APPROVED FOR RELEASE: 2007/02/08: CIA-RDP82-00850R000300080046-0

APPROVED FOR RELEASE: 2007/02/08: CIA-RDP82-00850R000300080046-0

UDC 551.465(263)

SOME CHARACTERISTICS OF VARIABILITY OF THE THERMOHALINE STRUCTURE OF THE EQUATORIAL REGION OF THE ATLANTIC

Moscow METEOROLOGIYA I GIDROLOGIYA in Russian No 10, Oct 80 pp 70-77

[Article by S. N. Moshonkin, State Oceanographic Institute, manuscript submitted 22 Apr 80]

[Text]

Abstract: On the basis of data obtained in the First Global Experiment of GARP in the winter of 1979 the author examines the peculiarities of mesoscale variability of the thermohaline structure of the active layer in the ocean. There was found to be a stable noncoincidence of the lower boundaries of layers quasi-homogeneous with respect to temperature and salinity over a prolonged period of time. The lower boundary of the homogeneous layer experiences fluctuates with a semidiurnal period as a result of internal waves. Its variability with a time scale of about 2-3 days is associated for the most part with the variability of wind velocity. In the case of a weak wind the predominant role is played by the heat flux through the surface. A situation with a sharp decrease in thickness of the quasi-homogeneous layer was discovered. The influence of precipitation creating a freshened sublayer is examined. The patterns of distribution of characteristics in the pycnocline are outlined. The hypothesis of self-similarity for temperature is checked.

The thermohaline structure of the upper layer of the ocean is analyzed on the basis of data obtained in the course of two special observation periods of the First Global Experiment. The observations were made in the neighborhood with the coordinates 5°N, 29°W during the period 13 January through 13 February and from 25

APPROVED FOR RELEASE: 2007/02/08: CIA-RDP82-00850R000300080046-0

APPROVED FOR RELEASE: 2007/02/08: CIA-RDP82-00850R000300080046-0

February through 14 March 1979. This region was selected specially for implementation of the First Global Experiment as being characteristic for the equatorial region of the Atlantic in hydrological respects. Temperature and salinity were measured with a probe-bathometer each three hours. Two stages of semihourly observations were also carried out (two and three days).

The vertical resolution of the probe-bathometer in the layer 0-200 m was 1 m; the accuracy in measuring temperature was ±0.03°C and the accuracy in measuring salinity was about ±0.03°/oo. Salinity was computed on the basis of the conductivity of sea water. The specifics of work with cable probes was discussed, for example, in [7]. The discreteness of measurements along the vertical was variable, which was dependent on the rate and uniformity of lowering of the instrument and the frequency of its interrogation. In the upper 100-m layer it averaged 2 m and in the layer 100-200 m — 4 m.

The following meteorological data were used in determining the influence of atmospheric processes on variability of the thermohaline structure of waters: radiation heat budget of the ocean surface (direct and scattered solar radiation minus the radiation of the reflected and effective radiation), air temperature, wind velocity at the level 26 m from the water surface and the quantity of falling precipitation.

For the purposes of computations and analysis the data on temperature and salinity were subjected to monitoring and orderly arrangement. Then the vertical temperature and salinity profiles were reduced to the uniform discreteness of 1 m by interpolation with the use of a cubic polynomial [1].

Figure 1a shows the density distribution in the section, obtained as a result of soundings of the upper layer of the ocean each half-hour while the ship was at drift. All the considered hydrological stations in the experiment were concentrated in the region of this section (the maximum distance between them was about 12 miles). It can be seen that the density isolines in the section are situated almost horizontally and the trend of the fluctuations is small. It can therefore be surmised that the upper layer is horizontally homogeneous and initially it is possible to neglect the complex problem of separating the temporal and spatial variability [7].

The vertical profiles of temperature, salinity and density (Fig. 1b,c) are frequently complicated by a microstructure (scales from a meter or more). A stepped structure of different scales is present. Density inversions observed for the most part in the seasonal pycnocline are also elements of the microstructure. Here they are always caused by intensive vertical changes in salinity and have a scale of 3-5 m. Sometimes there are density inversions in the quasihomogeneous layer as well (for example, see Fig. 1c -- profiles for 0600 hours on 30 January). But they are rapidly liquidated by convection.

The quasihomogeneous layer was clearly discriminated in the distribution of temperature and salinity throughout the period of observations. The thicknesses of the layers quasihomogeneous with respect to temperature and salinity virtually coincided for a large part of the observation period. The only exception was the

APPROVED FOR RELEASE: 2007/02/08: CIA-RDP82-00850R000300080046-0

APPROVED FOR RELEASE: 2007/02/08: CIA-RDP82-00850R000300080046-0

period 13-21 January (Fig. 1b; 2a,b). At this time the lower boundary of the layer quasihomogeneous with respect to salinity was on the average 10 m above the lower boundary of the thermal quasihomogeneous layer (Fig. 2a, Table 1). A typical situation of such a position of the boundaries during the mentioned period is illustrated in Fig. 1b.

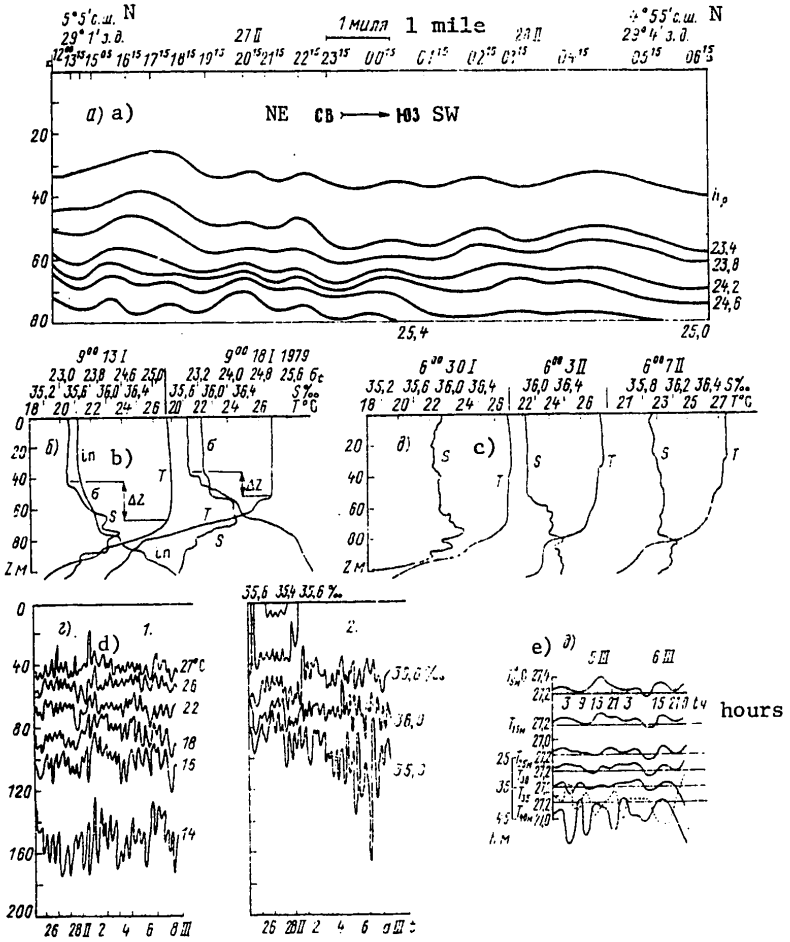

Fig. 1. Elements of thermohaline structure of upper layer of ocean. a) section of density structure of waters in observation region. Upper isoline -- lower boundary of layer quasihomogeneous with respect to density; b) vertical profiles of temperature, salinity and density during period of separation of lower boundaries of quasihomogeneous salinity and thermal layers (Δz -- distance between boundaries, in -- density inversion); c) evolution of temperature and salinity profiles during shallowing of quasihomogeneous layer; d) fragment of change of thermal (1) and salinity (2) structure of upper layer of ocean (interval -- three hours); e) change in water temperature in quasihomogeneous layer (dotted line -- lower boundary of layer).

APPROVED FOR RELEASE: 2007/02/08: CIA-RDP82-00850R000300080046-0

APPROVED FOR RELEASE: 2007/02/08: CIA-RDP82-00850R000300080046-0

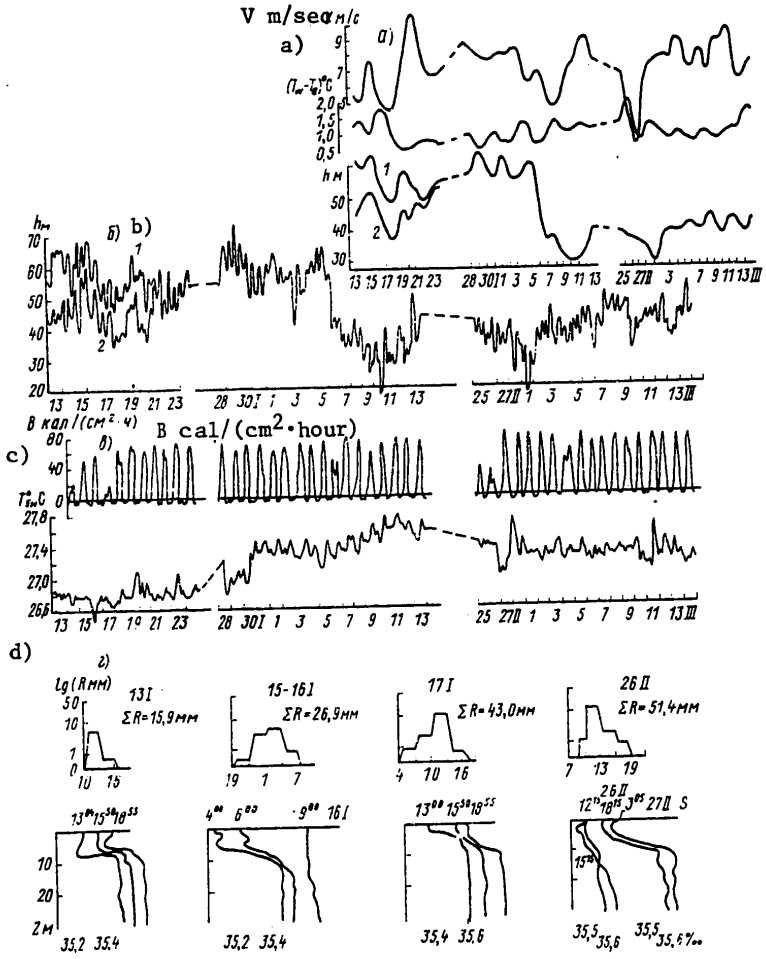

Fig. 2. Temporal variation of parameters of thermohaline structure of upper layer of ocean and meteorological characteristics. a) wind velocity at level 26 m from water surface, difference in water-air temperatures, thickness of layer quasihomogeneous with respect to temperature (1) and salinity (2) (mean daily values); b) thickness of quasihomogeneous layer (interval -- three hours). 1) thermal, 2) salinity, c) radiation thermal budget of surface (interval -- one hour) and water temperature at horizon 5 m (interval -- three hours); d) quantity of falling precipitation (R mm) during heaviest rains and change in vertical salinity profiles with time in upper 30-m layer. Adjacent successive salinity profiles are displaced by $1^{o}/oo$.

APPROVED FOR RELEASE: 2007/02/08: CIA-RDP82-00850R000300080046-0

APPROVED FOR RELEASE: 2007/02/08: CIA-RDP82-00850R000300080046-0

Table 1

Statistical Characteristics of Parameters of Thermohaline Structure of Upper Layer of Ocean and Wind, 1979

Time	Mean values			Dispersion Evaluations			Standard Deviations			Extremal values					
	$\bar{h}_T$	$\bar{h}_S$	$\bar{V}$	D_{h_T}	D_{h_S}	D_V	h_T	h_S	V	max h_T	min h_T	max h_S	min h_S		
13-24 Jan	56	47	7	24.8	24.5	4.9	5.0	5.0	2.2	70	42	59	34		
28 Jan-13 Feb	48	47	7	20.9	26.2	2.5	4.6	5.1	1.6	17	17	77	17		
25 Feb-14 Mar	38	39	7	14.2	16.5	4.2	3.8	4.1	2.0	51	24	53	17		

Notes: 1) during the period 25-27 January there were interruptions in the observations;

2) h_T, h_S -- thicknesses of layers quasihomogeneous with respect to temperature and salinity;

3) modulus of wind velocity at level 26 m from water surface.

APPROVED FOR RELEASE: 2007/02/08: CIA-RDP82-00850R000300080046-0

APPROVED FOR RELEASE: 2007/02/08: CIA-RDP82-00850R000300080046-0

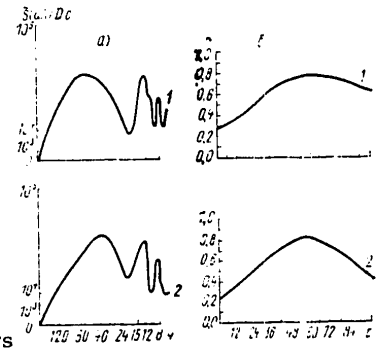

Fig. 3. Normalized spectral density and cross-correlation functions. a) spectra of fluctuations of thickness of quasihomogeneous layer (2) and isotherm 23°C (1) (25 February-14 March 1979); b) wind velocity cross-correlation functions and thicknesses of homogeneous layer; 1) time from 28 January through 13 February, 2) from 25 February through 14 March 1979.

Shear and eddy-wave turbulence, free convection, usually create layers homogeneous with respect to temperature and salinity of approximately the same thickness [2, 3]. The detected relative independence of the thermal and salinity structure can be attributed, for example, to the influence of the boundary conditions.

The considered series are short in extent and characterize the intramonthly variability and therefore it is easy to trace the nonstationarity and trend of the mean (Fig. 2). This made it necessary to carry out smoothing of the series, which was accomplished by means of two-day moving averaging (discreteness — three hours). The two-day period corresponds approximately to one-ninth - one-tenth of the total duration of the registered time series. In computing the dispersions (Table 1), autocorrelation functions and spectral density functions (Fig. 3a) the filtering of the initial series was accomplished by subtraction of the smoothed series. However, for computing the cross-correlation functions between the wind and the quasihomogeneous layer (Fig. 3b), as will be demonstrated below, it was desirable to filter out the low-frequency components. In this case processes with a time scale of 12 hours or less were suppressed.

Table 1 shows that during the entire observation period on the average the thickness of the quasihomogeneous layer is decreased. During this time the wind velocity and its dispersion remain at the same level. The general decrease in the thickness of the homogeneous layer is evidently associated with the constant heat influx from the atmosphere, increasing hydrostatic stability (Fig. 2c). However, this process does not occur uniformly (Fig. 2b).

The mean amplitude of fluctuations of the thickness of the quasihomogeneous layer, superposed on this general variation, is equal to 4.5 m. In general, however, the thickness of the quasihomogeneous layer varied in the range from 17 to 77 m. Always, even in a period of noncoincidence, the lower boundaries of layers quasihomogeneous with respect to temperature and salinity varied synchronously and therefore their statistical characteristics are similar.

APPROVED FOR RELEASE: 2007/02/08: CIA-RDP82-00850R000300080046-0

APPROVED FOR RELEASE: 2007/02/08: CIA-RDP82-00850R000300080046-0

Typical spectra of fluctuations of the thickness of the quasihomogeneous layer and isotherms in the seasonal thermocline have a similar form (Fig. 3a). The low-frequency peak corresponds to the maximum time scale of the filtered components of the fluctuations and therefore should be excluded from the analysis. The high-frequency maximum, corresponding to a time scale 8-9 hours, is possibly fictitious and with a discreteness of 3 hours can be caused by the effect of intermingling of frequencies [4]. A semidiurnal period is clearly discriminated. A distinguishing characteristic of the dynamics of the waters in the considered region is the constant presence of internal tidal waves in the thermohalocline. These wave movemements occur isopycnically without "traumatic" effects in the thermohaline structure of the waters [7]. Their amplitude, averaging 5 m, virtually does not change vertically in the seasonal pycnocline. The phase shift here differs little from zero (Fig. 1d). On the basis of the amplitude of fluctuations of the isopycnic lines it can be concluded that in the upper part of the main pycnocline the amplitude of the internal waves increases and can exceed by a factor of 2 to 4 the amplitude of waves in the seasonal pycnocline.

A joint analysis of fluctuations of the isopycnic lines in the seasonal pycnocline and the thickness of the quasihomogeneous layer shows that 12-hour fluctuations of the lower boundary of the quasihomogeneous layer are caused precisely by internal waves. The amplitude of these fluctuations on the average is 4 m. In general, however, it varies from 2 to 5 m (Fig. 2b). The lower boundary of the layer quasihomogeneous with respect to density in the process of semidiurnal fluctuations moves synchronously with the isopycnic lines of the upper part of the seasonal pycnocline (for example, see Fig. 1a). Accordingly, there is no substantial turbulent entrainment of the waters of the seasonal thermocline into the quasihomogeneous layer.

A period of 5-6 days is traced in fluctuations of the thickness of the quasihomogeneous layer (Fig. 2a). However, the length of the considered series is inadequate for a more or less rigorous statistical analysis of the noted periodicity. The amplitude of these fluctuations is equal to approximately 4-7 m. Their period is close to the inertial scale, which for the observation region is 5.75 days, and also to the synoptic scale. A similar quasiperiodicity is noted in the wind velocity fluctuations.

The collected data make it possible to trace the evolution of the quasihomogeneous layer, its dependence on external conditions. The greatest decrease in the thickness of the quasihomogeneous layer occurs during the period 5-10 February. During this time the lower boundary moves from 60 m to the 30-m horizon (Fig. 2a,b). This is associated with attenuation of wind velocity (Fig. 2a) and intensive heating. The water temperature in the quasihomogeneous layer attains its maximum values 27.3-27.7°C (Fig. 2c), that is, with a decrease in wind velocity turbulence in the upper layer decreases and the heat regularly arriving from the atmosphere is distributed into a thinner layer. The evolution of the temperature and salinity profiles in the process of formation of a secondary quasihomogeneous layer of lesser thickness is shown in Fig. 1c.

An appreciable decrease in the thickness of the quasihomogeneous layer occurred during the period 15-18 January and during the period 27 February-1 March (Fig. 2a,b). Both these cases were related to a preliminary decrease in wind velocity.

APPROVED FOR RELEASE: 2007/02/08: CIA-RDP82-00850R000300080046-0

APPROVED FOR RELEASE: 2007/02/08: CIA-RDP82-00850R000300080046-0

However, they were preceded by situations of a decrease in the fluxes of direct and scattered solar radiation associated with an increase in cloud cover (Fig. 2c). Therefore, there was not such an intensive decrease in the thickness of the quasihomogeneous layer as during the period 5-10 February.

The wind exerts a significant influence on the thickness of the quasihomogeneous layer. With an increase in wind velocity the thickness of the layer increases. For example, a velocity increase from 2.0 to 9.0 m/sec during the period 27 February-4 March corresponds to an increase in the thickness of the quasihomogeneous layer from 25-30 m on 1 March to 40-45 m on 6 March. However, with a decrease in wind velocity, as indicated above, the lower boundary of the homogeneous layer rises upward. An appreciable decrease in the thickness of the quasihomogeneous layer occurred with a wind velocity less than approximately 5.5 m/sec (Fig. 2a).

Figure 3b shows the cross-correlation functions for wind velocity and the thickness of the quasihomogeneous layer. Their maxima correspond to a shift of about 2.5 days. In this case the positive correlation coefficient attains a value 0.8, which indicates a high degree of closeness of the positive linear dependence. Such a situation corresponded to a large part of the observation time.

The product of wind velocity and the water-air temperature difference is proportional to the quantity of heat lost by the ocean during evaporation and contact heat exchange with the atmosphere [5]. Evaporation is combined with salinization of the water surface layer. It can be seen that the temporal variation of wind velocity and the water-air temperature difference is similar to the change in the thickness of the quasihomogeneous layer (Fig. 2a). This indicates that the mechanism of the influence of the wind on the deepening of the lower boundary of the quasihomogeneous layer has in part the nature of direct wind mixing, in part a convective character associated with generation of hydrostatic instability.

The cited computations of the cross correlation relate to time intervals when the heat flux through the ocean surface changed little from day to day (Fig. 2c). Otherwise it would be difficult to trace the noted simple correlation between the wind and the thickness of the quasihomogeneous layer. In order to establish more complete and reliable dependences of this type it is necessary to carry out, for example, multiple correlation. For this purpose, in addition to the wind, it is necessary to make use of data on all the heat balance components, the evaporation-precipitation difference, and also take into account the influence of the initial state of the thermohaline structure proper [9].

An important characteristic of the thermal structure of the active layer in the ocean is the water temperature in the quasihomogeneous layer. During the observation period it varied from 26.5°C to 27.8°C (Fig. 2c). The water temperature disturbances arising at the surface rapidly affect virtually the entire homogeneous layer, which indicates its intensive turbulence. The magnitude of the phase shift and the vertical decrease in the amplitudes of these disturbances in the quasihomogeneous layer can be judged from the example cited in Fig. 1e. The change in the radiation heat budget of the surface for the most part had a regular diurnal character (Fig. 2c). Within the quasihomogeneous layer, in accordance with the change

APPROVED FOR RELEASE: 2007/02/08: CIA-RDP82-00850R000300080046-0

APPROVED FOR RELEASE: 2007/02/08: CIA-RDP82-00850R000300080046-0

in the radiation budget, a diurnal variation of water temperature was observed. The amplitude of the diurnal harmonic at the surface was 0.1°C. The shift of the maximum of surface temperature relative to the maximum of the radiation budget was 2-4 hours. The influence of the cloud cover changed the picture substantially (13-17 January, 25-26 February), complicating the variation of water temperature with time in the quasihomogeneous layer.

The intensive falling of precipitation led to freshening in a layer with a thickness of 10-15 m (Fig. 2d). The lower boundary of this layer was clearly expressed; the salinity gradients here attain values close to the gradients on the boundaries of the "core" of highly saline subtropical waters in the seasonal halocline. The lifetime of the freshened layer, dependent on the intensity of turbulence in the upper layers of the water, the quantity and intensity of precipitation, varied from 3 hours to 2 days (Fig. 2d, 1d). The vertical heat flux in the quasihomogeneous layer changed considerably in such situations.

A clearly expressed seasonal thermohalopycnocline is situated under the quasihomogeneous layer. It occupies the layer from 40-50 to 80-120 m. A singular characteristic of the thermohaline structure of waters in the region is that the halocline is represented by a clearly expressed tongue of water of increased salinity transported by the subsurface countercurrent from the subtropical regions of salinization [8]. Here the salinity profile has several extrema (Fig. 1b,c). The vertical salinity gradients under and over the tongue attain their maximum values. The center of the "core" experiences fluctuations in the range 55-85 m (Fig. 1b,c,d). The salinity here then increases to 36.2-36.3°/oo and sometimes to 36.4°/oo in comparison with 35.6-35.8°/oo outside the tongue of highly saline waters.

In the layer 60-70 m, corresponding approximately to the center of the seasonal thermocline and the core of waters of increased salinity, the temperature gradients change with time in the range from -0.10 to -0.35 C/m. The salinity gradients change from -0.05 to 0.05°/oo. Whereas at the extrema of the vertical salinity profile the gradients are equal to zero, at the horizons of a sharp increase or decrease they attain in absolute value 0.07-0.09°/oo/m. The density gradients at the center of the seasonal pycnocline vary with time from $0.3 \cdot 10^{-6}$ g/cm^4 to $1.2 \cdot 10^{-6}$ g/cm^4, on the average approaching $0.7 \cdot 10^{-6}$ g/cm^4.

In the seasonal thermocline the temperature for the most part decreases linearly from 26-27 to 15-16°C in a layer with a thickness 40-60 m, but its profile in many cases is complicated by a well-expressed stepped structure, evidently representing traces of turbulent deepenings of the quasihomogeneous layer in the past. The vertical scales of these structural elements have values from 1 to 10 m or more. Precisely over the points of their maximum curvature the temperature gradients attain their maximum values.

The self-similarity hypothesis [6] was checked for the vertical structure of the seasonal thermocline. This hypothesis assumes a universality of the distribution of water temperature in the seasonal thermocline. In such a case the dimensionless temperature profile

$$\Theta(z, t) = (T_S(t) - T(z, t))/(T_S(t) - T_H(t))$$

is dependent only on the dimensionless parameter

$$\eta(t) = (z - h(t))/(H - h(t)).$$

APPROVED FOR RELEASE: 2007/02/08: CIA-RDP82-00850R000300080046-0

APPROVED FOR RELEASE: 2007/02/08: CIA-RDP82-00850R000300080046-0

Here T_S is water temperature in a quasihomogeneous layer of the thickness h, T_H is the temperature at the lower boundary of the seasonal thermocline H, T(z,t) is the temperature at individual horizons of the seasonal thermocline, t, z are time and depth.

Table 2

Statistical Characteristics for Checking Self-Similarity Hypothesis (Notations in Text)

	Situation of marked shallowing of quasihomogeneous layer excluded from series			Full series considered		
	mean value	evaluation of standard deviation	mean horizon, m	mean value	evaluation of standard deviation	mean horizon, m
0.3	0.538	0.110	78	0.459	0.165	77
0.5	0.792	0.054	99	0.704	0.164	98
0.7	0.923	0.021	119	0.876	0.091	118

As the lower boundary of the seasonal thermocline we used the horizon 150 m, situated in the upper part of the main thermocline. The profiles for 1200 hours for all days were subjected to processing. Individual results are given in Table 2. In general, it can be said that the self-similarity hypothesis is satisfactorily satisfied. The only exception is the period of intensive shallowing of the quasihomogeneous layer on 5-13 February. At this time the forms of the $\theta(\eta)$ profiles were characterized by diversity. As a result, the mean dimensionless temperature is decreased but the temperature dispersion increases sharply (see Table 2). Individual checks indicate that internal waves exert virtually no influence on self-similarity. The normalization condition leads to a small dispersion θ at the edges of the profile. However, in general the fluctuations of θ with depth attenuate (Table 2).

The seasonal jump layer of characteristics is underlain by the main thermohalopycnocline (Fig. 1d). The temperature and salinity gradients decrease sharply in its upper part, in individual sectors of the profiles attaining values close to the gradients in the upper quasihomogeneous layer. The homogeneity gradient in the main pycnocline on the average is equal to $0.7 \cdot 10^{-7}$ g/cm^4, that is, an order of magnitude less than the gradient in the seasonal pycnocline.

The author expresses appreciation to Yu. A. Ivanov for useful discussion of the work.

BIBLIOGRAPHY

1. Bakhvalov, N. S., CHISLENNYYE METODY (Numerical Methods), Moscow, Nauka, 1975.

APPROVED FOR RELEASE: 2007/02/08: CIA-RDP82-00850R000300080046-0

APPROVED FOR RELEASE: 2007/02/08: CIA-RDP82-00850R000300080046-0

2. Byshev, V. I., Ivanov, Yu. A., "Model of the Nonstationary Thermohaline Structure of the Upper Layer in the Ocean," OKEANOLOGIYA (Oceanology), Vol 14, No 2, 1974.

3. Byshev, V. I., Ivanov, Yu. A., "Dynamic Model of Formation of the Quasihomogeneous Layer in the Ocean," OKEANOLOGIYA, Vol 17, No 4, 1977.

4. Grigorkina, R. G., et al., PRIKLADNYYE METODY KORRELYATSIONNOGO I SPEKTRAL'NOGO ANALIZA KRUPNOMASSHTABNYKH OKEANOLOGICHESKIKH PROTSESSOV (Applied Methods of Correlation and Spectral Analysis of Macroscale Oceanological Processes), Leningrad, Izd-vo LGU, 1973.

5. Kalatskiy, V. I., MODELIROVANIYE VERTIKAL'NOY TERMICHESKOY STRUKTURY DEYATEL'NOGO SLOYA OKEANA (Modeling of Vertical Thermal Structure of Active Layer of Ocean), Leningrad, Gidrometeoizdat, 1978.

6. Kitaygorodskiy, S. A., Miropol'skiy, Yu. Z., "On the Theory of the Active Layer in the Ocean," IZV. AN SSSR, FIZIKA ATMOSFERY I OKEANA (News of the USSR Academy of Sciences, Physics of the Atmosphere and Ocean), Vol 6, No 2, 1970.

7. Fedorov, K. N., TONKAYA TERMOKHALINNAYA STRUKTURA VOD OKEANA (Fine Thermohaline Structure of Ocean Waters), Leningrad, Gidrometeoizdat, 1976.

8. Khanaychenko, N. K., SISTEMA EKVATORIAL'NYKH PROTIVOTECHENIY V OKEANE (System of Equatorial Countercurrents in the Ocean), Leningrad, Gidrometeoizdat, 1974.

9. Niiler, P. P., "Deepening of the Wind-Mixed Layer," J. MARINE RES., Vol 33, No 3, 1975.

APPROVED FOR RELEASE: 2007/02/08: CIA-RDP82-00850R000300080046-0

APPROVED FOR RELEASE: 2007/02/08: CIA-RDP82-00850R000300080046-0

UDC 556.16.01(47)

MODELING OF PROCESSES OF RUNOFF FORMATION IN THE RIVERS OF THE FOREST ZONE OF THE EUROPEAN USSR

Moscow METEOROLOGIYA I GIDROLOGIYA in Russian No 10, Oct 80 pp 78-85

[Article by Candidate of Physical and Mathematical Sciences V. I. Koren', USSR Hydrometeorological Scientific Research Center, manuscript submitted 27 Feb 80]

[Text]

Abstract: A study was made of the characteristics of formation of runoff in forested and field sectors of watersheds. The author proposes a mathematical model which takes into account the principal thermophysical processes in the aeration zone and can be used in continuous computation of meltwater, rain and meltwater-rain runoff for rivers in areas with different degrees of forest cover. The model parameters are determined by optimization methods. Checking of the formulated model in a number of small watersheds in the forest zone indicated a good convergence of the actual and computed hydrographs. The ratio of volumes of runoff from field and forested sectors agrees with physical concepts.

A number of models of runoff formation are presently used in making hydrological computations. The most important of these include a model of formation of rain-induced high water [5] and a model of formation of the hydrograph of spring high water [2]. Experience shows that in the application of these models great difficulties arise during the transition periods when there is very great change in the water-absorption properties of the watershed as a result of the freezing and thawing of the soil. Because of this it is impossible to formulate a continuous model for the short-range forecasting of water discharge.

In this article we propose a model which takes into account the principal thermophysical processes transpiring in the aeration zone, as a result of which it can be used for continuous computation of meltwater, rain and meltwater-rain runoff. The considered model is a generalization of the model obtained earlier for completely forested watersheds [1] for the case of partially forested river basins.

APPROVED FOR RELEASE: 2007/02/08: CIA-RDP82-00850R000300080046-0

APPROVED FOR RELEASE: 2007/02/08: CIA-RDP82-00850R000300080046-0

The conditions for the formation of runoff in forested and field sectors are substantially different. One of the principal factors governing the great differences in water absorption properties in the field and forest is the presence of a small (about 5-10 cm) very loose soil surface layer in the forest. The data cited in [7] on the mechanical composition of different soils show that beginning at a depth of 5-10 cm the porosity of soils in field and forested sectors differs very insignificantly, whereas in the layer 0-10 cm these differences are very significant. This circumstance makes possible some simplification of the model of runoff formation for partially forested watersheds.

We will arbitrarily shift the surface line in the forest to the interface between the upper (5-10 cm), very permeable layer, and the lower-lying soil layer with a considerably lesser porosity. In other words, we will assume that in the forest all the water reaching the soil surface is instantaneously absorbed by the upper 5-10-cm layer. Some of this water is filtered into the lower-lying layer and some flows away in a network of streamlets forming a runoff close in time to the surface runoff. In this case the model can be constructed in such a way that the dependences for computing most of the balance components in the field and forest differ only in the coefficients.

We will discriminate an upper soil layer with the thickness z and a maximum moisture capacity ω_m. In forested sectors the upper boundary of this layer will be the line of the arbitrary surface (Fig. 1). If it is assumed that phase transitions occur only on the freezing or thawing front, whereas in the zone of negative temperatures all the moisture freezes, it is relatively simple to obtain balance expressions for moisture in the solid and liquid phases

$$\frac{dW_{\text{т}\,i}}{dt} = v_i + r_{\text{т}\,i} \qquad (i = 1, 2, \ldots, 5), \tag{1}$$

[T = thawed; M = frozen]

$$\frac{dW_{\text{м}\,i}}{dt} = r_{\text{м}\,i} \qquad (i = 2, 4), \tag{2}$$

where $W_{\text{thaw } i}$, $W_{\text{froz } i}$ are the reserves of liquid and solid moisture components in the i-th layer, v_i is the intensity of change in the liquid component as a result of water exchange with the upper and lower layers, $r_{\text{thaw } i}$, $r_{\text{froz } i}$ are the intensities of change of the thawed and frozen components as a result of phase transitions at the upper or lower boundaries of the layer.

In accordance with Fig. 1, we will write expressions for computing the balance components (thawing of the soil from below is not taken into account):

$$r_{\text{т}\,i} = \left[\operatorname{int}\left(\frac{i+1}{2}\right) - \operatorname{int}\left(\frac{i}{2}\right)\right] \frac{dZ_{\text{н}\,i}}{dt} \frac{W_{\text{т}\,i-1}}{\Delta Z_{i-1}} - \frac{dZ_{\text{в}\,i}}{dt} \frac{W_{\text{т}\,i}}{\Delta Z_i} \qquad (i = 1, 2, \ldots, 5), \tag{3}$$

$$r_{\text{м}\,i} = \frac{dZ_{\text{н}\,i}}{dt} \frac{W_{\text{т}(i-1)}}{\Delta Z_{i-1}} - \frac{dZ_{\text{в}\,i}}{dt} \frac{W_{\text{м}\,i}}{\Delta Z_i} \qquad (i = 2, 4), \tag{4}$$

[B = upper; H = lower]

$$v_i = \frac{\Delta Z_i}{Z_{\text{н}\,i}} (h_{\text{в}} - E - q - q_{\text{т}\,i} - q_{\text{т}}) \qquad (i = 1, 2, \ldots, 4), \tag{5}$$

APPROVED FOR RELEASE: 2007/02/08: CIA-RDP82-00850R000300080046-0

APPROVED FOR RELEASE: 2007/02/08: CIA-RDP82-00850R000300080046-0

$$v_5 = q_1 - q_2 - q_{I2}, \tag{6}$$

where $Z_{low\ i}$, $Z_{up\ i}$ are the lower and upper boundaries of the i-th layer respectively, W is the total moisture reserve,

$$\Delta Z_i = Z_{low\ i} - Z_{up\ i},$$

h_{water} is water yield at the surface, E is total evaporation from a watershed, q is surface runoff, $q_{I\ 1}$, $q_{I\ 2}$ is the soil runoff from the freezing and lower, not freezing zones, q_1, q_2 is the loss of moisture through the lower boundaries of the freezing and nonfreezing zones, int(x) is the whole part of the variable x.

The interfaces between the frozen and thawed soil layers were computed using the approximate dependence [6] derived from the heat transfer equations with the following fundamental assumptions: there is no inflow of heat (cold) from below; the distribution of temperatures in the frozen (thawed) layer and in the snow cover is linear; with a negative (positive) temperature all the moisture is in a solid (liquid) state; the water filtering during thawing does not participate in the heat transfer processes:

[c = snow; $\rho_B = \rho_{water}$]

$$Z(t+dt) = -\lambda H/\lambda_c + \{[\lambda H/\lambda_c + Z(t)]^2 + 2\lambda|T|dt/\rho_B L\omega\}^{1/2}, \tag{7}$$

where H and T are the depth of the snow cover and air temperature during the considered time interval dt; Z(t) and Z(t + dt) is the position of the interface by the beginning and end of the computation time interval respectively; ω is the volumetric moisture content at the freezing (thawing) front; ρ_{water} is water density; L is the latent heat of fusion for ice; λ_{snow} is the thermal conductivity coefficient for snow; λ is the thermal conductivity coefficient for frozen (during freezing) and thawed (during thawing) soil.

Expressions (1)-(7) are correct for both field and forested sectors of a watershed. We will assume that the structure of the dependences for computing water yield, evaporation, soil runoff and loss of moisture into the lower-lying layers is identical for field and forested sectors. Then for their computation it is possible to use expressions obtained earlier for completely forested watersheds [1]. However, the parameters of these expressions can be different for field and forested sectors.

Another fundamentally important distinguishing characteristic of the formation of meltwater runoff in the field is the formation of "blocking" layers, as a result of which infiltration in such sectors is virtually completely absent. Such layers are usually not formed in the forest. As a result, during the period of snow melting the expressions for computing the dynamics of surface runoff in the field and forest should be fundamentally different.

As noted above, by the term "surface runoff" in the forest we mean runoff in the uppermost 5-10-cm soil layer. In this case the intensity of infiltration will be determined by the water absorption properties of the lower-lying soil layer. If the retention of water in the upper layer is also taken into account, it is

APPROVED FOR RELEASE: 2007/02/08: CIA-RDP82-00850R000300080046-0

APPROVED FOR RELEASE: 2007/02/08: CIA-RDP82-00850R000300080046-0

possible to obtain a dependence for computing surface runoff in the forest

[Л = forest; h_B = h_{water}] $$q_л = \begin{cases} (h_в - I)\left\{1 - \exp\left[-m\sum^{t}(h_в - I - E)\right]\right\}, & I < h_в \\ 0, & I \geq h_в, \end{cases} \quad (8)$$

where I is the intensity of infiltration through the arbitrary surface, m is the retention parameter.

For a field we will assume that infiltration occurs only in sectors where a "blocking" layer was not formed. In the remaining part infiltration is absent and the losses are formed due to surface retention, that is

[П = field; h_B = h_{water}] $$q_п = \begin{cases} (h_в - I)s_k F_k + h_в s(1 - F_k), & I < h_в \\ h_в s(1 - F_k), & I \geq h_в, \end{cases} \quad (9)$$

$$s_k = 1 - \exp\left\{-m\sum^{t}(h_в - I - E)\right\},$$

$$s = 1 - \exp\left\{-m\sum^{t}(h_в - E)\right\},$$

where F_k is the fraction of the area of field sectors in which a "blocking" layer was not formed.

The intensity of infiltration for field and forested sectors was computed using the expression

[T = thaw; M = froz] $$I = k(\omega_{mp} - \omega)z + i(\omega_т - \omega_{mp})^n(1 + 8\omega_м)^{-2}, \quad (10)$$

where ω_{mp} is the maximum possible productive moisture, ω_{thaw} is the volume content of liquid moisture, ω_{froz} is volumetric ice content, k, i, n are parameters,

$$\omega = \omega_{thaw} + \omega_{froz}.$$

A validation of expression (10) is given in [1].

For the formation of a "blocking" layer there must be some critical relationships of the water absorption characteristics of the soil. According to the laboratory investigations of V. D. Komarov [4], the "blocking" layer is formed only upon attaining some critical soil temperature whose value is dependent on soil moisture content. In practice, as an indirect characteristic of soil temperature it is common to use the depth of freezing. In [3], for example, a dependence is given for the fraction of the area in which a blocking layer was formed on the product of the mean depths of freezing for the watershed and soil moisture content obtained on the basis of experimental data.

Soil moisture content (ω) and depth of freezing (Z) vary greatly over the watershed. We will assume that for field sectors in a specific watershed there is some critical value $u_k = (Z\omega)_k$ which when exceeded gives a soil which is virtually impermeable. If it is assumed that Z and ω at each point in the watershed are independent and there are stable distribution curves for them, it is possible to

APPROVED FOR RELEASE: 2007/02/08: CIA-RDP82-00850R000300080046-0

APPROVED FOR RELEASE: 2007/02/08: CIA-RDP82-00850R000300080046-0

write the following expression for computing the fraction of the area over which a "blocking" layer is not formed:

$$F_k(u \leqslant u_k) = \int_0^{\infty} \int_0^{u_k/\omega} f(\omega) f(Z)\, d\omega\, dZ, \tag{11}$$

where $f(\omega)$ and $f(Z)$ are the distribution curves for soil moisture content and depth of freezing in the field sectors of the watershed. In describing these curves we use a rather flexible single-parameter gamma distribution of the modular coefficients:

$$f(K) = \frac{\alpha^{\alpha}}{\Gamma(\alpha)} K^{\alpha-1} e^{-\alpha K}, \tag{12}$$

where K is a modular coefficient equal to $Z_i/\overline{Z}$ or $\omega_i/\overline{\omega}$, is a distribution parameter equal to $1/C_v^2$, C_v is the variation coefficient of the corresponding variable, $\overline{Z}$, ω are the mean values of the variables for the watershed.

Substituting expression (12) into (11) and integrating the latter, we obtain

$$F_k = \frac{\alpha_{\omega}^{\alpha_{\omega}}}{\Gamma(\alpha_{\omega})\,\Gamma(\alpha_z)} \int_0^{\infty} K_{\omega}^{\alpha_{\omega}-1} e^{-\alpha_{\omega} K_{\omega}} \Gamma_g(\alpha_z)\, dK_{\omega}, \tag{13}$$

where α_{ω} and α_z are the parameters of the distribution curves for moisture content and depth of freezing respectively, $\Gamma_g(\alpha_z)$ is the incomplete gamma function and $g = \alpha_z u_k/\overline{Z}\,\overline{\omega}\,K_{\omega}$.

Expression (13) is too unwieldy for practical computations. Without a significant loss of accuracy it can be assumed that α_z are only whole numbers. Also taking into account that the nonuniformity of the distribution of depths of freezing for the forest zone is considerably greater than for soil moisture content, we will exclude the influence of variability of the moisture content over the watershed, that is, we will assume that $\alpha_{\omega} \to \infty$. In this case it is possible to simplify expression (13):

$$F_k \approx 1 - e^{-\alpha_z K_k} \sum_{i=1}^{\alpha_z} (\alpha_z K_k)^{\alpha_z - i} / \Gamma(\alpha_z - i + 1), \tag{14}$$

where $K_k = u_k/\overline{Z}\,\overline{\omega}$.

Numerical experiments indicated that the differences in computations using expressions (13) and (14) with $\alpha_{\omega} > \alpha_z$ (if $\alpha_z \leqslant 6$) are insignificant and henceforth we will use the dependence (14).

In computing the changes in F_k during the high-water period the moisture content of the soil in expression (14) was kept constant from the moment of onset of snow melting and the depth of freezing decreased by the value of snow thawing by a particular moment. Thus, F_k increased by the end of the high water period, tending to unity.

V. D. Komarov proposed the following dependence for computing the maximum possible losses (with a virtually unlimited water supply in the snow):

APPROVED FOR RELEASE: 2007/02/08: CIA-RDP82-00850R000300080046-0

APPROVED FOR RELEASE: 2007/02/08: CIA-RDP82-00850R000300080046-0

$$P_m = Ae^{-\alpha\bar{\omega}}e^{-\beta\bar{z}\bar{\omega}} = I(\bar{\omega})e^{-\beta\bar{z}\bar{\omega}}, \tag{15}$$

where A, α, β are parameters.

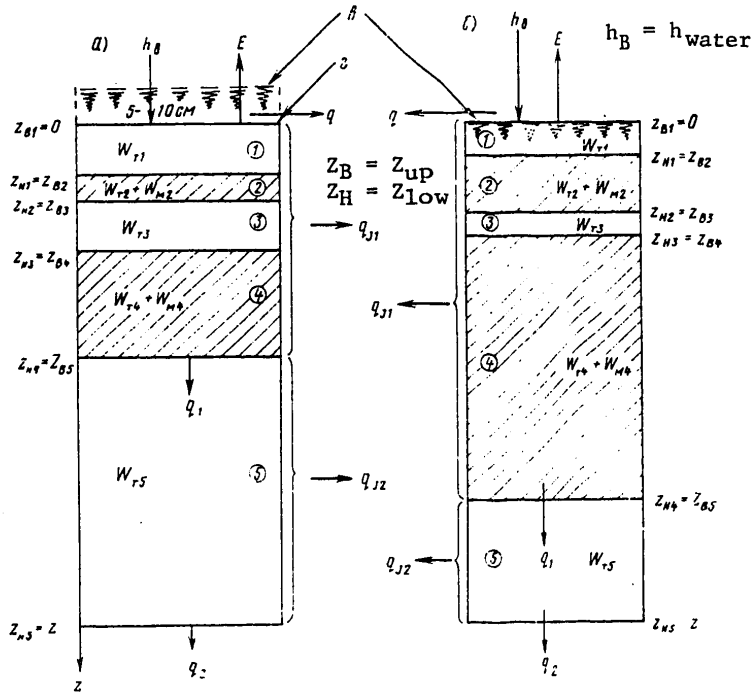

Fig. 1. Schematic section of soil for forested (a) and field (b) sectors of watershed: c) surface line, d) arbitrary surface line; 1, 3, 5 -- meltwater layer; 2, 4 -- freezing layers.

Integrating expression (9) with $S_k = s = 0$, $\alpha_z = 1$ and $F_k = \text{const}$, it is possible to determine the maximum possible losses during high water:

$$P_m' = \left(\int_0^T I dt\right)(1 - e^{-u_k/\bar{z}\bar{\omega}}). \tag{16}$$

In expression (16) the first cofactor is the potential total losses in infiltration and the second represents the fraction of the area in which they are formed. Expressions (15) and (16) are close in form, although each of the cofactors is

APPROVED FOR RELEASE: 2007/02/08: CIA-RDP82-00850R000300080046-0

APPROVED FOR RELEASE: 2007/02/08: CIA-RDP82-00850R000300080046-0

determined from different dependences. It can therefore be assumed that expression (15) also indirectly takes into account the fraction of the impermeable sectors for a case when soil moisture content is distributed uniformly over the area and the depth of freezing is close to a gamma distribution with the parameter $\alpha_z = 1$.

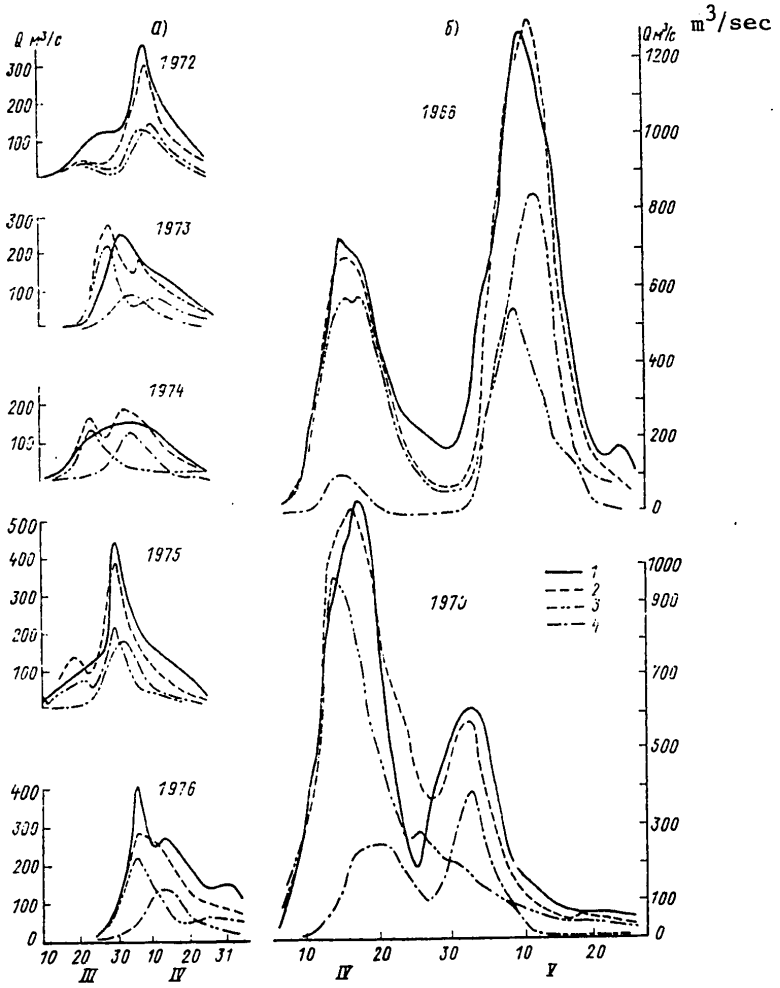

Fig. 2. Actual (1) and computed (2 -- total, 3 -- from field, 4 -- from forest) runoff hydrographs. a) Dnepr River, Dorogobuzh; b) Cheptsa River, Glazov.

All the balance equations for both field and forest were solved separately for snow-covered sectors of the watershed and sectors free of snow. The surface and soil runoffs from field and forested sectors were determined as the mean weighted values taking into account surface coverage with snow. In computing the runoff

APPROVED FOR RELEASE: 2007/02/08: CIA-RDP82-00850R000300080046-0

APPROVED FOR RELEASE: 2007/02/08: CIA-RDP82-00850R000300080046-0

hydrograph at the lowest-lying station the transformation was accomplished differently in dependence on the forest cover coefficient (γ). The surface and soil components of runoff (mean weighted values for the entire basin) were transformed for virtually completely forested or field watersheds ($0.25>\gamma>0.75$). In the remaining cases the forest and field components of surface runoff were transformed separately and the soil runoff was summed without additional transformations.

The formulated model includes a number of coefficients which can vary for different specific watersheds. Some of these coefficients take into account the influence of different zonal factors of runoff formation and vary slightly for watersheds situated within the limits of the same zone. The other parameters reflect the influence of local characteristics of runoff formation and can differ substantially for different watersheds situated even within the limits of uniform zones. In this connection the success of use of the model for specific watersheds is dependent to a great extent on the reliability of evaluation of the coefficients in the model reflecting both the zonal conditions of runoff formation and the local characteristics of the watershed.

The testing and perfecting of the model were carried out using data for five small (watershed area 5,000-10,000 km^2) watersheds in the forest zone in the basins of the Volga and Dnepr Rivers for which high waters are characteristic when there is a relatively stable snow cover. The forest cover coefficient for these watersheds varied from 0.25 to 0.80. Data were used from standard observations of the snow cover, daily temperatures and dew point spread, precipitation, and water discharge at the lowest-lying station. Data on variation of the depth of freezing and thawing of the soil were used only for a qualitative analysis of the results of computation of these characteristics.

The parameters were determined using the optimization method with a quality criterion equal to the sum of the squares of the deviations of the actual and computed water discharges [5]. The parameters were optimized in two stages. We initially optimized the most significant parameters which it was virtually impossible to measure or compute directly. The coefficients of equations (8)-(10) and the transformation parameters, in particular, can be assigned to this group. The number of these parameters for watersheds with different forest cover can vary from 9 to 13. The remaining parameters of the model (maximum moisture capacity of the soil, evaporation parameter, thawing coefficients) were not included in the optimization and their values were determined from field measurements or from balance relationships. A joint optimization of parameters of the first and second groups was accomplished in the second stage.

For all the considered watersheds the considered approach made it possible to obtain quite stable values of the parameters, as is confirmed by the virtually identical accuracy in computing water discharges for dependent and independent (the data were not used in the optimization) samples. This is also indicated by the weak variability of most of the parameters with transition from watershed to watershed. Accordingly, it can be expected that with application of the model to other watersheds in the forest zone it will be possible to reduce the number of parameters to be optimized.

APPROVED FOR RELEASE: 2007/02/08: CIA-RDP82-00850R000300080046-0

APPROVED FOR RELEASE: 2007/02/08: CIA-RDP82-00850R000300080046-0

The actual and computed runoff hydrographs for the two watersheds shown in Fig. 2 give some idea concerning the accuracy of computations of water discharges during the period of spring high water. A similar accuracy was obtained also for rain- and meltwater-rain-induced high waters. Figure 2 also shows hydrographs formed in field and forested sectors of watersheds. The forest cover coefficients for the watersheds of the Cheptsa and Dnepr Rivers as far as the considered gaging points were 0.40 and 0.42 respectively. In the graphs it is easy to trace considerable phase and amplitude differences of the hydrographs for field and forested sectors. Thus, if a watershed is considered as a purely field or purely forested sector it is scarcely possible to achieve a satisfactory accuracy in computing the hydrograph at the lowest-lying stations. The computations indicated that such an approximation is acceptable with forest cover coefficients falling in the range $0.25>\gamma>0.80$.

The runoff layers computed using the proposed model for high waters from the field sectors of these watersheds for all years exceed the corresponding values for forested sectors. The mean runoff coefficients for field and forest sectors of the Cheptsa basin were equal to 0.76 and 0.44, and for the Dnepr -- 0.77 and 0.62. These same runoff coefficients for the Cheptsa River were obtained in [7] with the separation of the total runoff during the high-water period into field and forested components by the method proposed by V. D. Komarov. The ratio of these components varies from year to year in a broad range (for the considered samples -- from 1.03 to 1.9).

In conclusion it can be noted that the resulting model takes into account the characteristics of runoff formation in field and forested sectors of watersheds and can be used in computing meltwater, rain and meltwater-rain runoff for small rivers in the forest zone with different degrees of forest cover.

BIBLIOGRAPHY

1. Bel'chikov, V. A., Koren', V. I., "Model of Formation of Meltwater and Rain Runoff for Forested Watersheds," TRUDY GIDROMETTSENTRA SSSR (Transactions of the USSR Hydrometeorological Center), No 218, 1979.

2. Zhidikov, A. P., et al., METODY RASCHETA I PROGNOZA POLOVOD'YA DLYA KASKADA VODOKHRANILISHCH I RECHNYKH SISTEM (Methods for Computing and Predicting High Water for Stages of Reservoirs and River Systems), Leningrad, Gidrometeoizdat, 1977.

3. Kapotov, A. A., "Evaluation of Runoff Loss on Infiltration During Spring High Water," TRUDY IV VSESOYUZNOGO GIDROLOGICHESKOGO S"YEZDA (Transactions of the Fourth All-Union Hydrological Congress), Vol 6, 1976.

4. Komarov, V. D., "Laboratory Investigations of the Permeability of Frozen Soil," TRUDY TsIP (Transactions of the Central Institute of Forecasts), No 54, 1957.

5. Koren', V. I., Kuchment, L. S., "Mathematical Model of Formation of Rain-Induced High Waters, Optimization of its Parameters and Use in Hydrological Forecasts," METEOROLOGIYA I GIDROLOGIYA (Meteorology and Hydrology), No 1, 1971.

APPROVED FOR RELEASE: 2007/02/08: CIA-RDP82-00850R000300080046-0

APPROVED FOR RELEASE: 2007/02/08: CIA-RDP82-00850R000300080046-0

6. Pavlov, A. V., TEPLOOBMEN PROMERZAYUSHCHIKH I PROTAIVAYUSHCHIKH GRUNTOV S ATMOSFEROY (Heat Exchange of Freezing and Thawing Ground and the Atmosphere), Moscow, Nauka, 1965.

7. Uskova, L. M., "Comparative Description of the Conditions for Formation and Coefficients of Runoff of Meltwater in Forested and Unforested Parts of a Basin," TRUDY GIDROMETTSENTRA SSSR (Transactions of the USSR Hydrometeorological Center), No 84, 1971.

APPROVED FOR RELEASE: 2007/02/08: CIA-RDP82-00850R000300080046-0

APPROVED FOR RELEASE: 2007/02/08: CIA-RDP82-00850R000300080046-0

UDC 556.166."45"(470.6)

PRINCIPAL CHARACTERISTICS OF MAXIMUM ANNUAL RUNOFF OF MOUNTAIN RIVERS IN THE NORTHERN CAUCASUS

Moscow METEOROLOGIYA I GIDROLOGIYA in Russian No 10, Oct 80 pp 86-92

[Article by Ye. F. Chekalovskiy, Giprorechtrans, manuscript submitted 3 Apr 80]

[Text]

Abstract: The moduli of maximum annual discharges with a 5% probability of excess, reduced to a watershed area of 200 km^2, are mapped on the basis of regional dependences. The dependence of the variation coefficient for maximum annual discharges on basin extent was established. A cartogram of the variation coefficient is given for a watershed area of 200 km^2, as well as a formula for conversion from this area to basins of other extents. The relationships of the variation and asymmetry coefficients for maximum annual runoff of the mountain rivers of the Northern Caucasus are given.

The maximum runoff of mountain rivers forming under the influence of a whole series of factors (melting of glaciers, high-mountain snows, showers and steady precipitation, bursting of dams formed by mudflows, etc.) is usually very difficult to break down into components. In addition, even if it is assumed that such a breakdown has been accomplished quite precisely, in computations of the flow discharge of a definite probability of excess it is necessary again to perform the quite unwieldy operation, not characterized by a high accuracy, of adding the probabilities of "high-water runoff" and "shower-induced runoff."

Accordingly, from our point of view, in the practice of planning of hydraulic structures on mountain rivers it is better to use the characteristics of maximum annual runoff determined considerably more simply, and in the last analysis, more precisely.

An analysis of the dependences of the moduli of maximum annual discharges on the area of the watershed, determined on the basis of observational data for 106 stations and posts located on the small mountain rivers of the Northern Caucasus (Fig. 1), makes it possible to arrive at the following conclusions:

APPROVED FOR RELEASE: 2007/02/08: CIA-RDP82-00850R000300080046-0

APPROVED FOR RELEASE: 2007/02/08: CIA-RDP82-00850R000300080046-0

1. With an area of the basins greater than 400 km^2 the degree of reduction of maximum mixed runoff occupies an intermediate value between the reductions of snow and shower runoff. For example, the reduction of the modulus of maximum annual discharge with a 5% probability of excess for rivers of the southern slope of the Black Sea chain of the Greater Caucasus is equal to 0.62, on the northern slope of this same sector of the water-divide crest it decreases to 0.50, within the limits of the zone of cuestas it is 0.47, and in the high-mountain zone beyond the Skalistyy Range is 0.44. On the other hand, for the lowland regions of the Northern Caucasus the value of the reduction index of snow runoff (not dependent on the probability) is 0.42, whereas for shower-induced runoff with a 5% probability it is 0.67.

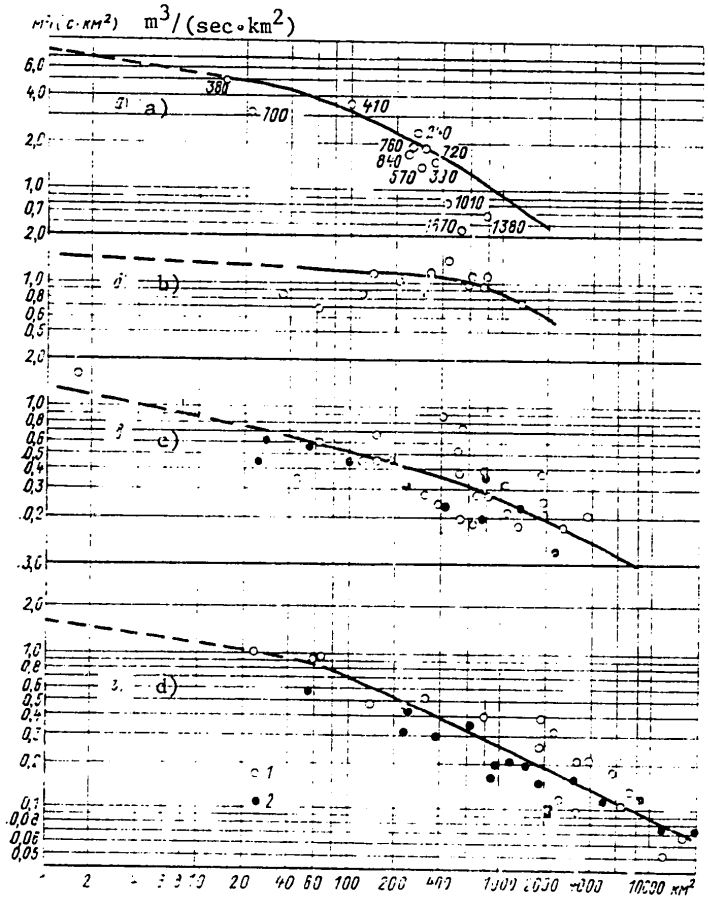

Fig. 1. Dependence of modulus of maximum annual discharge with 5% probability of excess on watershed area. a) southern slope of Black Sea chain (the figures denote the mean weighted elevation of the watershed), b) northern slope of Black Sea chain, c) high-mountain zone, d) zone of cuestas; 1) Kuban basin, 2) Terek basin.

APPROVED FOR RELEASE: 2007/02/08: CIA-RDP82-00850R000300080046-0

APPROVED FOR RELEASE: 2007/02/08: CIA-RDP82-00850R000300080046-0

Thus, a change in the reduction index with transition from one zone to another to some degree reflects the fraction of participation of shower-induced runoff in the formation of the maximum annual discharge. The greatest high waters on the rivers of the Black Sea coast of the Caucasus are formed for the most part by shower precipitation, whereas the maximum discharges in the high-mountain zone, as a rule, are the result of the intensive melting of glaciers and firn fields.

2. On rivers with a basin area less than 400 km^2 the reduction value decreases with a decrease in the extent of the watershed, resulting in dependences of a curvilinear character. This phenomenon is especially conspicuous on the rivers of the northern slope of the Black Sea chain, where continuous precipitation, simultaneously extending over considerable areas, is of very great importance in the formation of maximum runoff. Here the moduli of maximum runoff, with conversion from a watershed of 500 km^2 to an area of 10 km^2, increase by a factor of only 1.3.

On the basis of the dependences shown in Fig. 1 it was possible to compile a table making it possible to reduce the observational data to a watershed area of 200 km^2 (Table 1).

The value of the modulus of maximum runoff with a 5% probability of excess, reduced to a basin area of 200 km^2 q5(200), was mapped. A cartogram of the q5(200) value is a graphic illustration of the predominance of southwesterly moist air flows in the formation of maximum discharges in the territory of mountainous regions in the Northern Caucasus.

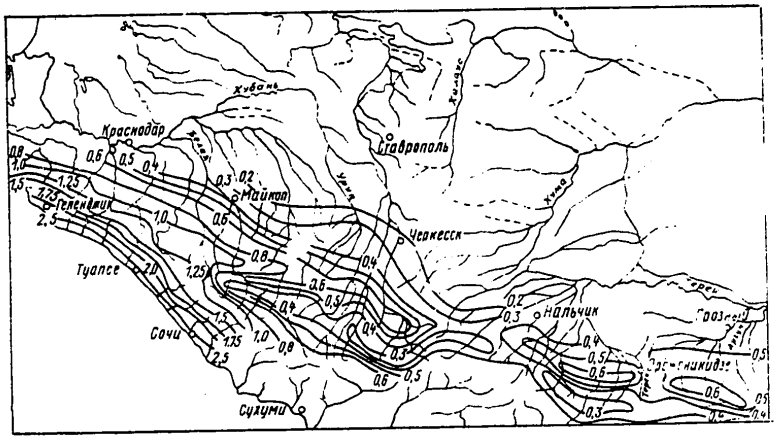

Fig. 2. Modulus of maximum annual runoff with a 5% probability of excess ($m^3/(sec \cdot km^2)$), reduced to a watershed area of 200 km^2.

On the slopes of the front ranges of the southern slope of the Black Sea chain, first encountered by these flows, the most vigorous rain-induced high waters are formed; in many cases in areas along the Black Sea they attain a catastrophic

APPROVED FOR RELEASE: 2007/02/08: CIA-RDP82-00850R000300080046-0

APPROVED FOR RELEASE: 2007/02/08: CIA-RDP82-00850R000300080046-0

FOR OFFICIAL USE ONLY

Table 1

Factors for Conversion from Maximum Annual Discharges With 5% Probability of Excess from Watershed Area

	Watershed area, km^2														
	11	5	10	25	50	75	100	200	300	400	500	750	1000	2000	3000
A	3.35	2.61	2.35	2.01	1.74	1.54	1.37	1.00	0.83	0.69	0.60	0.47	0.39	0.25	--
B	1.22	1.18	1.17	1.13	1.09	1.07	1.05	1.00	0.96	0.93	0.91	0.86	0.74	0.51	--
C	2.89	2.13	1.85	1.56	1.36	1.24	1.16	1.00	0.89	0.82	0.73	0.62	0.55	0.42	0.36
D	3.02	2.30	2.13	1.85	1.68	1.47	1.32	1.00	0.83	0.74	0.66	0.55	0.49	0.36	0.28

KEY:

A) Southern slope of Black Sea chain of Greater Caucasus

B) Northern slope of Black Sea chain

C) High-mountain zone (behind Skalistyy Range)

D) Zone of cuestas

FOR OFFICIAL USE ONLY

APPROVED FOR RELEASE: 2007/02/08: CIA-RDP82-00850R000300080046-0

APPROVED FOR RELEASE: 2007/02/08: CIA-RDP82-00850R000300080046-0

force. The q5(200) value here exceeds 2.5 $m^3/(sec \cdot km^2)$ and the moduli of the 5% runoff of small watercourses attain 7-9 $m^3/(sec \cdot km^2)$. With a rising of the terrain and an increase in the degree of its shielding from the southwesterly moisture-bearing flows q5(200) decreases to 1.5-2.0 $m^3/(sec \cdot km^2)$, whereas at the headwaters of the Mzymta it decreases to 1.0.

On the northern slope of the Black Sea chain in the most moistened sectors near the peaks the q5(200) value does not exceed 1.3-1.5 $m^3/(sec \cdot km^2)$, whereas at the foot of the slope it is equal to 0.6 $m^3/(sec \cdot km^2)$.

There is a very high territorial variability of maximum runoff in the upper course of the Belaya River. The moisture-bearing flows, passing around the Fisht-Oshten complex from the west, penetrate into the river valley situated along the Main Range and at the headwaters of the Belaya form rather high waters with q5(200) = 1.0-1.1 $m^3/(sec \cdot km^2)$. In the basins of its right-bank tributaries this parameter attains the same values (Kisha River at Lagernaya Karaulki 0.8; Dakh River at Dakhovskaya 1.1). In the basins of the left-bank tributaries of the Belaya, shielded from the moisture-bearing winds by the steep slope of the Skalistyy Range (Lagonaki Plateau), q5(200) is reduced to 0.4-0.5 $m^3/(sec \cdot km^2)$ (Zhelobnaya River at Guzeriplya 0.45).

North of the mouth of the Dakh River the Skalistyy Range, facing eastward, exerts a definite influence on the formation of runoff to the meridian of El'brus. In the basins of small watercourses, beginning near its precipitous slopes, the modulus of maximum runoff is equal to 0.6-0.8 $m^3/(sec \cdot km^2)$. There is a considerable increase in the maximum runoff on the "transit" rivers which intersect the range: in the longitudinal valley between the Main (Glavnyy) and Skalistyy Ranges q5(200) usually does not exceed 0.3-0.4, whereas after intersecting the Skalistyy Range it increases to 0.5-0.7 $m^3/(sec \cdot km^2)$.

Within the limits of the Central Caucasus the influence of the Skalistyy Range, in elevation considerably less than the Main (Glavnyy) and Side (Bokovoy) Ranges, decreases sharply; nevertheless its orographic line can still be traced on the map of isolines of the modulus of runoff by an increase in q5(200) to 0.5-0.6 $m^3/(sec \cdot km^2)$. These increases with individual breaks are continued to the Argun River.

The problem of the regularities which in the mountain regions control the value of the variation coefficient of maximum runoff and its distribution over a territory has been studied relatively little. In the computation schemes proposed by different researchers it is usually proposed that use be made of territorially averaged conversion factors from the computed value (usually 1-5%) to the stipulated value.

For example, the Transcaucasian Scientific Research Institute proposes that for the western regions of Transcaucasia use be made of conversion factors corresponding to a value of the variation coefficient 0.6 and $C_s = 4C_v$ [5].

A single value of the conversion factor with use of a log-normal curve is recommended for mountainous Crimea in [6]. A similar solution with the use of a binomial curve was adopted for the Kuban and Terek basins [4] and only for the

APPROVED FOR RELEASE: 2007/02/08: CIA-RDP82-00850R000300080046-0

APPROVED FOR RELEASE: 2007/02/08: CIA-RDP82-00850R000300080046-0

Armenian SSR have specialists developed a more detailed scheme for the determination of C_V in dependence on the extent of the basin and the elevation of the terrain [1].

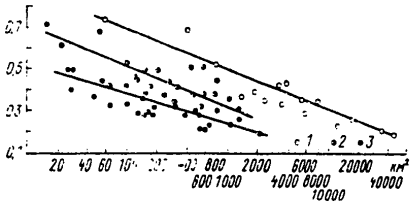

Fig. 3. Dependence of variation coefficient on watershed area. 1) zone of cuestas; 2) Black Sea chain; 3) high-mountain zone.

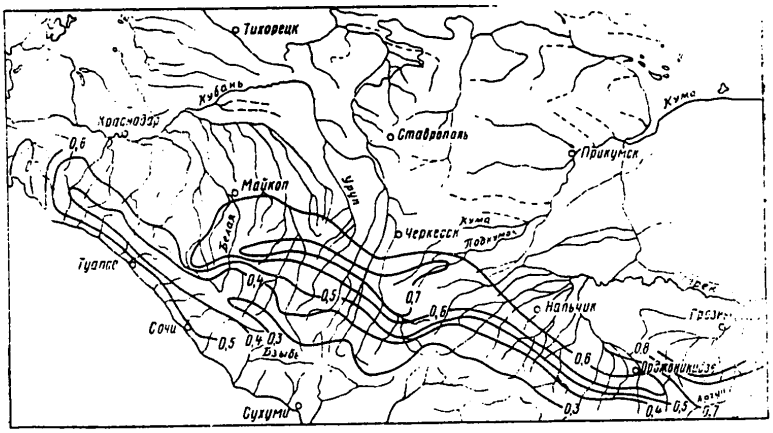

Fig. 4. Variation coefficient of maximum annual discharges reduced to a watershed area of 200 km^2.

Meanwhile, in the mountain regions of the Northern Caucasus the variation coefficient varies in the range from 0.2-0.3 to 1.0-1.2. Naturally, with conversion from the computed probability of excess to the stipulated error due to averaging C_V can attain extremely substantial values.

In the analysis of the principal regularities controlling the value of the variation coefficient of maximum annual runoff of mountain regions in the Northern Caucasus use was made of 110 runoff series with a duration of observations from 15 to 45 years.

The values of the variation coefficient in 70% of the cases do not exceed 0.5 and therefore C_V was determined by the moments method.

The value of the variation coefficient exhibits an explicit dependence on watershed area (Fig. 3). This dependence can be expressed by the formula

APPROVED FOR RELEASE: 2007/02/08: CIA-RDP82-00850R000300080046-0

APPROVED FOR RELEASE: 2007/02/08: CIA-RDP82-00850R000300080046-0

$$C_{v_F} = A - B \lg (F + 1). \quad (1)$$

The angle coefficient B for the three main zones (both slopes of the Black Sea chain and the zone of cuestas), in which the formation of maximum runoff occurs for the most part under the influence of rain precipitation, assumes one and the same value 0.19 and only for the high-mountain zone, where the runoff maximum is formed almost exclusively due to the melting of glaciers and snows in the high mountains, does the B value decrease to 0.14.

The physical sense of the A parameter is clear: this value of the variation coefficient applies to the smallest watersheds. However, it is more convenient not to use the parameter A, but the value of the variation coefficient reduced to a watershed area of 200 km^2 (C_{v200}). The following relationship obviously exists between A and C_{v200}:

$$A = C_{v_{200}} + B \lg 201 = C_{v_{200}} + 2{,}30\,B. \quad (2)$$

In the distribution of the C_{v200} value over the area (Fig. 4) we also see an increase in runoff variability along the orographic line of the Skalistyy Range. Here the C_{v200} value increases to 0.6-0.7 versus 0.3-0.4 in the high-mountain zone. The C_{v200} parameter attains its maximum values (0.9-1.0) at the foot of the front ranges bounding the Chechenskaya Plain on the south. Precisely in this region intensive shower activity develops, caused by local orocyclogenesis.

The asymmetry coefficient for runoff series was determined by trial and error using the G. N. Brovkovich graphs. The use of these graphs instead of the G. A. Alekseyev graph-analysis method which has come into wide use in the divisions of the State Committee on Hydrometeorology in this case is dictated by the circumstance that the variation of most series did not exceed 0.5. In the case of small values of the variation coefficient the influence of the asymmetry coefficient on the shape of the distribution curve is very small: a change in C_S/C_V from 2 to 6 will change the modular coefficient of 5% probability of excess by not more than 4%, which is several times less than the accuracy in determining the maximum discharges on the basis of hydrometric data. Naturally, striving to "fit" the curve as close as possible to the empirical points leads to completely improbable C_S/C_V ratios (10-15 or more).

Among the 74 determinations of the asymmetry coefficient made using the Brovkovich graphs a $C_S/C_V = 1$ value was obtained in three cases, $C_S/C_V = 2$ -- in 49 cases, $C_S/C_V = 3$ -- in 13 cases, $C_S/C_V = 4$ -- in 7 cases.

In two cases the shape of the distribution curve was uncertain; in the remaining cases it corresponded to a binomial model.

The obvious predominance of C_S/C_V in the limits 2-3 makes it possible to consider the recommendation in SN-435-72 (assume the C_S/C_V ratio for rivers with mixed sources to be equal to 3.0) to be entirely justified.

APPROVED FOR RELEASE: 2007/02/08: CIA-RDP82-00850R000300080046-0

APPROVED FOR RELEASE: 2007/02/08: CIA-RDP82-00850R000300080046-0

Thus, determination of the maximum discharge with any probability of excess, using the proposed scheme, is carried out in the following sequence.

1. The modulus of 5% runoff for a stipulated area is determined from the cartogram of the modulus of maximum runoff of 5% probability of excess, reduced to a watershed area of 200 km^2 (Fig. 2), and a table of conversion factors (Table 1) is used in determining the modulus of 5% runoff for a stipulated area.

2. The C_{v200} value is read from the cartogram (Fig. 4).

3. Using a formula determined by expressions (1) and (2),

$$C_{v_F} = C_{v_{200}} + B[2{,}30 - \lg(F+1)] \qquad (3)$$

it is possible to compute the variation coefficient for a particular area F. The parameter B in formula (3) for a high-mountain zone (beyond the Skalistyy Range) was assumed equal to 0.14; for the remaining territory it was equal to 0.19.

4. The conversion factor from a 5% probability of excess to the stipulated value is determined from a table of the normal deviations of the ordinates of the binomial curve from the mean with computed C_v and $C_s = 3C_v$.

The proposed scheme makes possible a quite reliable determination of the maximum discharges in the range of areas from 10 to 3,000 km^2. For computing the runoff of rivers from greater areas it is preferable to use interpolation between the processed data for series of observations.

The described scheme can be used not only for its direct purpose, that is, for computing the maximum discharges of unstudied rivers, but to some degree for evaluating the representativeness of a relatively short period of observations. In connection with the inadequate representativeness of short series there are cases when considerable high waters do not enter into the series, which leads to an understatement of the computed discharges and variation coefficient [3]. For example, the modulus of a 5% discharge, reduced to a watershed area of 200 km^2, according to observational data for the Armkhi River at Chmi village, is 0.10, which is 3-4 times less than the characteristic values for this region. This causes serious doubts of the possibility of use of this series for hydroengineering planning.

On the other hand, at times one catastrophic high water of extremely low probability of excess leads to an increase in the computed values by several times. For example, in 1953 on the Gizel'-Don and Tseya Rivers there were high waters with moduli (reduced to a watershed area of 200 km^2) equal to 0.7 and 1.2 respectively, that is, exceeding by a factor of 2-3 the 5% probability value characteristic for this region. The inclusion of this high water in the computation series increases the variation coefficient for the Gizel'-Don River from 0.38 to 1.02 and for the Tseya River from 0.33 to 1.16, which corresponds to C_{v200} of 1.06 and 1.20. Such values are not observed over the entire mountainous territory of the Northern Caucasus. An analysis of the conditions for the passage of this high water, taking into account that the bursting of mudflow dams participated in its formation [2], confirms that its probability approaches 0.1%.

APPROVED FOR RELEASE: 2007/02/08: CIA-RDP82-00850R000300080046-0

APPROVED FOR RELEASE: 2007/02/08: CIA-RDP82-00850R000300080046-0

The problem of determining the probability of excess of the high water greatest according to observational data for a group of N rivers over the course of n years for the time being has no definite solution. It is obvious that for using the "probability of probabilities" curve or a composite curve with determination of the probability of the first term of the series p = 1/Nn there must be a complete absence of correlation between the series, which for a limited territory is improbable. It is also illogical to assign such a high water to the probability 1/n, since for such an assumption it is required that the correlation coefficient be equal to 1.0. The true probability will fall between these two values.

The analysis of such high waters can be considerably facilitated when using geographical diagrams of the runoff characteristics similar to that proposed above.

BIBLIOGRAPHY

1. Antonyan, A. Ye., "On the Problem of Determining the Variation Coefficient for the Maximum Discharges of Rivers in the Armenian SSR," SB. NAUCHNYKH TRUDOV YEREVANSKOGO POLITEKHNICHESKOGO INSTITUTA (Collection of Scientific Papers of the Yerevan Polytechnic Institute), Vol 25, Yerevan, 1970.

2. Vilenkin, M. A., "Unusual High Water in Northern Osetia," PRIRODA (Nature), No 6, 1956.

3. Zalesskiy, F. V., "Construction of the Computed Curve for the Probability of Maximum Water Discharges," METEOROLOGIYA I GIDROLOGIYA (Meteorology and Hydrology), No 7, 1975.

4. RESURSY POVERKHNOSTNYKH VOD SSSR (Resources of USSR Surface Waters), Vol 8, Part 3, Leningrad, Gidrometeoizdat, 1973.

5. TEKHNICHESKIYE UKAZANIYA PO RASCHETU MAKSIMAL'NOGO STOKA REK V USLOVIYAKH ZAKAVKAZ'YA (Technical Instructions for Computing the Maximum Runoff of Rivers in Transcaucasia), Tbilisi, ZAKNIGMI, 1969.

6. Khloyeva, Ye. V., "On the Problem of Computations of the Maximum Water Discharges of Rivers in the Crimea," SB. RABOT PO GIDROLOGII (Collection of Papers on Hydrology), No 8, Leningrad, 1968.

APPROVED FOR RELEASE: 2007/02/08: CIA-RDP82-00850R000300080046-0

APPROVED FOR RELEASE: 2007/02/08: CIA-RDP82-00850R000300080046-0

UDC 556.(535.5+06)"32"

GENERAL SCHEME FOR COMPUTING AND PREDICTING THE BREAK-UP OF RIVERS

Moscow METEOROLOGIYA I GIDROLOGIYA in Russian No 10, Oct 80 pp 93-99

[Article by Candidate of Geographical Sciences L. M. Margolin, USSR Hydrometeorological Scientific Research Center, manuscript submitted 24 Jan 80]

[Text]

Abstract: The author proposes a physically validated and practical general scheme for computing and predicting the times of break-up of rivers based on the correlation between the modular coefficients of ice strength and water discharge on the day of the break-up. The variables of this correlation are characterized in the study by a number of easily determined basic hydrological and morphometric parameters of rivers and their basins. Thus, a step has been taken toward obtaining a universal method for computing and predicting the break-up of rivers. Proposals for further investigations are formulated.

In studying the ice regime of rivers, especially the formation, growth and destruction of the ice cover, researchers usually [2, 3] examine the mentioned phenomena in their totality, as a single process characteristic for most rivers.

Many years were required, for example, for creating a model of appearance of ice [4] common for all rivers. The broad application of this model became possible only after it was possible to find easily determined fundamental morphometric and hydraulic parameters of rivers which replaced component equations describing the appearance of ice.

The same difficulties were encountered in formulating a model of the break-up of rivers [1], which only at the beginning of the 1970's assumed its present form

$$\varphi h_{spr} \leqslant f(A_{spr}). \qquad (1)$$

According to this model, the break-up occurs when a critical relationship is reached by the ice strength, decreasing by spring (φh_{spr}), and the increasing water volume in the river (A_{spr}). The water volume in the river was characterized in this model for different rivers either by the water level or discharge or by their increment over some initial value primarily for obtaining a better

APPROVED FOR RELEASE: 2007/02/08: CIA-RDP82-00850R000300080046-0

APPROVED FOR RELEASE: 2007/02/08: CIA-RDP82-00850R000300080046-0

probability of the correlations. Until now the application of this model has been difficult and has been limited by the need for determining local correlations, the difference in whose form is physically difficult to explain.

Without question it is necessary to obtain a universal method for computing and predicting the times of river break-up. It must be regarded as the final result of solution of a number of complex intermediate problems involving a great many different factors determining the destruction of the ice cover under the influence of heat and the fracturing force of the flow. A factor of great importance is spring meteorological conditions, such as air temperature (alternation of heat and cold waves), intensity of solar radiation, its duration. The morphometric and hydraulic characteristics of the flow, channel, valley, and possibly the entire river basin are extremely important. We have in mind here the dimensions of the channel and its configuration in cross section and horizontally, the presence or absence of a floodplain, its extent, configuration and vegetation, river slopes, extent and configuration of the watersheds. Other factors of great importance are ice structure, the conditions for the formation of frazil and snow ice, outcrops of ground water, presence of tributaries with other breaking-up conditions, etc. It must be assumed that even the cited list of factors, determining the phenomenon of breaking-up of rivers, is not complete.

Allowance for all these factors is extremely difficult and on a practical basis is not too useful. It was desirable to introduce a search for the principal or complex indices of the process of breaking-up of rivers which with a sufficient accuracy could reflect the effect of this set of factors. For this reason, evidently, S. N. Bulatov [1] called the correlation which he established for the Lena River at Tabaga the first step in the development of a universal method for computing the break-up of rivers

$$\varphi h_{spr} \leqslant f_1\left(\frac{Q^2}{B^2}\right), \qquad (2)$$

where Q is water discharge on the day of the break-up, B is river width with a particular discharge.

The equation approximating this correlation was similar to the equations for four other rivers which he selected with different regimes.

In our opinion, the universality of these equations was a result of an attempt to reduce the parameters of the rivers to a single scale. In actuality, the Q/B ratio is none other than the specific water discharge, in some degree leveling the influence of the differences in river volumes. However, the river depths are also extremely different. There is an enormous range in variation of the extent of basins, their geographical location, and this means, in the conditions for runoff formation.

In connection with what has been stated, we assumed that first of all an attempt must be made to reduce to a single scale the runoff parameters governing the break-up of rivers. For this purpose the water discharges on the day of the break-up (Q_{spr}) for seven rivers in the northern part of the European USSR -- Severnaya Dvina, Yug, Sukhona, Vychegda, Mezen', Onega and Pechora -- were expressed in

APPROVED FOR RELEASE: 2007/02/08: CIA-RDP82-00850R000300080046-0

APPROVED FOR RELEASE: 2007/02/08: CIA-RDP82-00850R000300080046-0

fractions of unity, in the form of their ratio to the maximum values of water discharges on the day of break-up on each river (Q_{max}) for a long-term period. We assume further that the ice strength during the break-up (φh_{spr}) on different rivers can vary considerably due to the peculiarities not so much of their size as their regime. Accordingly, without at this stage dwelling on an analysis of the physics of the phenomenon, we also related this strength to the maximum ice strength during the break-up on each river during the long-term period. Denoting by φh_M the ratio $\varphi h_{spr}/\varphi h_{max}$ and by Q_M the ratio Q_{spr}/Q_{max}, using the data for all rivers we obtained the correlation of these parameters, approximated by the equation

$$\varphi h_M = 0{,}07 + 1{,}5\,Q_M^2 + 0{,}3\,(1-e^{Q_M}). \qquad (3)$$

The probability of nonexcess of the admissible error (2 days) in computing the break-up of the mentioned rivers on the basis of equation (3) was rather high -- from 89 to 100% and on the average was 92%. Attempts at using this equation for some rivers in other regions were less successful. We analyzed the reasons for this circumstance on the basis of a comparison of local correlations of the type (1) for rivers in different regions cited in Table 1.

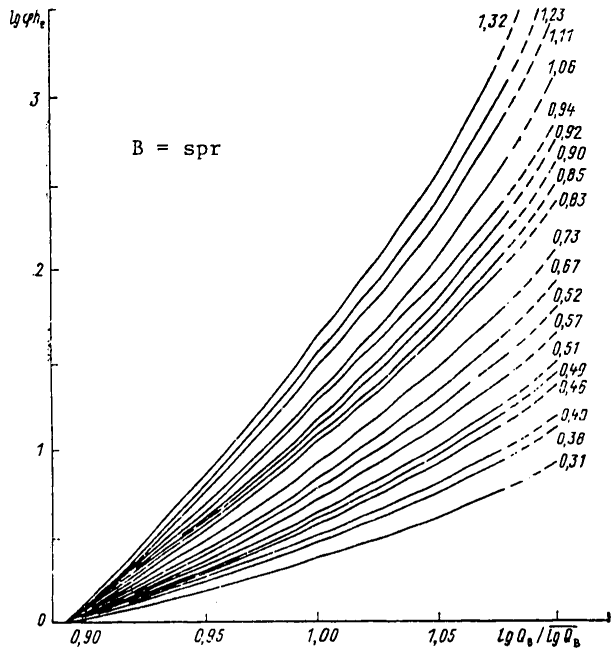

Fig. 1. Correlations $\lg \varphi h_{spr} \leqslant \psi'$ ($\lg Q_{spr}/\lg \overline{Q_{spr}}$) for investigated rivers. The figures on the curves are the norms for ice strength during break-up $\overline{\lg \varphi h_{spr}}$.

APPROVED FOR RELEASE: 2007/02/08: CIA-RDP82-00850R000300080046-0

APPROVED FOR RELEASE: 2007/02/08: CIA-RDP82-00850R000300080046-0

In this stage we considered it possible to limit ourselves to such a number of rivers, taking into account the great difference in their size, geographic location and accordingly the sharply different hydrological regime. For example, the greatest thickness of the ice on these rivers varies on the average from 40 to 150 cm, the water discharges during break-up vary from 250 to 80,000 m^3/sec, and the break-up time differs by more than two months.

For convenience in comparison of the local correlations the variables changing in a wide range were expressed in logarithmic form and for all the rivers dependences were constructed on a uniform scale:

$$\lg \varphi h_{spr} \leqslant f_2 \lg (Q_{spr}). \tag{4}$$

Each of them is entirely satisfactory. Their mean probability is 94%. An analysis of these correlations indicated that the use of the earlier cited relative values cannot be successful because the maximum values of the water discharges and ice strength during break-up can deviate substantially from the mean values of the adopted variables. The mean long-term values of water discharges and ice strength during the break-up are more indicative. This is discovered in constructing correlations of the form

$$\lg \varphi h_B \leqslant \psi' \left(\frac{\lg Q_B}{\overline{\lg Q_B}} \right), \tag{5}$$

[B = spr]

for all the investigated rivers, where $\lg Q_{spr}/\overline{\lg Q_{spr}}$ are the relative values of water discharge during the break-up.

The constructed curves emerge virtually from the same point on the x-axis (Fig. 1), showing that with the mean minimum water discharge causing the break-up the ice strength on all the rivers is close to zero. With an increase in Q_{spr} there is an increase in the variability of ice strength and therefore the computed curves are arranged regularly in the form of an abacus, differing with respect to the mean value of ice strength during the break-up.

The mean long-term water discharges during the break-up ($\overline{Q}_{spr}$), as well as the river runoff norms, are a function of watershed area:

$$\overline{\lg Q}_{spr} = \psi''(\lg F). \tag{6}$$

This correlation is approximated by the equations:

$$\overline{\lg Q}_B = 1{,}01 \lg F - 1{,}71, \tag{7}$$

[B = spr]

$$\overline{\lg Q}_B = 0{,}67 \lg F - 0{,}53, \tag{8}$$

where F is the watershed area, km^2.

Equation (7) was derived for zones of normal and excess moistening and is characterized by the correlation coefficient r = 0.97; equation (8) was established for the zone of inadequate moistening; its correlation coefficient is r = 0.99.

APPROVED FOR RELEASE: 2007/02/08: CIA-RDP82-00850R000300080046-0

APPROVED FOR RELEASE: 2007/02/08: CIA-RDP82-00850R000300080046-0

Carrying out replacement of the right-hand side of inequality (5) on the basis of equations (7), (8), we accordingly obtain the expressions

[B = spr]

$$\lg \varphi h_B \leqslant f_4' \left(\frac{\lg Q_B}{\lg F - 1{,}71} \right), \tag{9}$$

$$\lg \varphi h_B \leqslant f_5' \left(\frac{\lg Q_B}{0{,}67 \lg F - 0{,}33} \right). \tag{10}$$

The inequalities (9), (10) do not require special explanations since the right-hand sides of inequality (5) here lose their externally abstract form, in physical sense approaching the runoff moduli and characterizing the conditions of its formation in the watersheds.

Now, in greater detail, we will examine the variability of ice strength during the break-up in its geographic aspect. The analysis made it possible to establish that in order to obtain more indicative relative values of ice strength during break-up it is also better to use its mean long-term value, not its maximum value. This makes it possible to obtain some single dependence for different rivers between the relative values of water discharge and ice strength during the break-up. Empirically this was revealed as a result of derivation of such a dependence initially for five rivers (Severnaya Dvina, Pechora, Dnestr, Oka, Yenisey):

$$\frac{\lg \varphi h_B}{\overline{\lg \varphi h_B}} \leqslant f_6 \left(\frac{\lg Q_B}{\overline{\lg Q_B}} \right), \tag{11}$$

where $\lg \varphi h_{spr} / \overline{\lg \varphi h_{spr}}$ is the relative ice strength value.

This correlation (Fig. 2) was supplemented by data for the remaining 17 points (a total of more than 400 cases) and was entirely satisfactory. The probability of nonexcess of the admissible error in computing the break-up for all 22 points when using this correlation is 83-100% and on the average is 92%.

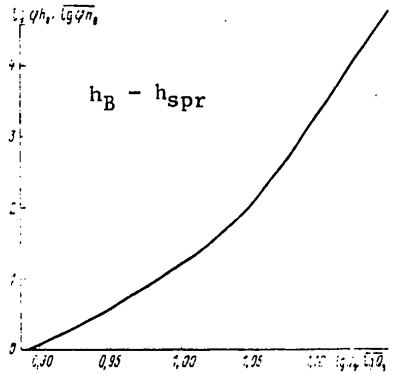

Fig. 2. Correlation $\lg \varphi h_{spr} / \overline{\lg \varphi h_{spr}} \leqslant f(\lg Q_{spr} / \overline{\lg Q_{spr}})$, common for investigated rivers.

APPROVED FOR RELEASE: 2007/02/08: CIA-RDP82-00850R000300080046-0

APPROVED FOR RELEASE: 2007/02/08: CIA-RDP82-00850R000300080046-0

A geographical analysis of the mean long-term ice strength values on break-up day shows that the mean $\overline{\lg \varphi h_{spr}}$ values are related to climate and increase with an increase in the severity of the latter. Precisely for this reason we have the relationship

$$\lg \varphi h_{spr} = \psi_1(\overline{h_{ice}}), \tag{12}$$

where $\overline{h}_{ice}$ is the mean long-term maximum ice thickness on the rivers.

However, the correlation coefficient for this relationship is low (r = 0.79) and for a number of rivers in the north and east the mean ice strength during the break-up $\lg \varphi h_{spr}$ is less than on some rivers in the south and west. A dependence in the form

$$\overline{\lg \varphi h_в} = \psi_2\left(\frac{1}{\overline{\Delta}}\right), \tag{13}$$

was also obtained, where $\overline{\Delta}$ is the mean long term duration of the melting of the ice from the date of disappearance of the snow from the ice to the date of break-up of the river.

This dependence shows that the longer the period of melting of the ice, the lesser is its strength during the break-up (φh_{spr}), primarily as a result of an increase in the quantity of heat reaching the ice cover. The correlation coefficient of this dependence is somewhat higher (r = 0.84). Then finding that there is almost no correlation between $\overline{h}_{ice}$ and $\overline{\Delta}$, we found it possible to proceed to the dependence

[B = spr; Л = ice]

$$\overline{\lg \varphi h_л} = \psi\left(\frac{\overline{h_л}}{\overline{\Delta}}\right), \tag{14}$$

which is approximated by the equation

$$\overline{\lg \varphi h_в} = 0{,}16\left(\frac{\overline{h_л}}{\overline{\Delta}}\right) + 0{,}006. \tag{15}$$

The correlation coefficient of this dependence is r = 0.94.

Substituting the $\overline{\lg \varphi h}$ value into the left-hand side of the inequality (11) (from equation (15)), we obtain the expression

$$\frac{\lg \varphi h_в}{0{,}16\left(\frac{\overline{h_л}}{\overline{\Delta}}\right) + 0{,}006} \leqslant J\left(\frac{\lg Q_в}{\lg Q_в}\right), \tag{16}$$

and carrying out replacements in it on the basis of equations (7), (8) and (15), we have

$$\frac{\lg \varphi h_в}{0{,}16\left(\frac{\overline{h_л}}{\overline{\Delta}}\right) + 0{,}006} \leqslant J_1\left(\frac{\lg Q_в}{\lg F - 1{,}71}\right), \tag{17}$$

$$\frac{\lg \varphi h_в}{0{,}16\left(\frac{\overline{h_л}}{\overline{\Delta}}\right) + 0{,}006} \leqslant J_2\left(\frac{\lg Q_в}{0{,}67 \lg F - 0{,}33}\right), \tag{18}$$

APPROVED FOR RELEASE: 2007/02/08: CIA-RDP82-00850R000300080046-0

APPROVED FOR RELEASE: 2007/02/08: CIA-RDP82-00850R000300080046-0

FOR OFFICIAL USE ONLY

Table 1

List of Rivers and Some Characteristics

River - station	Watershed area, km^2	Means		Mean date	
		maximum ice thickness, cm	water discharge on break-up day m^3/sec	departure of snow from ice	break-up
Pripyat'-Mozyr'	97200	38	457	12 March	24 March
Berezina-Bobruysk	20200	42	247	15 "	28 "
Don-Belyayevskiy	204000	48	1007	19 "	28 "
Dnepr-Rechitsa	58200	42	496	17 "	30 "
Oka-Kaluga	54900	57	1541	26 "	3 April
Oka-Kashira	68700	55	1620	28 "	6 "
Oka-Polovskoye	99000	60	2836	29 "	10 "
Oka-Kasimov	130000	50	2320	27 "	12 "
Oka-Murom	188000	52	2150	26 "	11 "
Severnaya Dvina-Abramkovo	220000	66	4560	14 April	28 "
Severnaya Dvina-Zvoz	285000	67	6540	14 "	30 "
Severnaya Dvina-Ust'-Pinega	348000	59	9550	14 "	2 May
Sukhona-Kalikino	49200	69	1315	6 "	21 April
Yug-Gavrino	34800	56	760	5 "	21 "
Vychegda-Syktyvkar	66900	60	740	8 "	27 "
Onega-Porog	55700	58	980	6 "	28 "
Mezen'-Malonisogorskaya	56400	73	2340	16 "	8 May
Pechora-Ust'-Shugor	67500	81	4270	24 "	9 "
Pechora-Ust'-Tsil'ma	248000	72	7950	24 "	14 "
Lena-Vitim	199000	81	3980	29 "	12 "
Lena-Tabaga	897000	155	14800	26 "	21 "
Yenisey-Igarka	2440000	106	79276	20 May	31 "

FOR OFFICIAL USE ONLY

APPROVED FOR RELEASE: 2007/02/08: CIA-RDP82-00850R000300080046-0

APPROVED FOR RELEASE: 2007/02/08: CIA-RDP82-00850R000300080046-0

Transforming these inequalities, we obtain the following:

$$\lg \bar{\varphi} h_0^{\lg F + 1.71} \leqslant J_1 \left(\lg Q_0^{0.16\left(\frac{\bar{h}_\beta}{\bar{\Delta}}\right)+0.006} \right), \tag{19}$$

$$\lg \bar{\varphi} h_0^{0.67 \lg F - 0.53} \leqslant J_2 \left(\lg Q_0^{0.16\left(\frac{\bar{h}_\beta}{\bar{\Delta}}\right)+0.006} \right). \tag{20}$$

Thus, we arrived at the dependence (11), common for different rivers, of the modular coefficients of ice strength and water discharges on the day of the break-up (Fig. 2). This correlation indicates the fundamental possibility of obtaining a general scheme for computing the time for the break-up of rivers. Its practical importance is evident. It precludes the necessity for constructing many variants of the correlations for each point on the rivers and makes it possible to compute and predict the time of opening-up on rivers with limited series of observations. This correlation was constructed on the basis of more than 600 cases and therefore it is more reliable than the local correlations. However, its use, the same as the local dependences, is made difficult by the need for making computations of $\bar{\varphi} h_{spr}$ and Q_{spr} and becomes completely impossible on rivers with a poorly studied regime. Dependences (16), (19) and (20) are promising in this connection. They were checked on the basis of data for 11 points on rivers with substantially different regime characteristics. The results of this checking were compared with the evaluation of computations using dependence (11) (Table 2).

It follows from this table that the substitution of empirically established correlations into (11) naturally leads to some decrease in the accuracy of computations. In subsequent investigations it is necessary to use more data. Then it will be possible to refine the dependences (6), (12), (13) by means of allowance for additional arguments. In this connection it seems possible to refine the inequalities (19), (20). The fact is that using in the study data only on the ice thickness h_{ice}, we do not take into account such important factors as the structure of the ice and the depth of the snow on the ice, and characterizing by the period of ice melting ($\bar{\Delta}$) the quantity of heat received by the ice and in part the peculiarities of river morphometry, we do not take into account the time required for the melting of the snow on the ice and the intensity of the heat influx, etc.

Table 2

Evaluation of Errors in Computing River Break-Up

River-station	Probability of nonexcess of admissible error, %		
	using empirical correlation (11)	with computations using inequalities (16)	(19), (20)
Pripyat'-Mozyr'	95	89	85
Berezina-Bobruysk	95	85	93
Don-Belyayevskiy	86	81	79
Dnepr-Rechitsa	88	88	80
Oka-Kashira	97	97	90
Oka-Murom	89	89	78
Severnaya Dvina-Abramkovo	100	93	93
Onega-Porog	86	81	80
Pechora-Ust'-Tsil'ma	89	87	86
Lena-Tabaga	100	97	89
Yenisey-Igarka	97	92	76

APPROVED FOR RELEASE: 2007/02/08: CIA-RDP82-00850R000300080046-0

APPROVED FOR RELEASE: 2007/02/08: CIA-RDP82-00850R000300080046-0

In conclusion we note that inequality (16) even now is of practical importance. For its application for any river it is sufficient to know the mean long-term times for the disappearance of the snow from the ice, the times of break-up of rivers, the greatest thickness of the ice and the mean long-term water discharge on the day of the break-up. For hydrometric posts in operation for 15-20 years the determination of these parameters will not be difficult.

BIBLIOGRAPHY

1. Bulatov, S. N., "Possibility of Creating a Universal Method for Computing the Break-up of Rivers," TRUDY GIDROMETTSENTRA SSSR (Transactions of the USSR Hydrometeorological Center), No 112, 1972.

2. Piotrovich, V. V., "Appearance, Growth and Disappearance of Ice on the Rivers of the European USSR," TRUDY TsIP (Transactions of the Central Institute of Forecasts), 1948.

3. Piotrovich, V. V., "Formation and Thawing of Ice on Lakes and Reservoirs and Computation of the Times of Ice Setting-In and Going-Out," TRUDY TsIP, 1958.

4. Shulyakovskiy, L. G., POYAVLENIYE L'DA I NACHALO LEDOSTAVA NA REKAKH, OZERAKH I VODOKHRANILISHCHAKH (Appearance of Ice and Onset of Ice Formation on Rivers, Lakes and Reservoirs), Moscow, Gidrometeoizdat, 1960.

APPROVED FOR RELEASE: 2007/02/08: CIA-RDP82-00850R000300080046-0

APPROVED FOR RELEASE: 2007/02/08: CIA-RDP82-00850R000300080046-0

UDC 551.326.3:629.124.791

HUMMOCKING AND THE RESISTANCE OF ICE TO A MOVING SHIP

Moscow METEOROLOGIYA I GIDROLOGIYA in Russian No 10, Oct 80 pp 100-104

[Article by Candidate of Geographical Sciences G. N. Sergeyev and Yu. N. Khromov, Arctic and Antarctic Scientific Research Institute, manuscript submitted 18 Feb 80]

[Text]

Abstract: The article gives a generalization of the principles for computing the mean thicknesses of the ice cover developed by different authors, with ice hummocking taken into account. It is shown that they cannot be used in calculating the ice penetrability of ships due to selectivity of the process of fracturing of ice by a moving ship. A method is given for computing the equivalent thicknesses of ice with hummocking taken into account which correspond to the resistance of smooth ice of a similar thickness.

The hummocking of the ice cover, forming under the influence of dynamic processes, is one of the most important indices of its state. The hummocks cause not only an increase in the nonuniformity of ice thickness, but also a considerable increase in the mean thickness of the ice cover as a whole.

According to the computations of P. A. Gordiyenko, the thickness of the ice cover in ice-covered seas, as a result of hummocking, increases on the average by 30% in comparison with the thickness of ice formed in a quiet ice formation process. In regions of increased hummocking this increase can attain 80% or more.

The ice volume in the hummocks is dependent primarily on the area of the ice covered by the hummocks and on the magnitude of the parts of the hummocks above and below the water which are in an isostatic state. This is indicated by the investigations of A. V. Bushuyev [2], which have convincingly shown that as a result of the considerable plasticity of the ice individual sectors of the ice cover are in isostatic equilibrium during both the summer and winter seasons. However, the mean extent of the ice sectors in which isostatic equilibrium is manifested is about 30 m.

APPROVED FOR RELEASE: 2007/02/08: CIA-RDP82-00850R000300080046-0

APPROVED FOR RELEASE: 2007/02/08: CIA-RDP82-00850R000300080046-0

Thus, the fundamental assumption of an isostatic state of hummocked areas, adopted by many researchers [1, 3, 6-8] in computations of the volume of ice in any region, is entirely legitimate. The profiles of the parts of hummocks above and below the water have been assumed to be either triangular [7] or trapezoidal with different ratios of their bases to the altitude [1, 3]. The space factor of hummock formations with ice fragments has usually been assumed to be 0.7. In old ice, as a result of the freezing of the fragments together, this factor is higher.

Height and settling (draft) are important morphological characteristics of hummock formations. The height of the hummock formations on the drifting ice has a great spatial variability. But in different kinds of computations the authors usually employ a mean height of hummocks [1, 5, 7, 8] which in most cases has been assumed equal to the thickness of the ice in sectors without hummocks. However, actual observations of the parts of hummock formations above and below the water, carried out during recent years [3, 5], revealed that the mean height of hummocks on perennial ice is 2.0-2.5 m, which is considerably less than the thickness of the ice in smooth sectors. On shore ice, excluding regions along the edge with thick ridges of hummocked formations, the mean height of the hummocks is usually considerably less than the thickness of the ice in sectors without hummocks.

Thus, the principle of equality of the mean heights of the hummocks to the thickness of the ice in sectors without hummocks is not always correct.

Actual observations of Soviet and foreign researchers, carried out by different methods, indicated that the mean ratio of the settling of the hummocks to their height above the water is in the range from 4.8 to 5.5 [3]. This ratio persists for almost the entire range of heights of hummocks in ice of different age.

These investigations make possible analytical computation of the approximate values of the mean thicknesses of the ice cover, with hummocking taken into account, which is extremely important in a study of the ice balance of freezing seas. However, the characteristics of hummocked formations and their distribution on different types of ice require further study.

Data on the mean thickness of the ice cover are of great practical interest in ensuring the navigation of ships in ice. In this case the hummocking of ice as an element increasing its mean thickness is regarded as a factor exerting additional resistance to a moving ship in the ice. It is necessary to determine whether the mean thickness of the ice cover, computed with hummocking taken into account, corresponds to the resistance of ice of a similar thickness without hummocks.

Special in situ observations were carried out for this purpose. The technical ice speeds of movement of icebreakers of the "Moskva" type were used as an index of ice resistance. In this case the icebreaker served as a sort of tool for carrying out measurements of resistance of the ice cover. By a comparison of the thicknesses of hummocked (on smoothed sectors between hummocks) and unhummocked ice, corresponding to identical values of the technical ice speed, it was possible to determine the corrections to the ice thickness necessitated by the different degree of hummocking of the ice cover. It was found that the corrections for ice thickness

APPROVED FOR RELEASE: 2007/02/08: CIA-RDP82-00850R000300080046-0

APPROVED FOR RELEASE: 2007/02/08: CIA-RDP82-00850R000300080046-0

in the case of identical hummocking had a higher value the greater was the total thickness of the ice beyond the hummock formations. The results of the investigations indicated that the resistance of the ice cover with an increase of hummocking by 1 scale unit on the average increases by as much as it would increase with an increase in the thickness of smooth ice by 25%. Thus, each scale unit of hummocking is equivalent to a layer of smooth ice equal to 25% of its thickness.

The equivalent thickness of the ice, with allowance for hummocking, for computing the ice passability of ships, can be computed approximately using the formula

$$H'_{equiv} = H_{smooth}(1 + 0.25\ T), \qquad (1)$$

where H_{equiv} is the mean thickness of the ice, with hummocking taken into account, equivalent in resistance to smooth ice of similar thickness, H_{smooth} is the ice thickness on smooth sectors amidst the hummocks, T is the hummocking of ice in scale units.

It should be noted that the resulting regularity is based on in situ observations carried out in drifting ice with increased hummocking (from 2-3 to 5 scale units). With lesser hummocking values it was impossible to obtain reliable corrections due to the inadequate accuracy in determining speeds and therefore they were obtained by the graphic interpolation method. The corrections to the ice thickness in smooth sectors obtained using formula (1) differ considerably from those obtained by some authors on the basis of theoretical computations.

Later in situ observations, made using icebreakers with engines having a power greater than 30,000 HP, indicated that the decrease in their technical ice speeds of movement with an increase in hummocking does not occur as uniformly as would be indicated by formula (1). An increase in hummocking from 0 to 1 scale unit causes virtually no decrease in the rate of movement. Hummocking of 2 scale units causes an appreciable decrease in speed, which becomes more clearly expressed with a further increase in hummocking.

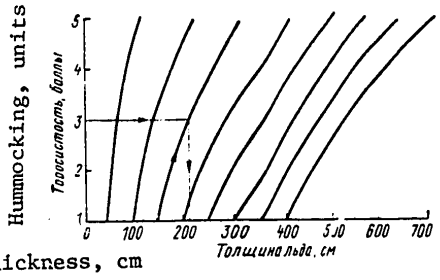

Fig. 1. Nomogram for determining the equivalent thickness of hummocked ice.

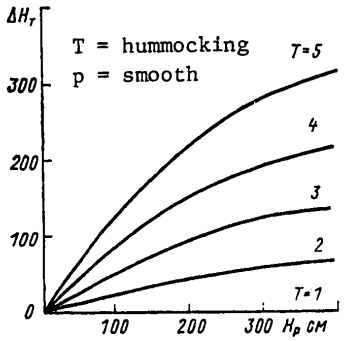

Fig. 2. Dependence of correction ΔH_T on ice thickness in smooth sectors H_{smooth} and hummocking T in scale units.

APPROVED FOR RELEASE: 2007/02/08: CIA-RDP82-00850R000300080046-0

APPROVED FOR RELEASE: 2007/02/08: CIA-RDP82-00850R000300080046-0

This can be attributed only to the selectivity of the icebreaker path and the process of fracturing of the ice by its hull. When there is wide spacing of the hummocked formations (infrequent hummocking) it is primarily sectors of even ice between the hummocks which are subject to breaking. The individual hummocks encountered along the icebreaker path can be bypassed or the hummocks force a sudden deviation of the ship from its course and the icebreaker then breaks thinner, smoother sectors of ice, bypassing the hummocks. In the case of greater hummocking (more than 2-3 scale units) the icebreaker is forced to break both smooth ice sectors and hummocked formations.

With a hummocking of 5 scale units the corrections to the thickness of one-year and younger ice are approximately 125% of the ice thickness in the unhummocked sectors, which agrees with the conclusion obtained using the velocities of movement of icebreakers of the "Moskva" type. For perennial ice with a thickness of 3.5-4.0 m the corrections for hummocking of 5 scale units could not be determined from in situ observations. Under real conditions such hummocking of perennial ice is encountered extremely rarely; since it is primarily younger ice which hummocks up here, its quantity amidst the perennial ice is usually small. Using extrapolation methods, it can be assumed that in the case of hummocking of perennial ice of 5 scale units the value of the correction to the thickness will not exceed 85-90% of its thickness in unhummocked sectors.

Our investigations made it possible to obtain a nomogram for determining the equivalent thicknesses of the drifting ice, whose resistance to a moving ship corresponds to the resistance of even ice of a similar thickness (Fig. 1). A merit of the nomogram is the possibility of direct determination of the equivalent thickness of the ice on the basis of data on ice thickness in unhummocked sectors and the degree of ice hummocking in scale units. The computed equivalent ice thicknesses can be used in determining the technical ice speeds for the movement of ships. This is done using ordinary graphs of their correlation with the thicknesses of smooth ice, representing the most widely observed type of dependence for different types of ships.

Despite the considerable nonuniformity of spatial distribution of the heights of hummocked formations on drifting ice, the cited graphs give entirely satisfactory results when carrying out computations of voyage planning of sea operations on ice paths. The results of these computations represent the necessary expenditures of time by the ship for covering segments of the path considerable in length for which the mean height of the hummocks is a reliable index.

In regions of well-developed shore ice (excluding edge zones with thick ridges of hummocks) the mean height of the hummocks will usually be the greater the later the shore ice sets in and in almost all cases is less than the thickness of the shore ice. After the shore ice sets in the formation of hummocks ceases and the hummocking which was formed before it had set in persists. Therefore, in computing the corrections to the thickness of the shore ice for allowing for hummocking (Fig. 2) as the initial thickness of the smooth ice it is necessary to use that at which the setting-in of the shore ice occurred. The equivalent thickness of the shore ice is computed using the formula

APPROVED FOR RELEASE: 2007/02/08: CIA-RDP82-00850R000300080046-0

APPROVED FOR RELEASE: 2007/02/08: CIA-RDP82-00850R000300080046-0

$$H_{equiv} = H_{smooth} + \Delta H_T, \quad (2)$$

where H_{smooth} is the thickness of the smooth shore ice at the moment of computation, ΔH_T is the correction to the thickness of the shore ice for hummocking, determined from the graph (Fig. 2).

In Fig. 2 the dependence was approximated by the equation

$$\Delta H_{Ti} = aH^z_{smooth}, \quad (3)$$

where ΔH_{T_i} is the correction to the ice thickness for different hummocking values (in scale units).

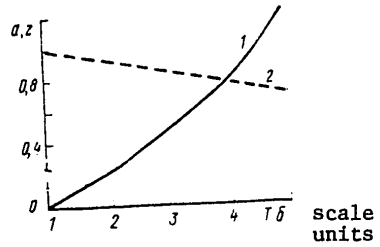

Fig. 3. Dependence of the coefficient a (1) and exponent z (2) in formula (4) on hummocking.

For each hummocking value we determined the values of the coefficient $a = f'(T)$ and the exponents $z = f''(T)$, represented in the graph (Fig. 3), which were also approximated and substituted into equation (3). As a result we obtain an analytical dependence of the correction ΔH_T on the thickness of the shore ice in smooth sectors and on hummocking

$$\Delta H_T = (0{,}0312\,T^2 + 0{,}125\,T - 0{,}1562)\,H_p^{1{,}7-0{,}07\,T}, \quad (4)$$

[p = smooth]

where H_{smooth} is the thickness of the shore ice in smooth sectors at the time of its setting-in, in m.

Formula (4) gives entirely reliable results of computations with thicknesses of smooth ice H_{smooth} up to 3 m and hummocking more than 1 scale unit. With an ice thickness greater than 4 m the errors in the computations can attain 20-30 cm. They must be taken into account by the introduction of a constant correction. This formula can also be used in computing corrections to the thicknesses of drifting ice of different age, but then H_{smooth} should represent the ice thickness in smooth sectors at any moment in time of interest.

This investigation makes it possible to exclude from the computations the most common and important of the characteristics of state of sea ice -- hummocking, replacing it by a correction to the thickness of smooth ice equal to the resistance to a moving ship. This circumstance made possible a fivefold decrease in the number of graphs characterizing the ice passability of a ship and increases considerably the volume of in situ observations necessary for obtaining the statistical relationships of the technical ice speeds of a ship and ice thickness.

APPROVED FOR RELEASE: 2007/02/08: CIA-RDP82-00850R000300080046-0

APPROVED FOR RELEASE: 2007/02/08: CIA-RDP82-00850R000300080046-0

The mean ice thicknesses computed by different methods, set forth in [1, 8], in most cases do not correspond to the resistance of smooth ice of a similar thickness.

In order to compare the resistance of smooth and hummocked ice it is first necessary to compute the equivalent thickness of the latter. This thickness can be determined either graphically (see Fig. 1) or analytically using formula (2) and the correction for hummocking can be determined either from a graph (see Fig. 2) or using formula (4).

The method for computing the equivalent thickness of ice can be used for both the cold and warm seasons of the year if the ice destruction does not exceed 3 scale units. It must be remembered that the data used in developing the method were obtained for shore and drifting ice with a continuity of 9-10 and 10 scale units. There is basis for assuming that in thinner ice areas this pattern does not hold true because selectivity of the path and the fracturing of the ice by the icebreaker should increase with a decrease in the continuity of the ice cover.

BIBLIOGRAPHY

1. Buzuyev, A. Ya., Shesterikov, N. P., "Dependence of the Mean Thickness of Shore Ice on Hummocking," PROBLEMY ARKTIKI I ANTARKTIKI (Problems of the Arctic and Antarctica), No 32, 1969.

2. Bushuyev, A. V., Volkov, N. A., Gudkovich, Z. M., Loshchilov, V. S., "Results of Expeditionary Investigations of the Drift and Dynamics of the Ice Cover of the Arctic Basin in the Spring of 1961," TRUDY AANII (Transactions of the Arctic and Antarctic Scientific Research Institute), Vol 257, 1967.

3. Gavrilo, V. P., Grishchenko, V. D., Loshchilov, V. S., "On the Problem of Field Investigations of the Morphology of Hummocks on Arctic Ice and Possibilities of Modeling of the Hummocking Process," TRUDY AANII, Vol 316, 1974.

4. Gordiyenko, P. A., Buzuyev, A. Ya., Sergeyev, G. N., "Study of the Ice Cover of Seas as a Navigation Medium," PROBLEMY ARKTIKI I ANTARKTIKI, No 27, 1967.

5. Grishchenko, V. D., "Statistical Characteristics of Some Parameters of the Upper and Lower Surfaces of Drifting Ice," TRUDY AANII, Vol 320, 1976.

6. Gudkovich, Z. M., Romanov, M. A., "Method for Computing the Distribution of Ice Thickness in Arctic Seas in the Winter," TRUDY AANII, Vol 292, 1970.

7. Zubov, N. N., L'DY ARKTIKI (Arctic Ice), Moscow, Izd-vo Glavsevmorputi, 1945.

8. Kirillov, A. A., "Allowance for Hummocking in Determining Ice Volume," PROBLEMY ARKTIKI (Problems of the Arctic), No 2, Leningrad, Morskoy Transport, 1957.

9. Klimovich, V. M., "Characteristics of Hummocks on Shore Ice," METEOROLOGIYA I GIDROLOGIYA (Meteorology and Hydrology), No 5, 1972.

10. Somov, M. M., "On the Mean Thickness of Ice in Marginal Seas," PROBLEMY ARKTIKI, No 6, 1939.

APPROVED FOR RELEASE: 2007/02/08: CIA-RDP82-00850R000300080046-0

APPROVED FOR RELEASE: 2007/02/08: CIA-RDP82-00850R000300080046-0

UDC 551.576.2

OBJECTIVE ANALYSIS OF THE QUANTITY OF CLOUDS

Moscow METEOROLOGIYA I GIDROLOGIYA in Russian No 10, Oct 80 pp 105-107

[Article by T. P. Kupyanskaya and I. A. Alekseyeva-Obukhova, USSR Hydrometeorological Scientific Research Center, manuscript submitted 22 Feb 80]

[Text]

Abstract: A numerical scheme for the objective analysis of total cloud cover, reduced to the lower level by the bilinear interpolation method, is proposed for a territory well covered by meteorological data. The data for surface observations of clouds for individual days in April-July 1979 are interpolated at the points of intersection of a regular grid of 15 x 16 points of intersection with an interval of 150 km. An evaluation of the results of the analysis is presented. It shows that the proposed objective analysis scheme will make it possible to obtain cloud cover data with an accuracy admissible for practical purposes.

One of the advantages of the synoptic weather forecasting method is the use, in its application, of all types of synoptic and aerological information, which makes possible the most complete analysis of the physical characteristics of current atmospheric processes and forecasting directions of their further development.

In the meteorological information contained in synoptic telegrams the data on visual observations of the forms of cloud cover and its extent are of great importance. These data are extensively used in the analysis of atmospheric fronts on weather maps. They are also indispensable in the prediction of cloud cover. In the studies of B. D. Uspenskiy [1, 2] it is validly noted that the introduction of observational data on the cloud cover as one of the initial meteorological fields in a numerical synoptic-hydrodynamic forecasting scheme is one of the real possibilities for increasing the accuracy in predicting temperature, humidity, precipitation and other meteorological elements.

The great volume of information on cloud cover, consisting of both the results of visual observations and of photographs of cloud systems obtained from meteorological satellites, indicates the complexity of the problem of including observations

APPROVED FOR RELEASE: 2007/02/08: CIA-RDP82-00850R000300080046-0

APPROVED FOR RELEASE: 2007/02/08: CIA-RDP82-00850R000300080046-0

of clouds among the initial meteorological fields. For this reason it is obvious that there should be progressive solution of the mentioned problem. The results of visual observations of total and low cloud cover are most accessible for use; such information is available in synoptic telegrams. It is important that the information on cloud cover contained in the telegrams can be processed on electronic computers.

The method for the representation of cloud observation data in a form employable in subsequent computations can be different, but the experience of development of a numerical synoptic-hydrodynamic forecast of atmospheric precipitation based on initial information more complete in comparison with other forecasting schemes shows that the most acceptable is a conversion from observational data on total and lower cloud cover at meteorological stations to the cloud quantity values at the points of intersection of a regular grid, that is, a changeover of this type of observations as well to objective analysis on an electronic computer.

In this article we will examine one of the possible schemes for the objective analysis of cloud cover over the European USSR and will give an evaluation of its accuracy.

Bilinear interpolation is the basis of the scheme for the objective analysis of data on the total quantity of clouds, expressed in tenths of lower cloud cover. Taking into account the complex structure of the cloud cover field, which is characterized by the presence of jumplike changes from a cloud cover to a clear sky or changes in the opposite direction, the radius of the region of interpolation of data on the quantity of clouds was limited to 150 km. In addition, some assumptions were made in the objective analysis scheme. Observations on the quantity of clouds at points not more than 30 km from the points of intersection of a regular grid were assigned directly to these points of intersection. In these same cases when two observation points were situated on a straight line passing through a point of intersection of a regular grid the quantity of clouds at this grid point of intersection was determined by linear interpolation of data at the mentioned two points. In the remaining cases in determining the quantity of clouds at the points of intersection of a regular grid we used bilinear interpolation of data at three observation points situated in a territory with a radius of 150 km with the center at the corresponding grid point of intersection.

As already noted, the objective analysis scheme provided for the collection of data on total cloud cover, reduced to the lower level. The N value, on the basis of data available in synoptic telegrams, was determined using the formulas

$$\begin{aligned} N &= N_{lower} + 0.7\, N_{middle} + 0.2\, N_{upper}, \\ N &= N_{lower} + 0.5\, (N_{total} - N_{lower}), \end{aligned} \qquad (1)$$

where N is the total quantity of clouds, expressed in tenths of lower cloud cover; N_{lower}, N_{middle} and N_{upper} are the quantities of clouds of the lower, middle and upper levels in tenths; N_{total} is the total quantity of clouds in tenths.

APPROVED FOR RELEASE: 2007/02/08: CIA-RDP82-00850R000300080046-0

APPROVED FOR RELEASE: 2007/02/08: CIA-RDP82-00850R000300080046-0

Table 1

Percentage of Coincidence of Analysis of Total Cloud Cover (N) and its Actual Quantity (N_{act}) With Error δ N

No.	Compared parameters	N in tenths 0-1	0-2	0-3	n1	n2
1	N and N_{act} at observation points not more than 30 km from grid points of intersection	53	63	73	4	67
2	N and N_{act} read from isolines on maps of total cloud cover	59	72	80	4	192
3	$\overline{N}$ according to data at two points between which an observation point was situated	46	71	84	4	61
4	$\overline{N}$ according to data at two points between which a point with data on $\overline{N}_{act}$ for a region with R = 150 km was situated	64	77	89	4	61
5	$\overline{N}$ and $\overline{N}_{act}$, found for points of grid intersection by averaging of quantity of clouds for regions with R = 150 km	63	78	88	24	1152
6	$\overline{N}$ according to objective analysis data at 5 points and $\overline{N}_{act}$ for regions with R = 150 km	57	86	97	2	82

In objective analysis the data on N were interpolated at the points of intersection of a regular grid. This grid for the European USSR with an interval 150 km had 15 x 16 points of intersection. For individual days in April, May, June and July 1979 there were 24 objective analyses of reduced cloud cover N on the basis of observations at 0300 hours Moscow time. We will examine the data in the table giving some idea concerning the quality of this analysis.

The data in the table on comparison of the results of objective analysis of the total quantity of clouds and the actual cloud cover indicate the following relationships between the compared parameters:

1. With errors from 2/10 to 3/10 the total quantity of clouds obtained using objective analysis in 63-73% of the cases coincides with cloud cover directly at the observation point.

Note. In the table n1 is the number of objective analyses, n2 is the number of points taken for comparison of N and N_{act}.

APPROVED FOR RELEASE: 2007/02/08: CIA-RDP82-00850R000300080046-0

APPROVED FOR RELEASE: 2007/02/08: CIA-RDP82-00850R000300080046-0

The relatively low percentage of coincidence between the comparable parameters is partially attributable to the fact that the interpolation method used leads to some averaging of data on the quantity of clouds. The percentage of coincidence between the comparable parameters, according to the data in the second line, is increased to 73-80% if the data on the actual cloud cover at the points of intersection of the regular grid are read from the isolines on the map of lower-level cloud cover, when drawing which there is inevitably a smoothing of individual peculiarities in the distribution of cloud cover.

2. According to the data in lines 4 and 5 in the table, the possibility of a coincidence of the results of objective analysis of cloud cover $\overline{N}$ and the actual quantities of clouds at the points of intersection of a regular grid is increased to 77-88% if the latter are found by means of averaging of the results of observations given on weather maps. The N_{act} values, indicated in lines 4-5 in the table, represent the mean N values computed using data from meteorological stations (from 2 to 5) in a territory with a radius of 150 km and its center at the corresponding point of intersection of a regular grid.

3. According to the data in line 6 in the table, the possibility of a coincidence between $\overline{N}_{act}$ and the results of objective analysis increases to 86-97% if as the latter we take the mean values on the basis of data at five points of intersection of a regular grid -- at a central and at the four nearest-lying points of intersection situated 150 km from the central point of intersection.

It follows from what has been set forth above that the considered numerical scheme for objective analysis makes it possible, with an accuracy admissible for practical purposes, to obtain data on the quantity of clouds averaged for the territory with a radius of 150 km. Accordingly, it is desirable that further investigations be made for the purpose of expansion of the region of objective analysis of cloud cover with the inclusion of regions with a thin network of meteorological observations, including the seas surrounding Europe.

The authors express appreciation to D. Ye. Bakatina, who participated in the processing of the materials cited in the article.

BIBLIOGRAPHY

1. Uspenskiy, B. D., "Quantitative Prediction of Continuous and Shower Precipitation," METEOROLOGIYA I GIDROLOGIYA (Meteorology and Hydrology), No 1, 1970.

2. Uspenskiy, B. D., "Status and Prospects of Synoptic Short-Range Weather Forecasting," METEOROLOGIYA I GIDROLOGIYA, No 10, 1972.

APPROVED FOR RELEASE: 2007/02/08: CIA-RDP82-00850R000300080046-0

APPROVED FOR RELEASE: 2007/02/08: CIA-RDP82-00850R000300080046-0

UDC 556.535.5

DETERMINATION OF ICE VISCOSITY UNDER NATURAL CONDITIONS

Moscow METEOROLOGIYA I GIDROLOGIYA in Russian No 10, Oct 80 pp 107-109

[Article by I. Ye. Kozitskiy, State Hydrological Institute, manuscript submitted 13 Aug 79]

[Text]

Abstract: Using the Maxwell model the author has derived a simple computation expression making it possible to compute the coefficient of ice viscosity on the basis of the results of measurements of a beam embedded in the ice cover and loaded on the free end.

In practical ice engineering problems are encountered which cannot be solved satisfactorily due to the absence of validated values of a series of physicomechanical characteristics of the ice cover responsible for its behavior under a load. One of these characteristics is the ice viscosity coefficient. As is well known, this coefficient is not a physical constant of ice, has a conditional character and is dependent on the state of the ice and the forces acting upon it. If these are taken into account, the uncertainty is not thereby removed because the value of the viscosity coefficient is dependent to a considerable degree on the method used in its determination.

For example, if the data available in the literature on the value of the ice viscosity coefficient are grouped in accordance with the type of method by means of which they were obtained it can be noted that the values closest to one another are observed within groups and the mean values for the groups manifest a tendency to a decrease, similar to that which we observe in a number of mean values of the ice plasticity limit obtained using the same set of methods (compression-flexure-dilatation-shearing) in a comparable temperature range.

The fact that the viscosity coefficient, obtained, for example, in the torsion of cylinders [2], is an order of magnitude less than the coefficient obtained in the flexure of beams [1], is easily attributable to the anisotropy of the properties of the internal friction of crystals.

During the torsion of ice cylinders elementary displacements in the crystals transpire along the basal plane perpendicular to the main crystallographic axis (sixth-order symmetry axis). This is caused by the horizontal direction of action of the external forces, on the one hand, and the horizontal orientation of the basal

APPROVED FOR RELEASE: 2007/02/08: CIA-RDP82-00850R000300080046-0

APPROVED FOR RELEASE: 2007/02/08: CIA-RDP82-00850R000300080046-0

plane during the natural growth of ice, on the other hand. In the flexure of beams the elementary deformations are caused by the action of normal compressive and dilatational stresses. In this case the glide and shear planes are oriented at an angle of about 45° to the horizontal.

As is well known, the flowability of ice crystals is essentially dependent on the direction of the shears and the glide plane. In particular, gliding occurs most easily along the basal plane of a particular type of crystals. It follows from this brief examination that in the solution of a specific ice engineering problem, requiring knowledge of the ice viscosity coefficient, the latter must be determined by a method ensuring comparability of the direction of action of the external forces and the direction of the basal planes of the crystals both in the sample to be tested and in an ice element in nature. Since the closest approach to the actual properties is attained in tests carried out under natural conditions and with large samples, such as so-called "keys," it is desirable to examine the possibility of using the beam flexure method for determining the viscosity coefficient. The coefficient obtained by the beam flexure method can be used in solving a broad class of problems in which the ice cover experiences flexure. In this case the computed dependences must be derived from definite physical concepts concerning ice as a material.

The ice viscosity coefficient is usually computed on the basis of measurements of the rate of deformation, making the assumption of presence of a linear dependence between the magnitude of the stresses and the rate of deformation. However, linearly a viscous medium is an extremely approximate model for ice. In such a medium deformations arise only with time, whereas at the time of load application the ice immediately experiences some "instantaneous" deformations. The simplest model of a hypothetical medium which can be used is the Maxwell model.

A corresponding rheological equation is derived taking into account that the total deformation ε is the sum of the elastic ε' and residual ε'' deformations of a viscous character:

$$\varepsilon = \varepsilon' + \varepsilon''. \tag{1}$$

If with simple dilatation $\dot{\varepsilon}' = \dot{\sigma}/E$ and $\dot{\varepsilon}'' = \sigma/3\mu$, where E is the elasticity modulus and μ is the viscosity coefficient, from (1) we obtain

$$\dot{\sigma} + \frac{\sigma}{T} = E\dot{\varepsilon}. \tag{2}$$

Here $T = 3\mu/E$ is a constant, the so-called relaxation time, ε is all ("instantaneous" elastic + viscous) the relative deformation in the case of a linear stressed state, $\dot{\sigma}$ and $\dot{\varepsilon}$ are the time derivatives of stress and strain.

We will demonstrate how the Maxwell model can be used for the above-mentioned purpose.

We will assume that the deformations of beam flexure conform to the law of plane sections (see Fig. 1).

APPROVED FOR RELEASE: 2007/02/08: CIA-RDP82-00850R000300080046-0

APPROVED FOR RELEASE: 2007/02/08: CIA-RDP82-00850R000300080046-0

$$\varepsilon = \frac{y}{\rho} = \varkappa y, \tag{3}$$

where $\varkappa$ is the curvature of the neutral layer, y is the distance from the neutral layer to the considered longitudinal fiber.

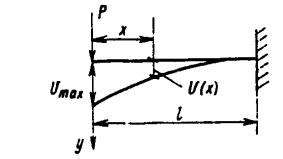

Fig. 1. Diagram used in deriving computed dependence.

From (2) and (3) we have

$$\dot{\sigma} + \frac{\sigma}{T} = E\dot{\varkappa}y, \tag{4}$$

where $\dot{\varkappa} = dx/dt$. Multiplying the left- and right-hand sides by $1 \cdot y \cdot dy$ and integrating in the limits from $y = -H/2$ to $y = H/2$, we obtain

$$\int_{-H/2}^{H/2} \dot{\sigma} y dy + \frac{1}{T} M_z = EI_z \dot{\varkappa}, \tag{5}$$

where M_z is the bending moment not dependent on time, $I_z = 1 \cdot H^3/12$ is the moment of inertia of the section relative to the neutral axis z.

Integrating the left- and right-hand sides for t, we obtain

$$M_z + \frac{M_z \cdot t}{T} = EI_z \varkappa, \tag{6}$$

or, bearing in mind that $\varkappa \simeq d^2v/dx^2$,

$$EI_z \frac{d^2v}{dx^2} = M_z \left(1 + \frac{t}{T}\right). \tag{7}$$

Here v is the bending of the beam in the direction of the y-axis. Assuming $M_z = Px$, we find, after integration for x and determination of the constants, the bending in any section

$$v_{(x,\,t)} = \frac{Pl^3}{3EI} \alpha \left(\frac{x}{l}\right)\left(1 + \frac{t}{T}\right) \tag{8}$$

(for the end of the beam $\alpha = 1$).

If the bending is now measured at one and the same point for two different moments in time t_1 and t_2 and the ratio

APPROVED FOR RELEASE: 2007/02/08: CIA-RDP82-00850R000300080046-0

APPROVED FOR RELEASE: 2007/02/08: CIA-RDP82-00850R000300080046-0

$$\frac{v_{(x_0,\ t_1)}}{v_{(x_0,\ t_2)}} = k \qquad \text{(we assume } k<1\text{)} \tag{9}$$

is computed with the constant force P, from (8) we obtain

$$T = \frac{kt_2 - t_1}{1 - k}. \tag{10}$$

Assuming E to be known, we determine the viscosity coefficient

$$\mu = \frac{1}{3} ET. \tag{11}$$

We note the following in conclusion. It is known that in natural tests it will be difficult to adhere to various methodological requirements, such as the stationarity of temperature conditions. In the considered test method, in a case when the air temperature changes during the time $t_2 - t_1$, the temperature bending Δv_t must be subtracted from $v_{(x0,\ t_2)}$. It is convenient to determine this bending with P = 0 using a "control" key block sawed from the ice together with the main sample.

BIBLIOGRAPHY

1. Kozitskiy, I. Ye., "Flexure of an Ice Beam and Ice Viscosity," TRUDY GGI (Transactions of the State Hydrological Institute), No 192, 1972.

2. Kozitskiy, I. Ye., Ponomarenko, O. F., "Experimental Investigations of the Viscosity of Natural Ice," TRUDY GGI, No 159, 1968.

APPROVED FOR RELEASE: 2007/02/08: CIA-RDP82-00850R000300080046-0

APPROVED FOR RELEASE: 2007/02/08: CIA-RDP82-00850R000300080046-0

UDC 551.501

STORING DATA FROM REGULARLY SCHEDULED RADIOSONDE OBSERVATIONS AND THEIR COMPUTERIZED PROCESSING

Moscow METEOROLOGIYA I GIDROLOGIYA in Russian No 10, Oct 80 pp 110-114

[Article by Candidate of Physical and Mathematical Sciences V. D. Kaznacheyeva, All-Union Scientific Research Institute of Hydrometeorological Information - World Data Center, manuscript submitted 15 Apr 80]

[Text]

Abstract: The article gives concise information on the archives of data from regularly scheduled radiosonde observations on different technical carriers. The author examines the basic principles for the creation of files of radiosonde observation data on magnetic tapes in the format of the YeS electronic computer and also problems relating to the climatological processing of aerological information.

The continuously increasing volumes of information on the atmosphere can be effectively processed only by making use of the possibilities of modern technical carriers and high-speed electronic computers.

The principal problems involved in creating and processing archival meteorological data on an electronic computer were examined in [3]; methods were proposed for describing the masses of meteorological data on technical carriers; possible future lines of development were discussed.

This article deals with the problems involved in the collection and climatological processing of data from scheduled radiosonde observations in the free atmosphere.

Concise summary of information on the archives of aerological information on technical carriers. Prior to July 1978 all the historical information on the atmosphere intended for the purposes of climatological processing was put on punch cards. At the present time the punched cards with aerological data for the stations of the USSR contain the results of standard radiosonde observations for the years 1936-1938. It is true that the number of stations with such a series of observations is relatively small and half of these observational series were

APPROVED FOR RELEASE: 2007/02/08: CIA-RDP82-00850R000300080046-0

APPROVED FOR RELEASE: 2007/02/08: CIA-RDP82-00850R000300080046-0

interrupted during the period of the Great Fatherland War. For the majority of stations the continuous series of observations begins with the post-war years. The total volume of the punched card files for the stations of the USSR for the period of observations up to 1975 is approximately $7.0 \cdot 10^7$ punched cards. [In July 1978 an automated system for the collection, checking, processing and registry of aerological data on a technical carrier after receipt from communication channels, developed at the Central Asiatic Regional Computation Center of the Central Asiatic Scientific Research Institute, was put into operation. In this system provision is made for the storage on magnetic tape of aerological information arriving through the communication channels. This precludes the necessity for first plotting the sounding data on punch cards.]

The punched card file contains observational data for foreign stations for the northern hemisphere since 1950 and for the southern hemisphere since 1960, a total of about 570 stations, primarily with two sounding times per day. The total volume of the file of punched cards for foreign stations up to 1975 is approximately $3.0 \cdot 10^7$ punched cards.

In creating the file of punched cards for Soviet stations use was made of the tables of standard radiosonde observations at the aerological stations of the USSR: TAE-16M (up to 1971 and for a number of stations up to 1972) and TAE-16A (from 1971-1972 to July 1978); the card file for foreign stations was created using using decoded data in telegrams on vertical sounding of the atmosphere received in the operational communication channels at the USSR Hydrometeorological Center. Naturally, the file of punched cards for foreign stations is considerably inferior with respect to completeness and the quality of data in comparison with the file of punched cards for Soviet stations, especially during the earlier years.

In the early 1970's efforts were undertaken to transfer historical meteorological information from punched cards to a binary microfilm (BMF). In particular, a binary microfilm was used in storing the punched card data on standard radiosonde observations for the aerological stations of the USSR with data at isobaric surfaces [6], at the ground surface, in the boundary layer for the 10-year period 1961-1970. The use of a binary microfilm as a technical carrier when working with an electronic computer made it possible for the handbooks to include new characteristics which had not been published earlier in Soviet reference publications on climate of the atmosphere. However, the storing of aerological data on a binary microfilm did not come into wider use due to the lack of effective technical and mathematical support.

In connection with the introduction of the YeS (Unified System) as the basic computer for the processing of archival hydrometeorological information specialists at the All-Union Scientific Research Institute of Hydrometeorological Information-World Data Center have been carrying out work on the transfer of historical information onto magnetic tapes for the YeS computer.

This work is carried out within the framework of the general program for creating a system for the information servicing of users on the basis of an automated hydrometeorological data bank (HMDB). The uniformity of the information base

APPROVED FOR RELEASE: 2007/02/08: CIA-RDP82-00850R000300080046-0

APPROVED FOR RELEASE: 2007/02/08: CIA-RDP82-00850R000300080046-0

necessary for the HMDB is achieved by the introduction of standard methods for the organization and description of the structure of masses of data using a data description language (DDL) specially developed at the All-Union Scientific Research Institute of Hydrometeorological Information [1] and also the use of standard technical carriers -- magnetic tapes (MT) for the YeS electronic computer.

Table 1

Models of Punched Card Files for Regularly Scheduled Radiosonde Observations, Archives of Aerological Data on Technical Carriers (Station Data)

Model No.	Content of model	Number of stations*			
		BMF	MT Minsk-32	MT YeS	Name of archives on MT of YeS computer
		Soviet stations			
I	Surface data from radiosonde observations	140	---	90	AEROZEM
II	Data in boundary layer	150	---	---	
III	Data at special points	---	---	90	AEROSOVOS
IV	Data at isobaric surfaces	150	140	140	AERIZA
V	Data in tropopause	---	---	90	AEROSTA
		Foreign stations			
I	Surface data and data in tropopause	---	---	60	AEROZINT
III	Data at special points	---	---	---	
IV	Data at isobaric surfaces	---	---	150	AEROZARI

*The number of stations is approximate.

As the first step in creating masses of aerological data the data from regularly scheduled radiosonde observations for the 10-year period from 1961 through 1970 selected as the most uniform from the point of view of sounding methods, measurement and processing accuracy, are being plotted in the DDL formats on magnetic tapes for the YeS.

At the present time masses of data have been created on magnetic tapes for the YeS computer for the isobaric surfaces, tropopause and levels of special points, as well as a mass of surface data for radiosonde observations for a selected network of Soviet and foreign stations during the period 1961-1970 (see Table 1) with a total volume of about $1.6 \cdot 10^7$ punched cards ($12.0 \cdot 10^8$ bytes).

APPROVED FOR RELEASE: 2007/02/08: CIA-RDP82-00850R000300080046-0

APPROVED FOR RELEASE: 2007/02/08: CIA-RDP82-00850R000300080046-0

The masses of aerological data registered on the magnetic tapes for the YeS computer have already been used effectively in carrying out a series of studies to meet the needs of scientific research institutes and agencies servicing the national economy.

Work on the creation of masses of aerological data on magnetic tapes for the YeS computer in the DDL formats ("Aerologiya" data bank) will be continued in the future. [Archival data can be obtained by special request to the Hydrometeorological Center (HMDC) of the All-Union Scientific Research Institute of Hydrometeorological Information (VNIIGMI-MTsD). Information on data available on different technical carriers is given in the catalogues of the HMDC.]

Features of organization of masses of aerological data on magnetic tapes for the YeS computer. It has developed historically that the accumulation of punched card files with aerological information for both Soviet and foreign stations has been with several models, each of which describes one such object as the boundary layer, isobaric surfaces, special points, tropopause, level of the maximum wind (see Table 1). Within the models the accumulation of a punched card file was carried out station-by-station and in chronological order. At first glance the separation of data from radiosonde observations into individual models may seem artificial, but it was valid for the climatological processing of data, since the method for carrying out this processing differs substantially for different models (for example, for isobaric surfaces, special points, tropopause, etc.).

In accordance with the developing peculiarities of collection and storage on punched cards, during the past years masses of archival aerological data on YeS magnetic tapes are being combined for individual models, within the model -- for individual stations, and within the station are arranged in a chronological sequence.

The masses of data, having an organization natural with respect to the collection and storage system, are called "base" data, and such an organization, according to [5], is optimum from the point of view of reliability of storage and maintenance of the stored mass of data.

The base mass of aerological information is a family of files, each of which contains information of the same type (that is, the information in one model of an aerological file of punched cards) for one station for a selected period of years. These have an identical internal structure but differ from one another with respect to spatial characteristics (station index). This family of files is incorporated on a large number of magnetic tapes and on one magnetic tape there can be data for several (their number is dependent on the type of archives) stations.

In accordance with the requirements on the organization of hydrometeorological data on magnetic tapes for the YeS electronic computer developed at the All-Union Scientific Research Institute of Hydrometeorological Information-World Data Center, each file of data on magnetic tapes is accompanied in such cases by a description file which in data description language contains documented information on the name of the specific file and the name of the entire mass of data: on the name of the country and institute where the data mass was created; the code in

APPROVED FOR RELEASE: 2007/02/08: CIA-RDP82-00850R000300080046-0

APPROVED FOR RELEASE: 2007/02/08: CIA-RDP82-00850R000300080046-0

the information is stored on the magnetic tapes; the structure of the data file, its constant indices, such as the name of the station, observation period, standard sounding times, etc.

A radiosonde ascent, constituting a logical unit of radiosonde observations, has been adopted as the structural unit of the data file (record). Each record is identified by a series of indices which give information on the temporal and spatial characteristics of a specific ascent: year, month, time of ascent (GMT) or the number of the ascent on the day, as well as the station index. The indices in the masses of aerological data constitute groups containing information on the totality of meteorological elements at different levels of radiosonde ascent, to wit: geopotential (pressure), air temperature, wind direction and velocity and on one of the characteristics of humidity (either on the dew point spread or on relative humidity). The values of each meteorological element within the group are supplied with a quality characteristic. The group is identified by a key element determining either pressure or altitude of the corresponding level. For example, for archives with data on the isobaric surfaces the key elements are the pressure values at the standard isobaric surfaces 1000, 850, 700, 500, 400, 300, 250, 150, 100, 70, 50, 30, 20, 10 mb; for archives with data on the tropopause -- the altitudes of the upper and lower boundaries of the tropopause, etc.

Thus, if the mass of aerological data is considered as some multdimensional mass of data, the indices identifying the physical parameters of the set of data can be arranged in accordance with the indices of the elements in the multidimensional mass of data.

Assume that X is any physical parameter from the archives of aerological data. Accordingly, the following indices should be supplied: number of the archives N (determines the object, model); observation station S; year G; month M; day D; time when observations are made T; altitude I at which the measurement is made, and finally, the name of the measured physical parameter V. In this case the totality of aerological data is an eight-dimensional mass

$$X_{NSGMDTIV}. \tag{1}$$

In (1) the sequence of indices corresponds to the already described base mass of aerological data.

Within the framework of a definite model and one station the set of data from the base mass can be regarded as six-dimensional

$$X_{GMDTIV}. \tag{2}$$

When it is necessary to have data with a structure different from the base mass the base masses can be transformed. The transformation procedure is carried out considerably more effectively on magnetic tapes than on punched cards. Accordingly, there is a change in the sequence of the indices. For example, the mass of data adequate in its structure to the ascent of a radiosonde, that is, the mass containing combined data for all models, arranged by altitude, will have the following sequence of the indices:

$$X_{SGMDTNIV}. \tag{3}$$

APPROVED FOR RELEASE: 2007/02/08: CIA-RDP82-00850R000300080046-0

APPROVED FOR RELEASE: 2007/02/08: CIA-RDP82-00850R000300080046-0

The ordering of data in a chronological sequence, which is observed in (1)-(3), is convenient for station-by-station statistical analyses and climatological generalizations. For other types of problems it may be necessary to have other variants of arrangement of masses of data. For example, for an investigation in the field of physical-statistical forecasting methods it is necessary to arrange the information in the sequence GMDTSIV, characterizing archives of the synoptic type. In this case the base masses of data must be rearranged. The desirability of storage of the rearranged mass of data is determined on the basis of the cost for obtaining it, the cost of storage and the probability of reconsulting this duplicating mass of data.

As an example of a base mass of data the figure shows the structure of the registry of a file of archival data on isobaric surfaces for USSR stations on magnetic tape for a YeS electronic computer.

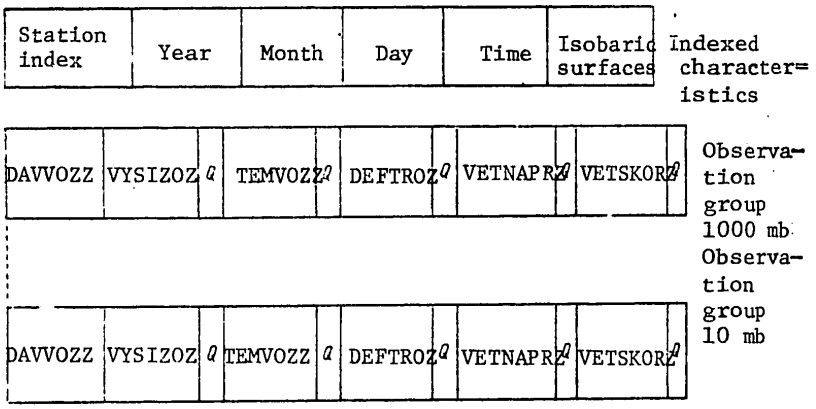

Fig. 1. Structure of registry of archives of data for isobaric surfaces for USSR stations on magnetic tape for YeS computer (name of archives AERIZA).

The name of the archives is AERIZA. The file of data contains a chronologically arranged series of records with the name NABLSROK of a variable length. Each such NABLSROK record consists of five index characteristics representing the key elements of the record with the names STANTSIYA, GOD, MESYATS, DEN', VREMYA (Station, Year, Month, Day, Time), as well as the auxiliary element SCHETPOV (Isobaric Surfaces), containing information on the number of isobaric surfaces in a specific ascent, and the corresponding number of groups with the name NABLPOV (Observed Surfaces). (NABLSROK = Observation Time)

The NABLPOV group represents the totality of data at one standard isobaric surface and contains a key element with the name DAVVOZZ, and also the five principal elements with the names VYSIZOZ (geopotential height), TEMVOZZ (air temperature), DEFTROZ (dew point spread), VETNAPRZ (wind direction), VETSKORZ (wind velocity) and the quality index (Q) accompanying each principal element. The NABLPOV groups and indices are arranged in the sequence of a decrease in the values of the key

APPROVED FOR RELEASE: 2007/02/08: CIA-RDP82-00850R000300080046-0

APPROVED FOR RELEASE: 2007/02/08: CIA-RDP82-00850R000300080046-0

element DAVVOZ. More detailed information can be found in the description of the specific archives stored at the HMDC at the VNIIGMI-MTsD.

Fundamental principles for control of the base archives of aerological information. A mandatory procedure in creating masses of data for prolonged storage and the carrying out of climatological processing is the checking of the information registered on the magnetic tape. In the event of discovery of an inconsistency when checking the indexed characteristics the observation is not included in the archives at all. As a result of checking the significant information a quality characteristic is assigned which has one of the following values: 0 -- correct value, 1 -- restored value, 2 -- doubtful value, 3 -- rejected value.

The primary checking of the quality of the information is carried out in the stage of creation of the base masses of data. The primary checking must be carried out with sufficiently tested methods free of subjective prejudices of the researcher and must also be adequately economical with respect to the time required to carry out this procedure. As a result of the checking in the creation stage there must be confidence in the data which are registered on the long-term carrier.

The correction of the rejected values in the base archives is considered possible if the original data from the radiosonde observations are available (for example, the TAE-3 tables sent from the station, etc.). In the absence of this type of data the correction of the rejected values in the base mass of historical data and the restoration of the missing data must be considered inadmissible.

Such an approach to checking work in the stage of creation of base masses of data is dictated by the imperfection of existing checking methods, different requirements on the accuracy of checking on the part of users, etc.

In the stage of data processing, for example, when carrying out statistical computations, more rigorous checking must be exercised. Depending on the requirements of the user on the quality of information and the availability of computer time the researcher can select a checking method acceptable to him, carry out the correction of rejected data and restore the missing data, taking into account that the checking and subsequent processing of the data are carried out from magnetic tapes representing copies of base masses of data. During the checking in the processing stage, in addition to the errors inherent in the data, there will also be exclusion of the errors arising in the storage of the data, associated, for example, with the ageing of the carrier, etc.

With the creation of masses of historical information from punched cards on magnetic tapes for the YeS computer it is possible to employ quite simple checking methods, such as checking for the limiting values of change of meteorological elements, since it is known that the file of punched cards of aerological data was created using data which have undergone critical checking at the stations or in data preparation groups and the errors present in the files of punched cards are usually associated with the preparation and use of the files of punched cards and fall in the category of knowingly rejected data.

In the future, in the processing of data already accumulated on magnetic tapes, it is desirable to use more rigorous methods of checking data, for example, multisided checking [2], etc.

APPROVED FOR RELEASE: 2007/02/08: CIA-RDP82-00850R000300080046-0

APPROVED FOR RELEASE: 2007/02/08: CIA-RDP82-00850R000300080046-0

Summary. The increasing volumes of data on magnetic tapes and the use of third-generation electronic computers are substantially broadening the possibilities of climatological processing of aerological information. Although this kind of processing can be carried out using existing packets of programs and well-developed data control units incorporated in the operational system of the YeS computer, the great diversity of structure of files of meteorological data on the magnetic tapes and the considerable volumes of this information make it desirable to create special processing systems. In this work it is necessary to take into account the peculiarities of meteorological information, such as the possible nonuniformity of the series of observations, the presence of gaps in data in the observation series, the diurnal and annual variation of meteorological elements [2, 4].

In the method for the climatological processing of aerological data, from which most of the aeroclimatology handbooks in the USSR are prepared, not all the peculiarities of this information are taken into account, for example, no allowance is made for the gaps in data in series of observations, the possible presence of a diurnal variation at the upper levels, etc. Accordingly, at the present time there is a need for improving the method for the climatological processing of aerological information, all the more so because the broad application of the method to the investigation of modern climate and the study of the dynamics of processes exerting an influence on its formation at a global scale requires a more correct evaluation of aeroclimatic statistics.

BIBLIOGRAPHY

1. Veselov, V. M., "Language for Describing Hydrometeorological Data," TRUDY VNIIGMI-MTsD (Transactions of the All-Union Scientific Research Institute of Hydrometeorological Information-World Data Center), No 43, 1978.

2. Gandin, L. S., Kagan, R. L., STATISTICHESKIYE METODY INTERPRETATSII METEOROLOGICHESKIKH DANNYKH (Statistical Methods for the Interpretation of Meteorological Data), Leningrad, Gidrometeoizdat, 1976.

3. Gruza, G. V., Kachurina, L. R., Reytenbakh, R. G., "Possibilities of the Processing of Archival Meteorological Data on an Electronic Computer," METEOROLOGIYA I GIDROLOGIYA (Meteorology and Hydrology), No 6, 1978.

4. Kobysheva, N. V., Narovlyanskiy, G. Ya., KLIMATOLOGICHESKAYA OBRABOTKA METEOROLOGICHESKOY INFORMATSII (Climatological Processing of Meteorological Information), Leningrad, Gidrometeoizdat, 1978.

5. Reytenbakh, R. G., "Problems in Organizing the Storage of Archival Hydrometeorological Data on Successive Access Carriers," TRUDY VNIIGMI-MTsD, No 43, 1978.

6. Khvostova, R. N., Kaznacheyeva, V. D., "Organization of an Informative Mass of Aerological Data for Isobaric Surfaces on a Photocarrier (Aerological Microfilm)," TRUDY VNIIGMI-MTsD, No 1, 1974.

APPROVED FOR RELEASE: 2007/02/08: CIA-RDP82-00850R000300080046-0

APPROVED FOR RELEASE: 2007/02/08: CIA-RDP82-00850R000300080046-0

UDC 551.46.073-52(215-13)

DEPLOYMENT OF FGGE DRIFTING BUOYS IN SOUTHERN HEMISPHERE

Moscow METEOROLOGIYA I GIDROLOGIYA in Russian No 10, Oct 80 pp 114-119

[Article by Candidate of Geographical Sciences E. I. Sarukhanyan and Yu. B. Vedenskiy, Arctic and Antarctic Scientific Research Institute, manuscript submitted 13 Feb 80]

[Text]

Abstract: The article examines the course of implementation of the FGGE special observation program for the deployment of drifting buoys in the zone from 20 to 65°S during the period from December 1978 through June 1979 and the participation of USSR ships in this program. The article describes the design of Norwegian buoys then deployed from aboard the scientific research ship "Professor Vize." Data are given on the calibration of the sensors of drifting buoys on the basis of shipboard observations and the number of buoys operating from January through November 1979 in the southern hemisphere. The prospects for scientific research use of the data collected from the drifting buoys are discussed.

In accordance with the program for the implementation of the First Global Experiment (FGGE) of GARP for collecting data on pressure and temperature of the sea surface in oceanic regions of the southern hemisphere poorly covered by observations provision was made for creating a special observation system, including a network of drifting buoys with water pressure and temperature sensors and artificial earth satellites, by means of which it would be possible to ascertain the location of buoys, collect data and transmit this information upon interrogation.

In this connection plans called for the deployment of about 300 drifting buoys in oceanic regions of the southern hemisphere in the zone from 20 to 65°S.

Such an observation system was developed by the beginning of the FGGE and in accordance with the operational plan for the global weather experiment [3] the buoys were to be deployed by the following countries: Australia (50), Canada (80), France (35), Norway (55), United States (50), Great Britain (9), New Zealand (10).

APPROVED FOR RELEASE: 2007/02/08: CIA-RDP82-00850R000300080046-0

APPROVED FOR RELEASE: 2007/02/08: CIA-RDP82-00850R000300080046-0

It was proposed that the buoys be deployed for the most part during the first special observation period of the FGGE (SOP-I) from December 1978 through March 1979 using vessels of Argentina, Australia, Brazil, Great Britain, Norway, New Zealand, USSR, United States, France, West Germany, Chile and Japan.

The task of constant monitoring of the course of buoy deployment was delegated to the center for logistics and deployment of buoys located at Vancouver, Canada. The collection of data from the drifting buoys was delegated to a center for data checking and processing at Toulouse, France.

The USSR, in accordance with its obligations for implementation of the FGGE, took an active part in the deployment of drifting buoys in the southern hemisphere. For this purpose scientific-research ships of the Arctic and Antarctic Scientific Research Institute of the State Committee on Hydrometeorology were assigned: "Professor Vize," "Professor Zubov" and "Mikhail Somov." They worked from November 1978 through April 1979 in the Antarctic Ocean under the program "POLEKS-Yug-79," which was a regional subprogram of the FGGE.

The drifting buoys, produced in Norway, Canada and New Zealand, were taken aboard the mentioned ships during visits to the ports of Haugesund (Norway), Las Palmas (Spain) in November 1978 and Wellington (New Zealand) in January 1979. According to the preliminary plan the USSR ships should deploy 17 buoys, but due to untimely delivery of buoys to Montevideo the ships received only 12 buoys for deployment.

Now we will discuss in somewhat greater detail the deployment of drifting buoys from aboard the scientific research ship "Professor Vize."

The ship took aboard four sets of drifting radiotelemetric meteorological buoys of the KhV-105 type, fabricated in Norway specially for support of the FGGE program. The buoys were intended for measurement of sea surface temperature and air pressure, and also for determination of drift currents and transmission of these data via the radiotelemetric satellite system "Service Argos" to the meteorological centers entering into this system.

The buoy was a completely hermetic, pear-shape container fabricated of glass plastic. The buoy had a hydraulic sail, a panel of synthetic fabric measuring 0.5 x 3 m, supplied with weights on the ends and suspended on a guide-rope with a length of 7 m to the bottom of the buoy for stabilization of the vertical position of the buoy in the water and effective movement in the current. The total length of the body of the buoy was 2.5 m, the maximum diameter was 0.8 m, the mass of the buoy was 63 kg and the mass of the sail was 35 kg.

Figure 1 is a diagram of the rigged buoy. The diagram shows the positioning of the sensors and the magnetic switch. At the end of the upper cylinder of the body of the buoy there is an air intake for the atmospheric pressure sensors and the transmitter antenna; in the lower part of the lower cylinder is the sensing element of the water temperature sensor. Attached by two screws on the upper horizontal part of the buoy is a magnetic plug; with its removal a magnetically controlled contact is triggered which cuts in the electric supply current and the

APPROVED FOR RELEASE: 2007/02/08: CIA-RDP82-00850R000300080046-0

APPROVED FOR RELEASE: 2007/02/08: CIA-RDP82-00850R000300080046-0

buoy begins to function. When the plug is put into position a magnetically controlled contact breaks the electric supply circuit and the buoy ceases to operate.

The buoy operates in the following way. With removal of the magnetic plug the electric current is fed to all buoy instruments. A transmitter operating at a frequency of 401 MHz is cut in each 60 sec for 1.0-1.5 sec.

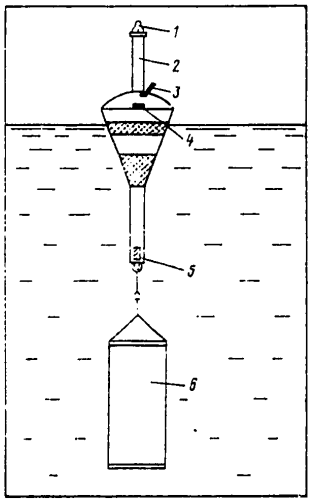

Fig. 1. Diagram of rigged buoy of KhV-105 type. 1) air intake of atmospheric pressure sensor; 2) positioning of sensor; 3) eye for rigging; 4) magnetic plug-switch; 5) sensing element of air temperature sensor; 6) hydraulic sail.

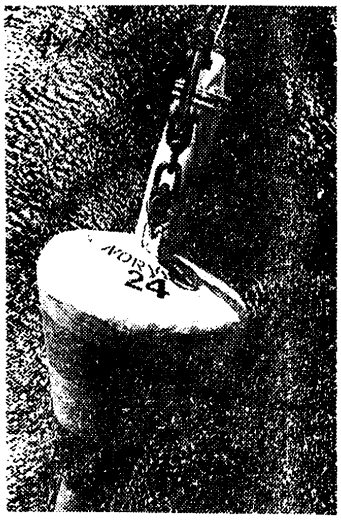

Fig. 2. Rigged buoy prior to lowering into water.

During transmitter operation a cycle of data containing the following parameters is transmitted: at the beginning of the cycle, the buoy identification code is transmitted in the "Service Argos" system; then the following parameters are successively transmitted:

1) air pressure (920-1050 mb)±1 mb (the sensor is calibrated in the temperature range from -5 to +35°C) -- 10 bits;
2) voltage of supply battery (0-21 V) ±0.6 V -- 6 bits;
3) water surface temperature (-5 - +35°C) ±1°C -- 8 bits;
4) temperature within buoy (-5 - +35°C) +1°C -- 8 bits.

All the parameters are measured continuously and their values are transmitted each 60 sec. The air pressure is integrated over a period of 15 minutes in a special accumulation device and is stored. A new air pressure value is entered in the accumulation device memory each 15 minutes and is read out for transmission in the course of the subsequent 15 minutes.

APPROVED FOR RELEASE: 2007/02/08: CIA-RDP82-00850R000300080046-0

APPROVED FOR RELEASE: 2007/02/08: CIA-RDP82-00850R000300080046-0

The technical servicing of the buoy and its placement was accomplished in accordance with the accompanying documentation and arrangements with a representative of the Norwegian manufacturer.

Three days prior to placement the buoy in its packaging (wooden crate) was placed in a vertical position on the ship's deck in such a way that the metal construction parts of the vessel as little as possible screened the antenna of the buoy receiver situated in the upper cylinder under the air intake and it was switched on by removing the magnetic plug with the inscription "activate." The activation was reported to the Norwegian Meteorological Institute (Oslo). The operation of the buoy transmitter was checked with an electronic tester which accompanied the delivered consignment of buoys.

The tester was a simple direct amplification receiver enclosed in a hermetically sealed plastic housing together with a self-contained 6 V power source (4 elements of the "MARS" type connected in series). The flat spiral antenna with a diameter of 70 mm was matched with a HF aperiodic transistorized amplifier and tuned to the middle of the range 401 MHz. The receiver detector was loaded with a photodiode which served as an indicator of HF radiation. Another photodiode serves as an indicator for the electric current tester. In order to check the operation of the buoy transmitter it is sufficient to raise the tester up to its antenna in such a way that the plane of the spiral antenna of the tester is perpendicular to the vertical axis of the upper cylinder of the buoy. With the normal operation of the transmitter a red photodiode (indicator) will light up for 1.0-1.5 sec each minute. The transmitter operation was checked twice a day and immediately after being lowered into the water. Prior to being lowered into the water the buoy was checked in horizontal and vertical positions.

Measurements of air temperature and pressure in the neighborhood of placement of the buoy sensor were made for three days prior to lowering into the water each three hours and for a day before its lowering — each hour in order to check the measuring channels of the buoy. These data were sent to the Norwegian Meteorological Institute which through the "Service Argos" system also received data on air pressure and temperature measured by the sensors of a buoy situated on the ship's deck. The Norwegian Meteorological Institute sent these data to our address for comparison of the buoy readings with shipboard observations.

The results of the calibration carried out for the Norwegian buoys show (Table 1) that the maximum deviation of buoy data with respect to pressure does not exceed 0.7 mb and with respect to temperature -- 0.7°C. Thus, the measurements of the meteorological parameters by the buoy sensors fall within the limits of the required accuracy.

The buoy was lowered into the water from the ship's stern. After outfitting of the buoy with a hydraulic sail and checking the transmitter operation the buoy was hoisted over the side and held by the crane boom at a distance of 2-4 m from the water surface by means of an opening hook fitting into the rigging eye on the buoy. Figure 2 is a photograph of the buoy prior to its lowering into the water. Then the rolled-up sail was deployed. Thereafter, when it began to float freely in the water the hook holding the buoy was released. The placement of the buoy was immediately

APPROVED FOR RELEASE: 2007/02/08: CIA-RDP82-00850R000300080046-0

APPROVED FOR RELEASE: 2007/02/08: CIA-RDP82-00850R000300080046-0

FOR OFFICIAL USE ONLY

Table 1

Comparison of Readings of Sensors of Drifting Buoy With Shipboard Observations Made by the Scientific Research Ship "Professor Vize" in 1978

Buoy number	Date and time, GMT	Temperature, °C		Pressure, mb	
		buoy data	shipboard observations	buoy data	shipboard observations
14 NOR	26 November 1700 hours	29.17	29.4	1010.8	1010.3
	28 November 1814 hours	27.76	28.0	1009.1	1008.9
	30 November 1753 hours	25.77	26.0	1010.1	1009.7
15 NOR	27 November 1515 hours	31.17	31.4	1009.4	1009.9
	30 November 1753 hours	26.85	26.0	1010.4	1009.7
16 NOR	3 December 1855 hours	27.53	28.0	1017.6	1017.9
	4 December 1843 hours	27.92	28.2	1016.0	1016.6
17 NOR	3 December 1855 hours	28.54	28.0	1017.5	1017.9
	4 December 1843 hours	27.46	28.2	1016.1	1016.6

Table 3

Placement of Drifting Buoys in Antarctic Ocean During FGGE Period [2] 1979

Date	Number of placed buoys	Number of buoys transmitting data	Number of buoys with reliable pressure-temperature data	Number of buoys with reliable pressure data spaced 500 km apart, %
5 January	125	115	105	52
29 January	185	165	140	70
28 February	206	180	145	59
1 April	234	197	155	71
1 May	252	195	155	70
1 June	296	233	184	80
1 July	301	226	176	77
1 August	302	213	155	72
1 September	302	194	137	67
1 October	302	183	121	66
1 November	302	157	102	62

FOR OFFICIAL USE ONLY

APPROVED FOR RELEASE: 2007/02/08: CIA-RDP82-00850R000300080046-0

APPROVED FOR RELEASE: 2007/02/08: CIA-RDP82-00850R000300080046-0

Table 2

Placement of FGGE Drifting Buoys by USSR Ships

Date of placement	Buoy code number	Coordinates	Ship
28 November 1978	32 CAN	25°00'S 08°00'E	"Professor Zubov"
2 December 1978	14 NOR	20°00'S 25°00'W	"Professor Vize"
3 December 1978	15 NOR	27°00'S 30°00'W	"Professor Vize"
4 December 1978	16 CAN	25°00'S 05°00'W	"Mikhail Somov"
5 December 1978	16 NOR	29°30'S 39°14'W	"Professor Vize"
7 December 1978	17 NOR	33°59'S 47°59'W	"Professor Vize"
12 December 1978	33 CAN	60°00'S 30°00'E	"Professor Zubov"
18 December 1978	29 CAN	55°00'S 40°00'E	"Professor Zubov"
8 January 1979	30 CAN	40°00'S 40°00'E	"Professor Zubov"
2 February 1979	28 CAN	61°28'S 95°00'E	"Mikhail Somov"
4 February 1979	27 CAN	58°00'S 118°00'E	"Mikhail Somov"
27 February 1979	N315Ye82	65°00'S 165°00'E	"Mikhail Somov"

APPROVED FOR RELEASE: 2007/02/08: CIA-RDP82-00850R000300080046-0

APPROVED FOR RELEASE: 2007/02/08: CIA-RDP82-00850R000300080046-0

reported to the Norwegian Meteorological Institute. The communication gave the coordinates and time of placement and also the meteorological parameters at the time of placement.

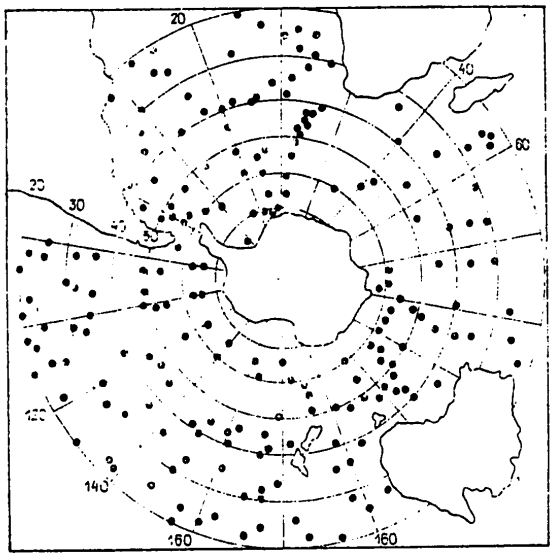

Fig. 3. Diagram of placement of FGGE drifting buoys in southern hemisphere on 5 April 1979 [4].

During the period from December 1978 through February 1979 USSR ships placed 12 buoys in different regions of the Antarctic Ocean (Table 2). The ships of other participating countries operated with equal success and by the end of the first FGGE observation period more than 200 drifting buoys had been placed in the southern hemisphere and more than 150 of these buoys provided reliable information on pressure and temperature of the sea surface (Table 3). As indicated by Fig. 3, the buoys were quite uniformly spaced over the area of the Antarctic Ocean.

During subsequent months, during the second FGGE observation period (SOP-II), the placement of the buoys was continued and by August 1979 a total of 302 buoys were placed in the southern hemisphere. As indicated by the data in Table 3, from April through August between 155 and 180 buoys provided reliable information on water temperature and pressure. More than 70% of these buoys were separated from one another by a distance not exceeding 500 km.

A comparison with independent observations (such as that carried out on the scientific research ship "Professor Vize") was possible for 68% of all the buoys. This comparison indicated that the mean deviation of pressure measured by the buoy sensor does not exceed 1.5 mb [5]. It was not possible to make such a comparison for water temperature measurements.

APPROVED FOR RELEASE: 2007/02/08: CIA-RDP82-00850R000300080046-0

APPROVED FOR RELEASE: 2007/02/08: CIA-RDP82-00850R000300080046-0

As already mentioned, the drifting buoys were interrogated using the "Service Argos" system, which included a series of satellites revolving around the earth, launched into a polar orbit. The period of revolution of the satellites was 90 minutes. The satellites observed the position of the drifting buoys and also received and stored telemetric information transmitted from the buoy through the radio channel. The stored information was transmitted upon interrogation during transit in the zone of radiovisibility of the meteorological centers included in the "Service Argos" system.

The storage of data and its analysis was accomplished at the center for the collection and checking of information (Toulouse) and the center for logistics and deployment of buoys (Vancouver).

At the present time the analysis of data received from the FGGE buoys is carried out at the Arctic and Antarctic Scientific Research Institute and at a number of other institutes of the State Committee on Hydrometeorology.

A report prepared in 1979 by a group of Canadian specialists on the use of data from FGGE drifting buoys [1] gives the results of a preliminary analysis of the data. These results include a map of the trajectories of buoys from 1 January through 28 February 1979, maps of pressure and temperature of the sea surface and its anomalies (averaged for five-day periods) for February 1979. Maps of the drift of buoys in different sectors of the Antarctic Ocean from November 1978 through June 1979 are also given in a preliminary report prepared by specialists of the Toulouse center for the collection and checking of information [5].

We can mention several directions in research for which the use of data from FGGE drifting buoys will be extremely effective.

In particular, as already indicated by experience, the use of these data in synoptic analysis will lead to the creation of more perfect forecasting methods. Thus, in particular, during the period of operation of drifting buoys there was an increase in the success of forecasts of storm conditions in the high latitudes of the southern hemisphere as a result of better description of synoptic processes [5].

The use of the collected data in the climatological study of the pressure and sea surface temperature in the southern hemisphere is of great interest since the earlier investigations were based primarily on irregular shipboard observations. In this connection it is promising to use data on pressure and temperature of the water surface for constructing the spatial spectra of nonuniformity of fields, study of their structure, intraannual and seasonal variability and the relationships between the pressure and water temperature fields, which is of great importance for the problem of large-scale interaction between the ocean and the atmosphere.

These data are also reliable test material for numerical models of general circulation of the atmosphere and ocean which now exist or which are being developed.

APPROVED FOR RELEASE: 2007/02/08: CIA-RDP82-00850R000300080046-0

APPROVED FOR RELEASE: 2007/02/08: CIA-RDP82-00850R000300080046-0

The collected materials are unique from the point of view of oceanographic investigations. As indicated by the preliminary results of analysis of the buoy trajectories, when using the collected data it is possible on this basis to describe circulation of the surface waters of the Antarctic Ocean and anticyclonic circulations in the South Atlantic and the southern part of the Pacific Ocean and detect zones of eddy formation and evolution of eddies and study the dynamics of frontal zones.

Taking into account that the duration of operation of the greater number of drifting buoys is about a year, possibilities arise for study of the variability of surface circulation of waters of the Antarctic Ocean at different time scales.

After evaluating the FGGE special observation system for the placement and use of drifting buoys as a whole, the conclusion can be drawn that such a system represents a qualitatively new stage in the approach to global investigations of the ocean and atmosphere. The broad-scale coverage in time and space coordinates, the great technical possibilities of concentration of flows of information from an extensive area of the ocean, the processing of information immediately after its collection (to all intents and purposes in the measurement process) -- all this makes it possible to consider such systems as an extremely promising method for in situ investigations on a global scale.

BIBLIOGRAPHY

1. Boston, N. E. J., Helbig, J. A., Keely, R., Thomas, I., Wilson, J. R., DRIFTING BUOY PRODUCTS FROM THE FIRST GARP GLOBAL EXPERIMENT (FGGE). A PROGRESS REPORT, Vancouver-Ottawa, 1979.

2. CRITICAL REVIEW OF THE PERFORMANCE OF THE FGGE DRIFTING BUOY SYSTEM, prepared by the Committee of Participants for the FGGE Drifting Buoy System, Secretariat of WMO, Geneva, 1979.

3. GLOBAL ATMOSPHERIC RESEARCH PROGRAMME. GLOBAL WEATHER EXPERIMENT. THE FGGE SPECIAL OBSERVING SYSTEMS, Part D, Southern Hemisphere Drifting Buoy System, Implementation Operations Plan, WMO, Vol 5, 1978.

4. LOGISTICS AND DEPLOYMENT PLAN FOR THE SOUTHERN HEMISPHERE DRIFTING BUOY SYSTEM, Circular No 2, Revisions to Vol 5, Part D, Annex, Geneva, 1979.

5. PERFORMANCE OF THE FGGE DRIFTING BUOY SYSTEM FROM 6 MARCH TO 30 JUNE 1979. Preliminary Report Prepared by FGGE Buoy Central Centre, Secretariat of WMO, Geneva, 1979.

APPROVED FOR RELEASE: 2007/02/08: CIA-RDP82-00850R000300080046-0

APPROVED FOR RELEASE: 2007/02/08: CIA-RDP82-00850R000300080046-0

REVIEW OF MONOGRAPH BY B. B. SHUMAKOV: 'HYDROMELIORATION PRINCIPLES OF ESTUARY IRRIGATION' (GIDROMELIORATIVNYYE OSNOVY LIMANNOGO OROSHENIYA), LENINGRAD, GIDROMETEOIZDAT, 1979, 215 PAGES

Moscow METEOROLOGIYA I GIDROLOGIYA in Russian No 10, Oct 80 pp 120-121

[Article by Doctor of Technical Sciences K. I. Shavva]

[Text] The rapid growth of industry and population in our country poses before agriculture a highly important task: obtaining the greatest quantity of different types of agricultural production with minimum expenditures of money and work.

One of the most effective methods for the intensification of agriculture is the melioration of lands, and in particular, estuary irrigation.

Estuary irrigation as a measure for increasing the yield of different agricultural crops is exceptionally effective, especially in those cases when the possibility of regular irrigation is limited due to the absence of permanent water sources. A distinguishing characteristic of estuary irrigation is that it makes use of local runoff.

At the present time a relatively large number of studies are devoted to the problems involved in computing the parameters of estuary irrigation systems. These examine individual scientific and practical problems involved in the planning of shallow or deep estuaries.

The publication of this fundamental monograph by B. B. Shumakov is unquestionably a noteworthy event. In this book, on the basis of generalization of available scientific studies, his own experimental materials and theoretical analyses, the author in a broad aspect examines hydrological-meteorological problems involved in the planning and computation of estuary irrigation systems with allowance for the peculiarities of formation of local runoff in the watershed and the processes of thawing and percolation of water into the soil of the estuary.

The reviewed monograph is the result of many years of field, laboratory and theoretical investigations of the author.

The book contains an introduction, five chapters, a summary and a bibliography of 213 items.

APPROVED FOR RELEASE: 2007/02/08: CIA-RDP82-00850R000300080046-0

APPROVED FOR RELEASE: 2007/02/08: CIA-RDP82-00850R000300080046-0

Despite the relatively small size (13.5 quires, 215 pages), the book broadly covers the problems which it treats.

The introduction describes the development of estuary-type irrigation in the USSR through the years. It is noted that in our country in 1973 the area of estuary irrigation was 1,004,800 hectares, of which 24 to 94% was flooded in individual years. After the high-water season of 1966 (when 80% of the area of the estuaries was inundated) the total area of estuary irrigation, due to destruction of the estuaries, was reduced by 150,000 hectares. On the average for the decade only 6.1% of these areas was used for sown crops and 90.1% was occupied by natural hay fields.

The experience of progressive farms has shown that when fodder and grain crops are cultivated in estuaries their effectiveness is increased by a factor of 3-5. The author very correctly asserts that for the planning of highly effective, reliably operating, technically perfect estuary irrigation systems it is necessary to develop a unified method for their planning, theoretically validated for different hydrological, soil-climatic and relief conditions.

The long-range calculations made by the author show that in the coming years the area of estuary-type irrigation in the USSR can be expanded to 11 million hectares and the fodder base for livestock raising can be considerably strengthened.

The first chapter examines the influence of estuary irrigation on the yield of different agricultural crops. It is shown that the yield increment for different crops when using estuary irrigation is from two (corn for silage) to six or more times (natural hay fields) in comparison with unirrigated lands. The influence of estuary irrigation on an increase in soil fertility, on soil-forming processes, on their stratification, and also on the possibility of using artificial estuaries as a means for contending with the water erosion of soils is also considered. Also discussed is the water balance of watersheds under natural conditions and in a case when local runoff waters are used for estuary irrigation. The author shows that the water regime of soils in estuaries differs radically from the water regime of unirrigated lands.

As a result of use of estuary irrigation an additional 2,500-4,000 m^3/hectare of moisture is obtained.

The second chapter is devoted to a study of the peculiarities of formation of local runoff on the watersheds and determination of its principal characteristics.

The author notes that an estuary irrigation system will operate correctly and the water resources will be used systematically and effectively only under the condition that the annually developing regime is closely matched with the regime of a water source of local runoff, and this must be taken into account in planning the systems.

The third chapter is devoted to an extremely timely scientific problem -- choice of the optimum percentage of the computed probability of runoff used for estuary irrigation.

APPROVED FOR RELEASE: 2007/02/08: CIA-RDP82-00850R000300080046-0

APPROVED FOR RELEASE: 2007/02/08: CIA-RDP82-00850R000300080046-0

B. B. Shumakov correctly notes that despite the exceptional importance of this problem it has still not been finally solved.

The extent of the planned estuary system, the volume of harvested agricultural production, the regularity (frequency) of inundation of the entire area over a long-term period, the size and design of hydroengineering structures in the system, and also the required volume of capital investments for the construction of the system and its economic effectiveness are dependent on the computed percent of runoff probability.

Relatively many studies have been devoted to different aspects of the economic validation of the computed probability of estuary irrigation. The author analyzes these studies attentively and quite soundly points out their merits and shortcomings. Most of this chapter is devoted to the exposition of a method, developed by the author, for selecting the optimum computed probability of estuary irrigation systems. A peculiarity of this method is that in contrast to existing methods it takes into account all types of capital investments in the construction of estuary irrigation systems (expenditures on planning-engineering field work, construction of earthen dams, hydroengineering structures and agricultural exploitation of the area of estuary irrigation), and in addition, at the basis of planning of estuary irrigation systems is the condition of assurance of reliable and damage-free use of diking and all hydroengineering structures. For this purpose the author has proposed corresponding equations for determining the computed discharges of water-discharge structures.

The author has demonstrated that in determining the optimum percentage of probability of runoff the main role is played by the relationship between the maximum discharge and the flow capacity of water bypasses.

The "purpose function" used is the time required for recuperation of the capital investments required for the construction of estuary irrigation systems due to the mean annual additional net income obtained from the irrigated areas.

The computation equations proposed by the author are universal and suitable for determining the optimum percentage of probability for estuaries with a shallow inundated layer and for deep-water estuaries.

In our opinion, the developed methods for determining the optimum probability percentage for estuary irrigation systems set forth in this chapter constitute a considerable contribution to development of the theory of optimization of irrigation system parameters.

The fourth chapter is devoted to a theoretical validation of the elements of estuary irrigation technology, that is, determining the optimum dimensions of earthen walls, hydroengineering and very simple discharge structures, validation of the norms for estuary irrigation, etc. In this chapter a considerable place is devoted to the water balance of deep- and shallow-water very simple and "level" estuaries. The graph analysis method and schemes for computing the water balance of a system of multilevel estuaries with a shallow inundation layer, when the high-water hydrograph has the form of a triangle, are described. These schemes are of great practical interest for planners. For the first time, for shallow-level estuary

APPROVED FOR RELEASE: 2007/02/08: CIA-RDP82-00850R000300080046-0

APPROVED FOR RELEASE: 2007/02/08: CIA-RDP82-00850R000300080046-0

The author describes a graph-analysis method and schemes for computing the water balance of a system of multilevel estuaries with a shallow layer of flooding when the high-water hydrograph has the form of a triangle. These schemes are of great practical interest for planners. For the first time the author, for multilevel estuary irrigation systems, proposes the use of soft intake and inflatable structures as discharge structures; these, to a considerable degree, will simplify and reduce the cost of such discharge structures.

The final chapter of the monograph is devoted to classifications and schemes for estuary irrigation. The central place in this chapter is devoted to a discussion of general schemes for determining the principal parameters of different types of estuaries (slope estuaries, estuaries in closed depressions, "swale" and "ravine" estuaries fed by discharge waters from reservoirs, etc.). At the end of the chapter is a scheme developed by the author for the meliorative regionalization of estuary irrigation in the southeastern part of the European USSR.

B. B. Shumakov has written an original and valuable book in which he has successively, on a rigorous scientific basis and at a modern scientific level, set forth the theoretical principles of estuary irrigation. The appearance of this book has been met with great interest by many specialists. We feel that it will also be highly regarded by specialists and will be of great practical use for planners, workers in agriculture, specialists in land improvement, agrometeorologists and hydrologists, as well as students at land improvement institutes.

APPROVED FOR RELEASE: 2007/02/08: CIA-RDP82-00850R000300080046-0

APPROVED FOR RELEASE: 2007/02/08: CIA-RDP82-00850R000300080046-0

SIXTIETH BIRTHDAY OF BORIS MORISOVICH GINZBURG

Moscow METEOROLOGIYA I GIDROLOGIYA in Russian No 10, Oct 80 p 122

[Article by the hydrologists of the USSR Hydrometeorological Center]

[Text] Doctor of Geographical Sciences Boris Morisovich Ginzburg, head of the Ice Forecasts Laboratory at the USSR Hydrometeorological Center, marked his sixtieth birthday on 26 September.

After graduating from the Higher Hydrometeorological Institute in 1944, B. M. Ginzburg worked at the Central Institute of Forecasts first as a hydrological engineer and then as a senior scientific specialist and since 1976 has been a laboratory head at the USSR Hydrometeorological Center.

B. M. Ginzburg is one of the leading scientists in the field of ice forecasts. His studies of methods for long-range forecasts of ice phenomena on rivers and reservoirs have come into wide use in the routine practice of the Hydrometeorological Service. A cycle of studies which he carried out for the geographical generalization

APPROVED FOR RELEASE: 2007/02/08: CIA-RDP82-00850R000300080046-0

APPROVED FOR RELEASE: 2007/02/08: CIA-RDP82-00850R000300080046-0

and computation of the probabilistic characteristics of the times of ice phenomena (including for rivers in the zone of the Baykal-Amur Railroad) is of great importance.

During recent years he has directed investigations of the problem of hydrological support for the lengthening of navigation seasons on rivers. B. M. Ginzburg combines scientific research with much routine work. Over the course of many years he has directed the preparation of ice forecasts for the rivers of our country and thereby supported the central Party, government and national economic organizations. On the basis of the results of his investigations he has published more than 40 scientific studies. He devotes much attention to the training of scientific personnel and guides graduate students and degree candidates.

Boris Morisovich has participated in the work of hydrological congresses and in many union and international conferences on hydrology and has presented scientific reports to them.

The Communist B. M. Ginzburg actively participates in the Party-political life of the community. For more than 25 years he has carried out much work on the dissemination of foreign policy propaganda in Krasnopresnenskiy Rayon. At present he is chairman of a section of the methodological council of the Krasnopresnenskiy Rayon Committee CPSU, a member of the methodological council of the House of Political Education of the Moscow Committee CPSU and a propagandist.

B. M. Ginzburg is full of creative energies and inexhaustible vigor. We wish him good health, long years of life and further successes in scientific and routine work.

APPROVED FOR RELEASE: 2007/02/08: CIA-RDP82-00850R000300080046-0

APPROVED FOR RELEASE: 2007/02/08: CIA-RDP82-00850R000300080046-0

SEVENTY-FIFTH BIRTHDAY OF PAVEL PAVLOVICH VORONKOV

Moscow METEOROLOGIYA I GIDROLOGIYA in Russian No 10, Oct 80 pp 122-123

[Article by A. V. Karaushev, V. T. Kaplin and B. G. Skakal'skiy]

[Text] Professor Pavel Pavlovich Voronkov, Doctor of Geographical Sciences, outstanding professional hydrochemist, one of the organizers of hydrochemical research in the Hydrometeorological Service system, marked his 75th birthday on 30 August. Over the course of 40 years the scientific activity of P. P. Voronkov was associated with the State Hydrological Institute, where he progressed from graduate student to director of the hydrochemistry laboratory.

P. P. Voronkov actively participated in many sea expeditions of the State Hydrological Institute carried out under the direction of the outstanding oceanologist K. M. Deryugin and his first scientific investigations were devoted to a hydrochemical study of the Far Eastern and Northern seas. In 1936 Pavel Pavlovich was awarded the academic degree of Candidate of Sciences for his dissertation on the hydrochemical regime of Peter the Great Bay, and in the year which followed he became head of the hydrochemistry laboratory of the State Hydrological Institute. During 1936-1941 he published 12 scientific articles and also a series of methodological studies and manuals on chemical oceanography. The scientific activity in the the field of marine chemistry has brought Pavel Pavlovich fame and authority among the hydrochemists of our country. The Great Fatherland War interrupted the scientific work of P. P. Voronkov. He was called into the ranks of the Red Army and fought on the approaches to Leningrad.

After returning to the State Hydrological Institute in December 1945, Pavel Pavlovich organized extensive expeditionary investigations directed to a comprehension of the processes of formation of the chemical composition of surface waters of the land. These covered extensive areas of the forest, wooded steppe and steppe landscape zones of the European USSR and also regions of virgin and idle lands in Kazakhstan. Emphasis was on the waters forming in small drainage basins, that is, local runoff waters. These investigations gave the necessary material for understanding the peculiarities of the processes of formation of the chemical composition of waters in the different phases of their runoff -- along the slopes of drainage basins and in the ground layers. P. P. Voronkov defined the principal genetic categories of waters, which enabled him to formulate the principles of hydrochemical study of local runoff.

APPROVED FOR RELEASE: 2007/02/08: CIA-RDP82-00850R000300080046-0

APPROVED FOR RELEASE: 2007/02/08: CIA-RDP82-00850R000300080046-0

The results were of great fundamental importance for the development of hydrochemistry in a genetic direction. The principal achievements in the field of genetic hydrochemistry were set forth by P. P. Voronkov in two monographs which were published in 1955 and 1970. In the monographs fundamental generalizations were presented on the patterns of formation of the chemical composition of waters of the local runoff type in different landscape zones.

Pavel Pavlovich was awarded the degree of Doctor of Geographical Sciences in 1957 for his theoretical studies in the field of the hydrochemistry of surface waters.

The principles of hydrochemical mapping lying at the basis of compilation of hydrochemical maps of local runoff, formulated by P. P. Voronkov, constitute a major contribution to the development of Soviet hydrochemistry.

Pavel Pavlovich always devoted much attention to scientific-methodological activity. The highly important results of his scientific work were incorporated in the instructions and methodological recommendations on the carrying out and rationalization of hydrochemical investigations, and also in study aids. The hydrochemical sections of the multivolume scientific-practical publication RESURSY POVERKHNOSTNYKH VOD SSSR (Surface Waters of the USSR), during the course of whose compilation hundreds of hydrochemists in our country acquired great experience in solving complex problems of modern hydrochemistry, were compiled under his direction and with his direct participation.

P. P. Voronkov published three monographs and more than 70 scientific articles having great theoretical and practical importance. He trained many professional hydrochemists and assisted them in developing a creative approach to study of the hydrochemical processes developing in the drainage basins and in water bodies. Among the students and followers of P. P. Voronkov there are specialists working at the State Hydrological Institute, Hydrochemical Institute, Institute of Biology of Internal Waters USSR Academy of Sciences, Institute of Hydrobiology Ukrainian Academy of Sciences and at a number of other institutes. Pavel Pavlovich was always ready to share his knowledge and enormous research experience in the field of hydrochemistry with his colleagues. At the present time Pavel Pavlovich is enjoying well-earned rest. We wish him health and many more long years of life.

APPROVED FOR RELEASE: 2007/02/08: CIA-RDP82-00850R000300080046-0

APPROVED FOR RELEASE: 2007/02/08: CIA-RDP82-00850R000300080046-0

CONFERENCES, MEETINGS AND SEMINARS

Moscow METEOROLOGIYA I GIDROLOGIYA in Russian No 10, Oct 80 pp 123-127

[Article by L. S. Gandin, K. Ya. Kondrat'yev, K. M. Lugina and Yu. G. Slatinskiy]

[Text] A scientific seminar on "The Role of Satellite Meteorological Information in the Prediction of Weather and the Theory of Climate" was held at the Main Geophysical Observatory during the period 24-25 April 1980. It was organized by the Interdepartmental Council on the Problem "Space Meteorology."

After introductory words by Ye. P. Borisenkov, director of the Main Geophysical Observatory, I. F. Berestovskiy (State Committee on Hydrometeorology) presented information on the present status and prospects of development of observations from Soviet satellites of the "Meteor" series. Then a detailed review of the problem of use of data from thermal sounding from satellites in numerical weather forecasting was presented by Corresponding Member USSR Academy of Sciences K. Ya. Kondrat'yev (Main Geophysical Observatory). Relying primarily on the attempts of foreign scientists to include sounding data from American satellites in the initial information in numerical forecasting, the speaker convincingly demonstrated that the results of these investigations have not justified the hopes placed on them. Only very recently have communications appeared on some successes in this direction.

M. A. Petrosyants told about the organization and experience in use of satellite information at the USSR Hydrometeorological Center in the routine analysis and prediction of weather by synoptic methods. Cloud cover photographs have already been successfully used for this purpose for many years. Taking into account the needs of forecasters, the speaker expressed a number of requirements on the volume and quality of this type of satellite information. M. A. Petrosyants also discussed the problem of use of data from temperature sounding from satellites in numerical forecasting and demonstrated that the practical realization of the corresponding methods is unthinkable without a substantial increase in the capabilities of electronic computers in comparison with the present-day capabilities of the USSR Hydrometeorological Center.

The latter subject was examined in greater detail in a report by S. L. Belousov, prepared by him in collaboration with A. N. Bagrov. It told of the work being carried out at the USSR Hydrometeorological Center directed to the introduction

APPROVED FOR RELEASE: 2007/02/08: CIA-RDP82-00850R000300080046-0

APPROVED FOR RELEASE: 2007/02/08: CIA-RDP82-00850R000300080046-0

of four-dimensional analysis. Systems for the primary processing of routine information, including data from satellite temperature sounding, have been developed and have been successfully tested. Work is being done on a changeover from level-by-level objective analysis to layer-by-layer objective analysis, which will facilitate use of satellite data on relative geopotential transmitted in the now operational code SATEM. Objective analysis of the surface fields of pressure and temperature on the basis of data from the synoptic network of stations and shipboard observations is in use. However, the now operative system totally exhausts the possibilities of the BESM-6 electronic computer in an operational regime. Accordingly, the introduction of four-dimensional analysis is possible only with an increase in computer capabilities.

S. A. Mashkovich (USSR Hydrometeorological Center) told about numerical experiments which he carried out in collaboration with Ye. L. Metelitsa on multi-element objective analysis of the geopotential, wind and temperature fields by the optimum interpolation method with geostrophically and hydrostatically congruent functions. As indicated by the experiments, the method makes it possible to obtain fields of a meteorological element close to real with an extremely small volume of data on this element and even with their total absence. This is achieved by making use of information on other elements.

Two reports by L. S. Gandin (Main Geophysical Observatory) dealt with some investigations made by the speaker and his associates on the problems involved in analysis and checking of data from satellite temperature sounding. It was shown that the random errors of the latter, in contrast to the errors in radiosonde observations, have a considerable spatial correlation, allowance for which is extremely important in the interpretation of data from satellite sounding and makes it possible to obtain realistic evaluations of their information content. A corresponding generalization of the optimum interpolation method was examined. In joint objective analysis this allows simple use of data from satellite and radiosonde observations. On the basis of actual material it was demonstrated that about 7-8% of the telegrams with satellite sounding data contain blunders caused primarily by distortions in the communication channels. Methods have been developed for checking these data, directed to the detection and elimination of serious errors.

The studies of O. M. Pokrovskiy and his colleages (Main Geophysical Observatory) were represented by a series of individual reports. They developed an approach already formulated relatively long ago and based on use of the primary information from satellite sounding -- data on the long-wave spectral brightnesses. This approach deserves preference, from the scientific point of view, in comparison with the usual use of vertical temperature profiles constructed on the basis of these data. It is shown that within the framework of this approach it is possible to expect a considerable increase in the accuracy of objective analysis. At the same time, for the realization of this approach there must be a fundamental restructuring of the methods for processing and transmitting a particular type of information. In addition, as noted by M. A. Petrosyants, in this approach the requirements on electronic computers far exceed the existing capabilities of the latter.

APPROVED FOR RELEASE: 2007/02/08: CIA-RDP82-00850R000300080046-0

APPROVED FOR RELEASE: 2007/02/08: CIA-RDP82-00850R000300080046-0

V. I. Titov told about a system which he developed and which is being used at the Moscow Division of the All-Union Scientific Research Institute of Hydrometeorological Information for the storing of satellite data on cloud cover, based on determination of the degree of coverage of areas of latitude-longitude squares by clouds. These data are in a form convenient for consultation.

Unfortunately, a planned report on the storing of data from satellite temperature sounding was not presented. However, it is known that this important matter is not being dealt with satisfactorily.

Specialists of the State Scientific Research Center for the Study of Natural Resources, the coordinating center on this problem, spoke out within the framework of the general discussion. V. A. Pakhomov told in detail about the temperature sounding data from the "Meteor" satellites and about work on the interpretation of the data carried out at the State Scientific Research Center for the Study of Natural Resources.

I. A. Chetverikov presented a brief communication on the methods and algorithms for processing this information.

In summarizing the seminar results, it must be stated that in our country definite work is being carried out for creating methods for using satellite sounding data in numerical weather forecasting but for the time being it is limited to problems related to the restoration of the fields of meteorological elements on the basis of data from satellite measurements. The development of a meteorological space observation system, the need for using the masses of GARP data, the tasks of increasing the accuracy and timeliness of weather forecasts -- all this dictates the urgent necessity for a radical broadening and deepening of the front of investigations with the objective of developing methods for the effective use of satellite meteorological information in numerical weather forecasts and support of this type of research with high-capacity electronic computers.

L. S. Gandin and K. Ya. Kondrat'yev

The All-Union Conference on Anthropogenic Modification of Climate was held in Leningrad at the State Hydrological Institute during the period 1-4 April. It was attended by more than 200 specialists from 38 organizations of the State Committee on Hydrometeorology, USSR Academy of Sciences, Academies of Sciences of the union republics, Ministry of Higher and Intermediate Special Education RSFSR and USSR Geology Ministry.

Twenty-seven reports were presented at the conference. They dealt with different aspects of the influence of economic activity on climate (influence of carbon dioxide on climate -- five reports, influence of atmospheric aerosol on climate -- four reports, patterns of recent climatic changes — nine reports, use of paleoclimatic data for evaluating climatic conditions of the future -- eight reports).

The introductory report by Corresponding Member USSR Academy of Sciences M. I. Budyko validated the necessity for developing the forecasting of possible changes in climate under the influence of economic activity with the use of presently

APPROVED FOR RELEASE: 2007/02/08: CIA-RDP82-00850R000300080046-0

APPROVED FOR RELEASE: 2007/02/08: CIA-RDP82-00850R000300080046-0

existing climatic models, the results of instrumental observations, historical and geological data.

E. K. Byutner, O. K. Zakharova, A. G. Lapenis and I. Ye. Turchinovich devoted their report to an investigation of the distribution of anthropogenic carbon in the atmosphere, ocean and biological sphere. The authors demonstrated that from 45 to 60% of the carbon dioxide obtained from the combustion of fossil fuel remains in the atmosphere.

K. I. Kobak, et al. demonstrated that at the present time the cutting of forests, especially in the tropical zone, is proceeding at a greater intensity than their renewal and this is exerting a substantial influence on the atmospheric CO_2 balance.

A report by V. P. Dymnikov, S. Ya. Galin and V. L. Perov told about numerical experiments for evaluating the influence of change in the CO_2 concentration on climate. Particular attention was devoted to allowance for the influence of cloud cover, which in contrast to preceding experiments did not remain fixed, but changed in accordance with the parameters of the model.

A report by I. I. Mokhov and V. K. Petukhov also mentioned the substantial influence of change in cloud cover on the sensitivity of the climatic system to a change in the CO_2 content. In the example of a model averaged for a hemisphere, with allowance for empirical data, the authors evaluate the contribution of different factors to the sensitivity of the surface temperature field to a change in the CO_2 concentration. It is also noted that in addition to the influence of cloud cover an appropriate parameterization of the precipitation field is important.

A report by A. S. Ginzburg and T. V. Panova dealt with some results of computations of radiation fluxes in a three-dimensional model of general circulation formulated by I. V. Trosnikov (USSR Hydrometeorological Center) with different CO_2 contents.

A report by K. S. Shifrin and his colleagues was devoted to an allowance for stratospheric aerosol in computations of radiation fluxes. A detailed investigation of this factor shows the need for taking it into account in climatic models. This requires a careful modeling of the stratospheric aerosol layer and its possible anthropogenic changes. A report by M. I. Asaturov was devoted to this problem.

G. N. Nikol'skiy cited comparative evaluations of the effect of anthropogenic and natural factors on the characteristics of atmospheric transparency.

A report by S. A. Volovikov, S. S. Khmelevtsov and A. S. Kabanov was devoted to allowance for the influence of heat and moisture on the mean annual global temperature in simple climatic models.

G. V. Gruza, E. Ya. Ran'kova and Ye. G. Apasova told of an investigation of the statistical characteristics of the surface fields of temperature and precipitation on the basis of an analysis of archival data available at the All-Union

APPROVED FOR RELEASE: 2007/02/08: CIA-RDP82-00850R000300080046-0

APPROVED FOR RELEASE: 2007/02/08: CIA-RDP82-00850R000300080046-0

Scientific Research Institute of Hydrometeorological Information-World Data Center. Some problems involved in the statistical analysis of aerological data were set forth in a report by V. D. Kaznacheyeva and L. K. Kleshchenko.

K. Ya. Vinnikov, P. Ya. Groysman and N. P. Kovynev, by use of the empirical model which they developed, investigated the interrelationship between global temperature and the local fields of this element and also the pressure and precipitation fields.

A report by P. P. Arapov and G. I. Mosolova gave an analysis of the frequency of recurrence of moisture anomalies in the continental regions of the northern hemisphere on the basis of historical data and the results of instrumental observations. The problems involved in the relationship between the quantity of atmospheric precipitation and the change in air temperature were discussed in a report by O. A. Drozdov. The author demonstrated that an increase in global temperature by approximately 2°C in comparison with the present-day level will lead to a decrease in the meridional temperature gradients and the precipitation associated with them in the continental regions of the temperate latitudes. A further increase in air temperature will be accompanied by an increase in the quantity of precipitation due to convective factors.

K. M. Lugina, in her report, dealt with some aspects of evaluation of the necessary density of the network of stations for the purposes of global monitoring of the temperature regime.

A report by I. P. Gerasimov and A. A. Velichko was devoted to the characteristics of climatic changes in the Late Cenozoic, which was characterized by a particularly great variability.

A. B. Ronov and A. N. Bolukhovskiy discussed reconstruction of the climate of the Late Mesozoic and Cenozoic. On the basis of petrographic data it was possible to construct maps characterizing the aridity of climates on the continents during this epoch.

A report by V. A. Zubakov dealt with problems relating to the chronology of climatic variations in the Late Cenozoic.

Reconstructions of the climates of two periods of the Pleistocene, characterized by a different thermal regime, were demonstrated in a report by A. A. Velichko.

The problems involved in reconstruction of the climate of the Holocene on the basis of data from a pollen analysis were discussed in the reports of V. A. Klimanov and M. V. Muratova and I. A. Suyetova. On the basis of a great volume of factual material, the first of them described an investigation of the climate of this period for the European USSR; the second presented maps characterizing the thermal regime and humidity of the climate of the Holocene in the territory of the USSR and North America.

I. I. Borzenkova examined quantitative methods for evaluating the climates of the Tertiary as possible analogs of the climate of the future. On the basis of a generalization of the results of an oxygen-isotope analysis of deep-water cores

APPROVED FOR RELEASE: 2007/02/08: CIA-RDP82-00850R000300080046-0

APPROVED FOR RELEASE: 2007/02/08: CIA-RDP82-00850R000300080046-0

from different regions of the earth it was possible to visualize changes in the temperature of the upper layers of the ocean during a period from 65-70 million to 1 million years, for example, for different latitude zones of the southern and northern hemispheres.

A report by V. N. Adamenko demonstrated possible reconstructions of pressure-circulation conditions in epochs of warmings and coolings occurring during the last five millenia by means of use of different paleoclimatic data.

At the final session there was an extensive discussion and conference resolutions were adopted.

The great practical importance of materials on impending climatic changes requires an increase in the effectiveness of investigations in this direction. In particular, in order to improve the organization of work on this problem the conferees proposed the creation of a commission of representatives of scientific institutes participating in work on the problem of anthropogenic modification of climate.

The resolution gave a formulation of the following fundamental problems whose solution is necessary for satisfaction of the existing needs for information on climatic conditions of the future.

1. Improvement of computations of concentrations of atmospheric CO_2 with more precise allowance for the transfer of CO_2 into the deep layers of the ocean and exchange of CO_2 between the atmosphere and the biological medium.

2. Implementation of computations of changes of the principal elements of the meteorological regime as a result of an increase in the CO_2 concentration (and also gases forming small impurities in the atmosphere and exerting an influence on the greenhouse effect) with the use of climatic models with different degree of detail in which the feedbacks between climate-forming factors and elements of the meteorological regime are taken into account most precisely.

3. Investigation of the empirical dependences between climate-forming factors and the meteorological regime based on an analysis of data on the annual variation of meteorological elements, recent climatic changes and the climate of the geological past. For this purpose there must be expansion of the data banks of instrumental meteorological observations. A broadening of satellite observations with an increase in their quality is of particular importance. It is necessary to organize the implementation of observations of the balance of glaciers and of the state of the ocean, including contamination of their surfaces. It is necessary to construct detailed global maps of the climates of the past, including maps for the epoch of the climatic optimum, interglacial periods and maps for different parts of the Tertiary.

4. Construction of global maps and preparation of a reference book in the form of tables characterizing the climate of the next five-year period.

5. Development of methods for using data on the climate of the future for solving economic problems, taking into account the limited accuracy and detail of these data.

K. M. Lugina

APPROVED FOR RELEASE: 2007/02/08: CIA-RDP82-00850R000300080046-0

APPROVED FOR RELEASE: 2007/02/08: CIA-RDP82-00850R000300080046-0

A session of the scientific-technical council of the Administration of the Hydrometeorological Service Ukrainian SSR was held in Kiev on 24 April. There was discussion of the problem of the status of study of the hydrometeorological regime of the Black Sea and the Sea of Azov and measures for improving this work in the sea network. Participating in the session were leading workers of the Administration of the Hydrometeorological Service Ukrainian SSR and also representatives of the Sevastopol' Division of the State Oceanographic Institute and the Sea Section of the Crimean Hydrometeorological Observatory. The results of work of the sea and river mouth subdivisions of the Administration of the Hydrometeorological Service Ukrainian SSR on study of the hydrometeorological regime of the coastal zone and open sea were reported by G. V. Yatsevich (Crimean Hydrometeorological Observatory) and Yu. G. Slatinskiy (Sevastopol' Division State Oceanographic Institute).

It was noted in the reports and communications of session participants that during the years of the Tenth Five-Year Plan the Administration of the Hydrometeorological Service Ukrainian SSR, with the active participation of the Sevastopol' Division of the State Oceanographic Institute, has done much work on the rationalization of the sea network and types of observations, an increase in the volume of scientific-research and expeditionary work, and also of special observations of individual elements of the hydrometeorological regime. Each year the sea and river mouth network of the Administration of the Hydrometeorological Service Ukrainian SSR receives a great volume of operational and regime information. Regularly, at the established times, 47 subdivisions make measurements of water temperature and level observations are made at 36 stations using a depth gage. Level variations are registered at 15 hydrometeorological stations using SUM apparatus. In the sea network there are also 12 gaging stations outfitted with GM-12 wave recorders - perspectrographs. During winter about forty subdivisions participate in the implementation of the program for daily ice observations.

The sea and river mouth subdivisions of the Administration of the Hydrometeorological Service Ukrainian SSR receive a great volume of information in the course of implementing expeditionary work under the programs of scientific-research themes and also when making observations on secular profiles and at roadstead stations. It was noted at the session that in 1979 a total of 5,800 individual and 230 multihour stations were occupied in the course of expeditionary work. This made it possible to obtain about 46,500 measurements of temperature and salinity in the open sea. Roadstead runs and multihour stations at roadstead points were also carried out or occupied over the course of the year. A total of 936 individual and 36 multihour stations were occupied.

The sea and river mouth network of the Administration of the Hydrometeorological Service Ukrainian SSR also has seven hydrochemical laboratories which each year carry out a great volume of work on study of the hydrochemical regime of the seas. In particular, in 1979 about 58,000 hydrochemical determinations were made. Great efforts were also made for broadening work on monitoring the state of the environment.

It was noted at the session that on the basis of observational data from the sea and river mouth network the Administration of the Hydrometeorological Service Ukrainian SSR has prepared a series of major generalizations concerning the

APPROVED FOR RELEASE: 2007/02/08: CIA-RDP82-00850R000300080046-0

APPROVED FOR RELEASE: 2007/02/08: CIA-RDP82-00850R000300080046-0

hydrometeorological regime of the coastal zone and open sea. During the last decade alone three volumes of the SPRAVOCHNIK PO GIDROLOGICHESKOMU REZHIMU MOREY I UST'YEV REK (Handbook on the Hydrological Regime of Seas and River Mouths) have been published. This included a special volume on the hydrology of the mouth region of the Danube, seven annual reviews of the state of the hydrometeorological regime of the Black Sea and the Sea of Azov, etc. The Sea Section of the Crimean Hydrometeorological Observatory compiled a fundamental catalogue of observations of waves and the Sevastopol' Division of the State Oceanographic Institute prepared a two-volume reference book on the hydrometeorological regime of the shelf zone of the Black Sea and the Sea of Azov.

Much attention is being devoted to the analysis and generalization of current regime information. The Sevastopol' Division of the State Oceanographic Institute is regularly compiling bulletins, reviews, marine almanacs and other types of generalizations.

It was noted at the session that an exceptionally important role in study of the hydrometeorological regime of the shelf zone of the Black Sea is being played by the river mouth subdivisions of the Danube and Nikolayevskaya Hydrometeorological Observatories. Each year each hydrometeorological observatory, in addition to standard and special coastal observations, carries out different types of work under the programs for scientific-research themes, generalization of materials in the form of marine almanacs and in the form of scientific-technical reports, and also the servicing of interested organizations in their regions. Each year each hydrometeorological observatory conducts 17-20 expeditions under the programs of the scientific research themes for the collection of materials for evaluating the influence of major water management measures on the hydrological and hydrochemical regimes of the mouth regions of rivers. All this type of work is carried out in close contact with the river mouth laboratories of the Sevastopol' Division of the State Oceanographic Institute, which routinely monitors the completeness and quality of the collected materials and in case of necessity introduces corrections into the research plans and programs.

In speaking of the prospects for the development of research in the basin of the Black Sea and the Sea of Azov in the Eleventh Five-Year Plan, the participants in the session noted that the realization of major water management measures in the Danube-Dnepr interfluve and the redistribution of runoff associated with this requires a deeper study of the hydrometeorological regime of individual regions of the sea for the purpose of evaluating the possible consequences both in the next few years and in the more remote future. In this connection a study is being made of the problem of the possibility of expanding some of the existing subdivisions. It was also noted that there is an insistent need for creating a new river mouth subdivision in the lower reaches of the Dnestr in the system of the Administration of the Hydrometeorological Service Ukrainian SSR. This will make it possible to ensure the information needed for all planning-engineering work in this region.

In the adopted resolution the session participants outlined a complex of specific measures whose realization would make possible a substantial improvement in the formulation of work in the sea network for studying the hydrometeorological regime of the seas and preparation of the necessary reference aids for the needs of the country's national economy.

Yu. G. Slatinskiy

APPROVED FOR RELEASE: 2007/02/08: CIA-RDP82-00850R000300080046-0

APPROVED FOR RELEASE: 2007/02/08: CIA-RDP82-00850R000300080046-0

NOTES FROM ABROAD

Moscow METEOROLOGIYA I GIDROLOGIYA in Russian No 10, Oct 80 pp 127-128

[Article by B. I. Silkin]

[Text] As reported in the JOURNAL OF APPLIED METEOROLOGY, Vol 19, 1980, and in NEW SCIENTIST, Vol 86, No 1203, 1980, the American meteorologists R. Viscanta (Purdue University, Indiana) and R. A. Daniels (Illinois University) have studied the effect of the degree of atmospheric contamination on the temperature of the underlying surface. They have formulated a two-dimensional mathematical model which takes in the air space over a large city to an altitude of 2 km. The model included different factors, including the role of various contaminating chemical agents and local topography. The computations were made using computers at the National Atmospheric Research Center at Boulder, Colorado.

The investigation led to the conclusion that the gases and aerosols contaminating an urban atmosphere can cause a decrease in surface temperature by 2°C. As a result, at nighttime, the temperature will be 1°C higher than in a city with an uncontaminated air space.

In the region surrounding a city the temperature variations should be directed in the opposite direction: during the daytime there is a relative warming, and at nighttime -- a relative cooling. However, the amplitude of this phenomenon outside the city is less. It does not exceed approximately 0.5°C.

Although these variations may seem insignificant in comparison with ordinary diurnal temperature fluctuations, in the opinion of R. Viscanta and R. A. Daniels such changes in thermal structure can lead to a real decrease in atmospheric turbulence. A result of this is a less active mixing of air masses between the city and the surrounding terrain. And this, in turn, has the result that at the end of the second half of the day the concentration of contaminating agents directly over the land surface increases by approximately 14%.

***

As reported in SCIENCE NEWS, Vol 116, No 7, 1979, scientific specialists at NOAA in the United States E. W. Varret, F. Parungo and R. Peischel carried out an investigation of the relationships existing between the nature of contamination, cloud cover and precipitation.

APPROVED FOR RELEASE: 2007/02/08: CIA-RDP82-00850R000300080046-0

APPROVED FOR RELEASE: 2007/02/08: CIA-RDP82-00850R000300080046-0

The studies were made in the Los Angeles, California region, well known for its smog. Observations were made of the extent, composition and chemical properties of the air particles present in air space. The control area was a region with little development of industry and little auto transport.

It was established that in the terrain subject to smog the atmosphere contains an excess number of tiny moisture droplets unfavorable for the process of their fusion and the formation of precipitation. Despite this, and this was quite unexpected by the researchers, the cloud cover subject to contamination over petroleum refineries, on the other hand, like the uncontaminated air, contains a great many large moisture droplets which with a high degree of probability can be transformed into rain. The difference is that the larger particles, arising in the petroleum refining process, are better condensation nuclei than the fine particles making up the smog. In addition, the nitrates and nitric acid particles released during the refining of petroleum absorb more water at a lower humidity than sulfate particles, forming smog.

Thus, the operation of a petroleum refinery increases the probability of rain in a particular region, but this rain has an increased acidity.

***

As reported in EDIS (ENVIRONMENTAL DATA AND INFORMATION SERVICE), Vol 11, No 2, 1980, NOAA in the United States has published its five-year plan for many-sided climatological investigations, which according to a resolution of the US Congress, should be implemented not only by this department, but also by NASA, the Department of Energy, the National Science Foundation and the US Department of Defense.

The plan consists of three parts: 1) "Evaluation of Climate Modification," 2) "Systematic Study of Climate" and 3) "Data, Information and Servicing." The objective of the first of these is a qualitative and quantitative determination of the biological, physical, socioeconomic and resource consequences of the changes (both natural and anthropogenic) in climate. Models are being formulated showing the influence of such changes on the yields of the most important crops, the production and saving of energy, the production of fodder for livestock, fishing, etc. The social and economic consequences of the changes caused by a variable climate are to be subjected to analysis; the factors leading to droughts, spreading of deserts, soil erosion and contraction of water resources will be determined.

The second section provides for the study of the physical mechanisms of climate. The factors associated with the accumulation and expenditure of heat in the ocean and the modification of different processes in relation to the state of climate will be determined. Their modeling (partial and complex) should make it possible to ascertain the degree of sensitivity of climate to natural and anthropogenic factors and check the limits of predictability of changes.

The third section enumerates the measures to be taken for increasing the accuracy, reliability and accessibility of climatological data, including data from monitoring of the ocean and information obtained from a system of artificial satellites

APPROVED FOR RELEASE: 2007/02/08: CIA-RDP82-00850R000300080046-0

APPROVED FOR RELEASE: 2007/02/08: CIA-RDP82-00850R000300080046-0

measuring the radiation of the earth's surface and the incident radiation reflected by the upper atmosphere. A separate item in the program is a study of the influence exerted on climate by atmospheric carbon dioxide and the creation of experimental groups predicting climatic changes.

In the United States about 100 million dollars is annually appropriated for all work in the field of climatology. The new program is intended to enhance the efforts to coordinate the efforts of all departments participating in such studies. A special subdivision of NOAA, headed by E. S. Epstein, has been established for this purpose.

COPYRIGHT: "Meteorologiya i gidrologiya", 1980
[3-5303]

5303 -END-
CSO: 1864

APPROVED FOR RELEASE: 2007/02/08: CIA-RDP82-00850R000300080046-0